

ICR

ANNUAL REPORT 1998

Kyoto University
Institute for Chemical Research

Volume 5

ICR ANNUAL REPORT 1998 (Volume 5)

For the calendar year 1 January 1998 to 31 December 1998

Editors:

Professor Minoru KANEHISA (Editor in chief)
Professor Atsuhiko OKA
Professor Kunihiro OSAKI

Managing editor:

Haruo NAKAGAWA

Published and distributed by:

Institute for Chemical Research (*ICR*), Kyoto University
<http://www.kuicr.kyoto-u.ac.jp/>

Note: *ICR* Annual Report available from the *ICR* Library,
Institute for Chemical Research, Kyoto University,
Uji, Kyoto 611-0011, Japan.

Tel: +81-(0)774-38-3009

Fax: +81-(0)774-38-4370

Copyright © 1999 Institute for Chemical Research, Kyoto University

Enquiries about copyright and reproduction should be addressed to:
ICR Annual Report Committee, *ICR* Library, Institute for Chemical Research,
Kyoto University, Uji, Kyoto 611-0011, Japan.

ISSN 1342-0321

Printed by

Nakanishi Printing Co. Ltd.
Shimotachiuti-dori Higashi-iru, Kamigyo-ku, Kyoto 602-8048, Japan.
TEL:+81-(0)75-441-3155. FAX:+81-(0)75-417-2050;441-3159.
E-mail:HBE02610@niftyserve.or.jp hide@nacos.com
HP URL <http://www.nacos.com/>

31 March 1999

CONTENTS

Preface

TOPICS AND INTRODUCTORY COLUMNS OF LABORATORIES	1
Electronic Structures of TiN and TiC — Extension of Molecular Orbital Method into Crystals Hirohide Nakamatsu, Bin Song, Rika Sekine, Kazuo Taniguchi and Takeshi Mukoyama (STATES AND STRUCTURES — Atomic and Molecular Physics).....	4
Polymerization Process of 1,6-di(N-carbazolyl)-2,4-hexadiyne Epitaxially Grown Films Studied by Cryo-TEM Noboru Kawase, Seiji Isoda, Hiroki Kurata, Tetsuya Ogawa and Takashi Kobayashi (STATES NAD STRUCTURES — Crystal Information Analysis)	6
Deformation Behavior of Extruded Blown Film of High Density Polyethylene Syozo Murakami, Kenji Urayama and Shinzo Kohjiya (STATES AND STRUCTURES — Polymer Condensed States)	8
Noncatalytic Cannizzaro-type Reaction of Formaldehyde in Hot Water Yasuo Tsujino, Chihiro Wakai, Nobuyuki Matubayasi, and Masaru Nakahara (INTERFACE SCIENCE — Solutions and Interfaces)	10
Experimental and Theoretical Studies on Thermal Isomerization Reaction of Methyl 4-(Dimethylamino)-benzenesulfonate in the Crystalline State Masao Oda and Naoki Sato Structure-Function Relationships in Alamethicin Ion-Channels: Effects of a Gln7 to Glu7 Mutation Koji Asami, Yasuaki Nagai and Yasuo Nagaoka (INTERFACE SCIENCE — Molecular Aggregates)	12
Arsenic Speciation Including 'Hidden' Arsenic in Natural Waters Hiroshi Hasegawa, Masakazu Matsui and Yoshiki Sohrin (INTERFACE SCIENCE — Separation Chemistry)	14
Magnetization reversal in submicron magnetic wire studied by using giant magnetoresistance effect Teruo Ono, Hideki Miyajima, Kunji Shigeto and Teruya Shinjo (SOLID STATE CHEMISTRY — Artificial Lattice Alloys)	16
Synthesis, Thermal Stability, Structural Features and Electromagnetic Properties of $\text{Bi}_{2+x}\text{Sr}_{2-x}\text{CuO}_{6+\delta}$ ($0 \leq x \leq 0.4$) T. Niinae and Yasunori Ikeda (SOLID STATE CHEMISTRY — Quantum Spin Fluids)	18
New $S = 1/2$ Alternating Chain Compound - High Pressure Form of $(\text{VO})_2\text{P}_2\text{O}_7$ - Masaki Azuma, Takashi Saito, Zenji Hiroi and Mikio Takano (SOLID STATE CHEMISTRY — Multicomponent Materials)	20
Photochemical Reactions of Ge-Related Centers in Germanosilicate Glass Prepared by Sol-Gel Process Massahide Takahashi, Jisun Jin, Takashi Uchino and Toshinobu Yoko (SOLID STATE CHEMISTRY — Amorphous Materials)	22
Rheo-Dielectric Behavior of Oligostyrene and Polyisoprene Hiroshi Watanabe, Tadashi Inoue and Kunihiko Osaki (FUNDAMENTAL MATERIAL PROPERTIES — Molecular Rheology)	24

A New Discovery of Microphase Separation Initiating In the Induction Period of Polymer Crystallization : characteristic wavelengths at high temperatures Keisuke Kaji, Shuji Matsunaga, Go Matsuba, Toshiji Kanaya, Koji Nishida and Masayuki Imai (FUNDAMENTAL MATERIAL PROPERTIES — Polymer Materials Science)	26
Dynamics of Flexible High-Molecular-Weight Polymers in Dilute Solution under Circular Couette Flow Yoshisuke Tsunashima (FUNDAMENTAL MATERIAL PROPERTIES — Molecular motion analysis)	28
Synthesis of Vinyl Ether-Based Polymacromonomers with Well-Controlled Structure Masahiko Minoda, Kenji Yamada, Masayuki Miyazaki, Kohji Ohno, Takeshi Fukuda and Takeaki Miyamoto (ORGANIC MATERIALS CHEMISTRY — Polymeric Materials)	30
Hydrocarbon Molecules with Novel Structure: a Dehydroannulene with Silver(I)-Complexing Ability and a Double C ₆₀ Adduct of Pentacene Koichi Komatsu, Tohru Nishinaga, Yasujiro Murata, Tetsu Kawamura and Noriyuki Kato (ORGANIC MATERIALS CHEMISTRY — High-Pressure Organic Chemistry)	32
Synthesis, Structure and Reaction of {Tris[2-(dimethylamino)phenyl]germyl}lithium Atsushi Kawachi, Yoko Tanaka and Kohei Tamao (SYNTHETIC ORGANIC CHEMISTRY — Synthetic Design)	34
The First Synthesis of an Optically Active Molecular Bevel Gear with Only Two Cogs on Each Wheel Kaoru Fuji, Takeo Kawabata and Takahiro Oka (SYNTHETIC ORGANIC CHEMISTRY — Fine Organic Synthesis)	36
Conformational Effect (Induced-Fit) on Catalytic Activity of α -Chymotrypsin Yasushi Kawai, Takashi Matsuo and Atsuyoshi Ohno (BIOORGANIC CHEMISTRY — Bioorganic Reaction Theory)	38
Artificial Nine Zinc-Finger Peptide with 30-Base Pair Binding Sites Tatsuya Kamiuchi, Emiko Abe, Miki Imanishi, Tamaki Kaji, Makoto Nagaoka and Yukio Sugiura (BIOORGANIC CHEMISTRY — Bioactive Chemistry)	40
CYP2D Microsatellite Polymorphism in Lewy Body Variant of Alzheimer's Disease and Parkinson's Disease Seigo Tanaka, Naomi Matoh and Kunihiro Ueda (BIOORGANIC CHEMISTRY — Molecular Clinical Chemistry)	42
Crystal structures of two tropinone reductases: Different reaction stereospecificities in the same protein fold. Keiji Nakajima, Atsuko Yamashita, Hiroyuki Akama, Toru Nakatsu, Hiroaki Kato, Takashi Hashimoto, Jun'ichi Oda and Yasuyuki Yamada (MOLECULAR BIOFUNCTION — Functional Molecular Conversion)	44
Non-stereospecific Transamination Catalyzed by Pyridoxal Phosphate-dependent Amino Acid Racemases of Broad Substrate Specificity Nobuyoshi Esaki, Tohru Yoshimura, Kenji Soda and Young Hee Lim (MOLECULAR BIOFUNCTION — Molecular Microbial Science)	46
The Crystal Structure of Zinc-Containing Ferredoxin from a Thermoacidophilic Archaeon Tomomi Fujii and Yasuo Hata (MOLECULAR BIOLOGY AND INFORMATION — Biopolymer Structure)	48
Two-component Response Regulators from <i>Arabidopsis thaliana</i> Contain a Putative DNA-binding Motif Hiroe Sakai, Takashi Aoyama, Hidemasa Bono and Atsuhiko Oka (MOLECULAR BIOLOGY AND INFORMATION — Molecular Biology)	50

NLS (Nuclear Localization Signal) Prediction Keun-Joon Park and Minoru Kanehisa (MOLECULAR BIOLOGY AND INFORMATION — Biological Information Science)	52
Design of the Superconducting RFQ for PIAVE Linac Toshiyuki Shirai, Vladimir Andreev, Giovanni Bisoffi, Michele Comunian, Augusto Lombardi, Andrea Pisent and Anna M. Porcellato (NUCLEAR SCIENCE RESEARCH FACILITY — Particle and Photon Beams)	54
Simulation Study of Three-Dimensional Laser Cooling Method for Fast Stored Ion Beams Takahiro Kihara, Hiromi Okamoto and Yoshihisa Iwashita (NUCLEAR SCIENCE RESEARCH FACILITY — Beams and Fundamental Reaction)	56
Mitochondrial Proteins Interacting with Guide RNAs Hiroyuki Sugisaki (RESEARCH FACILITY OF NUCLEIC ACIDS)	58
LABORATORIES OF VISITING PROFESSORS	60
SOLID STATE CHEMISTRY—Structure Analysis	
FUNDAMENTAL MATERIAL PROPERTIES—Composite Material Properties	
SYNTHETIC ORGANIC CHEMISTRY—Synthetic Theory	
PUBLICATIONS	62
SEMINARS	78
THESES	83
ORGANIZATION AND STAFF	87
PERSONAL	91
NAME INDEX	94
KEYWORD INDEX	97

Preface

In 1998, Japan was hit by its worst economic crisis since the Second World War. Therefore, it has been attempted to force through plans to convert large numbers of national research institutes, and possibly some universities, into semiautonomous corporations or “agencies”, by threatening to cut the budgets. On the other hand, the Earth’s environmental ecology, the cloning of Dolly the lamb, and endocrine disruptors(chemical compounds suspected of mimicking natural sex hormones) became high-profile current scientific topics.

This year, a critical review of the research activity, management, and future plans of the ICR is being carried out by eight external reviewers who are leading authorities in various chemical fields. The aim of this external review is to provide a basis for extensive development of the ICR. The Festival of the Uji Campus where includes the Institute of Advanced Energy, the Wood Research Institute, the Institute for Food Science, the Disaster Prevention Research Institute, and the Radio Atmospheric Science Center, in addition to the ICR, was held with the theme “Earth Cosmos Life” on November 20-21, 1998.

The ICR Annual Report continues to strive to provide timely and important information on the scientific activities of the ICR. Currently, 27 full professors, 24 associate professors, and 43 instructors work in the ICR, and about 230 graduate students study at the ICR. At the end of March, 1998, Professor J. Oda of the Laboratory of Functional Molecular Conversion, who has contributed a great deal to the development of the ICR, retired from the ICR and was appointed to a Professorship at Fukui Prefectural University, His successor is Professor K.Sakata from Shizuoka University. Dr. K. Yamada has been promoted from Associate Professor of Tohoku University to Full Professor in the Laboratory of Artificial Lattice Compounds in the ICR. Associate Professor, S. Kakigi, of the Laboratory of Particle and Photon Beams, also retired. We have appointed Drs. T. Kawabata, Y. Iwashita and T. Terashima as Associate Professor of the ICR. The two-year term of Director finished for Professor T.Shinjo in March. Since April, I have served as the Director for the ICR, as this successor.

Finally, I would like to congratulate Professor K. Fuji for the Pharmaceutical Society of Japan Award, and Professor K. Komatsu for the Divisional Award of the Chemical Society of Japan. In addition, the Pharmaceutical Society of a Award for Young Scientists was awarded to Associate Professor S. Fukaki, whom I would like to congratulate.

January, 1999



Yukio Sugiura
DIRECTOR

**TOPIC AND INTRODUCTORY COLUMNS
OF LABORATORIES**

Key to headline in the columns

RESEARCH DIVISION – Laboratory (Subdivision)*

* See also “Organization and Staff” on page 87.

Abbreviations used in the columns

Prof Em	Professor Emeritus	GS	Graduate Student
Prof	Professor	DC	Doctor’s Course (Program)
Vis Prof	Visiting Professor	MC	Master’s Course (Program)
Assoc Prof	Associate Professor	UG	Undergraduate Student
Lect	Lecturer	RF	Research Fellow
Lect(pt)	Lecturer	RS	Research Student
Instr	Instructor		
Assoc Instr	Associate Instructor	D Sc	Doctor of Science
Techn	Technician	D Eng	Doctor of Engineering
Guest Scholar	Guest Scholar	D Agr	Doctor of Agricultural Science
Guest Res Assoc	Guest Research Associate	D Pharm Sc	Doctor of Pharmaceutical Science
Univ	University	D Med Sc	Doctor of Medical science

Electronic Structures of TiN and TiC —Extension of Molecular Orbital Method into Crystals

Hirohide Nakamatsu,^{†1} Bin Song,^{†2} Rika Sekine,^{†3} Kazuo Taniguchi and
Takeshi Mukoyama

Density of states and theoretical X-ray emission spectra for the valence bands of TiN and TiC are obtained with a molecular orbital method. To describe electronic structures of crystals, local clusters for the molecular orbital calculations are extended, including the effects from the outside of the cluster in the crystal. The theoretical results are in good agreement with the experimental ones.

Keywords : molecular orbital/ TiN/ TiC/ electronic structure/ extended cluster model/ X-ray emission spectra

X-ray spectroscopy is one of the most powerful tools for elucidating electronic structures of substances. Valence band structures are studied with X-ray photoelectron spectra (XPS) and X-ray emission spectra (XES). XPS reflects density of states (DOS), while XES reflects partial density of state. According to the dipole selection rule on the radiative transition, K X-ray emission reflects p components and L_3 X-ray emission corresponds to s and d components. Therefore, detailed valence band structures are clarified by observing both spectra.

Fischer provided a diagram suitable to understand the relation among the X-ray emission spectra for various inner shell excitations[1]. The molecular orbital levels were shown to explain this relation. However, his and the followers' model clusters used to represent solids in the molecular orbital framework were insufficient to make

direct and quantitative comparison with the experimental results.

Molecular orbital methods provide an atomic view of materials and are, therefore, useful to get valuable insight about understanding electronic structures and designing materials. They can be also applied to widely extended systems such as solid states.

XES for TiN and TiC have been discussed with cluster calculations though the theoretical spectra were not satisfactory. The simplest TiX_6^n ($X=C$ or N) model cluster is still used to interpret the origins of the peaks in XES. Gubanov et al. [2] interpreted the XES spectra of these compounds with molecular orbital calculations. But in the $Ti L_3$ spectrum for TiN, the calculated peak intensity ratios were strikingly different from the experimental ones. His theoretical spectra could not explain bands at

STATES AND STRUCTURES — Atomic and Molecular Physics —

Scope of Research

In order to obtain fundamental information on the property and structure of materials, the electronic states of atoms and molecules are investigated in detail using X-ray, SR, ion beam from accelerator and nuclear radiation from radioisotopes. Theoretical analysis of the electronic states and development of new radiation detectors are also performed.



Professor
MUKOYAMA,
Takeshi
(D Eng)



Assoc. Prof
ITO,
Yoshiaki
(D Sc)



Instructor
KATANO,
Rintaro
(D Eng)



Instructor
NAKAMATSU,
Hirohide
(D Sc)

Students:

YAMAGUCHI, Koichiro (DC)
SHIGEMI, Akio (DC)
SUZUKI, Chikashi (DC)
TOCHIO, Tatsunori (DC)
VLAICU, A. Mihai (DC)
MASAOKA, Sei (DC)
ISHIZUKA, Takashi (DC)
ITO, Kunio (MC)
SHIGEOKA, Nobuyuki (MC)
NAKANISHI, Yoshikazu (RF)
YASUI, Jun (RF)

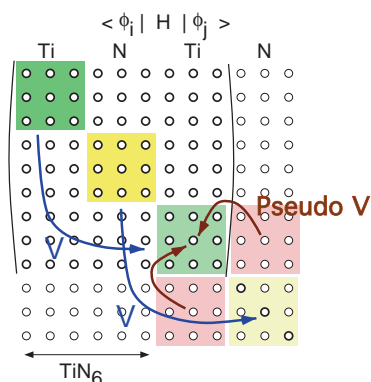


Figure 1. Energy matrix for a cluster extended to include the environment.

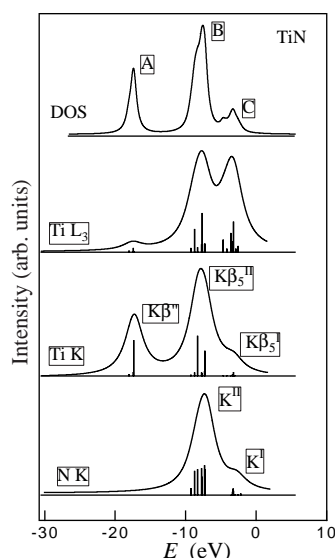


Figure 2. Theoretical DOS and XES for TiN.

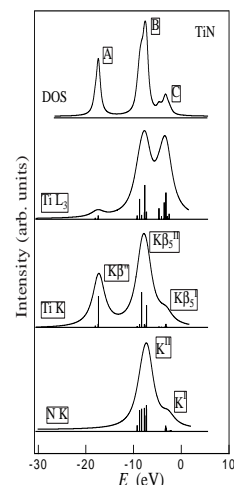


Figure 3. Experimental photoelectron spectra [3], Ti L₃, Ti K and N K XES [4] for TiN.

high energy parts of the spectra. He stated that the discrepancies of the uppermost bands for TiN could arise from defect structures in the crystal.

The simple TiX₆ⁿ⁻ cluster has a sudden change of bonding environment at the periphery and causes peculiar charge distribution different from the actual crystal. In the present work, to provide theoretical spectra of high quality, an extended cluster model is developed. These clusters can improve the periphery of clusters and the electroneutrality in the stoichiometric composition of crystals. Furthermore, to make a precise comparison, Ti L₃ XES for TiN and TiC are measured, using the synchrotron radiation.

We take a way that the environment around the cluster is involved in the energy matrix for the cluster. Explanation of this matrix is shown in Fig. 1, where the matrix elements for a cluster include the contributions from outside of the cluster in the crystal. The cluster is embedded in ambient potentials which are duplicated from the potentials of the central atoms. Pseudopotentials are placed upon these potentials so that the wave functions of the embedded cluster feel the exclusive character of the wave functions of the ambient atoms. The electroneutrality of the Ti-X stoichiometric pair is achieved by varying the depth of the pseudopotentials. This procedure reduces the change of the chemical potential of electrons at the ends of the embedded cluster. The electroneutrality is the postulate in this method to connect the cluster smoothly to the environment.

X-ray emission probability was obtained in the dipole approximation. Intensities for three kinds of the Ti atoms in the cluster were summed up to evaluate all the forms of the wavefunctions in the cluster. This summation corresponds to collecting the different momenta of the wavefunctions. To generate the theoretical spectra, a Lorentzian curve was placed at each eigenenergy.

The theoretical DOS and XES obtained are compared with the experimental spectra and the relation among the spectra is illustrated. The theoretical valence

DOS and XES for TiN are plotted in Fig. 2 and the experimental spectra are in Fig. 3. The spectra for TiC are not shown here for the limit of space. The experimental spectra were arranged, referring to the ionization energies of the corresponding initial levels of the excitations. This means the ionization energy for the valence band is plotted for the experimental spectra. Consequently, we have arranged the different XES on the same ground.

For TiN, the theoretical XES in Fig. 2 agree well in shape and position with the experimental spectra of the Ti L₃, Ti K and N K XES shown in Fig. 3. The present theoretical spectra have the uppermost peaks marked with Kβ₅[†] and K[†] in the Ti K and N K XES, which could not be explained with the simplest cluster TiX₆ⁿ⁻ calculations. The calculated peak intensities for Ti L₃, Ti K and N K are also in good agreement with the corresponding experimental ones.

Our original papers[5,6] present details of valence electronic structures and covalent interaction between the metal and non-metal atoms for TiN, TiC and TiO₂.

References

- †1 The present address is Dept. of Physics, Zhejiang University, Hangzhou 310027, China.
- †2 Dept. of Chemistry, Shizuoka University, Ohya, Shizuoka, 422-8529 Japan.
- †3 Osaka Electro-Communication University, Neyagawa, Osaka, 572-8530 Japan.
1. Fischer D. W. and Baun W. L.: *J. Appl. Phys.*, **39**, 4757 (1968).
2. Gubanov V A, Ivanovskii A L, Shveikin G P and Weber J: *Solid State Commun.*, **29**, 743 (1979).
3. Johansson L I, Stefan P M, Shek M L and Nørlund Christensen A: *Phys. Rev.*, **B22**, 1032 (1980).
4. Weinberger P: *Theoret. Chim. Acta (Berl.)*, **42**, 169 (1979).
5. Song B, Nakamatsu H, Mukoyama T and Taniguchi K: *Advances in X-Ray Chemical Analysis, Japan*, **29**, 191-202 (1998).
6. Song B, Nakamatsu H, Sekine R, Mukoyama T and Taniguchi K: *J. Phys. Cond. Matter*, **10**, 9443-9454 (1998).

Polymerization Process of 1,6-di(N-carbazolyl)-2,4-hexadiyne Epitaxially Grown Films Studied by Cryo-TEM

Noboru Kawase, Seiji Isoda, Hiroki Kurata, Tetsuya Ogawa and Takashi Kobayashi

Thin films of 1,6-di(N-carbazolyl)-2,4-hexadiyne (DCHD) grown epitaxially on (0 0 1) surface of KCl through vacuum-deposition were examined on their polymerization process induced by heat treatment. The structural changes due to polymerization in the films were investigated by electron diffraction and high resolution (HREM) cryo-TEM.

Keywords: 1,6-di(N-carbazolyl)-2,4-hexadiyne / polymerization process / low temperature high resolution imaging

Since Wegner has demonstrated in 1969 that solid-state polymerization of diacetylenes can be characterized as a diffusionless and lattice controlled process[1], many solid-state reactions in diacetylene derivatives have been examined on their unique features[2,3]. As for 1,6-di(N-carbazolyl)-2,4-hexadiyne (hereafter abbreviated DCHD), Enkelmann *et al.*[4] has reported in 1977 that DCHD monomer crystals can be topochemically polymerized by heat treatment or γ -irradiation. In the present study, the high resolution electron microscopic work was performed by cooling the specimen at a low temperature with a cryo-specimen-holder and employing a minimum electron irradiation system for image recording. The structural correlation of thin poly-DCHD film with the monomer film grown epitaxially on a substrate are examined by high resolution imaging to elucidate the polymerization process.

A small amount of the DCHD powder was heated and

sublimed on KCl substrate at 50°C in the vacuum of 5×10^{-5} Pa. The polymerization of DCHD was carried out by heating at 150°C in a nitrogen atmosphere.

A high resolution image of polymer crystal obtained by heating a monomer film on the KCl substrate at 150°C for 5 h is shown in Fig.1(a). The high resolution image shows a part of a needle-like crystal. At inner part of the crystal (the right part of the image), lattice fringes of 0.43nm are observed along two directions. The angle between these lattice fringes is about 59° and the angle of the fringe with the *b*-axis is about 60°, which agrees well with values calculated from the polymer crystal, assuming that the lattice fringes come from the (1 1 1)- and (1 $\bar{1}$ 1)-planes. The area, therefore, can be assigned as a projection of polymer crystal along the [1 0 $\bar{1}$]. At the edge of the crystal, lattice fringes of 0.83nm are running along the *b*-axis, which corresponds to the spacings of (0 0 2). This lattice plane could not satisfy the Bragg condi-

STATES AND STRUCTURES — Crystal Information Analysis —

Scope of research

Structures of materials and their structural transition associated with chemical reactions are studied through the direct observation of atomic or molecular imaging by high resolution microscopy. It aims to explore new methods for imaging with high resolution and for obtaining more detailed chemical information. The following subjects are studied: direct structure analysis of ultrafine crystallites and ultrathin films, crystal growth and adsorption states of organic materials, and development on high resolution energy filtered imaging as well as electron energy-loss spectroscopy.



Prof
KOBAYASHI,
Takashi
(D Sc)



Assoc Prof
ISODA,
Seiji
(D Sc)



Instr
OGAWA,
Tetsuya
(D Sc)



Instr
NEMOTO,
Takashi
(D Sc)



Assoc Instr
MORIGUCHI,
Sakumi

Guest Scholar:

FRÖHSHEIMER, Mathías

Students:

IRIE, Satoshi (DC)

KUWAMOTO, Kiyoshi (DC)

KOSHINO, Masanori (DC)

YAJI, Toyonari (DC)

SUGA, Takeo (DC)

FUJIWARA, Eiichi (DC)

TSUJIMOTO, Masahiko (MC)

YOSHIDA, Kaname (MC)

FURUKAWA, Chieko (MC)

AKAGI, Nozomu (MC)

TERADA, Shohei (MC)

HAHAKURA, Seiji (MC)

ADACHI, Yoshio (MC)

KANEYAMA, Syutetsu (MC)

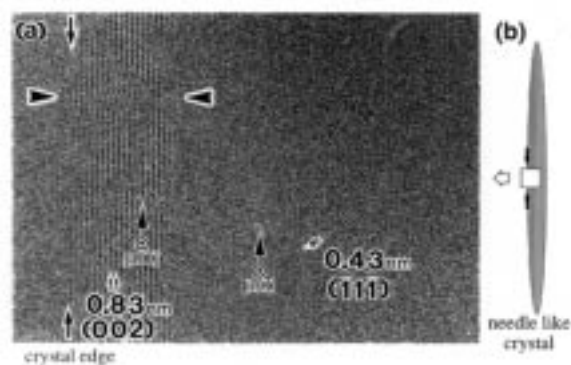


Figure 1. High resolution image of fully polymerised film by thermal treatment for 5 h at 150°C, where the vertical arrows indicate the crystal edge.

tion if the polymerization of monomer crystal occurs topochemically. When the poly-DCHD changes its orientation from the topochemical one by rotating about 28° around the b -axis, the (002) lattice fringes become observable in HREM. The poly-DCHD crystals seem to grow in many cases by changing drastically their orientation at the crystal edge, because such rotation is needed probably to relax a stress produced during the polymerization. In addition to this orientation change, crystal distortion is observed at the edges indicated by the two black arrowheads in Fig.1(a). This distortion may be introduced by collision of two growing polymer crystals from the opposite sides along the b -axis. Thus the DCHD molecules change their orientation, especially at the crystal edge where it is easy to expand the volume and to change orientation.

To examine the process of polymerization, it is necessary to observe intermediate stages of the polymerization. A high resolution image at such intermediate stage of polymerization is shown in Fig.2(a) as a projection nearly along $[1\ 0\ \bar{1}]$ axis of polymer. Various lattice fringes having different spacings can be found in the crystal, which are corresponding to those of (202). From this micrograph it becomes clear that the polymer and the monomer crystallites coexist as small domains in partially polymerized crystal. The regions of $d \sim f$ and h show intermediate lattice spacings between those of monomer and polymer, so that these regions are considered to be a mixed crystal or a solid solution of monomer and polymer molecules. Since all values of lattice spacings observed in the image are between those of (202)-spacings of monomer and polymer crystals, it can be concluded that various transient states of crystal structure coexist at microscopic level in partially polymerized crystal. This result supports the previous X-ray study on bulk specimen[5], and gives new information. That is, the transient state is an aggregation of very small crystal-

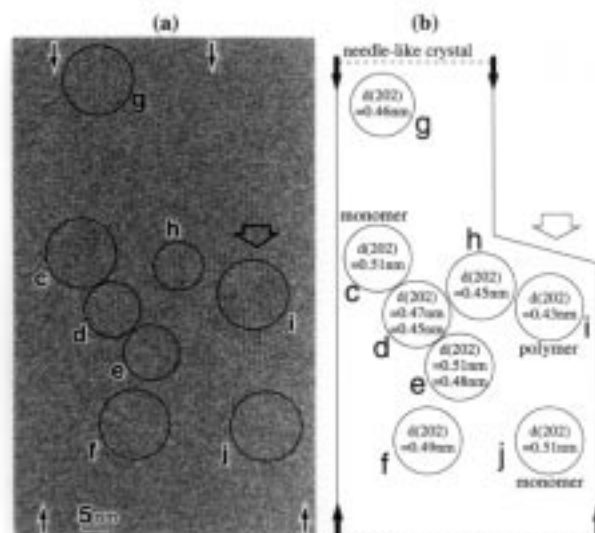


Figure 2. (a) High resolution image of partially polymerised film for 3 min at 150°C. (b) Schematic illustration corresponding to (a).

lites having slightly different lattice spacings in the needle-like crystal which was originally a single crystal of monomer. In addition to this, it is interesting that the almost polymerized region i is found at a crystal edge indicated by the wide white arrow, where the monomer crystal was ended along the b -axis. On the other hand, at the inner parts of the crystal, polymerization did not start or did not complete as indicated by the lattice fringes with different spacings in the figure. Then the thermal polymerization could start from such a defect at crystal edge. As polymerization proceeds, the small domains of solid-solution may coalesce coherently each other along the chain axis, resulting in a large fibrous domain as observed in Fig.1.

Finally the large domain at edges of needle-like crystal, considered to be a domain fully polymerized at an early stage, may change its orientation drastically, probably to relax a stress produced by polymerization at inner part of the crystal.

References

1. Wegner, G.: *Z. Natur. Teil B*, **24**, 824 (1969).
2. Baughman, R. H.: *J. Appl. Phys.* **43**, 4362 (1972).
3. Yee, K. C.: *J. Polym. Sci., Polym. Phys. Ed.* **16**, 431 (1978).
4. Enkelmann, V. and Wegner, G. *et al.*: *Chem. Phys. Lett.* **52**, 314 (1977).
5. Enkelmann, V. and Leyrer, R. J. *et al.*: *J. Mater. Sci.* **15**, 168 (1980).

Deformation Behavior of Extruded Blown Film of High Density Polyethylene

Syozo Murakami, Kenji Urayama and Shinzo Kohjiya

Deformation behavior of extruded blown film of polyethylene, which contains oriented lamellae normal to the extruded direction (MD), is investigated by scanning electron microscope and X-ray scattering techniques. Type of structural change in deformation process strongly depends on angle between stretching direction and MD. A structural model is proposed to explain the experimental results systematically.

Keywords : High density polyethylene / Extruded blown film/ Deformation / SEM/ X-ray diffraction

Deformation process of semi-crystalline polymers is strongly influenced by temperature and orientation of crystalline lamellae with respect to deformation direction. Aims of this study are to clarify mechanisms for unfolding of polymer chains, and to elucidate change from lamellar structure to fiber structure in deformation process. Extruded blown (EB) film of high density polyethylene (HD-PE) contains oriented crystalline lamellae, where polymer chains are parallel to extruded direction (MD:machine direction) and they are folding in ca.18nm thickness. In other words, the lamellae are originally oriented in direction normal to the extrusion direction (TD:transverse direction). There have been many investigations concerning deformation behavior of polyethylene [1,2]. In these studies, the stretching direction was perpendicular to original orientation of polymer chains. In this study, stretching of the EB film of HD-PE in various directions (involving parallel one to MD) is conducted, and the structural changes during the deformations are studied by X-ray scattering measurements and scanning electron microscopy (SEM).

HD-PE (Sholex 6009) was melted at 180°C and extruded from a circular orifice into air. Crystallization proceeded under elongation stress by drawing ratio of about 56 times. From the resultant films, specimens for mechanical and X-ray measurements were cut to obtain strips in various directions to MD. After the measurements, specimens were treated with fuming nitric acid for SEM observations (HITACHI S-310).

SEM observation shows that these films feature ordered stacking of untwisted lamellar crystals normal to MD (Fig.1). The thickness of a lamellar observed in SEM was about 100nm, while that from long period based on two-point diagram in SAXS pattern was about 18nm ((a) in Fig.1). These results suggest 5-6 sheets of folding of chain. Recently, we observed a lamella of about 18nm in AFM [3] in accord with the SAXS result. Stress-strain (S-S) curves are found to be much different per elongation direction. In the elongation along TD, the stress suddenly decreased when the film was elongated to the yield point, and thereafter the necking propagated steadily with a constant stress value. Optical observation revealed that necking boundary line was very sharp and perpendicular to elongation direction (parallel to MD) [4]. These deformation behavior are well explained by Kobayashi's silk hat model assuming that the polymer chains are pulled out of lamellae by unfolding [5]. In the elongation along MD, on the contrary, the film was apparently uniformly elongated without significant decrease of stress at the yield point. The necking boundary lines appeared at oblique angles about $\pm 50^\circ$ to MD due to the lamellar slipping, and gradual increase in number of necking line was observed during the drawing. In spite of these necking, shapes of the S-S curves were smooth, but the micronecking occurred one after another in many parts over the specimens.

Figure 1 shows a SEM image for EB film in the undeformed state. "A" in Fig. 1 shows the long connecting line of overlap-

STATES AND STRUCTURES — Polymer Condensed States —

Scope of research

Attempts have been made to elucidate the molecular arrangement and the mechanism of structural formation/change in crystalline polymer solids, polymer gels and elastomers, polymer liquid crystals, and polymer composites, mainly by electron microscopy and/or X-ray diffraction/scattering. The major subjects are: synthesis and structural analysis of polymer composite materials, preparation and characterization of polymer gels and elastomeric materials, structural analysis of crystalline polymer solids by direct observation at molecular level resolution, and in situ studies on structural formation/change in crystalline polymer solids.



Prof
KOHJIYA,
Shinzo
(D Eng)



Assoc Prof
TSUJI,
Masaki
(D Eng)



Instr
URAYAMA,
Kenji
(D Eng)



Instr
TOSAKA,
Masatoshi



Instr
MURAKAMI,
Syozo
(D Eng)

Students:

HIRATA, Yoshitaka (DC)
SHIMIZU, Toshiki (DC)
MURAKAMI, Takeshi (DC)
BEDIA, Elinor L.(DC)
FUJITA, Masahiro (DC)
KAWAMURA, Takanobu (DC)
KAMIJO, Takashi (MC)
KASAI, Yutaka (MC)
YOKOYAMA, Keisuke (MC)
HAMAJIMA Hirokazu (MC)
UENO Yukiyoishi (UG)
ISHIMARU, Kazunori (UG)
TERAKAWA, Katsumi (RF)
ASAEDA, Eitaro (RF)
DE SARKAR, Mousumi (RS)

ping parts of lamellae grown from different nucleus, and they pile alternatively. Probably, straight chains are assumed to be interpenetrating into center parts of lamellae (shish parts of Pennings' shish-kebab [6]) in EB film. Figure 2 indicates a SEM image for necked EB film drawn parallel to MD. It is found that oriented lamellae parallel to elongation direction appear by elongation instead of "A" in Fig.1. The parts corresponding to "A" in Fig. 1 and straight chains are first elongated and then the lamellae are bended, twisted, or rotated by the stress. By further stretching, tie molecules or link-fibrils [7] which link between lamellae are cut and the distance between lamellae is widen and lamellae orientation is changed to the stretching direction, and consequently the film is elongated by unfolding same as TD elongation [8].

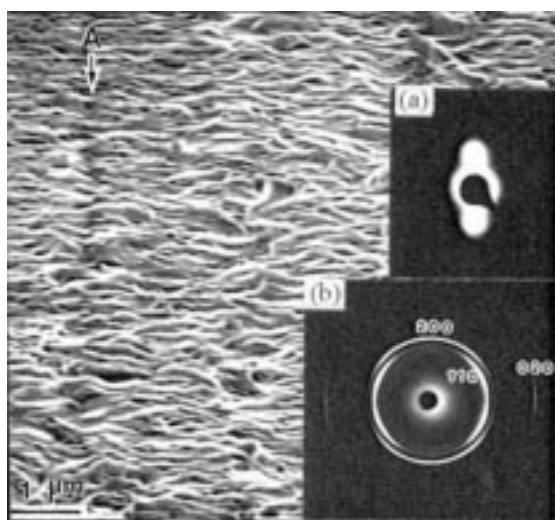


Figure 1. SEM of EB film etched with fuming HNO_3 . (a) is SAXS pattern of two-point diagram showing long period of about 18nm. (b) shows WAXD pattern with X-ray beam normal to surface of film.

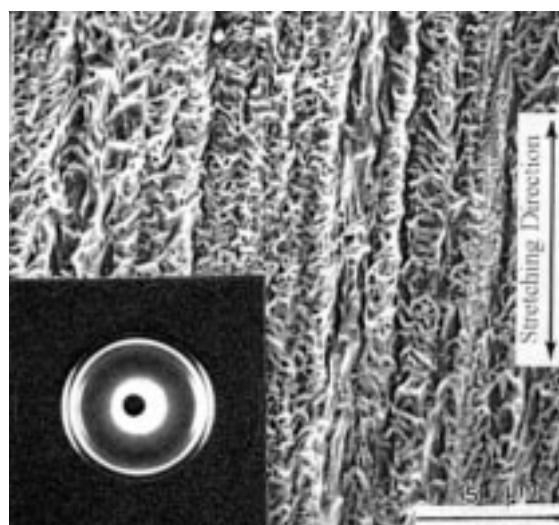


Figure 2. SEM of necked EB film drawn parallel to MD at room temp. Inset shows WAXD pattern whose most inner diffraction is 001 monoclinic one.

It was found by time-resolved X-ray diffraction patterns that the deformations induced phase transformation from orthorhombic to monoclinic form whose reflection appeared transiently inside orthorhombic 110 reflection during stretching at the temperatures below 50°C , as is shown in Fig. 2 [9]. This 001 monoclinic reflection (here b-axis is taken as fiber axis which is according to Seto et al. [10]) plane corresponds to orthorhombic 110 one, and the reflection appears in the stretching parallel to MD. The monoclinic reflection appeared from just before the onset of necking. However, in the stretching parallel to TD, monoclinic reflection did not appear. This is explained by assuming that the phase transformation occurs at a point of lamellae and no distortions such as bending, twisting and rotating occur in any other parts of lamellae. It should be noted that the b-axis is the growing direction of lamellae and parallel to TD. In the stretching to this direction, the transformation of lamellar structure to fiber structure appears to occur via successive unfolding starting from one part of lamellae due to stress concentration in the film. On the other hand, in the stretching parallel to MD, the transform appeared at many parts in specimen accompanied by various types of distortion. Based on these observations and correlations between structural changes and stress-strain relations, a structural model for elongation process is newly proposed, which is shown schematically in Fig.3. The model can explain the experimental results obtained here, thus elucidating the deformation mechanism of semi-crystalline polymer films in general. Further investigations on this model are in progress at our laboratory.

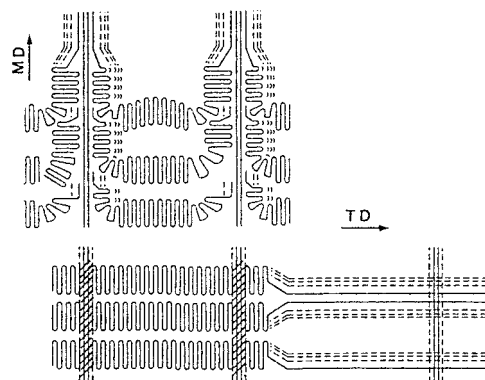


Figure 3. Structure model for chain-unfolding in stretching EB film.

References

1. B. Wunderlich, "Macromolecular Physics", Vol. 1, Academic Press, NY and London, 1973.
2. P. Ingram, H. Kiho and A. Peterlin, *J. Polym. Sci., Part C*, **16**, 1857 (1967).
3. K. Shimamura, T. Uchida, S. Murakami and S. Kohjiya, *Sen-i Gakkai Preprints*, G-198 (1998).
4. S. Murakami, K. Shimamura and S. Kohjiya, *NIHON REOROJI GAKKAISHI*, **25**, 193 (1997).
5. K. Kobayashi, in "Polymer Single Crystal", Ed. by P. H. Geil, Interscience, New York, p.478, 1963.
6. A. J. Pennings, J. M. A. van der Mark and A. M. Kiel, *Kolloid-Z.Z.Polym.*, **237**, 336 (1970).
7. H. P. Keith, F. J. Padden and R. G. Vadimsky, *J. Appl. Phys.*, **37**, 4027 (1966).
8. S. Murakami, S. Kohjiya and K. Shimamura, *Polymer Preprints, Japan*, **45**, 2807 (1996), *ibid.*, **46**, 4013 (1997).
9. S. Murakami, K. Tanno, M. Tsuji and S. Kohjiya, *Bull. Inst. Chem. Res., Kyoto Univ.*, **72**, 418 (1995).
10. K. Tanaka, T. Seto and T. Hara, *J. Phys. Soc., Japan*, **17**, 873 (1962).

Noncatalytic Cannizzaro-type Reaction of Formaldehyde in Hot Water

Yasuo Tsujino, Chihiro Wakai, Nobuyuki Matubayasi, and Masaru Nakahara

In water at 250 °C and 4 MPa, methanol and formic acid are produced from the disproportionation reaction of formaldehyde without a catalyst, although at mild conditions, this reaction usually occurs in the presence of a large amount of base catalyst. Formic acid further undergoes the hydride transfer reaction with formaldehyde, and the final yield of methanol exceeds 50%.

Keywords : Hydrothermal reaction / NMR / C₁ chemistry / Formaldehyde / Cannizzaro reaction

Water in the high-temperature and high-pressure (HTHP) conditions receives much attention recently as a novel and clean medium for chemical reactions of environmental and industrial importance. In order to understand and control a wide variety of organic reactions in HTHP water, it is important to establish physical organic chemistry of aqueous solutions at high temperatures and high pressures.

Formaldehyde is one of the most important reaction intermediates in C₁ chemistry. For example, it is expected to be an intermediate of decomposition of dichloromethane in HTHP water, and dichloromethane is transformed through formaldehyde into methanol and formic acid. Thus, it is natural to focus on the reaction

of formaldehyde in HTHP water. In addition, formaldehyde is a strongly reduced form of CO₂ and its reaction is of interest from the viewpoint of CO₂ cycle.

In order to form formaldehyde in HTHP water, 1.5 M (mol/dm³) of *s*-trioxane is dissolved into heavy water at room temperature. The sample solution was sealed into a quartz capillary with inner diameter of 2.5 mm. The sample tube was placed in the furnace and the temperature was raised from room temperature to 250 °C. The time 0 of the reaction was then set to be the time at which 250 °C was reached. After a reaction finished, the capillary was removed from the furnace quickly and cooled down to the room temperature. The solution was

INTERFACE SCIENCE — Solutions and Interfaces —

Scope of research
Structure and dynamics of a variety of ionic and nonionic solutions of physical, chemical, and biological interests are systematically studied by NMR under extreme conditions. High pressures and high temperatures are employed to shed light on microscopic controlling factors for the structure and dynamics of solutions. Vibrational spectroscopic studies are carried out to elucidate structure and orientations of organic and water molecules in ultra-thin films. Crystallization of protein monolayers, advanced dispersion systems at liquid-liquid interfaces, and biomembranes are also investigated.



Prof
NAKAHARA, Masaru
(D Sc)



Assoc Prof
UMEMURA, Junzo
(D Sc)



Instr
MATSUMOTO, Mutsuo
(D Sc)



Instr
MATUBAYASI, Nobuyuki
(Ph D)



Assoc Instr
OKAMURA, Emiko
(D Pharm Sci)



Assoc Instr
WAKAI, Chihiro
(D Sc)

Research

Assistants(pt)

KIMURA,
Noriyuki (D Sc)
TANO,
Takanori (D Sc)

Students

BOSSEV,
Dobrin (DC)
KONISHI,
Hirofumi (DC)
KIMURA,
Tomohiro (DC)
MCNAMEE,
Cathy (DC)
TOYA, Hiroshi (MC)
IMADA,
Tomokatsu (MC)
KAWAI,
Kunichika (MC)
TSUJINO,
Yasuo (MC)
KAKITSUBO,
Ryou (MC)

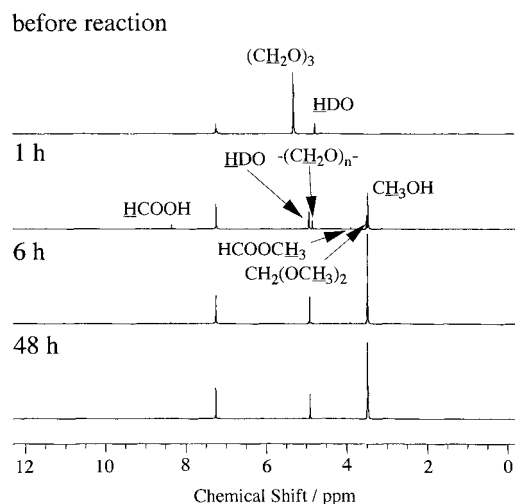
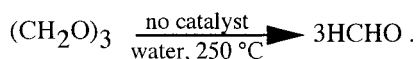


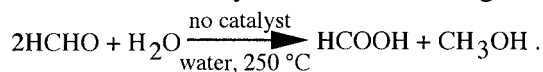
Figure 1. The ^1H -NMR spectra of *s*-troxane in D_2O reacted at $250\text{ }^\circ\text{C}$ as a function of time. (external reference; C_6H_6 , 7.27 ppm)

subjected to NMR measurements (JEOL, EX-270 wide-bore) and the gas components were analyzed with gas chromatography (Shimadzu GC-14B) equipped with a thermal conductivity detector.

Figure 1 shows how the ^1H -NMR spectrum of the solution reacted at $250\text{ }^\circ\text{C}$ varies with time. At the time of 1 h, two peaks emerge with disappearance of the *s*-trioxane peak; one is methanol and the other formic acid. In HTHP water, formaldehyde is formed from *s*-trioxane by ring-opening as follows,



After the formation of formaldehyde, the disproportionation reaction of formaldehyde occurs without catalysts in the following,



According to the classical Cannizzaro reaction, the disproportionation reaction proceeds under the presence of a large amount of catalysts. Although the autoprotolysis constant of water at $250\text{ }^\circ\text{C}$ and 4 MPa is larger than that at ambient condition, this does not cause the occurrence of disproportionation reaction since the OH^- concentration is still much smaller than that required for the classical Cannizzaro reaction. In the HTHP state studied here, therefore, the fact that the reaction occurs without catalysts suggests the possibility that water takes part in the HTHP Cannizzaro-type reaction. As the

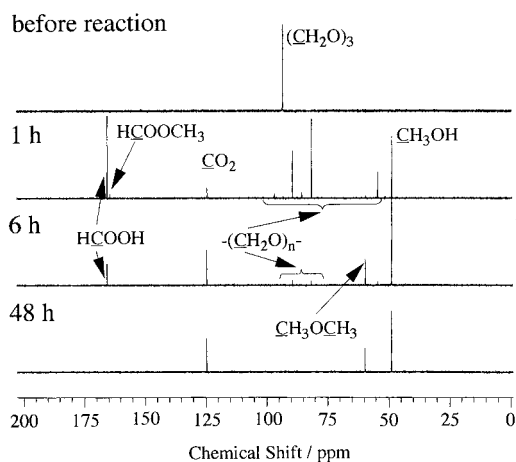
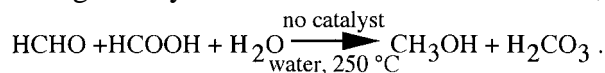


Figure 2. The ^{13}C -NMR spectra of *s*-troxane in D_2O reacted at $250\text{ }^\circ\text{C}$ as a function of time. (reference; CH_3OH , 49.0 ppm)

reaction time varied, the methanol peak grew with disappearance of formic acid and oligomers of formaldehyde.

It is of interest to note that the yield of methanol is found to reach about 70% in our reaction, exceeding the predicted value from the classical Cannizzaro-type reaction (50%). In Figure 2, we show ^{13}C spectra for the reaction system. The spectrum at each time in Figure 2 represents the same system as the corresponding spectrum in Figure 1. Figure 2 provides a possible mechanism for excessive methanol formation. Notably, CO_2 is detected in Figure 2. In fact, the production of CO_2 in the gas phase is also confirmed from gas chromatography. This indicates that the oxidized aldehyde, formic acid, participates in the methanol formation in HTHP water. Thus, formic acid is considered to undergo the hydride transfer and react as follows,



This reaction causes further formation of methanol. In addition, CO was not detected in the gas phase of our reaction, in agreement with quantum-chemical calculations. The hydride transfer reaction shown above is considered to occur when both formic acid and formaldehyde exist in HTHP water. With the reaction time, methanol peak and CO_2 peak in Figure 2 grew, accompanied with the decrease of the peak intensities of oligomers and formic acid. This mechanism also accounts for the disappearance of the formic acid peak in Figure 1.

Experimental and Theoretical Studies on Thermal Isomerization Reaction of Methyl 4-(Dimethylamino)benzenesulfonate in the Crystalline State

Masao Oda and Naoki Sato

Solid-state thermal isomerization reaction from methyl 4-(dimethylamino)benzenesulfonate to *N,N,N*-trimethylbenzeneaminium-4-sulfonate has been studied by X-ray diffraction and spectroscopic experiments and *ab initio* MO calculations. The examination of the experimental results in comparison with the calculated results such as molecular total energies, intramolecular charge distributions, a transition-state structure, intrinsic reaction coordinates and lattice energies has provided us with much essential information to elucidate the process, mechanism and energetics of the reaction.

Keywords: Organic solid-state reaction/ Thermal isomerization/ Methyl cation transfer/ *Ab initio* MO calculation

In searching for an organic solid-state reaction which could be employed as a phenomenon deriving novel electronic properties with dynamical natures, the thermal isomerization reaction from methyl 4-(dimethylamino)benzenesulfonate (MDBS) to a zwitterion of *N,N,N*-trimethylbenzeneaminium-4-sulfonate (TBS) in the crystalline state has been studied by both experiments of X-ray diffraction, infrared absorption, electronic absorption and emission and *ab initio* MO calculations using the RHF/MP2/6-31G* method to elucidate its mechanism [1,2], since this reaction is characterized by intermolecular methyl cation transfer.

This reaction can admit two kinds of ionic intermediates, that is, 4-(dimethylamino)benzenesulfonate (A, anion intermediate) and methyl *N,N,N*-trimethylbenzeneaminium-4-sulfonate (C, cation one), and they should exist at high concentrations during the reaction according to the two-step mechanism which was hitherto accepted. However, by comparing changes in

infrared absorption spectra through the reaction with the results from normal vibration analyses of the four chemical species involved by the RHF/6-31G* method, it is shown that concentrations of both intermediates have been less than the observation limits by the infrared absorption spectroscopy applied. This indicates that the thermal isomerization above proceeds not as a two-step reaction but as a chain one.

Concerning the heat of this reaction, *i.e.* $\Delta_r H^\circ \approx -63 \text{ kJ mol}^{-1}$, an interpretation that it is derived directly from the energy difference in total energies of MDBS and TBS in the isolated states seems to be contradictory to the results of lattice energy calculations of the two materials by other workers. To solve this problem total energies of both species in the isolated states were calculated with taking account of the electron correlation, and it has been clarified that MDBS is more stable than TBS by about 90 kJ mol^{-1} when their geometrical structures are kept to be the same as those in the respective single crystals. Further,

INTERFACE SCIENCE — Molecular Aggregates —

Scope of research

The research at this subdivision is devoted to correlation studies on structures and properties of both natural and artificial molecular aggregates from two main standpoints: photoelectric and dielectric properties. The electronic structure of organic thin films is studied using photoemission and inverse photoemission spectroscopies in connection with the former, and its results are applied to create novel molecular systems with characteristic electronic functions. The latter is concerned with heterogeneous structures in microcapsules, biopolymers, biological membranes and biological cells, and the nonlinearity in their dielectric properties is also studied in relation to molecular motions.



Professor
SATO, Naoki
(D Sc)



Associate Professor
ASAMI, Koji
(D Sc)



Instructor
KITA, Yasuo
(D Sc)



Instructor
YOSHIDA, Hiroyuki
(D Sc)

Students

SAKUMA, Taro (DC)
SHIMADA, Kenji (MC)
TSUTSUMI, Kiyohiko (MC)
NAGAI, Yasuaki (MC)
TAKAHASHI, Ryo (MC)
YOKOI, Tomoko (MC)

lattice energies of both crystals have been re-evaluated using the intramolecular charge distributions obtained from those calculations to show that the heat of reaction is realized by the large difference of lattice energy overturning the difference of molecular total energy as a result [1].

The initiation reaction of the thermal isomerization reaction in the crystalline state can be expected to be a methyl cation transfer between two neighboring MDBS molecules. Such a structure that the methylsulfo group of a MDBS molecule looking on the nitrogen atom of the adjacent molecule is characteristic of the molecular structure of MDBS in the crystal, which is different from that resulted from the geometrical optimization calculation of an isolated molecule, and is suitable for the isomerization reaction. This notable conformation of the methylsulfo group is explained by the molecular structure stabilized by the molecular packing in the crystal [2].

Further, the geometrical optimization calculations of the reaction transition state derived from a pair of two MDBS molecules placed in the free space have been carried out using the RHF/6-31G* method to consider the initiation stage of the reaction, since any *ab initio* MO methods to calculate the transition-state structure with taking account of crystal field effects and the arrangement of a pair of molecules in the crystal as the initial structure that are expected from the sound scientific point of view

have not yet been established so far. A concerted form of the transition state with a coordination number of five for the carbon atom of the transferring methyl cation was obtained as the optimized structure from those calculations. Normal vibration analysis for this structure shows only one vibrational mode with an imaginary wavenumber at $562.90i \text{ cm}^{-1}$ that corresponds to intermolecular transfer of the methyl cation being detached from an O atom of the methylsulfo group in one MDBS molecule and connected with the N atom of the dimethylamino group in the other molecule. By examining the results of intrinsic reaction coordinate calculations around the transition-state structure in comparison with the geometrical arrangements of the atoms in the MDBS crystal to be involved in the reaction, it is implied that the cooperative rotation of molecules around their long axes coupled with the molecular structural deformation can bring about a notable structure characteristic for the transition state of the initiation reaction [2].

References

1. Oda M and Sato N, *Chem. Phys. Lett.*, **275**, 40-45 (1997).
2. Oda M and Sato N, *J. Phys. Chem. B*, **102**, 3283-3286 (1998).

Structure-Function Relationships in Alamethicin Ion-Channels: Effects of a Gln7 to Glu7 Mutation

Koji Asami, Yasuaki Nagai and Yasuo Nagaoka

Effects of a Gln7 to Glu7 mutation in alamethicin on its ion-channel properties have been studied by the single-channel recording with planar bilayer lipid membranes. The mutation affected the channel conductance, current-voltage relationship, and ion-selectivity.

Keywords : Ion-channel/ Alamethicin/ Ion transport/ Bilayer lipid membrane

Alamethicin, a 20-residue peptide isolated from *Trichoderma viride*, forms ion-channels in artificial bilayer lipid membranes. The ion-channels, in which alamethicin helices are packed together in a parallel fashion around a central ion permeable pore, are basically similar to the pore region of biological ion-channels and therefore provide a useful model system for analyzing the ion transport mechanism of ion-channels. In the alamethicin ion-channels, the hydrophilic residue Gln7 faces the pore space and locates in the middle of the channels, being expected to play a key role in channel stability and ion transport. In this study, we have examined effects of a mutation of Gln7 to Glu7 with a negative charge on ion-channel formation and ion transport properties.

Native alamethicin (Gln7) showed ion-channels with six conductance levels, which may correspond to helix-

bundles of 4-9 peptides. The replacement of Gln7 with Glu7 had little effect on the channel stability but considerable effects on the ion transport properties as follows: (1) The frequency of occurrence of the levels 1 and 2 was extremely reduced. (2) The ion-channel conductance increased for all the levels. (3) The current-voltage relationships changed from a supralinear form to a linear one at low levels and from a linear form to a sublinear one at high levels. (4) The ion selectivity between K^+ and Cl^- changed from a non-selective type to a K^+ -selective one for all the levels. These findings suggest that the introduction of Glu7 with a negative charge induces (1) an increase in pore size by electrostatic repulsion between adjacent helices, (2) some reduction in the height of energy barrier for ion transport in the channels, and (3) high cation-selectivity.

Arsenic Speciation Including `Hidden` Arsenic in Natural Waters

Hiroshi Hasegawa, Masakazu Matsui, and Yoshiki Sohrin

Recent studies indicate the existence in natural waters of `hidden` arsenic which had previously been undetected by hydride generation technique. A speciation method for arsenic species has been developed in which hidden arsenic was classified into two fractions by their lability to the photochemical degradation procedure: the ultraviolet-labile fraction and the ultraviolet-resistant fraction. We discussed the hidden arsenic fraction as the key to explaining arsenic speciation in natural waters.

Keywords : Arsenic/Speciation/Organoarsenicals/Ultraviolet irradiation/Microwave digestion/Arsenic methylation/Natural water

Chemical speciation is the determination of the individual concentrations of the various forms of an element that together make up the total concentration of that element. So far as arsenic species in natural waters are concerned, the inorganic forms (arsenate [AsO(OH)₃; As(V)] and arsenite [As(OH)₃; As(III)] and the methylated forms (methylarsonic acid [CH₃AsO(OH)₂; MMAA(V)] and dimethylarsinic acid [(CH₃)₂AsO(OH); DMAA(V)]) have been reported to be the main species. The bulk of the total dissolved arsenic is inorganic species in seawater and in fresh water, whereas methylarsenicals are found to comprise significant amounts in the surface layers and above the sediment surface. Several observations showed that methylarsenicals in surface waters exhibit a seasonal cycle in which the maximum concentrations of methylarsenicals appear during the summer. Although

there is abundant evidence regarding methylarsenicals produced biologically in natural waters, apparent differences were observed in seasonal changes of phytoplankton densities and methylarsenicals.¹⁻²

On the other hand, other organoarsenicals make up the bulk of the arsenic stock in organisms. Arsenosugars are ubiquitous in algae and arsenobetaine is the predominant form in marine animals. Arsenosugars and arsenobetaine can not be detected with the conventional hydride generation analyses, which have been applied to natural water samples. These facts suggest the presence of additional organoarsenicals that had previously been undetected in natural waters by hydride generation atomic absorption spectrometry. We established the new speciation method for these 'hidden' arsenic species using ultraviolet irradiation and microwave digestion, and studied their applications to estimate the arsenic compo-

INTERFACE SCIENCE — Separation Chemistry —

Scope of research

Our research activities are concerned in the behavior of chemical substances in geochemistry and the biochemical reactions. Major subjects of the research are followings: (1) Biogeochemistry of trace elements in the hydrosphere. Analytical methods for trace elements are developed using the selective complex formation systems. The behavior of trace elements in hydrosphere is explored to realize the significance of them for ecosystem. (2) Design and synthesis of the selective complex formation systems. Ligands (host molecules) that have novel functions in separation of metal ions and guest molecules are designed and synthesized.



Prof
MATSUI,
Masakazu
(D Sc)



Assoc Prof
UMETANI,
Shigeo
(D Sc)



Instr
SASAKI,
Yoshihiro
(D Sc)



Instr
HASEGAWA,
Hiroshi
(D Sc)



Techn
SUZUKI,
Mitsuko
(D Sc)

Lect(pt):

SOHRIN, Yoshiki (D Sc)

Students:

YOSHIDA, Yumi (DC)
MITO, Saeko (DC)
AZUMA, Yohei (MC)
NAITO, Kanako (MC)
NORISUE, Kazuhiro (MC)
KOHYAMA, Haruhiko (MC)
OOHASHI, Chikako (MC)
FUKUI, Yoshiharu (MC)

sition in natural waters.³

Hidden arsenic can be classified into different fractions by their lability to the photochemical degradation procedure: the ultraviolet-labile fraction and the ultraviolet-resistant fraction. We estimate the ultraviolet-labile fraction as the increment in measurable arsenic concentration before and after the ultraviolet irradiation, and the ultraviolet-resistant fraction as the difference in measurable arsenic after the ultraviolet irradiation and the microwave digestion. Figure 1 shows typical photoproduction of inorganic and methylarsenic species in ultraviolet-irradiated samples. Initially, both filtered and unfiltered samples contained only inorganic arsenic (9.3 nM and 11.5 nM, respectively), and methylarsenic concentration was below detection limits. Inorganic and dimethylarsenic concentrations rapidly increased immediately after irradiation, and attained equilibrium in 1-3 h. The lake waters as well as other Uranouchi waters also showed similar speciation changes to those described above, although they varied as to their increments in arsenic concentration. The total bulk concentration in natural waters was determined by microwave digestion with added potassium persulphate combined with CT-HG-AAS. Organoarsenicals are decomposed into As(V) by persulphate, and microwave irradiation speeds the oxidative decomposition by its rapid heating ability.

Figure 2 shows the measured arsenic fractions in Uranouchi Inlet and Lake Biwa. UV-InorgAs, UV-MMA, and UV-DMA are the corresponding inorganic, monomethyl, and dimethylarsenic concentration in the ultraviolet-labile fraction. The observed results strongly suggest that hidden arsenic exists in both seawater and in fresh water. Uranouchi Inlet clearly showed higher concentrations of hidden arsenic than Lake Biwa, in spite of the similar composition of the inorganic and methylarsenic fractions. This pattern was consistent with the higher dissolved organic carbon (DOC) of

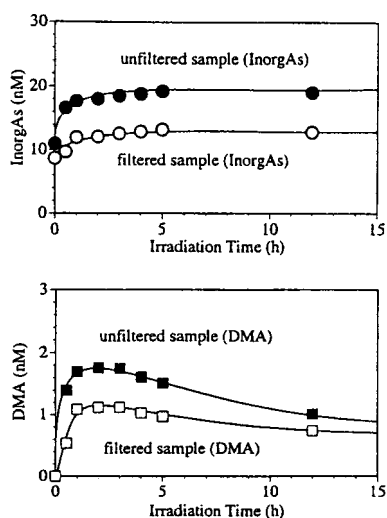


Figure 1. Effect of irradiation time with a 400 W high-pressure mercury lamp on arsenic speciation. Samples were collected from surface waters (depth; 0 m) of Uranouchi Inlet, on April 30, 1997. Monomethylarsenic was below the detection limit by CT-HG-AAS.

Uranouchi Inlet relative to Lake Biwa. The values of DOC were 2-4 mgC/l and <0.3 mgC/l in Uranouchi Inlet and Lake Biwa, respectively. Between filtered and unfiltered samples, the difference of hidden arsenic was significant compared with that of inorganic and methylarsenicals. It is likely that the hidden arsenic in the >0.45 μm size fraction was derived from the organoarsenicals in biological organic detritus.

The highest concentration of the ultraviolet-resistant fraction was observed on June 23 in Uranouchi Inlet with the highest dimethylarsenic concentration and a lower concentration of the ultraviolet-labile fraction. It appears that the increased dimethylarsenic concentration was due to photodegradation of hidden arsenic by strong sunlight in early summer. However, when exposed to the filtered light above a wavelength of 280 nm from a mercury lamp, both unfiltered samples of seawater and fresh water showed no significant change in the arsenic speciation. It is evident that photoproduction of UV-InorgAs, UV-MMA, and UV-DMA occurred in response only to the ultraviolet region of 250-280 nm when a high-pressure mercury lamp was used as an illuminator. These results indicate that photochemical degradation by sunlight rarely contributes to the production of methylarsenic compounds in natural waters.

References

1. Hasegawa H *Appl. Organomet. Chem.* **10**, 733-740 (1996).
2. Sohrin Y, Matsui M, Kawashima M, Hojo M, Hasegawa H *Environ. Sci. Technol.* **31**, 2712 (1997).
3. Hasegawa H, Matsui M, Okamura S, Hojo M, Iwasaki N and Sohrin Y *Appl. Organomet. Chem.*, in printing.

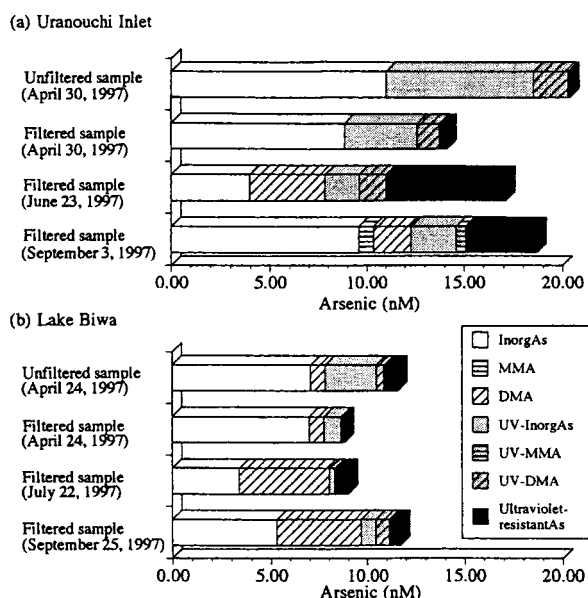


Figure 2. Bar diagram showing the mean concentration and distribution of arsenic in natural waters. Samples were collected from surface waters (depth; 0 m) of (a) Uranouchi Inlet on April 30, 1997, and (b) the southern basin of Lake Biwa on

Magnetization reversal in submicron magnetic wire studied by using giant magnetoresistance effect

Teruo Ono, Hideki Miyajima, Kunji Shigeto and Teruya Shinjo

The magnetization reversal phenomenon in a submicron magnetic wire with a trilayer structure consisting of NiFe(20nm)/Cu(10nm)/NiFe(5nm) was investigated by measuring the electric resistance in an external magnetic field. A giant magnetoresistance (GMR) effect of about 0.8 % was observed when the magnetizations in two NiFe layers are oriented antiparallel. It is demonstrated that magnetization reversal phenomena can be very sensitively investigated by utilizing the GMR effect.

Keywords: magnetization reversal/ submicron magnetic wire/ magnetic domain wall/ giant magnetoresistance

In very narrow ferromagnetic wires, due to the magnetic shape anisotropy, the magnetization is restricted to be directed either parallel or antiparallel to the wire axis. Normally, it is considered that magnetization reversal takes place by nucleation and propagation of a magnetic domain wall which lies in a plane perpendicular to the wire axis. The process of magnetization reversal attracts interests especially at low temperatures where a quantum tunneling process may be dominant. The magnetization measurement of magnetic wires, however, is difficult in general because the volume is very small.

We present magnetoresistance measurements of a single submicron magnetic wire based on a non-coupled

type GMR effect. The GMR is the electrical resistance change caused by the change of the magnetic structure in multilayers. This means, in turn, the magnetic structure of the system can be detected by resistivity measurements. Especially in the wire case, where the direction of the magnetization is restricted to be parallel or antiparallel along the wire axis, the GMR change is directly proportional to the magnitude of the switching layer magnetization. Here, we applied this method to a single NiFe(20nm)/Cu(10nm)/NiFe(5nm) trilayer wire. In magnetoresistance measurements the magnetic field was applied along the axis of the wires. The resistivity was determined using a four-point DC technique. As seen in

SOLID STATE CHEMISTRY — Artificial Lattice Alloys —

Scope of research

By using vacuum deposition method, artificial multilayers have been prepared by combining various metallic elements. The recent major subject is an interplay of magnetism and electric transport phenomena such as the giant magnetoresistance effect. Fundamental magnetic properties of metallic multilayers have been studied by various techniques including Mössbauer spectroscopy using Fe-57, Sn-119, Eu-151 and Au-197 as microprobes, and neutron diffraction. Preparation of microstructured films is attempted and novel magnetic and transport properties are investigated.



Prof
SHINJO, Teruya
(D Sc)



Assoc Prof
HOSOITO, Nobuyoshi
(D Sc)



Instr
MIBU, Ko
(D Sc)



Techni
KUSUDA, Toshiyuki

Guest Research Associate:

HASSDORF, Ralf (D Sc)
MATSUKAWA, Nozomu

Students:

NAGAHAMA, Taro (DC)
HAMADA, Sunao (DC)
SHIGETO, Kunji (DC)
ALMOKHTAR, A. M. M. (DC)
TANAKA, Satsuki (MC)
FUJIMOTO, Tatsuya (MC)

Figure 1, the samples have four current-voltage terminals, where the voltage is probed over a distance of 20 μm . Furthermore, the samples have an artificial neck (0.35 μm width) introduced at 1/3 distance from one voltage probe in order to control the magnetic domain wall propagation.

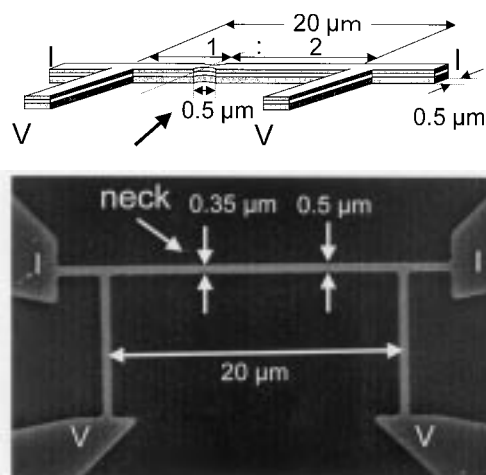


Figure 1. Schematic illustration and SEM image of the sample.

Figure 2 shows the resistance of our trilayer system as a function of the applied external field at 300 K. Prior to the measurement, a magnetic field of 100 Oe was applied in order to achieve magnetization alignment in one direction. Then the resistance was measured in steps of 1 Oe as the field was swept towards the counter direction. The result of our magnetoresistance measurement essentially displays four very sharp leaps. The first and second leap correspond to the magnetization reversal of the thin NiFe layer whereas the third and fourth leap correspond to the magnetization reversal of the thick NiFe layer. There is clear evidence resulting from a preliminary study on NiFe wire arrays deposited onto V-groove substrates that for the thickness range to be considered, the thicker NiFe layer has a larger coercive force than the thinner one. Here we discuss how the magnetization reversal takes place in the sample. As long as the counterfield is smaller than a critical field, the magnetizations of both thin and thick NiFe layers align parallel and the resistance shows the lowest value. As the applied magnetic field exceeds 5 Oe, the resistance abruptly jumps and is kept constant up to 10 Oe. Then, exceeding 10 Oe, the resistance abruptly jumps again and maintains the largest value up to 22 Oe. The result indicates that the antiparallel magnetization alignment is realized at an external field between 11 and 22 Oe, where the resistance shows the largest

value. The ratio of the resistance changes at the first and second leap is 1:2. This means that one third of the total magnetization of the thin NiFe layer changes its direction at the first leap in Fig. 2, since the GMR change is directly proportional to the switching layer magnetization. The ratio of one third corresponds to the ratio of length between the left voltage probe and the neck to the overall length of the wire between the voltage probes. Therefore, in this case, a magnetic domain wall nucleates in the shorter part of the wire and propagates to the neck, where it is pinned up to 10 Oe. The second leap when exceeding 10 Oe corresponds either to depinning of the magnetic domain wall from the neck or to nucleation and propagation of another magnetic domain wall on the other side of the neck. These two possibilities cannot be distinguished from the result shown in Fig. 2. The magnetization reversal of the thick NiFe layer takes place in the same manner as in the thin NiFe layer described above.

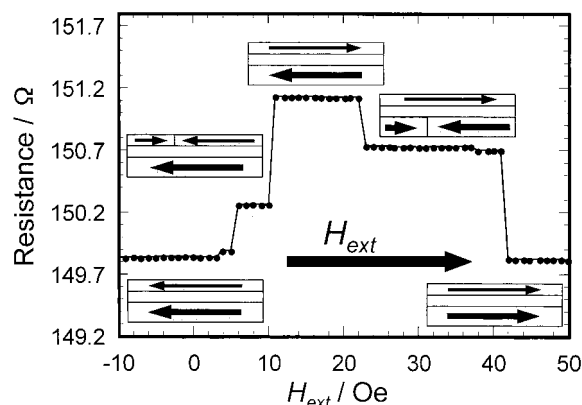


Figure 2. Resistance as a function of the external field at 300 K.

So far, we reported on magnetoresistance measurements of submicron magnetic wire based on GMR effect and found that magnetic domain wall propagation is controlled by the neck artificially introduced into the wire. It should be noted that the method reported here corresponds to a very high sensitive magnetization measurement. For the sample reported above, the sensitivity is as high as 10^{-13} emu (10^7 spins). The method, in principle, can be applied to smaller samples as far as the resistance of the samples can be measured and the relative sensitivity increases with decreasing sample volume.

REFERENCES

- Ono T, Miyajima H, Shigeto K and Shinjo T, *Appl. Phys. Lett.* **72**, 1116-1117 (1998).

Synthesis, Thermal Stability, Structural Features and Electromagnetic Properties of $\text{Bi}_{2+x}\text{Sr}_{2-x}\text{CuO}_{6+\delta}$ ($0 \leq x \leq 0.4$)

T. Niinae and Y. Ikeda

The thermal stability and structural modulation were studied systematically in a wide range of $0 \leq x \leq 0.4$ for the 2201 phase in the Bi-Sr-Cu-O system, $\text{Bi}_{2+x}\text{Sr}_{2-x}\text{CuO}_{6+\delta}$, and it was found that these properties varied remarkably at $x \approx 0.1$. Compositions $0 \leq x < 0.1$ remained stable only in a narrow low T -high P_{O_2} region and their modulation period changed stepwisely, not continuously, and reversibly between 4.9b (oxidized) and 5.5b (reduced) when the oxygen content was changed only by 0.65%. In relation to this we propose for $0 \leq x < 0.1$ specifically that the change in oxygen content induces the exchange of small amounts of Bi and Sr ions between the "BiO" and "SrO" sheets. The superconductivity of the cation-stoichiometric composition ($x = 0$) was also studied as a function of oxygen content.

Keywords: Phase diagram / $\text{Bi}_{2+x}\text{Sr}_{2-x}\text{CuO}_{6+\delta}$ / Substitution / Modulation / Superconductivity

The "2201" phase in the Bi_2O_3 -SrO-CuO system is known to adapt itself to various Bi:Sr:Cu ratios. Our previous phase diagrammatic study done at 840°C in the air [1] showed that the monophasic range was $0.1 < x < 0.6$ and $0 < y < x/2$ for $\text{Bi}_{2+x}\text{Sr}_{2-x}\text{Cu}_{1+y}\text{O}_z$ and that for $0 \leq x \leq 0.1$ three kinds of phases including the Bi-poorest end of the above mentioned solid solution, $\text{Bi}_{17}\text{Sr}_{16}\text{Cu}_7\text{O}_z$, and $\text{Sr}_{14}\text{Cu}_{24}\text{O}_{41}$ coexisted. More recently it has been reported that the solubility range is extended toward $x = 0$ at high oxygen pressures. Kato et al. successfully obtained a cation-stoichiometric sample with $x = 0$ at 840°C and $P_{\text{O}_2} = 30$ atm, which was an over-doped metal that became a superconductor when annealed in N_2 [2].

In this report we will shed a new light on the relation among Bi content, oxygen content, thermal stability, and structural features of the 2201 phase by comparing behaviors of monophasic samples with $0 \leq x \leq 0.4$ systematically which were all prepared under conventional conditions like $P_{\text{O}_2} = 1$ atm and 800°C.

All the samples were prepared by an ordinary ceramic

method from Bi_2O_3 , SrCO_3 , and CuO, each with a purity of 99.9%. Appropriate mixtures of these starting materials were pressed into pellets and heated at 600°C-840°C for 20h-120h in total with intermittent grinding, mixing and pelletizing processes. Three different atmospheres including an oxygen stream of 1 atm, the air, and an Ar stream of 1 atm were used. Certain samples were post-annealed in the Ar atmosphere at different temperatures between 200-700°C for 12-240h depending upon the temperature.

Cation-stoichiometric $\text{Bi}_2\text{Sr}_2\text{CuO}_{6+\delta}$ was successfully obtained by firing the starting mixture in flowing O_2 first at 720°C and finally at 800°C. The tetragonal cell parameters of $a = 5.361$ Å, $c = 24.65$ Å calculated from the X-ray diffraction peaks were almost identical to those ($a = 5.37$ Å, $c = 24.65$ Å) of Kato et al.'s sample with $\delta = 0.2$ which was synthesized under $P_{\text{O}_2} = 30$ atm and post-annealed in flowing N_2 . We note here that small amounts of $\text{Bi}_{17}\text{Sr}_{16}\text{Cu}_7\text{O}_z$ and others were detected after a further treatment at 820°C, showing the stability of $\text{Bi}_2\text{Sr}_2\text{CuO}_{6+\delta}$

SOLID STATE CHEMISTRY — Quantum Spin Fluids—

Scope of research

Quantum oxide systems such as high- T_c superconducting cuprates, $\text{La}_{2-x}\text{Sr}_x\text{CuO}_4$ and a spin-ladder, $(\text{Sr,Ca})_{14}\text{Cu}_{24}\text{O}_{41}$ are synthesized in the form of single crystals using traveling-solvent-floating-zone and laser abrasion techniques. Detailed equilibrium phase diagram of Bi cuprate systems is investigated. Main subjects and techniques are: mechanism of high- T_c superconductivity: origin of quantum phase separation in strongly correlated electron systems: spin excitations in quantum spin systems: interplay between spin and charge flow in doped spin systems: neutrons scattering by using triple-axis as well as time-of-flight techniques.



Prof
YAMADA, Kazuyohi
(DSc)



Assoc Prof
TERASHIMA, Takahito
(D Sc)



Instr
IKEDA, Yasunori



Techn
FUJITA, Masaki
(D Sc)

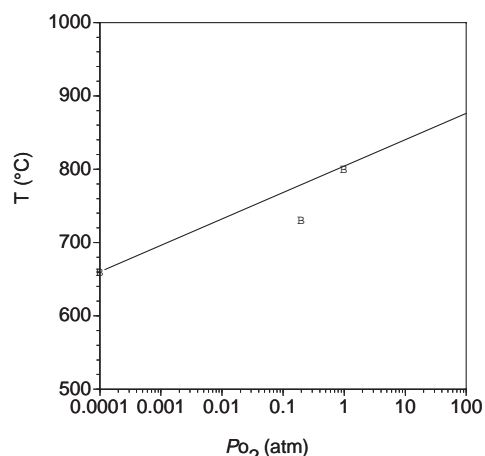


Figure 1. Temperature-oxygen pressure diagram with a border line below which the cation-stoichiometric composition remains stable. The closed squares are the present data and the open square is from ref. 2.

being limited to $T \leq 800^\circ\text{C}$ at $P_{\text{O}_2} = 1$ atm.

We tested the synthesis at a lower oxygen pressure as follows. Shown in Fig. 1 is a P_{O_2} - T diagram with a border line below which the cation-stoichiometric composition remains stable.

Monophasic samples with higher Bi contents of $0 < x \leq 0.4$ were also prepared at both $(T/^\circ\text{C}, P_{\text{O}_2}/\text{atm}) = (800, 1)$ and $(730, 0.2)$. The composition dependences of the lattice parameters, a and c , are plotted in Fig. 3. As Bi content increases from $x = 0$ to 0.4, the c parameter decreased by 0.8%, while a increased by 0.6%. In further detail, the c parameter showed a small jump at $x \approx 0.1$ and, at the same time, the slope, da/dx , became sharper for $0.1 \leq x$. This anomaly concerning the lattice parameters is one of the several features that separate the composition range of $0 \leq x \leq 0.4$ into two with a border line at $x \approx 0.1$.

In parallel to this, the thermal stability examined at $P_{\text{O}_2} = 0.2$ atm and 1 atm also showed a gap at $x \approx 0.1$. Saying typically, the decomposition temperature was as high as $\approx 880^\circ\text{C}$ for $x = 0.125$ in the air but it dropped to $\approx 780^\circ\text{C}$ for $x = 0.10$ in the same atmosphere.

It is well-known that the 2201 structure is incommensurately modulated with its wave vector, q , lying in the b^*-c^* plane. We found the same type of modulation in all the present samples by means of XRD and TEM. The coefficients b_m and c_m of the vector $q = b_m b^* + c_m c^*$ showed an interesting stepwise composition dependence again at $x \approx 0.1$. These coefficients were evaluated from the XRD data using the following equation

$$1/d_{hklm}^2 = h^2/a^2 + (k+mb_m)^2/b^2 + (l+mc_m)^2/c^2, \quad (1)$$

where d_{hklm} stands for the d value of a superlattice peak $(hkl, \pm m)$. We obtained a set of parameters $(a=b/\text{\AA}, c/\text{\AA}, b_m, c_m) = (5.361, 24.65, 0.205, 0.455)$ from the XRD pattern for the $x = 0$ sample prepared at 800°C and $P_{\text{O}_2} = 1$ atm.

Through a cyclic treatment of the former sample at 730°C in the air and at 800°C in flowing O_2 we noticed that the change was quite reversible. We further noticed that b_m and c_m were changed stepwisely, not continuously, from $(b_m, c_m) = (0.205, 0.455)$ to $(0.185, 0.288)$ by reducing treatments as can be seen most typically for the sample annealed at 400°C in Ar (see Fig.3). These two types are mixed in samples annealed under intermediate conditions

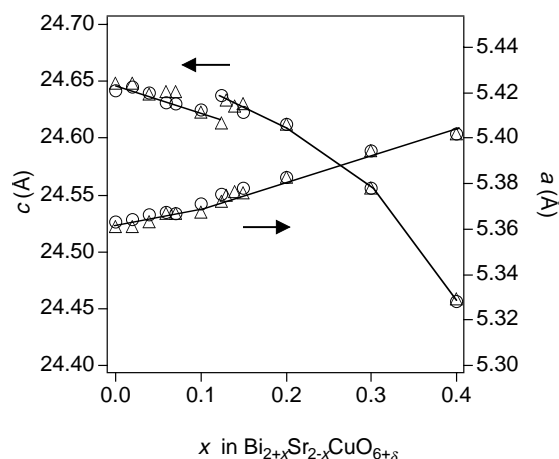


Figure 2. Composition dependence of the subcell lattice parameters. The triangles are for the samples prepared at 800°C in O_2 , and the circles are for those prepared at 730°C in the air.

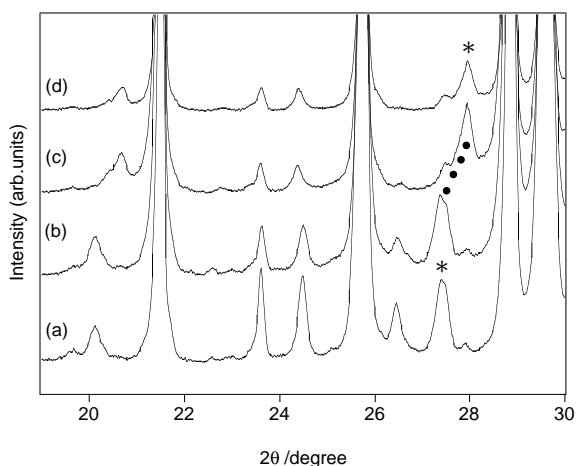


Figure 3. Partial enlargements of the XRD patterns of $\text{Bi}_2\text{Sr}_2\text{CuO}_{6+\delta}$ as-prepared in O_2 at 800°C (a), post-annealed in Ar at 200°C (b), 400°C (c), and 600°C (d).

like 730°C in the air. There seems no doubt that a slight change in oxygen content switches the modulation mode from one to the other, without changing the a and c parameters remarkably.

We conducted TEM observations on the two typical samples with $x = 0$, one as-prepared in O_2 and the other annealed in Ar at 600°C . The modulation wavelength varied from $\lambda = 4.9b$ for the as-prepared sample to $\lambda = 5.5b$ for the annealed one, which are consistent with the XRD results of $\lambda = 4.88b (= b/0.205)$ and $5.41b (= b/0.185)$, respectively.

From the resistance and magnetization measurements it has been revealed that it is only the portion with $(b_m, c_m) = (0.185, 0.288)$ that is superconducting but the portion with $(b_m, c_m) = (0.205, 0.455)$ is an over-doped metal.

References

1. Y. Ikeda, H. Ito, S. Shimomura, Y. Oue, K. Inaba, Z. Hiroi, M. Takano, *Physica C*, **159**, 93 (1989).
2. M. Kato, K. Yoshimura, K. Kosuge, *Physica C*, **177**, 52 (1991).

New $S = 1/2$ Alternating Chain Compound - High Pressure Form of $(VO)_2P_2O_7$ -

Masaki Azuma, Takashi Saito, Zenji Hiroi, and Mikio Takano

Crystal structure and magnetic properties of the high pressure phase of $(VO)_2P_2O_7$ were investigated, and it was found that this compound comprised $S = 1/2$ Heisenberg alternating antiferromagnetic chains. The magnetic susceptibility and the high-field magnetization data consistently showed the presence of a spin gap of about 25 K. Single crystals were grown by slowly cooling the stoichiometric melt in the high pressure cell.

Keywords: 1 dimensional magnet, Spin gap, High pressure synthesis

The unexpected discovery of high- T_c superconductivity in cupric oxides has strongly stimulated the research of the quantum mechanical interplay of the electronic spin, charge, and orbital degrees of freedom in $3d$ transition metal (M) oxides. The interplay is composition- and structure-sensitive, and hence it is meaningful to try to increase the variety of the M -O lattice and also the variety of the counter-cations and counter-anions that would finely tune the electronic state of the M -O lattice even by using unconventional synthesizing techniques. In this respect we have reported the high-pressure (HP) synthesis of a pair of spin-ladder cupric oxides, $SrCu_2O_3$ (two-legged) and $Sr_2Cu_3O_5$ (three-legged), the HP synthesis of oxides containing Fe^{4+} and Ru^{4+} exhibiting interesting

metal-insulator transitions, and others. Described below is a recent study of a new one-dimensional (1D) system in which the spin degree of freedom is killed quantum mechanically.

No doubt it is interesting to study how to control the electronic degrees of freedom. For example, if the ground state of a condensed system is the spin singlet state, where the spin degree of freedom is killed, there opens a way to create the freedom by mixing the excited magnetic state using an external field. In this sense there has been a growing interest in antiferromagnetic (AF) systems having a spin gap. Spin gap is the energy gap between the singlet ground state and the lowest magnetic excited state. Such a gap has been found mainly in one dimensional (1D) systems like spin-1/2 alternating

SOLID STATE CHEMISTRY — Multicomponent Materials —

Scope of research

Novel inorganic materials that have new, useful or exotic features such as superconductivity, ferromagnetism and quantum spin ground state are synthesized by novel methods. Recent topics are:

- High- T_c superconducting copper oxides with higher T_c or J_c
- Perovskite-based compounds with unusual magnetic and electronic properties.
- Low-dimensional spin system showing dramatic quantum effects.



Prof
TAKANO, Mikio
(D Sc)



Assoc Prof
HIROI, Zenji
(D Sc)



Instr
AZUMA, Masaki
(D Sc)

Students:

NIINAE, Toshinobu (DC)
KAWASAKI, Shuji (DC)
YAMADA, Takahiro (DC)
FURUBAYASHI, Yutaka (DC)
HAYASHI, Naoaki (DC)
OKUMURA, Makoto (MC)
SAITO, Takashi (MC)
TAMADA, Takayuki (MC)
TOGANO, Hiroki (MC)
ISHIWATA, Shintaro (MC)
ODAKA, Tomoori (MC)
TERASHIMA, Takashi (MC)

Research Fellow:

CHONG, Iksu

chains, spin-1 chains (called the Haldane system) and spin-1/2 ladders like SrCu_2O_3 discovered by us.

$(\text{VO})_2\text{P}_2\text{O}_7$ has long been known as an active catalyst for the selective oxidation of butane to maleic anhydride. The V^{4+} ions in this compound possess spin-1/2. A neutron scattering experiment [1] revealed that this compound was best described as a spin-1/2 alternating chain system in which the magnitude of AF interaction changes alternately as $-\text{V}^{4+}-(J_1)-\text{V}^{4+}-(J_2)-\text{V}^{4+}-(J_1)-\text{V}^{4+}-(J_2)-\text{V}^{4+}$. However, unfortunately, the structure is too complex to study the interesting magnetism in detail [2].

We recently found that this compound undergoes a pressure-induced transition to a similar but much simpler structure [3]. And the measurements of magnetic susceptibility, high-field magnetization, and specific heat have indicated consistently and unambiguously that the HP phase is a good example of the spin-1/2 Heisenberg alternating AF chain system having a spin gap.

The HP phase was obtained by treating the ambient pressure (AP) phase at 2 GPa and 700 °C for 30 min. using a cubic-anvil type HP apparatus. The structure determined by means of X-ray diffraction and neutron diffraction is illustrated in Fig. 1. As known through the neutron scattering study on the AP phase [1], the strongest AF interaction (J_1) is mediated by the PO_4 tetrahedra, while the second strongest one (J_2) works between a pair of edge-sharing VO_5 pyramids. These interactions alternate along the c axis as can be seen in Fig. 1b.

Figure 2a shows the temperature dependence of magnetic susceptibility. After subtracting a paramagnetic contribution due to an impurity V^{4+} of 2.6 %, the data showed an exponential decay toward zero as expected for a spin gap system. The data could be well fitted to the alternating chain model with parameters $J_1 = 136$ K, $J_2/J_1 = 0.9$, and $g = 1.98$, from which the spin gap was estimated to be about 25 K.

Figure 2b shows the magnetization measured at 0.4 K using a pulsed magnetic field. The Brillouin-function like behavior below 15 T is due to the impurity ions. Above 20 T, the data increases steeply indicating that the singlet ground state and the triplet excited state cross each other. Assuming that the gap between these states changes as $\Delta(H) = \Delta(0) - g\mu_B H$, $\Delta(0) = 26$ K has been obtained, which is in good agreement with the susceptibility data mentioned above.

Single crystals were obtained by slowly cooling the molten liquid from 1200 to 600 °C in 40 h at 3GPa. More detailed studies on these powder and single crystal samples by means of NMR, μSR , ESR, Raman scattering, and neutron scattering are in progress.

This work is one of a variety of researches being carried out using the HP technique and also a film technique

in the present laboratory for the purpose of discovering new fundamental and practical properties of 3d transition metal oxides.

References

- [1] T. Barnes, and J. Riera, Phys. Rev. B 50, 6817 (1994).
- [2] Z. Hiroi, M. Azuma, Y. Fujishiro, T. Sairo, M. Takano, F. Izumi, T. Kamiyama and T. Ikeda, submitted to J. Solid State Chem.
- [3] M. Azuma, T. Saito, Y. Fujishiro, Z. Hiroi, M. Takano, F. Izumi, T. Kamiyama T. Ikeda, H. Kageyama and T. Goto, to be submitted to Phys. Rev. B

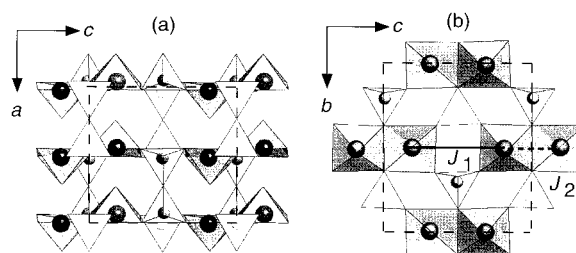


Figure 1. High-pressure phase of $(\text{VO})_2\text{P}_2\text{O}_7$ viewed along the b -axis (a) and the a -axis (b). Large and small spheres represent V and P ions, respectively. The alternation of the AF interaction along the c axis can be seen in (b).

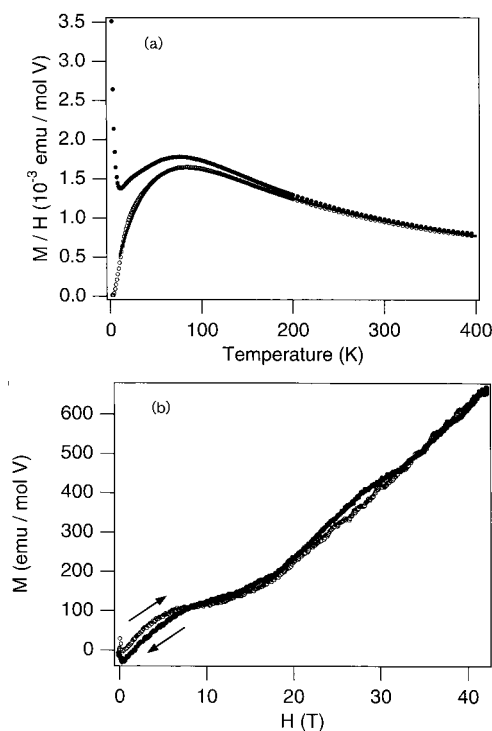


Figure 2. Temperature dependence of magnetic susceptibility (a). The data before and after the subtraction of the impurity contribution are shown with closed and open circles, respectively. The solid line is a fit to the alternation chain model. The field dependence of magnetization at 0.4 K (b).

Photochemical Reactions of Ge-Related Centers in Germanosilicate Glass Prepared by Sol-Gel Process

Masahide Takahashi, Jisun Jin, Takashi Uchino and Toshinobu Yoko

Germanosilicate glasses are prepared by a sol-gel method and the UV-photosensitivity of glasses is investigated by optical absorption, ESR, and photoluminescence measurements. Large changes in optical absorption are observed for the sol-gel-derived glass by the ultraviolet laser irradiation; a decrease in 5-eV band and increases in absorption around 4.5 and > 5.7 eV. Photoluminescence intensity under 248-nm excitation decreases with an increase in laser fluence and also with decrease in the 5-eV band. This result strongly implies the novel photochemical reaction from Ge²⁺ to Ge E' induced by excimer laser irradiation.

Keywords : Germanosilicate glasses / Defect / Photosensitivity / Sol-gel method / Fiber grating

Photosensitivity of GeO₂-SiO₂ glasses has been caught much attention because the Bragg grating can be easily printed in the fiber core, which is usually made of germanosilicate glasses, by ultraviolet (UV) laser irradiation [1]. It has been considered that the index change by UV laser irradiation is closely related to the photochemical processes of Ge-related defects in the germanosilicate glasses [2]. Previous studies indicated that the Ge-related defects have higher photosensitivity and the formation of Ge E' center is the key for the photorefractive effect in the glasses. In order to investigate the mechanism of UV induced refractive index change, the compositional and/or structural effect on the photochemical processes should be systematically clarified. The aim of this study is to elucidate photochemical processes induced by UV-irradiation in the germanosilicate glass.

The defect states of glasses before and after the UV

irradiation (KrF- and ArF-excimer lasers and Hg lamp) are analyzed by means of the optical absorption, photoluminescence (PL) and electron spin resonance (ESR) spectroscopy. Germanosilicate glass of 10GeO₂-90SiO₂ composition in molar ratio is prepared from tetraethoxysilane and tetraethoxygermanium through the sol-gel procedure.

Figure 1 shows the changes in optical absorption by the KrF irradiation. Change in optical absorption in the range of 3.8 to 6.4 eV is observed. The change in optical absorption of the glass seems to be almost comparable to that of the VAD fiber preform. ESR spectra after excimer laser irradiation indicate the existence of germanium electron-trapped centers (GEC) and Ge E' center. Fig. 2 (e) shows the ESR spectrum of unirradiated VAD-glass, which is corresponding to Ge E' center [3]. Spectral profile of low fluence (Fig. 2 (a)) indicates the formation of

SOLID STATE CHEMISTRY -Amorphous Materials-

Scope of Research

Inorganic amorphous materials with various functions are the targets of research in this laboratory. (1) To obtain a clear view of glass materials and the bases for designing functional glasses, we investigate the structure of glasses using X-ray and neutron diffraction analysis, high resolution MAS-NMR, and ab initio MO calculation. (2) To develop materials with high optical nonlinearity, we search heavy metal oxide-based glasses and transition metal oxide thin films, and evaluate the nonlinear optical properties by Z-scan methods. (3) Photosensitivity of glasses for optical fibers and waveguides is investigated to design efficient fiber gratings and optical nonlinear materials. (4) Using sol-gel method, synthesis and microstructure control are carried out on various functional oxide thin films.



Prof
YOKO,
Toshinobu
(D Eng)



Instr
UCHINO,
Takashi
(D Eng)



Instr
TAKAHASHI,
Masahide
(D Sc)



Assoc. Instr
JIN,
Jisun
(D Eng)

Guest Research Associates:

ZHAO, Gaoling (D Eng)

Students:

SAKIDA, Shinichi (DC)

TAKAISHI, Taigo (DC)

TOKUDA, Youmei (DC)

NIIDA, Haruki (MC)

TATSUMI, Masao (MC)

MIYAWAKI, Seikyo (MC)

KAJITA, Daisuke (MC)

HIROSE, Motoyuki (MC)

KUBO, Akiko (UG)

TSUKIGI, Kaori (UG)

TAKEUCHI, Toshihiro (UG)

DORJPALAM, Enkhtuvshin
(RS)

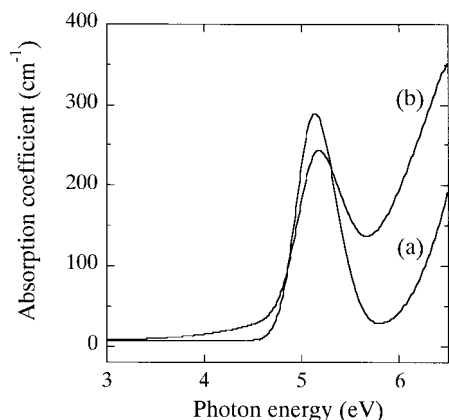


Figure 1. Absorption spectra before and after KrF laser irradiation (80mJ/cm² per pulse, 10⁴shot)

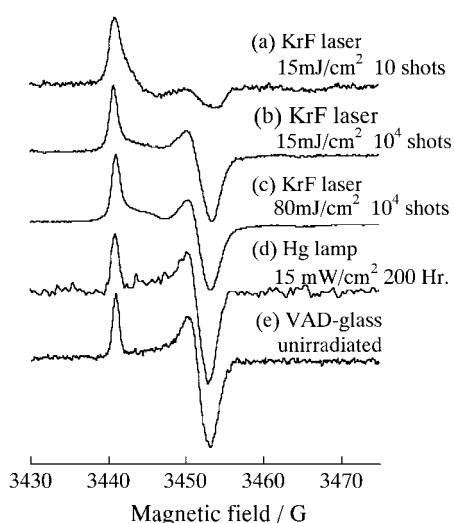


Figure 2. ESR signals of the glasses after UV irradiation and unirradiated fiber preform.

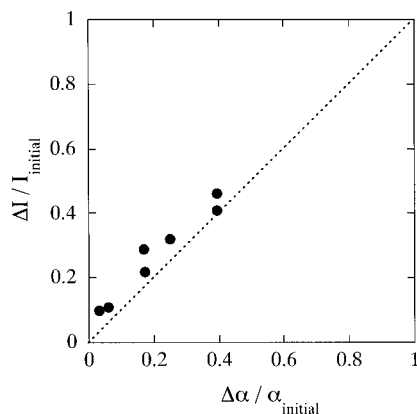


Figure 3. Correlation between decrease in PL intensity, $\Delta I/I_{\text{initial}}$, and bleaching of the 5-eV band, $\Delta\alpha/\alpha_{\text{initial}}$, by excimer laser irradiation.

GEC [4]. With increasing laser fluence, the profile approaches to that of Ge E' center (Fig.2 (a) to (c)). Irradiation of an Hg lamp induced only Ge E' center (Fig. 2 (d)).

Figure 3 shows a correlation between the bleaching of 5-eV band and the decrease in PL intensity by KrF laser

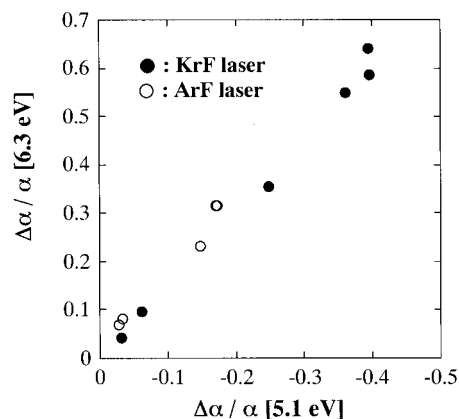
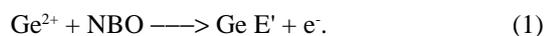


Figure 4. Changes in absorption coefficient of the 5-eV band and 6.3 eV band.

irradiation. Linear correlation indicates that bleaching of the 5-eV band is due mainly to a decrease in Ge²⁺ (NODV). This relationship is also exhibited by ArF-laser excitation. Therefore, we propose that the bleaching of the 5-eV band by irradiating excimer laser is due to the decrease of Ge²⁺.

The decrease of Ge²⁺ by excimer laser irradiation would be explained by photoionization of Ge²⁺ by multiphoton absorption. The lone pair electron of Ge²⁺ can be excited to the conduction band by successive two-photon absorption through long-lived T₁ state as an intermediate level. Furthermore, the ionized Ge²⁺ may form Ge-O bonding with nonbridging oxygen nearby. The final product of this process would be Ge E'. Fig. 4 shows a correlation between the decrease in the 5-eV band and the increase in 6.3 eV band corresponding to Ge E' center by irradiating KrF and ArF laser. The linear correlation indicates that Ge²⁺ is converted into Ge E' by excimer laser irradiation. In addition, changes in defect concentration of Ge²⁺ and Ge E' are almost equal. Therefore, we propose the following photochemical reaction by excimer laser excitation,



The conversion efficiency of Ge²⁺ to Ge E' is much larger for KrF laser excitation than for ArF laser at the same fluence. The photon energy of KrF laser agrees with the excitation energy of S₀ to S₁ transition in Ge²⁺. The excited S₁ state relaxes to long-lived T₁ state through intercombinational conversion. These facts follow the above reaction (1) because the 5-eV photons from KrF laser excite Ge²⁺ to long-lived T₁ state with higher efficiency than 6.3-eV photons from ArF laser.

References

- [1] G. Meltz, W. W. Morey and W. H. Gren, Opt. Lett. 14 (1989) 823.
- [2] T. E. Tsai, C. G. Atkins and E. J. Frieble, Appl. Phys. Lett. 61 (1992) 390.
- [3] R. A. Weeks and T. Purcell, J. Chem. Phys. 43 (1965) 483.
- [4] E. J. Frieble, D. L. Griscom and G. H. Sigel Jr., J. Appl. Phys. 45 (1974) 3424.

Rheo-Dielectric Behavior of Oligostyrene and Polyisoprene

Hiroshi Watanabe, Tadashi Inoue, and Kunihiro Osaki

Flow effects were examined for dielectric behavior of oligostyrene (OS; $M = 950$) and *cis*-polyisoprene (PI; $M = 8200$). OS-1 has monomeric dipoles perpendicular to its backbone and the terminal dielectric relaxation results from the segmental motion, while for PI-8 having parallel dipoles this relaxation reflects the global chain motion. The dielectric loss ϵ'' and viscosity η were measured for OS and PI at T well above respective T_g under steady shear flow at rates $\dot{\gamma} \ll 1/\tau_1$, with τ_1 being the linear viscoelastic terminal relaxation time. The ϵ'' and η of PI were independent of $\dot{\gamma}$, as usually expected under such slow flow. In contrast, OS exhibited acceleration of the dielectric relaxation and the shear-thinning of η at $\dot{\gamma} \ll 1/\tau_1$. This thinning was related to flow-induced changes in some sort of dynamic structure, probably a cooperative domain structure, and the dielectric change detected acceleration of the segmental motion due to this structural change.

Keywords : Rheo-dielectric behavior/ Global mode/ Segmental mode/ Shear-thinning/ Cooperative domain structure

Viscoelastic relaxation of flexible polymer chains has a considerably broad distribution of relaxation modes, and the fast and slow modes reflect the chain motion at small (segmental) and large (global) length scales, respectively. A recent rheo-optical study [1] revealed that the viscoelasticity-structure relationship is not identical for these fast and slow modes (the segmental and global modes). For the global mode, the mechanical stress is in proportion to an anisotropy of axial orientation of the chain backbone and the conventional stress-optical rule [2] is valid. In contrast, the segmental mode is related to an anisotropy of the planar orientation of the segments.

The segmental mode of polystyrene has been found to exhibit strong thinning under elongational flow at rates much smaller than the characteristic frequency of this

mode [3]. This result is of particular interest in a sense that the thinning behavior could provide us with detailed insight for a *dynamic structure* in glassy materials.

Dielectric techniques are useful in investigation of this structure. For polymer chains having electrical dipoles, the chain motion results in not only viscoelastic but also dielectric relaxation. Specifically, the segmental motion is observed as the dielectric dispersion (often referred to as the α dispersion) if the chains have the dipoles perpendicular to their contour, while the global motion is dielectrically detected if the chains have the parallel dipoles [4]. Taking advantage of these dielectric features, we have carried out rheo-dielectric measurements for model materials, oligostyrene (OS) of the molecular weight $M_w = 950$ ($M_w/M_n = 1.13$) and *cis*-

FUNDAMENTAL MATERIAL PROPERTIES — Molecular Rheology —

Scope of research

The molecular origin of various rheological properties of materials is studied. Depending on time and temperature, homogeneous polymeric materials exhibit typical features of glass, rubber, and viscous fluids while heterogeneous polymeric systems exhibit plasticity in addition to these features. For a basic understanding of the features, the molecular motion and structures of various scales are studied for polymeric systems in deformed state. Measurements are performed of rheological properties with various rheometers, of isochronal molecular orientation with flow birefringence, and of autocorrelation of the orientation with dynamic dielectric spectroscopy.



Prof
OSAKI, Kunihiro
(D Eng)



Assoc Prof
WATANABE, Hiroshi
(D Sc)



Instr
INOUE, Tadashi
(D Eng)



Techn
OKADA, Shinichi

Students:

SATO, Tomohiro (DC)
KAKIUCHI, Munetaka (DC)
ABE, Shuichi (MC)
KUWADA, Syozo (MC)
MATSUMIYA, Yumi (MC)
ISOMURA, Takenori (MC)
NISHIMURA, Masaki (MC)
UEMATSU, Takehiko (UG)

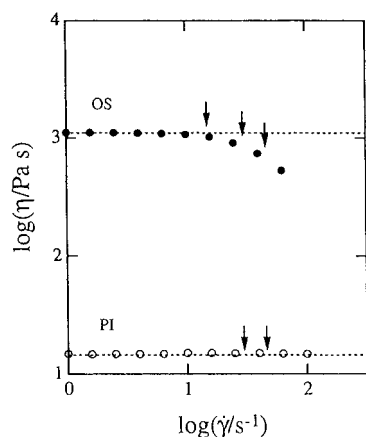


Fig.1 Steady state viscosity of OS at 42°C and PI at 23°C. The arrows indicate the shear rates for the rheo-dielectric data shown in Figure 2.

polyisoprene (PI) of $M_w = 8200$ ($M_w/M_n = 1.05$) [5]. The results are summarized here.

For the low-M OS molecules having the perpendicular dipoles, both of the terminal viscoelastic and dielectric relaxation processes reflect the segmental mode. In contrast, the PI chains have the parallel dipoles and their terminal processes are dominated by the global mode. The terminal relaxation time τ_1 at equilibrium was viscoelastically determined as [5]

$$\tau_1 = 1.3 \times 10^{-5} \text{ s for OS at } T_r = 42^\circ\text{C} \quad (1)$$

$$\tau_1 = 4.0 \times 10^{-5} \text{ s for PI at } T_r = 23^\circ\text{C} \quad (2)$$

The reference temperatures T_r are well above respective T_g ($\cong 7^\circ\text{C}$ for OS and $\cong -75^\circ\text{C}$ for PI).

For OS and PI at respective T_r , Figure 1 shows the steady state shear viscosity $\eta(\dot{\gamma})$ determined at shear rates $\dot{\gamma} \ll 1/\tau_1$. The dashed lines indicate plots of the magnitude of complex viscosity $|\eta^*(\omega)|$ against the angular frequency ω . The corresponding dielectric loss ϵ'' , measured in the quiescent state and under steady shear flow at $\dot{\gamma}$ indicated with the arrows in Figure 1, are shown in Figure 2.

For PI, completely Newtonian behavior is observed and the Cox-Merz rule is valid at $\dot{\gamma}$ examined (cf. Figure 1). This result indicates that the equilibrium global motion is not affected by the slow flow at $\dot{\gamma} \ll 1/\tau_1$. Correspondingly, the ϵ'' data detecting the global chain motion are insensitive to $\dot{\gamma}$ (cf. Figure 2).

For OS, Figure 2 demonstrates no detectable flow effect on the ϵ'' data at $\dot{\gamma} < 15 \text{ s}^{-1}$. However, with further increase of $\dot{\gamma}$ up to 46 s^{-1} , the terminal tail of the ϵ'' curve (where $\epsilon'' \propto \omega$) is shifted to higher ω side and the dielectrically detected segmental motion becomes faster, despite a fact that the flow at those $\dot{\gamma}$ is still much slower than the equilibrium segmental motion. As noted in Figure 1, the $\eta(\dot{\gamma})$ data of OS deviate from the $|\eta^*(\omega)|$ data

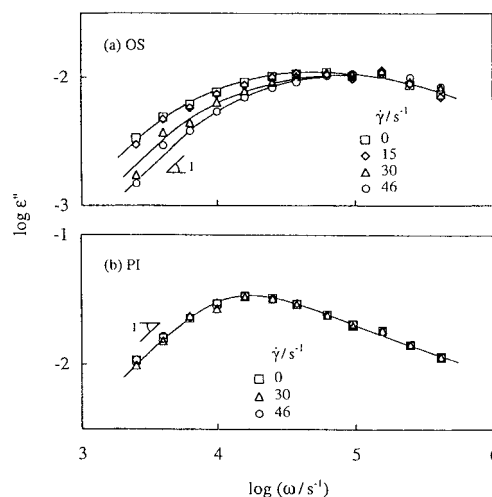


Fig.2 Dielectric loss ϵ'' of OS at 42°C and PI at 23°C determined under steady shear flow. For comparison, the data in the quiescent state are also shown.

and exhibit thinning at $\dot{\gamma} \geq 15 \text{ s}^{-1}$. This thinning for the segmental mode, noted also for polystyrene under very slow elongational flow [1], quite possibly results from the flow-induced acceleration of the segmental motion.

This result suggests that the OS system includes some sort of *dynamically heterogeneous* structure: Such a structure can be distorted under the slow flow, thereby affecting the segmental motion therein and inducing the thinning of η . This dynamic structure might be a cooperative domain structure [6] characteristic to glassy materials. At time scales of the segmental motion, the dynamic heterogeneity could have survived in the OS system even at $T_r > T_g$. We speculate that the flow may reduce the cooperative domain size thereby weakening the cooperativity in the segmental motion to accelerate this motion and induce the thinning of η . At this moment, no structural data proving/disproving this speculation are available. Further studies are desired for the structure under flow.

References

- [1] T. Inoue, H. Okamoto, K. Osaki, *Macromolecules*, **1991**, *24*, 5670.
- [2] H. Janeschitz-Kriegl, *Polymer Melt Rheology and Flow Birefringence*, Springer Verlag: Berlin, 1983.
- [3] T. Inoue, D. S. Ryu, K. Osaki, *Macromolecules*, **1998**, *31*, 6977.
- [4] W. H. Stockmayer, *Pure Appl. Chem.*, **1967**, *15*, 539.
- [5] Y. Matsumiya, H. Watanabe, T. Inoue, K. Osaki, M.-L. Yao, *Macromolecules*, **1998**, *31*, 7973.
- [6] T. Kanaya, A. Patkowski, E. W. Fischer, J. Seils, H. Gläser, K. Kaji, *Macromolecules*, **1995**, *28*, 7831.

A New Discovery of Microphase Separation Initiating In the Induction Period of Polymer Crystallization : characteristic wavelengths at high temperatures

Keisuke Kaji, Shuji Matsunaga, Go Matsuba, Toshiji Kanaya,
Koji Nishida and Masayuki Imai

On the basis of the previous new discovery that a spinodal decomposition type of microphase separation occurs during the induction period for glass crystallization when a polymer is crystallized at low temperatures just above the glass transition temperature, the effect of crystallization temperature on the characteristic wavelength has been studied using poly(ethylene terephthalate) (PET) because this is an important factor for spinodal structures determining the whole skeleton of higher-order structure of crystalline polymers. For melt crystallization when PET is crystallized directly from the melt at high temperatures below the melting point, the characteristic wavelength is obtained to be a few micrometers which is two orders of magnitude larger than that for the glass crystallization. This may provide a possible elucidation for the large difference in size and density of spherulites between the glass and melt crystallization.

Keywords : Melt Crystallization / PET / Microphase Separation / Characteristic Wavelength

In previous papers [1] we reported a new discovery that a spinodal decomposition type of microphase separation is initiated in a very early stage of the induction period for glass-cold crystallization, ie when poly(ethylene terephthalate) (PET) is crystallized from the glass just above the glass transition temperature. This phenomenon is induced by orientational fluctuations or partial parallel orientation of rigid polymer segments when the average persistence length of the polymer molecules becomes larger than a critical value [2]. Such a mechanism is schematically shown in Figure 1. This is because the increase of the lengths of rigid segments causes the increase of their excluded volumes, making the system unstable, and the parallel orientation reduces their volumes. In the late stage of the spinodal decomposition the characteristic wavelength Λ_c grows with time, and when it attains a critical value the crystal

nucleation is initiated in the orientationally ordered regions. In polymer crystallization the characteristic wavelength is a very important factor since it is only a parameter characterizing the spinodal structure and considered to determine the whole skeleton of higher-order structure of crystalline polymers, so that it is interesting to investigate the temperature dependence of Λ_c . The observation of such a spinodal decomposition would, however, be possible only when the crystallization temperature is near either the glass transition temperature or the melting temperature, corresponding to a low segment mobility or a small supercooling depth, respectively, because a considerably long induction period is necessary to perform time evolution measurements.

In the present study the change of the characteristic wavelength has been investigated for melt-hot crystallization, ie when PET is crystallized directly

FUNDAMENTAL MATERIAL PROPERTIES – Polymer Materials Science –

Scope of research

The structure and molecular motion of polymer substances are studied using mainly scattering methods such as neutron, X-ray and light with the intention of solving fundamentally important problems in polymer science. The main projects are: the mechanism of structural development in crystalline polymers from the glassy or molten state to spherulites; the dynamics in disordered polymer materials including low-energy excitation or excess heat capacity at low temperatures, glass transition and local segmental motions; formation process and structure of polymer gels; the structure and molecular motion of polyelectrolyte solutions; the structure of polymer liquid crystals.



Prof
KAJI, Keisuke
(D Eng)



Assoc Prof
KANAYA, Toshiji
(D Eng)



Instr
NISHIDA, Koji

Students

MATSUBA, Go (DC)
OGAMI, Akinobu (MC)
SHIBATA, Manabu (MC)
YAMAMOTO, Hiroyoshi (MC)
YAMASHITA, Ryoji (MC)
KITO, Takashi (UG)
SAITO, Mitsuru (UG)

Research Fellow

TSUKUSHI, Itaru
TAKESHITA, Hiroki
HOSIER, Ian

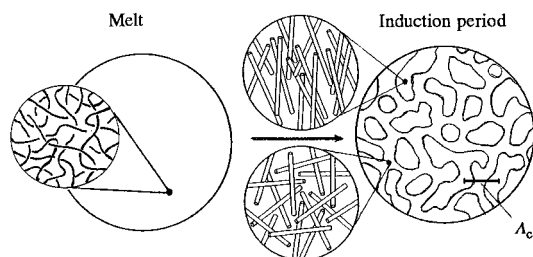


Figure 1. Microphase separation induced by orientational fluctuations of rigid polymer segments before crystallization.

from the melt at high temperatures below the melting point. A PET sample with $M_n=25,000$ and $M_w/M_n=2.5$ was melted at 290°C ($T_m=267^\circ\text{C}$) in the SAXS camera at the High-Intensity X-Ray Laboratory of Kyoto University, and SAXS measurements were carried out *in situ* when the sample was crystallized by jumping down to 244°C in this camera. The induction period was about 120min in this case. Figure 2 shows the time evolution of the difference intensity for this sample after subtraction of the scattering intensity from the melt sample at 290°C ; (a) and (b) correspond to the induction period and crystallization stage, respectively. As seen from Figure 2a, the intensity for $Q < 0.02 \text{ \AA}^{-1}$ increases with time in the induction period, but no peak corresponding to the characteristic wavelength is observed. It may be considered that for the hot crystallization the characteristic wavelength is too large to be observed within a resolution of the used SAXS camera and the intensity at low Q 's is due to the contribution from the

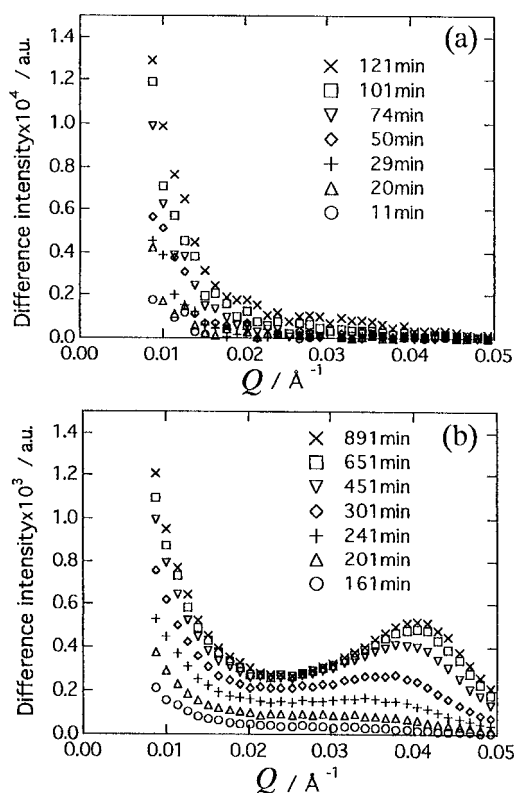


Figure 2. Difference SAXS intensity curves of PET measured *in situ* as a function of crystallization time. Crystallized at 244°C from the melt.

tail of the peak of such a characteristic wavelength. As is clear from Figure 2b, even after crystallization it continues to increase with time, suggesting that the phase separation continues to grow without being interrupted by crystallization, which was also confirmed from polarized light microscopic observations. Further, after crystallization a well-known broad peak of long period due to the alternation of crystalline and amorphous layers starts to appear and increases in intensity with time. Here it should be noted that the peak position slightly shifts toward the higher Q with time. This phenomenon, which was first discovered by Zachmann et al [3], is clearly reconfirmed here where the separation from the strong low Q scattering is large enough to neglect the effect of overlapping. Zachmann et al tentatively explained such a strange result of the decrease of long period with time using a model that nascent crystalline lamellae having rough wavy surfaces come to have more and more smooth surfaces with annealing time, resulting in the decrease of long period. A more possible alternative elucidation by us is based on the distribution of lamellar thickness; the microphase separation produces two different regions, more-ordered and less-ordered in orientation and the former region first provides thicker lamellae and the latter region later thinner ones because of its higher density of entanglements. These thinner lamellae produced later decrease the observed average long period, shifting the scattering peak toward the higher Q .

In order to estimate the order of magnitude of characteristic wavelengths for the hot crystallization confocal scanning laser microscopic (CSLM) and polarized optical microscopic (POM) observations have been carried out. The former observation for the crystallization at 220°C indicated a spinodal pattern with $\Lambda_c \approx 1 \mu\text{m}$ in the induction period [4]. If this value is true, the characteristic wavelengths for the hot crystallization would be two orders of magnitude larger than those for the cold crystallization. The POM observations showed a clear spinodal-like pattern after the beginning of crystallization; the dense and dilute domains of spherulites could clearly be distinguished and the interdomain spacings were estimated to be several tens μm at 240°C though they increased with crystallization time [5]. Such large difference in characteristic wavelength might give a possible explanation for a well-known great difference in number density of spherulites between both cases [6]; the two orders of magnitude in characteristic wavelength correspond to the six orders of magnitude in number density of spherulites.

References

1. Imai M, Kaji K and Kanaya T, *ICR Annual Report*, **1**, 26 (1994).
2. Doi M and Edwards S F, *The Theory of Polymer Dynamics*, Oxford (1986) Chapters 9 and 10.
3. Gehrke R, Riekel C and Zachmann H G, *Polymer*, **30**, 1528 (1989).
4. Imai M, Kaji K and Sakai Y, *Proceedings of the First Symposium, Polymer Crystallization & Phase Separation Research Committee*, Osaka, September 1996, page 7.
5. Matsunaga S, Matsuba G, Nishida K, Kanaya T, Kaji K and Imai M, *Polymer Preprints, Japan*, **45**, 823 (1996).
6. Van Krevelen D W, *Properties of Polymers*, Elsevier (1990) page 592.

Dynamics of Flexible High-Molecular-Weight Polymers in Dilute Solution under Circular Couette Flow

Yoshisuke Tsunashima

Chain dynamics of poly(α -methylstyrene) of high molecular weight in benzene, a good solvent, in dilute solution was investigated by dynamic light scattering under Couette flow. At the shear gradient above $2.8\text{--}4.5\text{s}^{-1}$, the internal modes of motions were exclusively suppressed and only the center-of-mass translational diffusion motion of the chain was detected. Whereas, in the intermediate shear region, the decay rate for the internal mode was constant, and that of the diffusion mode increased with increasing the shear rate. The obtained universal ratio Ω/D_0q^2 was located close to the theoretical curve predicted for the flexible chains with the *microscopic* description of chain dynamics in Θ state. This quantitative agreement between theory and experiments means that the coupled kinetic equations for chain segments and solvent in the same dynamic level is indispensable for describing rigorously chain dynamics in dilute solution.

Keywords: Dynamic light scattering/ Shear flow/ Diffusion/ Internal motions/ Dynamic coupling

In the quiescent, i.e., thermodynamically equilibrium state, dynamics of flexible linear polymers in dilute solution has not been understood fundamentally because the well-qualified experimental results disagreed quantitatively with the hydrodynamic descriptions of the polymer chain so far proposed theoretically. The reasons may be assigned to the following assumptions which have been made heretofore in the theoretical descriptions of chain dynamics in the quiescent state (the so-called *macroscopic* description of chain dynamics): (i) the polymer segments waggle in continuous viscous fluid (where the solvent motions are smeared and neglected) in accordance with a diffusion-type equation of the segment configurational distribution and (ii) the hydrodynamic disturbance of the fluid velocity caused by different polymer segments is described approximately by the Oseen tensor. This tensor was derived as a solution of the Stokes equation which neglects the nonlinear inertia term $(\mathbf{v} \cdot \nabla)\mathbf{v}$ of the Navier-Stokes (NS) general equation of motion,

$$\partial\mathbf{v}/\partial t + (\mathbf{v} \cdot \nabla)\mathbf{v} = \mathbf{K} - \nabla\mathbf{p}/\rho + \nu\Delta\mathbf{v}, \quad (1)$$

with \mathbf{v} the fluid velocity. However, the inertia term disappears essentially in the Couette flow. The Couette flow is thus a rigorous solution of the NS general equation of motion, as well as the Stokes equation. Therefore, if experiments were made under the Couette flow, not in the quiescent state, the results will give us new understanding to solve the disagreements between experimental facts and theoretical predictions. In this paper, we apply the dynamic light scattering (DLS) to the dilute solutions of high molecular-weight polymer sample in a good solvent in circular Couette flow and discuss the adequacy of the *microscopic* description¹ proposed for chain dynamics in dilute solution.

A monodispersed poly(α -methylstyrene) (PMS) fraction of $M_w = 6.85 \times 10^6$ was dissolved in benzene and the dilute solutions of different polymer mass concentration c ($c = 2.0 \sim 8.1 \times 10^{-4} \text{ g cm}^{-3}$) were prepared by filtering through a $0.2\mu\text{m}$ pore-size filter. The solution was set in

FUNDAMENTAL MATERIAL PROPERTIES — Molecular Dynamic Characteristics —

The Research activities in this subdivision cover structural studies and molecular motion analyses of polymers and related low molecular weight compounds in the crystalline, glassy, liquid crystalline, solution, and frozen solution states by high-resolution solid-state NMR, dynamic light scattering, electron microscopy, X-ray diffractometry, and so on, in order to obtain basic theories for the development of high-performance polymer materials. The processes of biosynthesis, crystallization, and higher-ordered structure formation are also studied for bacterial cellulose.



Prof
HORII
Fumitaka
(D Eng)



Assoc Prof
TSUNASHIMA
Yoshisuke
(D Eng)



Instr
KAJI
Hironori
(D Eng)



Assoc Instr
HIRAI
Asako
(D Eng)



Techn
OHMINE
Kyoko

Guest Res Assoc:

JOCHEN, Schacht (Ph.D)

Students:

ISHIDA, Hiroyuki (DC)

KAWANISHI, Hiroyuki (DC)

KUWABARA, Kazuhiro (DC)

OHIRA, Yasumasa (DC)

MASUDA, Kenji (DC)

HATTORI, Kimihiko (MC)

OHTSU, Takafumi (MC)

TAJIRI, Kouji (MC)

MIYAZAKI, Masayuki (MC)

MORIMOTO, Hidetoshi (MC)

ADACHI, Masayuki (UG)

MATSUDA, Eisuke (UG)

the 2mm-gap between the concentrically rotating rotor and the stator (glass cylinders) which stood perpendicularly. In the gap, the one-dimensional shear flow with a constant low-shear gradient γ was induced by the eddy current.² The single-frequency Ar-ion laser light of 3W was plunged perpendicularly to the rotor and, at given γ of $\gamma=0\sim 4.5s^{-1}$, the intensity time correlation function $A(t)$ of the V_v component of the scattered light from the sample solution at the angle $\theta=75.6^\circ$ was measured at $27^\circ C$ by homodyne method through a laboratory-made software correlator. The measured $A(t)$ was analyzed with the histogram method to obtain the decay rate Γ_i of the chain modes of motions i .

At all c examined, $A(t)$ curves were composed of two decay modes (slow and fast modes) at γ except the highest shear gradient γ_{max} of one slow mode. The slow mode with decay rate Γ_1 was the translational diffusion which represents the center-of-mass motion of the polymer chain, where the diffusion coefficient was $D_1 (= \Gamma_1 q^{-2})$ with q the scattering vector. The fast mode with decay rate Γ_2 was the intramolecular motions. The observation of slow mode alone at γ_{max} means that the intrachain motions are suppressed with the increase of the shear field. The γ and c dependence of D_1 below γ_{max} shows that, at fixed c , the D_1 increases with γ , as is the case for polystyrene-latex in aqueous solution² and for PMS of $M_w=2.71\times 10^6$ in benzene.³ However, with decreasing c , the D_1 changes from a descending to an ascending incline at higher γ . The double extrapolation to $\gamma, c\rightarrow 0$ gives the equilibrium value at infinite dilution $D_1(0,0)$. On the other hand, Γ_2/q^3 for internal motions at each c was constant independent of γ . Thus, the increasing decay rate with γ for translational mode and the γ -independent decay rate for internal modes indicate that, in shear field, the chain moves with a constant characteristic intramolecular frequency, though the translational motion is made faster by shear flow.

The first cumulant Ω , which represents all the motions the chain performs, was combined with the γ dependence of the translational motion and then the universal ratio $\Omega/D_0 q^2$ at the infinite extrapolations to $c\rightarrow 0$ and $\gamma\rightarrow \gamma_{solvent}$ was estimated to be 1.9 at $qR_G=3.03$. Here D_0 is the translational diffusion coefficient at infinite dilution and R_G is the radius of gyration of the chain. The obtained universal value is shown by a filled triangle () in Figure 1, where data for polystyrene and polyisoprene in Θ state () and the theoretical lines 1 and 2 calculated by the microscopic description of chain dynamics for Θ and good solvents¹ respectively are also given. The present data point is located near the line 1 and the feature is coincident with our recent one () obtained at low shear gradient for PMS of $M_w=2.71\times 10^6$ in benzene.⁴ It is very

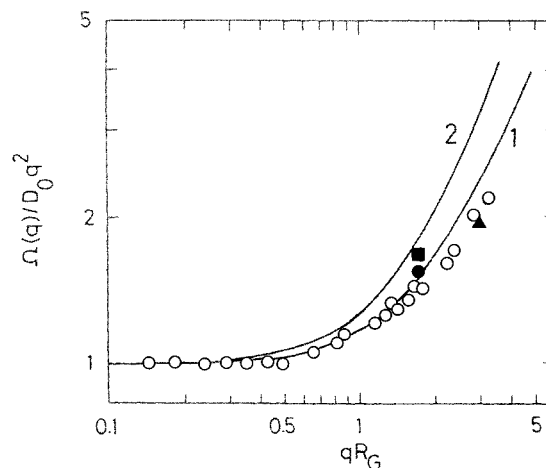


Figure 1. The $\Omega/D_0 q^2$ vs. qR_G plots for flexible polymers in dilute solution.

suggestive that data obtained in Couette flow in good solvent (,) are close to the data in Θ state () and are distinguished clearly from the data in good solvent in the quiescent state⁴ () which is located between lines 1 and 2. The microscopic description of polymer chain dynamics¹ is composed of the coupled kinetic model equations for polymer and solvent, where the segment velocity $\mathbf{c}(\tau, t)$ at the chain contour position τ and the solvent velocity $\mathbf{u}(\mathbf{r}, t)$ at the fluid position \mathbf{r} are expressed in the same dynamic level:

$$\frac{\partial \mathbf{c}(\tau, t)}{\partial t} = -\zeta_0^{-1} \delta \mathbf{H}\{\mathbf{c}\} / \delta \mathbf{c}(\tau, t) + \int d\mathbf{r} \mathbf{u}(\mathbf{r}, t) \delta(\mathbf{r} - \mathbf{c}(\tau, t)) + \mathbf{f}_c(\tau, t) \quad (\text{polymer}) \quad (2)$$

$$\frac{\partial \mathbf{u}(\mathbf{r}, t)}{\partial t} = \eta_c \nabla^2 \mathbf{u}(\mathbf{r}, t) - \int d\mathbf{r}' [\delta \mathbf{H}\{\mathbf{c}\} / \delta \mathbf{c}(\tau, t)] \times \delta(\mathbf{r} - \mathbf{c}(\tau, t)) + \mathbf{f}_u(\mathbf{r}, t) \quad (\text{solvent}) \quad (3)$$

with the incompressibility condition $\nabla \cdot \mathbf{u} = 0$. $\mathbf{H}\{\mathbf{c}\}$ is the chain potential and \mathbf{f} is the random force. In conclusion, the present result in Couette flow, which realizes an ideal fluid state in the hydrodynamic sense, can be explained by the microscopic view in Θ state, not in good solvents, and supports the necessity of the microscopic description in chain dynamics in dilute solution.⁵ The slight disagreement between data and the theoretical line 1 suggests further works in theoretical treatments in Θ state.

References

1. Shiwa Y, Tsunasima Y, *Physica A*, **197**, 43(1993).
2. Tsunasima Y, *J. Phys. Soc. Jpn.*, **61**, 2763 (1992).
3. Tsunasima Y, *J. Chem. Phys.*, **102**, 4673 (1995).
4. Tsunasima Y, *Proc. Kiban-B, the Grant-in-Aid for Scientific Research (Hakone)*, **102**, 61 (1997).
5. Tsunashima Y, Kawanishi H, *Polym. Prepr. Jpn.*, **46**, 3789 (1997).

Synthesis of Vinyl Ether-Based Polymacromonomers with Well-Controlled Structure

Masahiko Minoda, Kenji Yamada, Masayuki Miyazaki, Kohji Ohno,
Takeshi Fukuda and Takeaki Miyamoto

The present paper focuses on the atom transfer radical polymerization (ATRP) of vinyl ether (VE)-based macromonomers with a methacryloyl group at the chain end. Living cationic polymerization of isobutyl VE (IBVE) initiated with the HCl adduct of a VE carrying a pendant methacryloyl group in conjunction with ZnI_2 yielded the macromonomer (MA-PIBVE) with a narrow molecular weight distribution (MWD) ($M_w/M_n < 1.1$). The ATRP of MA-PIBVE was carried out using a halide initiator and the $CuBr/4,4'$ -di-*n*-heptyl-2,2'-bipyridine catalytic system. The number-average molecular weight of the polymacromonomer increased in proportion to the monomer conversion, while the MWDs stayed fairly narrow ($M_w/M_n \sim 1.2$). Thus polymacromonomers with controlled chain lengths for both the backbone and the side chain have been synthesized for the first time through a combination of living cationic polymerization and ATRP techniques.

Keywords: Polymacromonomer / Living cationic polymerization / Controlled radical polymerization

Recently there has been increasing interest in polymacromonomers, which are prepared by the homopolymerization of macromonomers. They are regular multi-branched macromolecules characterized by an extremely high branch density along the backbone. They can have unique molecular morphologies ranging from star-shaped spheres to rod-like cylinders, depending on the degrees of polymerization (DP) of the backbone and branch chains. For instance, polymacromonomers with a sufficiently large DP and long branches have been reported to exhibit a lyotropic phase. It was not until recently that the radical homopolymerization of a macromonomer in a highly concentrated medium yielded polymacromonomers with a high DP. Still more

difficult has been the living polymerization of macromonomers in a controlled manner.

On the other hand, the recent development in the controlled/ "living" radical polymerizations employing several initiating systems has provided possibilities for the synthesis of polymers with well-controlled structure. The transition metal-catalyzed atom transfer radical polymerization (ATRP) is one of the versatile techniques to achieve a controlled radical polymerization. Herein, we report on the ATRP of isobutyl vinyl ether (IBVE)-based macromonomers with the methacryloyl group at the initiating end (MA-PIBVE). This macromonomer is synthesized by living cationic polymerization. The combined use of living cationic polymerization and ATRP has led

ORGANIC MATERIALS CHEMISTRY — Polymeric Materials —

Scope of research

Basic studies have been conducted for better understandings of the structure/property or structure/function relations of polymeric materials and for the development of various types of polymers with controlled structure and/or novel functions. Among those have been the studies on (1) the mechanism and kinetics of "living" radical polymerization and its applications to the synthesis of well-defined polymers and copolymers of varying architecture, (2) the synthesis and properties of cellulose- and oligosaccharide-based functional polymers, and (3) the structure of polymer gels, ultrathin films and polymer alloys.



Prof
MIYAMOTO,
Takeaki
(D Eng)



Assoc Prof
FUKUDA,
Takeshi
(D Eng)



Instr
TSUJII,
Yoshinobu
(D Eng)



Instr
MINODA,
Masahiko
(D Eng)

Students:

OHNO, Kohji (DC)
OKAMURA, Haruyuki (DC)
YAMADA, Kenji (DC)
YAMAMOTO, Shinpei (DC)
GOTO, Atsushi (DC)
EJAZ, Muhammad (DC)
IZU, Yasumasa (MC)
YAMAMOTO, Shuichi (MC)
ENDO, Masaki (MC)
MARUMOTO, Yasuhiro (MC)
KAJITANI, Kazunobu (UG)
SATO, Koichi (UG)
ZHOU, Qi (RF)

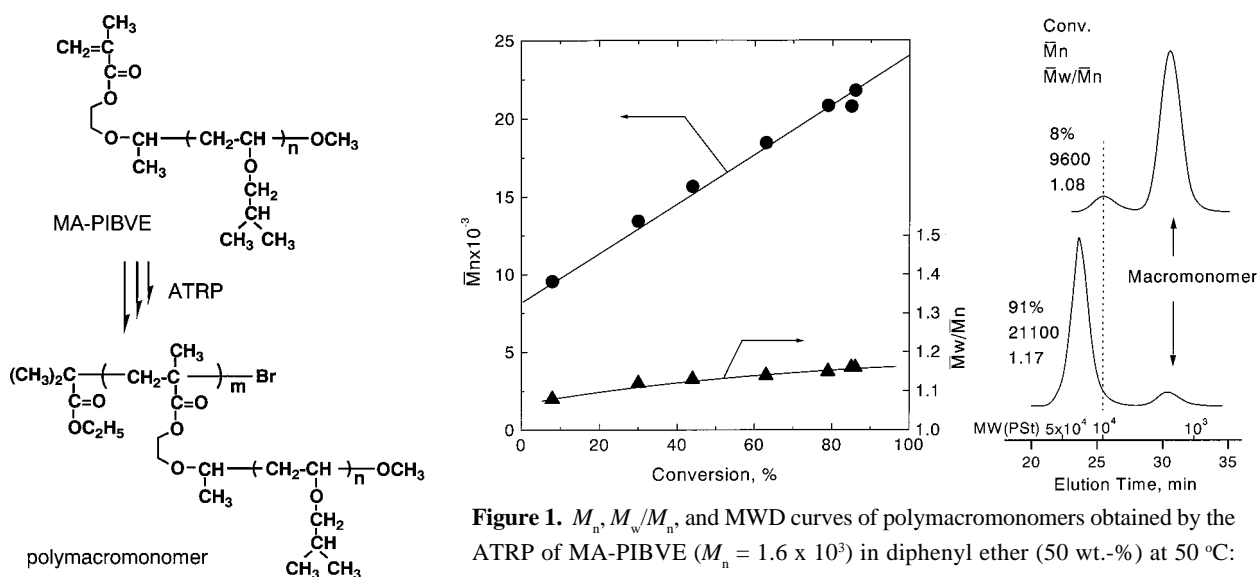


Figure 1. M_n , M_w/M_n , and MWD curves of polymacromonomers obtained by the ATRP of MA-PIBVE ($M_n = 1.6 \times 10^3$) in diphenyl ether (50 wt.-%) at 50 °C: $[M]_0/[ethyl\ 2\text{-bromoisobutyrate}]_0/[CuBr]_0/[dHbipy]_0 = 30/1/1/2$ (molar ratio).

to a new type of well-defined polymacromonomer that is controlled with respect to both backbone and side chain lengths and length distributions [1].

Synthesis of Macromonomers

The living cationic polymerization of IBVE was conducted by the HCl adduct of 2-(vinylxy)ethyl methacrylate (VEM-HCl) as the initiator in conjunction with zinc iodide (ZnI_2) to give the macromonomer (MA-PIBVE) with a narrow molecular weight distribution ($M_w/M_n < 1.1$). The number-average end functionality (F_n) estimated by the 1H NMR analysis was close to unity, indicating that the macromonomer has one methacryloyl group at the initiating end. The estimated number-average degrees of polymerization (DP_n s) of MA-PIBVE were in good agreement with the IBVE/initiator (VEM-HCl) feed molar ratios. All the obtained macromonomers have a narrow molecular weight distribution (MWD) and controlled DP_n .

ATRP of Macromonomers

The polymerization of MA-PIBVE by ATRP was conducted under a homogeneous condition using 4,4'-di-*n*-heptyl-2,2'-bipyridine (dHbipy) as the ligand, which coordinates copper(I) to solubilize the resulting complexes in the polymerization medium. The polymerization was carried out using ethyl 2-bromoisobutyrate as the initiator in conjunction with copper(I) bromide (CuBr) in diphenyl ether solution (50 wt.-%) at 50 °C [2]. The polymerization of MA-PIBVE ($M_n = 1.6 \times 10^3$) with a molar ratio $[M]_0/[I]_0/[CuBr]_0/[dHbipy]_0 = 30/1/1/2$ smoothly occurred without an induction period, and the conversion reached ca. 90% in 5 h. Moreover, the plot of $\ln[M]_0/[M]$ versus time was linear up to about 70%-conversion, indicating that the number of growing radicals remained constant. Deviations from the linear line were observed at higher conversions. This might be attributed to the increasingly high viscosity of the polymerization medium

rather than to irreversible termination reactions such as recombination of growing radicals.

As shown in Figure 1, the number-average molecular weights (M_n) of the obtained polymacromonomers increased linearly with the conversion, while the MWDs stayed fairly narrow with $M_w/M_n < 1.2$. These M_n and M_w/M_n values were estimated by polystyrene-calibrated GPC, and hence they are apparent values. Static light scattering measurements were made for one of the polymacromonomers. The weight-average molecular weight (M_w) determined by light scattering was 5.0×10^4 . This value is much larger than the GPC value ($M_w = 2.4 \times 10^4$) but reasonably well agrees with the theoretical value of 4.2×10^4 calculated from $M_w = M_{n,calcd} \times (M_w/M_n)_{GPC}$, where $M_{n,calcd}$ is the M_n value calculated with the initiator to (converted) monomer ratio, and $(M_w/M_n)_{GPC}$ is the GPC polydispersity index. All these results support the "living" nature of the ATRP of MA-PIBVE. The small value of M_w (or M_n) estimated by GPC suggests the multi-branched structure of the polymacromonomer that is more compact in hydrodynamic volume than the linear analog with a similar molecular weight.

Experiments were also carried out with higher $[M]_0/[I]_0$ ratios. Preliminary experiments using MA-PIBVE of $M_n = 1.6 \times 10^3$ with the molar ratios of $[M]_0/[I]_0/[CuBr]_0 = 60/1/1$ and $100/1/1$ showed that the polymerization proceeded too slowly or did not occur at all. We then attempted polymerization with an increased $[CuBr]_0/[I]_0$ ratio to promote polymerizability. In all cases up to the ratio of $[M]_0/[I]_0 \sim 200$, the polymerization proceeded in a controlled manner to give polymacromonomers with a narrow MWD.

References

- [1] Yamada, K. et al., *Macromolecules*, **1999**, *32*, 290.
- [2] Wang, J. S. et al., *J. Am. Chem. Soc.*, **1995**, *117*, 5614.

Hydrocarbon Molecules with Novel Structure: a Dehydroannulene with Silver(I)-Complexing Ability and a Double C₆₀ Adduct of Pentacene

Koichi Komatsu, Tohru Nishinaga, Yasujiro Murata, Tetsu Kawamura, and Noriyuki Kato

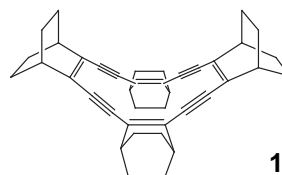
The first silver(I) complexes of tetrahydro[16]annulene fused with four bicyclo[2.2.2]octene units were synthesized, and the incorporation of the silver atom into the cavity center was shown by X-ray crystallography. The degree of complexation was affected by the counteranion. In contrast to the AgOTf complex, the AgSbF₆ complex was found to be more strongly coordinated to the dehydroannulene ligand. On the other hand, the solid-state reaction using high-speed vibration milling technique was applied to cycloaddition of fullerene C₆₀ to pentacene. There was obtained a new C₆₀ double adduct as a unique product for the solid-state reaction.

Keywords: dehydroannulene / silver complex / C₆₀ / cycloaddition / mechanochemistry

1. A Dehydroannulene with Silver(I)-Complexing Ability [1].

Dehydroannulene is a macrocyclic conjugated π -system containing acetylene linkage(s). Previously we reported the synthesis of a series of dehydroannulenes fused with bicyclo[2.2.2]octene frameworks [2]. The heightening of the HOMO of the π -systems due to the σ - π conjugation with the σ -bonds in rigid bicyclic frameworks has been demonstrated by electrochemical measurements.

The electron donation from the HOMO of the π -system should work favorably for complexation of a metal ion in the cavity of the cyclic π -system. Thus, when



tetrahydro[16]annulene **1** was allowed to react with an equimolar amount of either AgSbF₆ or AgOTf, the corresponding silver complexes were obtained as red crystals in 92 or 84% yield. The results of X-ray crystallography indicated that the silver ion is encapsulated in the middle of the cavity of the π -system, and is more strongly coordinated by the ligand for **1**·AgSbF₆ than for **1**·AgOTf.

ORGANIC MATERIALS CHEMISTRY —High-Pressure Organic Chemistry—

Scope of Research

Fundamental studies are being made for creation of new functional materials with novel structures and properties and for utilization of high pressure in organic synthesis. The major subjects are: synthetic and structural studies on novel cyclic π -systems; chemical transformation of fullerene C₆₀; utilization of carbon monoxide and dioxide for organic synthesis under the transition-metal catalysis.



Prof
KOMATSU
Koichi
(D Eng)

Instr
MORI
Sadayuki
(D Eng)

Instr
KUDO
Kiyoshi
(D Eng)

Instr
NISHINAGA
Tohru
(D Eng)

Techn
YASUMOTO
Mitsuo

Assoc Instr
TANAKA
Toru

Students:

MATSUURA, Akira (DC)
IZUKAWA, Yoshiteru (MC)
TAKAHASHI, Masayo (MC)
FUJIWARA, Koichi (MC)
KATO, Noriyuki (MC)
WAKAMIYA, Atsushi (MC)
ITO, Miho (UG)
NODERA, Nobutake (UG)

Research Fellow:

MURATA, Yasujiro (D Eng)

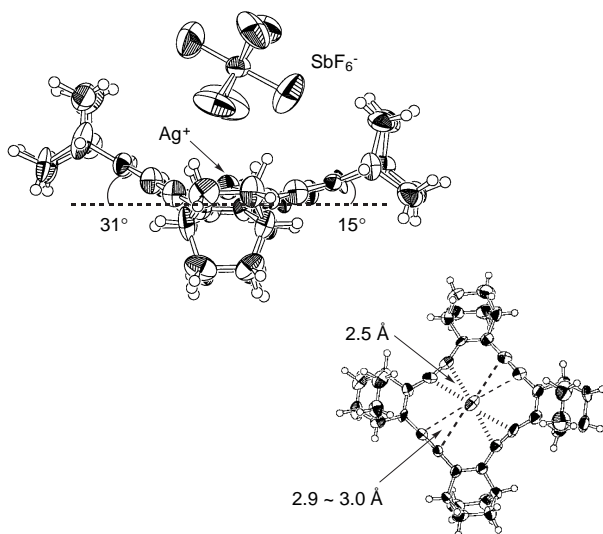


Figure 1. Molecular structure of $1 \cdot \text{SbF}_6$ determined by X-ray crystallography. A side view and a top view (with SbF_6 eliminated for clarity).

The Ag-C(alkyne) distance of $1 \cdot \text{AgOTf}$ varies only from 2.714(7) Å to 2.863(7) Å, indicating almost equal coordination with the four acetylene units whereas the ligand of $1 \cdot \text{SbF}_6$ is slightly deformed due to the stronger coordination with a pair of acetylene units which are opposite with each other. The Ag-C distance at the stronger coordination site is 2.52(1)–2.54(1) Å as shown in Figure 1.

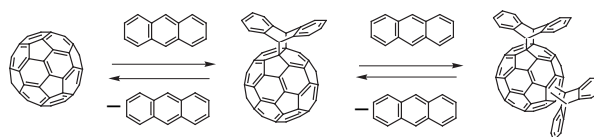
These results are in good agreement with the Mulliken charge calculated at the HF/STO-3G level for the silver atoms of AgSbF_6 and AgOTf using the X-ray structures. Apparently the annulene-type ligand in the present work is reducing the positive charge on the silver atom and the extent of this reduction is larger for the case of AgSbF_6 . This type of coordination is presumed to be principally due to the interaction between the HOMO of the ligand and the LUMO of the metal, and the annelation with the bicyclic frameworks, which raises the HOMO level of the π -system, has strengthened this interaction as expected.

2. A Double C_{60} Adduct of Pentacene.

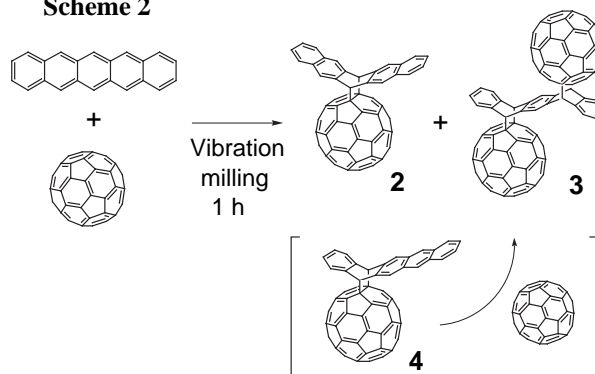
The mechanochemical solid-state reaction of fullerene C_{60} using a technique of high-speed vibration milling has been successfully utilized in our group in the nucleophilic addition of organozinc reagent [3] and the selective dimerization of C_{60} to give the first fullerene dimer C_{120} [4].

When this technique was applied to the [4+2] cycloaddition of C_{60} with anthracene, it was found that an apparent equilibrium state can be established within

Scheme 1



Scheme 2



about 30 minutes in spite of the heterogeneous solid-state reaction conditions (Scheme 1).

The similar high-speed vibration milling of C_{60} with pentacene was found to afford not only the symmetrical monoadduct **2** but the double C_{60} adduct **3** as shown in Scheme 2. Adduct **3** was not obtained by the reaction in solution in toluene, and is supposed to be formed by highly selective trapping of the non-symmetrical monoadduct **4** from the anti-face by the second C_{60} molecule, which exists abundantly in the surroundings of **4** under the present solvent-free conditions. Thus, in this particular case, the present reaction conditions appear to be favorable for the trapping of the kinetic product.

The electrochemical measurement on the double C_{60} adduct **3** indicated that there is no appreciable through-space interaction between the two C_{60} cages within the molecule.

References

1. Nishinaga T, Kawamura T and Komatsu K, *Chem. Commun.*, **1998**, 2263.
2. Nishinaga T, Kawamura T and Komatsu K, *J. Org. Chem.*, **62**, 5354 (1997).
3. Wang G-W, Murata Y, Komatsu K and Wan TSM, *Chem. Commun.*, **1996**, 2059.
4. Wang G-W, Komatsu K, Murata Y and Shiro M, *Nature*, **387**, 583 (1997).

Synthesis, Structure and Reaction of {Tris[2-(dimethylamino)phenyl]germyl}lithium

Atsushi Kawachi, Yoko Tanaka and Kohei Tamao

{Tris[2-(dimethylamino)phenyl]germyl}lithium (**1**) has been prepared from the corresponding hydrogermane (**3**) with *tert*-butyllithium. X-ray analysis of **1** shows that **1** exists as a mono-chelated monomer, where the lithium atom is coordinated with one of the amino groups and with two THF molecules. Reaction of **1** with elemental selenium gives 2,2,4,4-tetrakis[2-(dimethylamino)phenyl]-1,3,2,4-diselenadigermetane (**2**). The nitrogen donor induces a novel type of reaction for the formation of the heterocyclic compound.

Keywords: Germyllithium / 2-(Dimethylamino)phenyl ligand / Chelation / Solid-state structure / Diselenadigermetane

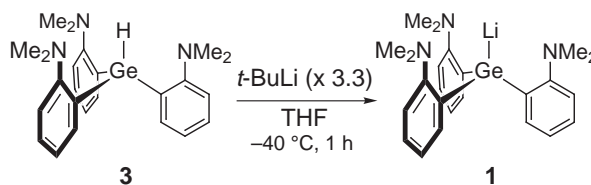
Among a variety of Group 14 element-alkali metal compounds, germyllithium compounds have been well studied from the synthetic view point, but structural studies have been less developed. Thus germanium-lithium bond character is still unclear. We report here the preparation of {tris[2-(dimethylamino)phenyl]germyl}lithium (**1**) and its structure in the solid state. We also report the reaction of **1** with elemental selenium to result in formation of 1,3,2,4-diselenadigermetane **2**.

1. Synthesis and Structure of **1** [1]

The germyllithium **1** was prepared by deprotonation of the hydrogermane **3** [2] with *tert*-butyllithium (3.3 mol amt.) in THF at $-40\text{ }^{\circ}\text{C}$ in 93% yield, as shown in Scheme 1; the yield was estimated by quenching with D_2O . When **3** was treated with a deficient amount of *tert*-butyllithium (1.2 mol amt.), **1** could

be isolated as pale yellow crystals in 33% yield after recrystallization from toluene at $-20\text{ }^{\circ}\text{C}$.

Scheme 1



X-ray analysis of the crystal reveals that **1** has a monomeric structure in the solid state, as shown in Figure 1. The most striking feature is the highly distorted geometry around Ge(1) due to the unsymmetrical interaction of Li(1) with the amino group. Li(1) bonded to Ge(1) is coordinated with N(1) of one of the three NMe_2 groups, forming a five-membered chelate ring consisting of Li(1), Ge(1), C(1), C(2), and N(1). Li(1) is also coor-

SYNTHETIC ORGANIC CHEMISTRY

–Synthetic Design–

Scope of research

(1) Synthesis, structural studies, and synthetic applications of organosilicon compounds, such as pentacoordinate silicon compounds, functionalized silyl anions, and functionalized oligosilanes. (2) Design and synthesis of novel π -conjugated polymers containing silacyclopentadiene (silole) rings, based on new cyclization reactions and carbon-carbon bond formations mediated by the main group and transition metals. (3) Chiral transformations and asymmetric synthesis via organosulfur and selenium compounds, especially via chiral episulfonium and episelenonium ions.



Prof
TAMAO,
Kohei
(D Eng)



Assoc Prof
TOSHIMITSU,
Akio
(D Eng)



Instr
KAWACHI,
Atsushi
(D Eng)



Instr
YAMAGUCHI,
Shigehiro
(D Eng)

KATKEVICS, Martins (Guest Scholar); JIN, Ren-Zhi (Guest Scholar); ASAHARA, Masahiro (D Eng); NAKAMURA, Hiroshi (D Eng); TANAKA, Yoko (DC); AKIYAMA, Seiji (DC); MAEDA, Hirofumi (DC); TSUJI, Hayato (DC); ENDO, Tomonori (MC); ITAMI, Yujiro (MC); GOTO, Tomoyuki (MC); SAEKI, Tomoyuki (MC); HIRAO, Shino (UG); MINAMIMOTO, Takashi (UG)

minated with O(1) and O(2) of two THF molecules arising from the reaction solvent. The Li(1)–Ge(1) bond length (2.598(9) Å) is the shortest among those of the characterized germyllithium compounds (2.613(3)–2.759(24) Å). The Li(1)–N(1) bond length (2.15(1) Å) is longer than the sum of the covalent radii (Li 1.23 Å; N 0.70 Å), but normal as the coordinative Li–N bonds (2.01–2.17 Å). The intramolecular coordination of N(1) to Li(1) reduces the angle of Li(1)–Ge(1)–C(1) to 83.9(3)°. As a result, Li(1), Ge(1), C(9), and C(17) are almost coplanar; the sum of the three angles of Li(1)–Ge(1)–C(9), Li(1)–Ge(1)–C(17), and C(9)–Ge(1)–C(17) is 359.5°. In spite of the distorted geometry, however, there are no significant differences among the three Ge–C bonds (2.042(6), 2.030(5), and 2.054(5) Å) and the three C–Ge–C angles (96.8(2), 99.2(2), and 98.4(2)°). It is also noted that the sum of the latter (294.4°) is strongly reduced from the sp³ tetrahedral value (328°). Thus, the geometry of **1** may be designated pyramidal rather than distorted tetrahedral.

We performed an *ab initio* calculation of **1**•(THF)₂ at HF level using the 6-311+G* basis set on Li and Ge atoms and the 6-31G basis set on H, C, N, and O atoms. The molecular orbital analysis of the anionic electrons (HOMO) indicates that the lithium atom is located not along the vector of the anionic electrons but aside. This may be represented as an intramolecular separated ion pair, which is not unusual if the Ge–Li interaction is weak while the N–Li coordinative interaction is relatively strong.

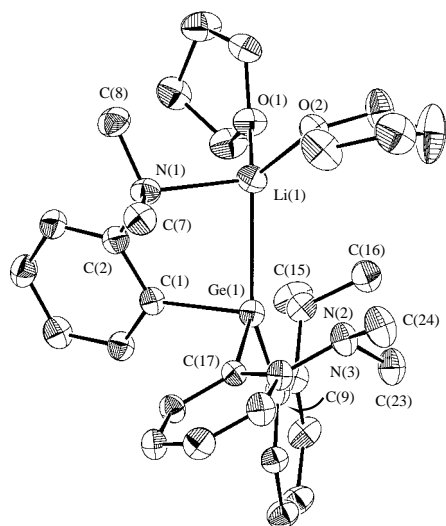
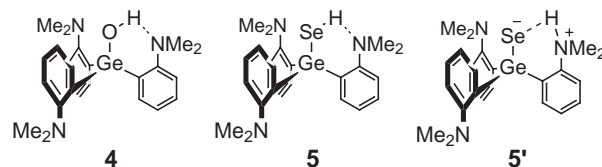


Figure 1. Molecular structure of **1**•(THF)₂ with 30% probability ellipsoids (H atoms omitted for clarity)

2. Reaction of **1** with Selenium [3]

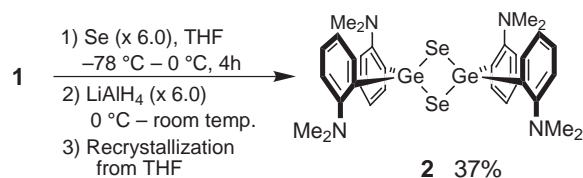
Previously we reported the preparation and structure of tris[2-(dimethylamino)phenyl]germanol (**4**),

which contains the germanium–oxygen bond and exhibits intramolecular hydrogen bonding between the hydroxyl group and one of the amino groups [2]. This finding prompted us to prepare and isolate a heavier Group 16 element analog, germaneselenol **5**.



The germyllithium **1** in THF was allowed to successively react with selenium powder and with lithium aluminum hydride, followed by hydrolysis. Crystallization of the product from THF did not afford **5** but unexpectedly afforded the diselenadigermetane **2** in 37% yield, as shown in Scheme 2.

Scheme 2



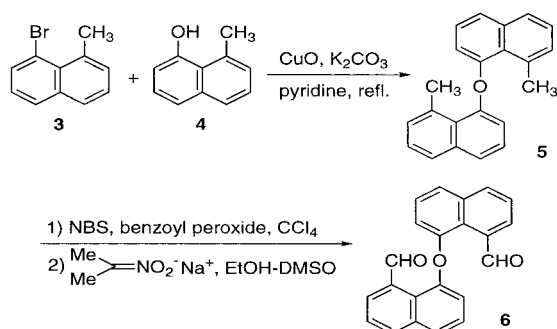
The molecular structure of **2** was determined by X-ray analysis. The Ge–Se bond lengths are 2.3678(6) and 2.3716(9) Å, which are among the normal Ge–Se single bond lengths (2.337–2.421 Å). The intramolecular Ge···Ge distance is 3.168(1) Å. The ratio of the Ge···Ge nonbonding distance to the Ge–Se bond length is 1.34, which is in good agreement with the values of the approximate homology rule proposed by Kabe and Masamune [4].

The mechanism of the formation of **2** is still unclear, but **2** turned out to be the secondary product from the zwitterionic species **5'**, perhaps via intra- and/or intermolecular protodegermylation, as indicated by the ¹H NMR results. Thus the nitrogen donor intramolecularly activates the selenol proton, inducing a novel type of reaction for the formation of the heterocyclic compound.

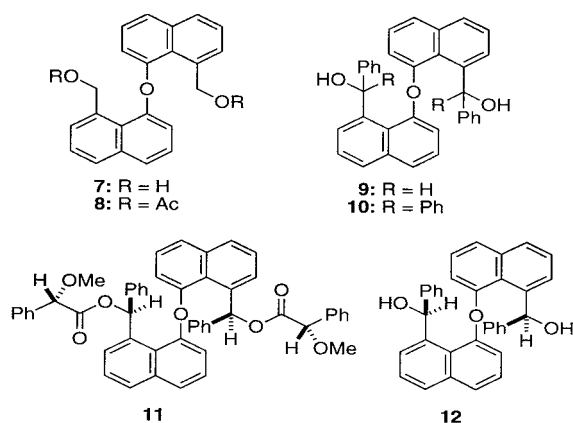
1. Kawachi A, Tanaka Y, and Tamao K, *Eur. J. Inorg. Chem.*, 461 (1999).
2. Kawachi A, Tanaka Y, and Tamao K, *Organometallics*, **16**, 5102 (1997).
3. Kawachi A, Tanaka Y, and Tamao K, *Chem. Lett.*, 21 (1999).
4. Kabe Y, Kawase T, Okada J, Yamashita O, Goto M, and Masamune S, *Angew. Chem., Int. Ed. Engl.*, **29**, 794 (1990).

physicochemical properties, the optically active molecular bevel gear with only two cogs on each wheel deserves to be studied as a chiral source for asymmetric syntheses and molecular recognition. We chose compounds of type 1 with substituents at the 8- and 8'-positions as a basic structure for the bevel gear with two cogs, because the naphthyl ring has a large blade area and because a substituent demanding large steric interaction should be required to prevent the gear slippage. Iwamura et al.³ reported that the gear slippage barrier of bis(9-triptycyl) derivative 2 was highest when two triptycyl groups were connected with the oxygen atom due to the orders of the relevant bond lengths and the stretching and bending force constants. Accordingly, we decided to connect two naphthyl rings with the oxygen atom to synthesize the compounds 1 (X=O), the enantiomers of which were expected to be isolated more easily than those of 1 (X=CH₂) and 1 (X=NH).

Scheme 1.

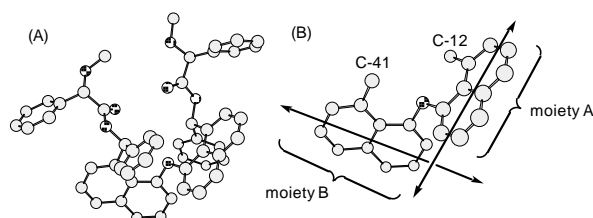


The synthesis of the 8,8'-diformyl-1,1'-binaphthyl ether 6 is shown in Scheme 1. The Ullmann ether synthesis with 1-bromo-8-methylnaphthalene (3) and 1-hydroxy-8-methylnaphthalene (4) gave binaphthyl ether 5 in 31% yield. Bromination of 5 with NBS followed by oxidation with sodium salt of 2-nitropropane afforded dialdehyde 6 in 61% yield. Reduction of 6 with lithium aluminum hydride gave the corresponding diol 7 in 98% yield, which was converted to diacetate 8 (92%). The diacetate 8 was shown to be a racemic mixture by HPLC analysis using a chiral column (see Supporting Information). The activation energy for the racemization (gear slippage) was found to be 93.3 kJ/mol at 20 °C ($t_{1/2} = 38$ min) by measuring the time-dependent decrease in the enantiomeric excess of 8 by HPLC.



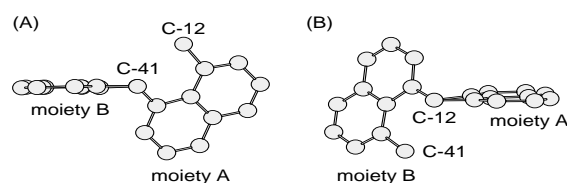
Introduction of a bulky group at the 8- and 8'-positions was expected to increase the activation energy sufficiently to isolate each enantiomer of the bevel gear with two cogs. The reaction of 6 with phenyllithium gave a diastereomeric mixture of alcohols 9. The Jones oxidation of 9 followed by the reaction with phenyllithium gave diol 10 in 30% yield for two steps. Each enantiomer of 10 was separated by preparative HPLC on a chiral column. The diester 11 was isolated in 7% yield from a mixture obtained by the reaction of 9 with (S)-(+)-*a*-methoxy-1-phenylacetic acid. Figure 1A and B shows the crystal structure of 11 and the effective transition moment of the two naphthyl rings, suggesting their negative chirality. An interesting finding of the X-ray analysis is that one of the naphthyl rings is almost planar, while another is slightly distorted (Fig. 2), though both naphthyl rings are expected to be completely identical, even with respect to the substituents at the peri-position. Hydrolysis of 11 gave optically active 12. The CD spectra of 11 and 12 gave rise to exciton-split bands

Figure 1. X-ray crystal structure of **11**, (A) showing full atoms except hydrogens, (B) showing the basic skeleton of **11** to indicate the direction of the effective transition moment.



with negative Cotton effects at longer wavelength. Comparison of the CD spectra of (+)- and (-)-10 with those of 11 and 12 led to the conclusion that the sense of chirality of (+)-10 is the same as those of them, and vice versa for (-)-10. The activation energy for gear-slippage (racemization) of optically active 10 was determined to

Figure 2. Two views of the X-ray structure of **11** emphasizing the difference between two naphthyl rings: (A) through the axis between C-41 and the ether oxygen; (B) through the axis between C-12 and the ether oxygen.



be 126.4 kJ/mol at 111 °C in toluene.

Utilization of this novel chiral source for molecular recognition and asymmetric syntheses is currently underway in our laboratory.

References

1. Glaser, R.; Blount, J. F.; Mislow, K. J. *Am. Chem. Soc.* 1980, 102, 2777 and references cited therein.
2. Kawada, Y.; Iwamura, H. *J. Am. Chem. Soc.* 1983, 105, 1449.
3. Kawada, Y.; Yamazaki, H.; Koga, G.; Murata, S.; Iwamura, H. *J. Org. Chem.* 1986, 51, 1472 and references cited therein.

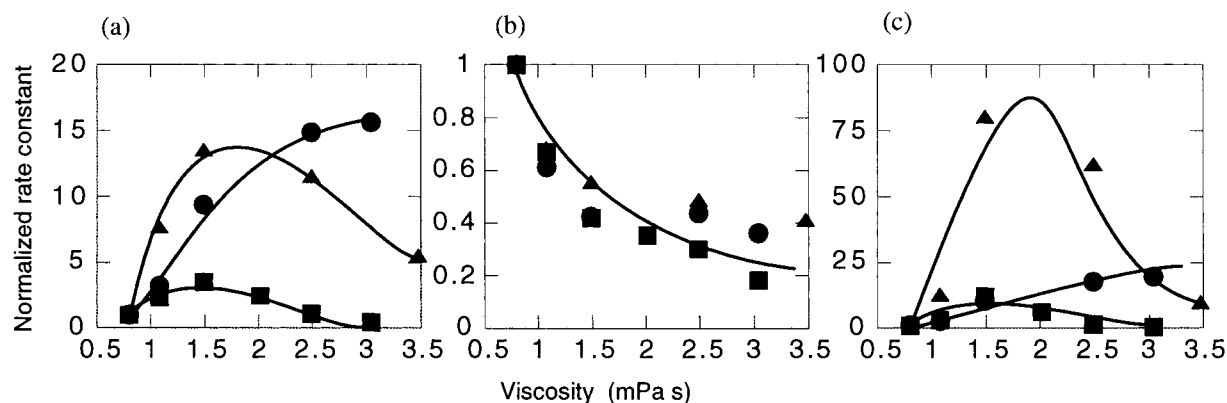
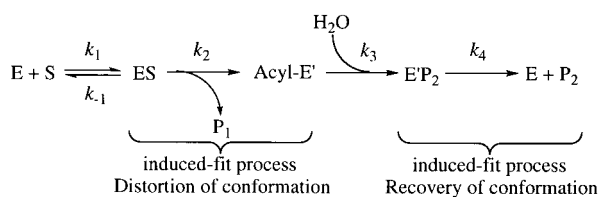


Figure 1. Dependence of kinetic parameters on medium viscosity: **1**, **2**, **3**: (a) k_{cat} , (b) k_2 , (c) k_3 .

i.e., a conformation that was not adopted to accommodate the acyl group, tends to eject the acyl group from its pocket so as to stabilize itself as the free enzyme. Thus, the decrease in k_2 is coupled by an increase in k_3 . However, the increase in k_3 with the increase in medium viscosity is not monotonic. Instead, it begins to decrease at about $\eta \approx 1.6$ mPa s. This is accounted for by the presence of an additional process in this step, which becomes unfavorable as the medium becomes more viscous. We assign this additional process to the product releasing step with a rate constant of k_4 . This assignment proposes that the conformation suitable for the acyl enzyme is also suitable for releasing P_2 , the acid part of the substrate. In other words, the release of free acid from the enzyme of undistorted conformation is not a simultaneous process. The release of P_2 requires energy corresponding to the release of distortion energy that exists in the conformationally distorted enzyme, and Scheme 1 is now revised to Scheme 2 by taking into account the induced-fit conformational adjustment for the release of P_2 .



Scheme 2

The shapes of the curves for k_{cat} shown in Fig. 1(a) are similar to those for k_3/k_4 shown in Fig. 1(c), which stems from the fact that this step is more sensitive process to the effect of induced-fit conformational adjustment than the k_2 step and the chemical (catalytic) reactivity of the enzyme is regulated by this process. It has been known that the rate-determining step in the enzymatic hydrolysis of an ester is the step in which the acyl enzyme is hydrolyzed into a free enzyme and an acid. Absolute values for k_2 and k_3 , as well as substrate

independence of the k_2 step shown in Fig. 1(b), also support the idea that the hydrolysis of acyl enzyme is (at least in part) the rate-determining step of the present reaction under normal conditions. However, interestingly, the rate-determining step is shifted to the k_2 step in the reactions occurring in highly viscous media for certain substrates. An exception is the reaction with **1**, where the rate-determining step is always in the k_3/k_4 step even in the most viscous medium studied.

The observation that the maximum position in the plot of k_3/k_4 step for **1**, if any, shifts to higher viscosity than the other amino acid substrates indicates that the reaction of this substrate is less sensitive to induced-fit conformational adjustment than the reactions of other substrates. The result obtained herein has good agreement with that obtained by proton inventory kinetics [3], where **1** was found to be associated by the movement of one proton whereas other amino acid substrates were associated with the movement of two protons at their respective transition states. In other words, **1** is not an appropriate substrate for studying the catalytic activity of α -chymotrypsin. Although, conventionally, **1** has been employed as a typical substrate in the study of catalytic activity of α -chymotrypsin, one should be very careful in extending the results obtained with **1** as a substrate to the discussion of the general mechanism of α -chymotrypsin hydrolysis.

Consequently, we now believe that both acylation/deacylation and release of products P_1/P_2 are dependent on the induced-fit conformational adjustment in the hydrolysis of an ester by α -chymotrypsin. More results should be accumulated using substrates of various types before we reach a conclusion.

References

1. D. E. Koshland, Jr., *Proc. Natl. Acad. Sci. U. S. A.*, **44**, 98 (1958).
2. Y. Kawai, T. Matsuo, and A. Ohno, *Bull. Chem. Soc. Jpn.*, **71**, 2187 (1998).
3. R. L. Stein, J. P. Elrod, and R. L. Schowen, *J. Am. Chem. Soc.*, **105**, 2446 (1983).

Artificial Nine Zinc-Finger Peptide with 30-Base Pair Binding Sites[†]

Tatsuya Kamiuchi, Emiko Abe, Miki Imanishi, Tamaki Kaji, Makoto Nagaoka, and Yukio Sugiura*

Newly designed zinc-finger peptide Sp1ZF9 containing nine Cys₂-His₂ type motifs has been manipulated. The DNA binding property of Sp1ZF9 was compared with those of native three zinc-finger Sp1(530-623) and artificial six zinc-finger Sp1ZF6 peptides. Although the equilibrium time was less than 0.5 hr for Sp1(530-623)-DNA complex, Sp1ZF6 and Sp1ZF9 required approximately 48 and 72 hrs respectively for full complex formation. Evidently, the footprinting analysis demonstrated that Sp1ZF9 and Sp1ZF6 bind at least 27 and 18 contiguous base pairs of DNA sequence, respectively. Sp1ZF9 showed two step bindings to DNA, namely first the recognition of GC (5'-GGG-GCG-GGGCC-3') sequence by the N-terminal Sp1 domain and next the recognition of the corresponding target sequences by the middle and C-terminal Sp1 domains. In contrast with unimolecular binding of Sp1ZF9 and Sp1ZF6, two Sp1(530-623) molecules bind to one GCIII (5'-GGG-GCG-GGG-GGG-GCG-GGG-GGG-GCG-GGGCC-3') site region. Of special interest is the fact that new nine zinc-finger peptide Sp1ZF9 can bind to DNA sequence of approximately 30-base pairs. Such multi zinc-finger peptides may be useful as genome-specific transcriptional switches in future.

Key Words: Zinc-finger protein/ transcription factor/DNA recognition/ multi finger/ artificial protein

DNA binding proteins selectively bind to specific DNA sequence, and play an important role in biological systems.¹ Zinc-finger domain of Cys₂-His₂ type is a typical class of DNA binding protein, and contains the sequence of (Tyr, Phe)-X-Cys-X_{2,4}-Cys-X₃-Phe-X₅-Leu-X₂His-X_{3,5}-His, usually in tandem arrays.²⁻⁵ The X- ray

crystal structures of the Zif268- and GLI-DNA complexes revealed the characteristic DNA binding mode of zinc finger proteins as follows: (1) recognition of three bases per one finger motif, (2) structure of tandemly repeated finger domain, and (3) binding to the sequence of asymmetric base pairs.⁶⁻⁹ Transcription factor Sp1 involves

BIOORGANIC CHEMISTRY- Bioactive Chemistry-

Scope or research

The major goal of our laboratory is to elucidate the molecular basis of the activity of various bioactive substances by biochemical, physicochemical, and synthetic approaches. These include studies on the mechanism of sequence-specific DNA cleavage by antitumor or carcinogenic molecules, studies on the DNA recognition of zinc-finger proteins, and model studies on the action of ion channels. In addition, artificial designed peptides have also been developed as useful tools in molecular biology and potentially in human medicine.



Prof
SUGIURA, Yukio
(D Pharm Sci)



Assoc Prof
FUTAKI, Shiro
(D Pharm Sci)



Assoc Instr
OKUNO, Yasushi

Students

AIZAWA, Yasunori (DC)
INOUE, Teruhiko (DC)
ARAKI, Michihiro (DC)
HARA, Yuji (MC)
IMANISHI, Miki (MC)
MATSUSHITA, Keizo (MC)
SAEGUSA, Nana (MC)
SUZUKI, Kazuo (MC)
OMOTE, Masayuki (MC)
KAJI, Tamaki (MC)
MIYAGAWA, Naoko (MC)
SUZUKI, Tomoki (MC)
HASHIMA, Mie (UG)
HORI, Yuichiro (UG)
UNO, Yumiko (UG)
YAMAUCHI, Kayoko (UG)

three Cys₂-His₂ type zinc-finger motifs at the C-terminus of protein,¹⁰ and is closely related to Zif268.¹¹ Indeed, Sp1 strongly binds to GGG-GCG-GGG sequence. On the basis of the nature of Cys₂-His₂ type zinc-finger motif and recognition bases of Sp1, we designed novel nine zinc-finger peptide Sp1ZF9 and also its DNA binding properties were compared with those of three finger Sp1(530-623) and six finger Sp1ZF6 peptides. DNA binding of nine zinc-finger protein TFIIIA is well known to be dominated by interaction of select few fingers.^{2, 8, 13-15} Therefore, it is of special interest to create new nine zinc-finger peptide that can bind to DNA sequence over an extended region of 30-base pairs. Such multi zinc-finger peptides may be hopeful in future gene therapy strategies. Certainly, molecules with high DNA binding affinity and long sequence specificity in the human genome are useful tools in molecular biology and potentially in human medicine.¹⁶⁻¹⁸

Design of multiple zinc-finger proteins: Novel multiple zinc-finger peptides, Sp1ZF6 and Sp1ZF9, were newly created from zinc-finger motif of transcription factor Sp1. These peptides were constructed by connecting C-terminal Sp1 molecule to N-terminal of a following one. The *Krüppel-type* linker (Thr-Gly-Glu-Lys-Pro) which is conserved in many zinc-finger proteins, was selected for connection of Sp1 finger domains. This linker plays in controlling the orientation and spacing of adjacent finger and also is involved in nonspecific interaction with phosphate backbone of DNA.^{6, 8, 19, 23, 24}

Binding specificity of Sp1(530-623), Sp1ZF6, and Sp1ZF9. In gel mobility shift assays, the binding sites were predicted from Sp1 recognition site (GGG GCG GGG).¹⁰ The equilibrium time was less than 0.5 hr for Sp1(530-623)-DNA complex. By contrast, Sp1ZF6 and Sp1ZF9 required approximately 48 and 72 hrs, respectively. To determine binding specificity of the multiple zinc-finger peptides, we performed the gel mobility shift assays with two DNA fragments. The binding affinity of Sp1(530-623) was no significant difference in three DNA fragments. Sp1ZF6 showed about 20-fold preferential binding to GCII compared with GC. Sp1ZF9 gave approximately 30-fold higher affinity with GCIII than GC. The results reveal that the length of the binding DNA sequence is dependent on

the number of these zinc-finger motifs. On the other hand, the binding affinities for GCIII complexes of Sp1ZF6 and Sp1ZF9 were considerably close. Probably, this is because GCIII sequence contains both GC and GCII sequences. Two Sp1(530-623) molecules bind to one GCIII fragment but Sp1ZF9(or Sp1ZF6) does with unimolecule.

DNA binding of multiple zinc-finger peptides: In order to examine the DNA binding site of Sp1ZF6 and Sp1ZF9 on GCIII, DNase I footprinting assays were performed. Under lower peptide concentration, Sp1(530-623) bound the GC-box of 3'-portion. With increasing the peptide concentration, the GC-box of 5'-portion was protected and also the hypersensitive breakages were detected at C(14) and G(15) within the middle GC-box. Clearly, two Sp1(530-623) peptides bound to GCIII. On the other hand, Sp1ZF6 and Sp1ZF9 exhibited different binding features from Sp1(530-623). Sp1ZF6 bound to longer sites than 18 bp of 3'-end in the GCIII. Sp1ZF9 protected slightly longer binding sites than the 27 bp target site.

Binding affinity of Sp1ZF9 to GCIII. To estimate accurately the binding affinity, the active peptide concentration should be calculated on the basis of only the preparation fraction which is active to bind to DNA. However, the larger peptide may be expected to be less likely to fold and more likely to be oxidized in long equilibrium period. By using the peptide prepared freshly, therefore, we determined approximate DNA binding affinity of Sp1ZF9. In the case of 72 hr, apparent equilibrium dissociation constant (K_d) was 1.2 ± 0.3 nM. Recently, we determined that the dissociation constant (K_d) of three zinc-finger Sp1(530-623) peptide for GC-box DNA is 3.5 ± 0.5 nM.²⁵

In conclusion, newly designed nine zinc-finger peptide Sp1ZF9 binds a contiguous 27-bp DNA. The multiple zinc-finger peptide has two steps of the sequence recognition and binding for peptide-DNA complex formation. Recently, zinc-finger motifs contacting with various sequences were selected by the technique of phage display.²⁹⁻³² The present results would provide good information for design of new DNA binding proteins to recognize long DNA sequence. Indeed, human Y-box binding protein gene promoter³³ and human immune activation (Act-2) gene³⁴ include GCIII-like long GC sequences. In future gene therapy, such multi zinc-finger proteins may be useful as genome-specific transcriptional switches.

CYP2D Microsatellite Polymorphism in Lewy Body Variant of Alzheimer's Disease and Parkinson's Disease

Seigo Tanaka, Naomi Matoh and Kunihiro Ueda

The Lewy body variant (LBV) has been recognized as a distinct subset of Alzheimer's disease (AD). In this study, we conducted an allelic association study in patients with pure AD, LBV and also Parkinson's disease (PD) by using the CYP2D microsatellite, the (dG-dT)_n dinucleotide repeat (n = 16 - 27) located between CYP2D8P and CYP2D7 genes. The alleles longer than 21 repeat (the long-type alleles) were excessively represented in LBV (allele frequency, 0.313) compared with the age-matched control (0.186) (odds ratio = 1.99, p = 0.019 by χ^2 test). This overrepresentation was also found in PD (0.298) (odds ratio = 1.86, p = 0.037), but not in pure AD (0.196). The long-type alleles showed a strong association with the CYP2D6 B mutation (odds ratio = 88.50, p < 0.001 by Fisher's exact test), but not with the D mutation or the deletion of CYP2D6 gene. These findings confirmed a close association of the CYP2D locus with LBV and PD, indicating the following two possibilities: the involvement of the CYP2D6 B mutation in pathogenesis of LBV and PD in a dominant-negative manner; or the linkage disequilibrium of the CYP2D microsatellite to another pathogenic gene locus. The microsatellite of the CYP2D locus could be an informative marker in the genetic study of LBV as well as PD.

Keywords : CYP2D6 / Microsatellite / Alzheimer's disease / Parkinson's disease / Lewy body

Alzheimer's disease (AD) and Parkinson's disease (PD) are considered complex multifactorial diseases, with an interaction of genetic susceptibility [1, 2] and environmental factors against a background of aging. The Lewy body variant (LBV) represents a clinico-pathologically defined subset of AD. It is characterized by the presence of Lewy bodies (LBs) in neocortical and subcortical regions of the AD brain. The LB is an intracytoplasmic neuronal inclusion and a hallmark of idiopathic PD.

Genetic analyses have revealed the association of the CYP2D6 B mutation with PD. CYP2D6 codes for one form of cytochrome P450 enzyme, which is responsible for hydroxylation of several substances. The CYP2D gene cluster consists of CYP2D8P, CYP2D7 and CYP2D6 genes in the order from 5' to 3' on chromosome 22 at q13.1-13.2. The B mutation of the CYP2D6 gene is a G to A transition at the intron 3 - exon 4 junction, which shifts the position of the 3' splice site, leading to a frameshift.

BIOORGANIC CHEMISTRY — Molecular Clinical Chemistry —

Scope of research

This laboratory was founded in 1994 with the aim of linking (bio)chemical research and clinical medicine. Thus, the scope of our research encompasses the structure, function and regulation of various biomolecules, the pathophysiological significance of bioreactions in relation to human diseases, and the application of molecular techniques to clinical diagnosis and therapy. Our current interest is focused on poly(ADP-ribosyl)ation, nuclear (de)localization of proteins in association with apoptosis, and the molecular etiology of Alzheimer's disease and related disorders.



Prof
UEDA, Kunihiro
(D Med Sc)



Assoc Prof
TANAKA, Seigo
(D Med Sci)



Instr
ADACHI, Yoshifumi
(D Med Sci)

Guest Scholar

BANASIK, Marek (D Med Sci)

Guest Res Assoc

STROSZNAJDER, Robert (Ph D)

Students

MINAKUCHI, Masayoshi (DC)

MATOH, Naomi (DC)

SHO, Toh (DC)

TAKEHASHI, Masanori (DC)

TAKANO, Emiko (RF)

WILLIAMS, Tyler (RS)

and inactivation of this enzyme.

In the CYP2D gene locus, the microsatellite, a (dG-dT)_n dinucleotide repeat, is located between the CYP2D8P and CYP2D7 genes. In this allelic association study, we analyzed the CYP2D microsatellite in patients with pure AD, LBV and PD [3]. This microsatellite, which is in the linkage disequilibrium with the CYP2D6 B mutation, proved to be a useful marker for assessment of CYP2D6 gene involvement in LB-associated diseases (LBV and PD).

I. Polymorphism of the CYP2D microsatellite.

We found 12 alleles in the CYP2D microsatellite. The size of PCR products ranged from 96 to 118 bp (Figure 1). The number of (dG-dT)_n repeat ranged from 16 to 27. We named each allele A16 to A27 by the repeat number.

II. CYP2D microsatellite polymorphisms in pure AD, LBV and PD.

We then analyzed the distribution of allele frequencies of CYP2D microsatellites in the control and disease groups. The frequencies of the short- and long-type alleles were significantly asso-

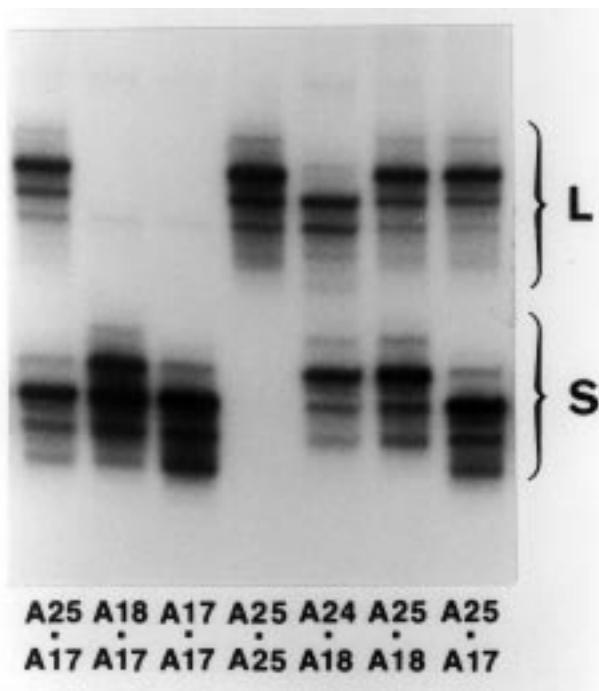


Figure 1. Autoradiogram of the CYP2D microsatellites. Genotypes are shown under respective lanes. The CYP2D microsatellite alleles were categorized into two groups; the short-type (A16 - A20) (S) and the long-type (A21 - A27) (L). The size of the A18 band was 100 bp. "Ghost" bands appeared, at 2-bp intervals, above and below the true band.

ciated with the control and disease groups. The long-type allele was excessively represented in LBV (0.313) compared with control (0.186) or pure AD (0.196). The PD patients also showed this overrepresentation (0.298).

III. CYP2D microsatellite polymorphisms and CYP2D6 B mutation.

The allele frequencies of CYP2D microsatellites were associated with the CYP2D6 B mutation. Its frequency was significantly higher in LBV (0.281) than in control (0.157) or pure AD (0.175). The PD patients also showed a higher value (0.234), although the difference did not reach a significant level in this study.

IV. CYP2D microsatellite polymorphisms and CYP2D6 D mutation.

We analyzed XbaI RFLP in order to investigate a relationship between the structure of the CYP2D gene cluster and CYP2D microsatellite genotypes. Four haplotypes of XbaI RFLP were identified by Southern blot analysis. The 11.5-kb haplotype, or the D mutant allele (deletion mutation), was not associated with the long-type allele. The results of the XbaI RFLP study, combined with those of the PCR analysis, indicated no overrepresentation of the CYP2D6 D mutation in any disease groups.

These findings confirmed a close association of the CYP2D locus with LBV and PD, indicating the following two possibilities: the involvement of the CYP2D6 B mutation in pathogenesis of LBV and PD in a dominant-negative manner; or the linkage disequilibrium of the CYP2D microsatellite to another pathogenic gene locus. The microsatellite of the CYP2D locus could be an informative marker in the genetic study of LBV as well as PD.

References

1. Kawamata, J., Tanaka, S., Shimohama, S., et al., *J. Neurol. Neurosurg. Psychiatry* 57: 1414-1416 (1994)
2. Tanaka, S., Kawamata, J., Shimohama, S., et al., *Dement. Geriatr. Cogn. Disord.* 9: 90-98 (1998)
3. Tanaka, S., Chen, X., Xia, Y., et al., *Neurology* 50: 1556-1562 (1998)

Crystal structures of two tropinone reductases: Different reaction stereospecificities in the same protein fold.

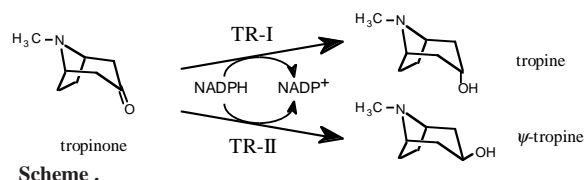
Keiji Nakajima, Atsuko Yamashita, Hiroyuki Akama, Toru Nakatsu, Hiroaki Kato, Takashi Hashimoto, Jun'ichi Oda, and Yasuyuki Yamada

A pair of tropinone reductases (TRs) share 64% identical amino acid residues, and belong to the short-chain dehydrogenase/reductase family. In the synthesis of tropane alkaloids in several medicinal plants, the TRs reduce a carbonyl group of an alkaloid intermediate, tropinone, to hydroxy groups having different diastereomeric configurations. To clarify the structural basis for their different reaction stereospecificities, we determined the crystal structures of the two enzymes at 2.4- and 2.3-Å resolutions. The overall folding of the two enzymes was almost identical. The substrate binding site was composed mostly of hydrophobic amino acids in both TRs, but the presence of different charged residues conferred different electrostatic environments on the two enzymes.

Keywords : X-ray crystallography/ Stereospecificity/ Enzymatic reaction/ alkaloids/ Tropinone reductase/ NADPH

Two tropinone reductases (TRs) constitute a branching point in the biosynthetic pathway of tropane alkaloids, which include such medically important compounds as hyoscyamine (atropine) and cocaine. TRs catalyze NADPH-dependent reductions of the 3-carbonyl group of their common substrate, tropinone, to hydroxy groups with different diastereomeric configurations: TR-I (EC 1.1.1.206) produces tropine (3 α -hydroxytropane), and TR-II (EC 1.1.1.236) produces pseudotropine (ψ -tropine, 3 β -hydroxytropane) (Scheme). The most intriguing question concerning the two TRs is what protein structures enable the enzymes to produce different stereoisomers from the same substrate, tropinone. Only a small number of the amino acid resi-

dues that differ between TR-I and TR-II may actually participate in determining the stereospecificities, and the overall foldings of the two enzymes may not be as different as predicted from their primary structures (1). To verify this idea, we determined the crystal structures of the TRs from *Datura stramonium* (2, 3). The structures revealed a simple evolutionary process adopted by the TRs to acquire their different stereospecificities.



MOLECULAR BIOFUNCTION — Functional Molecular Conversion —

Scope of research

Our research aims are to elucidate structure-function relationships of various biocatalysts in combination with organic chemistry, molecular biology and X-ray crystallography, and to clarify real physiological roles in tea plants of a glycosidase and β -primeverosidase, the latter which was found by ourselves to be mainly concerned with aroma formation during tea manufacturing. Main subjects are (1) Design and synthesis of transition-state analogue inhibitors of ATP-dependent ligases, (2) Chemical, biochemical and molecular biological studies on primeverosidase, (3) Time-resolved X-ray crystallographic study of glutathione synthetase, (5) Development of a new type of microbial lipase by evolutionary molecular engineering, (6) X-Ray crystallography of wild-type and mutant firefly luciferases, and (7) Overexpression and purification of pyruvate phosphate dikinase from Maize.



Prof
SAKATA, Kanzo
(D Agr)



Assoc Prof
HIRATAKE, Jun
(D Agr)



Instr
KATO, Hiroaki
(D Agr)



Instr
MIZUTANI, Masaharu
(D Agr)



Assoc Instr
NAKATSU, Toru
(D Agr)

INOUE, Makoto (DC)
Ma, Seungjin (DC)
ENDO, Masaharu (MC)
FUJII, Ryota (MC)
NAKANISHI, Hidemitsu (MC)
FURUKAWA, Hiroshi (MC)
IWAI, Takayasu (MC)
TAKEGAWA, Mizuki (MC)
GUO, Wenfei (PD, D Agr)

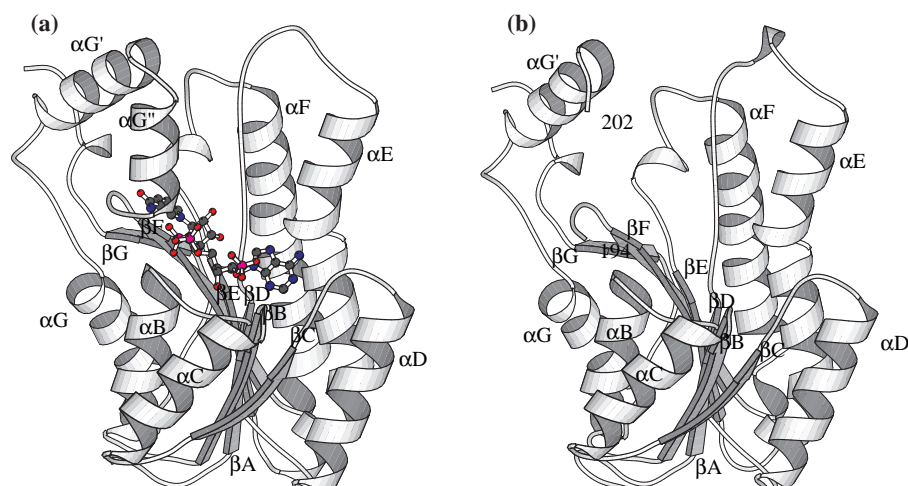


Figure 1.
Subunit structure of TR-I (a),
and TR-II (b).

The subunit structures of the TR-I and TR-II dimers are shown in Fig. 1. The two structures are almost indistinguishable from each other in both subunit folding. Conservation of the subunit structures between TR-I and TR-II was substantiated when the two structures were superimposed by the least squares method using all equivalent C α positions (rms deviation = 0.78 Å). Both TR subunits consist of a core domain that includes most of the polypeptide and a small lobe that protrudes from the core. A deep cleft was recognized between the core domain and the small lobe, which is presumed to be the binding site for tropinone. In the center of the core domain is a seven-stranded parallel β -sheet, flanked on each side by three α -helices, which constitutes the 'Rossmann fold' topology. This core structure is highly conserved among the SDR family members, despite relatively low residue identity between these enzymes (~30%). The small lobes of the two TRs are also very similar to each other, although the structure of this region is highly variable among SDRs for which crystal structures are known. In TR-II, the polypeptide corresponding to α G' is disordered, and therefore could not be modeled.

TR-I protein was crystallized in the presence of NADP⁺, and the bound cofactor molecules in the protein structure could be modeled unambiguously. As seen in Fig. 1a, NADP⁺ is located at the bottom of the cleft between the core domain and the small lobe.

Concurrent conservation of the catalytic residues and the cofactor-binding sites leaves only one explanation for the TR stereospecificities; tropinone should bind TR-I and TR-II in opposite orientations. The bound tropinone was predicted to contact several amino acids in both TRs (Fig. 2). These residues are located either at the two loops in the core domain or in the two α -helices that constitute the small lobe. The positive charge on the TR-I surface is due to His112, which in TR-II is replaced by Tyr100, a polar but not basic residue. The negative charge on the TR-II surface is generated by Glu156,

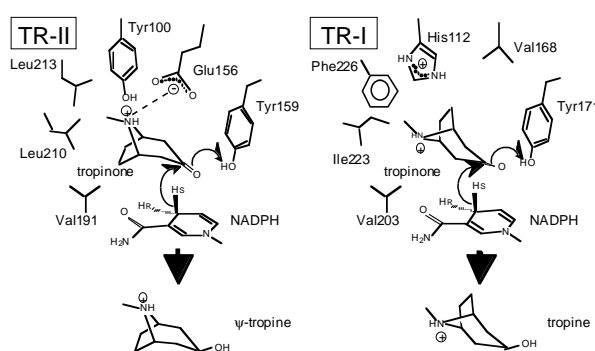


Figure 2. Schematic view of the predicted active sites of TR-I and TR-II.

which is replaced by the hydrophobic Val168 in TR-I. As the nitrogen atom of tropinone is positively charged under physiological pH conditions, the charge distributions in the tropinone-binding sites agreed well with the predicted orientations of tropinone. In contrast, TR-I uses a novel means to orient tropinone, namely repulsion between the positive charges of His112 and the nitrogen atom of tropinone. Apart from the charged residues described above, most of the amino acids that would contact tropinone within the binding sites, are hydrophobic. These residues would provide a favorable environment for the binding of tropinone which generally has a hydrophobic nature.

The structures presented here are the first for a pair of enzymes that are closely related evolutionarily but which have different reaction stereospecificities. Comparison of the two TR structures made clear that opposite reaction stereospecificities can be acquired in enzymes that have a conserved overall folding, by changing the amino acids in the substrate-binding site.

References

- (1) Nakajima K., *et al. PNAS* **90**, 9591-9595 (1993).
- (2) Nakajima K., *et al. PNAS* **95**, 4876 - 4881 (1998).
- (3) Yamashita A., *et al. Acta Cryst. D* **54**, 1405-1407 (1998).

Non-stereospecific Transamination Catalyzed by Pyridoxal Phosphate-dependent Amino Acid Racemases of Broad Substrate Specificity

Nobuyoshi Esaki, Tohru Yoshimura, Kenji Soda and Young Hee Lim

Pyridoxal 5'-phosphate-dependent amino acid racemases of broad substrate specificity catalyze transamination as a side-reaction. We studied the stereospecificities for hydrogen abstraction from C-4' of the bound pyridoxamine 5'-phosphate during transamination from pyridoxamine 5'-phosphate to pyruvate catalyzed by three amino acid racemases of broad substrate specificity. When the enzymes were incubated with (4'S)- or (4'R)-[4'-³H]-pyridoxamine 5'-phosphate in the presence of pyruvate, tritium was released into the solvent from both pyridoxamine 5'-phosphates. Thus, these enzymes abstract a hydrogen non-stereospecifically from C-4' of the coenzyme in contrast to the other pyridoxal 5'-phosphate-dependent enzymes so far studied which catalyze the stereospecific hydrogen removal. Amino acid racemase of broad substrate specificity from *Pseudomonas putida* produced D- and L-glutamate from α -ketoglutarate through the transamination with L-ornithine. Because glutamate does not serve as a substrate for racemization, the enzyme catalyzed the non-stereospecific overall transamination between L-ornithine and α -ketoglutarate. The cleavage and formation of the C-H bond at C-4' of the coenzyme and C-2 of the substrate thus occurs non-stereospecifically on both sides of the plane of the coenzyme-substrate complex intermediate. Amino acid racemase of broad substrate specificity is the first example of a pyridoxal enzyme catalyzing non-stereospecific transamination.

Keywords : Amino acid racemase/ Stereochemistry/ Pyridoxal phosphate

Although enzymatic racemization of amino acid is apparently simple, consisting of a non-stereospecific rearrangement of the substrate α -hydrogen, several different types of amino acid racemases are found in microorganisms. Aspartate racemase and glutamate racemase are independent of cofactors. Alanine racemase in several microorganisms, and amino acid racemases of broad substrate specificity of *Pseudomonas putida* depend

on pyridoxal 5'-phosphate (PLP). The reaction of amino acid racemase is initiated by transaldimination. In this step, PLP bound with the active-site lysyl residue through an internal Schiff base (Scheme I, A) reacts with a substrate to form an external Schiff base (B). The subsequent α -hydrogen abstraction results in the formation of a resonance-stable anionic intermediate (C). If the reprotonation occurs at C-2 of the substrate moiety on the

MOLECULAR BIOFUNCTION - Molecular Microbial Science -

Scope of research

Structure and function of biocatalysis, in particular, pyridoxal enzymes, NAD enzymes, and enzymes acting on xenobiotic compounds are studied to elucidate the dynamic aspects of the fine mechanism for their catalysis in the light of recent advances in gene technology, protein engineering and crystallography. In addition, the metabolism and biofunction of selenium and some other trace elements are investigated. Development and application of new biomolecular functions of microorganisms are also studied to open the door to new fields of biotechnology. For example, molecular structures and functions of thermostable enzymes and their application are under investigation.



Prof
ESAKI,
Nobuyoshi
(D Agr)



Assoc Prof
YOSHIMURA,
Tohru
(D Agr)



Instr
KURIHARA,
Tatsuo
(D Eng)

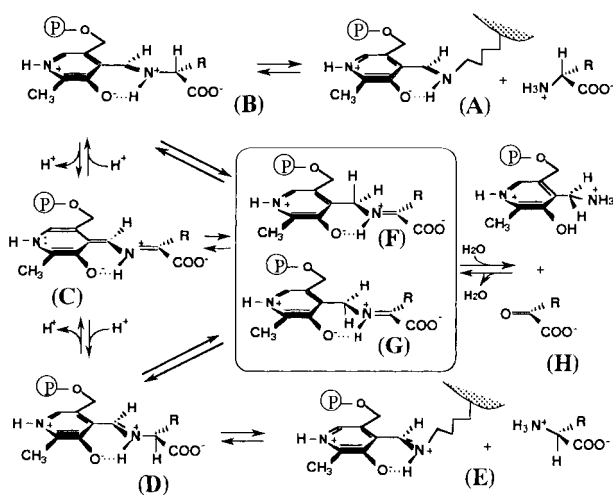
Technician: SEKI, Mio; UTSUNOMIYA, Machiko

Guest Research Associate: GALKIN, Andrey

Students: MIHARA, Hisaaki (DC); WATANABE, Akira (DC); BAHK, Song-Chul (DC); ICHIYAMA, Susumu (DC); KULAKOVA, Ludmila (DC); UO, Takuma (DC); YOSHIMUNE, Kazuaki (DC); KATO, Shin-ichiro (MC); NISHIYAMA, Tozo (MC); TAKEDA, So (MC); UEDA, Momoko (MC); WATANABE, Tasuku (MC); WEI, Yun-Lin (MC); ISUI, Ayako (MC); NAKAYAMA, Daisuke (MC); TOHDO Fumiko (MC); SAITOH, Mami (MC); YAMAUCHI, Takahiro (MC)

opposite face of the planar intermediate to that where the proton abstraction occurs, an antipodal aldimine is formed (D). The aldimine complex is subsequently hydrolyzed to form isomerized amino acid, and regenerates the bound PLP (E). The random return of hydrogen to the anionic intermediate is a characteristic of enzymatic racemization among various pyridoxal enzyme reactions. In aminotransferase reactions, the abstracted hydrogen is stereospecifically transferred to C-4' of the cofactor, and a ketimine intermediate is formed. The pyridoxamine 5'-phosphate (PMP) form of the enzyme and a keto acid are produced by hydrolysis of the ketimine intermediate. Amino acid racemases are reported to catalyze the transamination as a side reaction. The transamination catalyzed by amino acid racemases can be attained through a sequence either $A \rightarrow B \rightarrow F$ (or G) $\rightarrow H$, or $A \rightarrow B \rightarrow C \rightarrow F$ (or G) $\rightarrow H$ (Scheme I). An equivalent route can be delineated for the antipode: $E \rightarrow D \rightarrow F$ (or G) $\rightarrow H$, or $E \rightarrow D \rightarrow C \rightarrow F$ (or G) $\rightarrow H$. In transamination, mutual hydrogen transfer between the substrate and C-4' of the cofactor occurs. In all previous studies of transaminations catalyzed by aminotransferases as well as other pyridoxal enzymes, the hydrogen transfer between substrate and cofactor occurs strictly stereospecifically on the *si* or *re* face of the plane of the anionic intermediate. However, if the transamination catalyzed by amino acid racemases proceeds as depicted in Scheme I, the hydrogen transfer should occur non-stereospecifically on both faces of the planar intermediate. We were therefore interested in the stereospecificity for the hydrogen transfer during transamination catalyzed by amino acid racemases as a side-reaction, and provide the first evidence that hydrogen removal from C-4' of PMP occurs randomly on both faces of the substrate-cofactor imine plane during half transamination catalyzed by the amino acid racemases (1). We also show that the enzyme catalyzes non-stereospecific overall transamination between L-ornithine and α -ketoglutarate as well.

The absorption spectral change has demonstrated that



Scheme I. Reaction mechanism of amino acid racemase

the amino acid racemase of broad substrate specificity from *Ps. putida* catalyzes the transamination between PMP and pyruvate. When the PMP-form of an enzyme is converted to the PLP form by transamination with keto acid, one of the two hydrogens at C-4' of PMP is usually transferred stereospecifically to C α of the keto acid. We studied the stereospecificity of amino acid racemase for hydrogen abstraction from C-4' of PMP by measurement of the radioactivity of ^3H released from the PMPs which are stereospecifically tritiated at C-4' using the method described previously (2). Each 5 nmol of apo-amino acid racemase was incubated with 1 nmol of (4'*S*)- or (4'*R*)-[4'- ^3H]PMP and 5 nmol of sodium pyruvate. We deduce that PMP was completely converted to PLP because the PMP-form of the amino acid racemase from *Ps. putida* recovered 100 % of the activity theoretically expected. Tritium was released equally from both (4'*S*)- and (4'*R*)-[4'- ^3H]PMPs in the presence of amino acid racemases. The amount of tritium released from each PMP was about 50% of that which initially existed. The control experiment with D-AAT and AspAT showed that they catalyzed the stereospecific removal of tritium from (4'*R*)- or (4'*S*)-[4'- ^3H]PMP, respectively. These results confirm the stereospecific tritium labelling of both PMPs. Thus, the amino acid racemases catalyze the non-stereospecific abstraction of hydrogen from C-4' of PMP. They are the first class of pyridoxal enzyme catalyzing the hydrogen removal on both sides of the plane of a substrate-cofactor complex during transamination.

If the hydrogen is introduced non-specifically to C-2 of the keto acid moiety of the anionic intermediate on both sides of the planar intermediate during the half reaction of transamination, racemic amino acid is formed from the keto acid (Scheme I; $H \rightarrow F$ (or G) $\rightarrow C \rightarrow B \rightarrow A$, or $H \rightarrow F$ (or G) $\rightarrow C \rightarrow D \rightarrow E$). We studied the stereochemistry of glutamate formed from α -ketoglutarate by transamination with L-ornithine catalyzed by the amino acid racemase of *Ps. putida*. After the reaction, the products were derived to diastereomers with Marfey's reagent, and subjected to HPLC. Both enantiomers of glutamate and ornithine were found. The amino acid racemase from *Ps. putida* catalyzes the racemization of ornithine, but glutamate is inert as a substrate for the racemase reaction. Thus, both enantiomers of glutamate were directly formed by transamination, not by racemization of one enantiomer produced through transamination. The amino acid racemase from *Ps. putida* is the first example of a pyridoxal enzyme catalyzing non-stereospecific transamination.

References

1. Lim, Y.-H., Yoshimura, T., Kurokawa, Y., Esaki, N. and Soda, K. (1998) *J. Biol. Chem.* **273**, 4001-4005
2. Yoshimura, T., Nishimura, K., Ito, J., Esaki, N., Kagamiyama, H., Manning, J. M., and Soda, K. (1993) *J. Am. Chem. Soc.* **115**, 3897-3900

The Crystal Structure of Zinc-Containing Ferredoxin from a Thermoacidophilic Archaeon

Tomomi Fujii and Yasuo Hata

The crystal structure of ferredoxin from thermoacidophilic archaeon *Sulfolobus* sp. strain 7 was determined by X-ray diffraction analysis at 2.0 Å resolution. The structure of the archaeal ferredoxin consists of two parts: core fold part and the N-terminal extension part. The distinct structural feature of this archaeal ferredoxin lies in the zinc-binding center where the zinc ion is tetrahedrally ligated by four amino acid residues. The zinc ion in the zinc-binding center is located at the interface between the core fold and the N-terminal extension, and connects the β -sheet in the N-terminal extension and the central β -sheet in the core fold through the zinc ligation. Thus the zinc ion plays an important role in stabilizing the structure of the present archaeal ferredoxin by connecting the N-terminal extension and the core fold, which may be common to thermoacidophilic archaeal ferredoxins.

Key words ; X-ray analysis/ Zinc/ Iron-sulfur cluster/ Thermostability

Ferredoxins (Fds) are electron transfer proteins which have iron-sulfur clusters as their active sites, and are distributed over a wide range of living organisms. Various kinds of Fds isolated from different organisms are classified by the geometry of the Fe-S cluster into several types. The dicluster-type Fds frequently isolated from bacteria are well known to share a common protein fold known as the $(\beta\alpha\beta)_2$ fold ligating two cubane-like Fe-S clusters (2[4Fe-4S] or [3Fe-4S][4Fe-4S]). This type of Fds are also isolated from Archaea.

Archaea (archaeobacteria), which grow under extreme conditions such as high temperature, strong acidity, high salinity and anaerobicity, constitute a group of organisms which is distinct from Bacteria and Eucarya [1]. *Sulfolobus* sp. strain 7 is a thermoacidophilic archaeon which grows optimally at pH 2.5-3.0 and 75-80°C [2]. Ferredoxin from *Sulfolobus* sp. strain 7 is known to serve as an electron acceptor of a 2-oxoacid:Fd oxidoreductase. The *Sulfolobus* Fd molecule consists of

a polypeptide of 103 amino acid residues, and two Fe-S clusters [3]. The primary structure of the *Sulfolobus* Fd is distinct from those of bacterial Fds in two regions; the *Sulfolobus* Fd has an N-terminal extension of about 40 residues and an insertion of about 10 residues in the middle of the polypeptide chain. Such a characteristic extension and insertion in sequence has also been found in ferredoxins from other thermoacidophilic archaea. Therefore, the additional regions are expected to adopt informative conformations characteristic to thermoacidophilic archaeal Fds. In order to elucidate the stabilization mechanism and the evolutionary status of archaeal proteins by investigating structural features of thermoacidophilic archaeal Fds, we have determined the crystal structure of ferredoxin from *Sulfolobus* sp. strain 7 by X-ray analysis.

The *Sulfolobus* ferredoxin was crystallized by a batch method using ammonium sulfate as a precipitant. The crystals belong to the tetragonal space group $P4_32_12$ with

MOLECULAR BIOLOGY AND INFORMATION – Biopolymer Structure –

Scope of research

Our research aims are to elucidate structure-function relationships of biological macromolecules, mainly proteins, by using physicochemical methods such as spectroscopic and X-ray diffraction methods. The following attempts have been mainly made in our laboratory for that purpose. (1) Peptide secondary or supersecondary structures in aqueous or hydrophobic environments are studied to get a principle of protein architecture, employing various spectroscopic methods. (2) X-ray diffraction studies on protein structures in crystal and in solution are carried out by crystallographic and/or small-angle X-ray scattering techniques to elucidate structure-function relationships of proteins. (3) Molecular mechanism for myosin assembly is studied by proteolytic method, electron microscopy, and computer analysis of the amino acid sequence.



Prof
TAKAHASHI,
Sho
(D Sc)



Assoc Prof
HATA,
Yasuo
(D Sc)



Instr
HIRAGI,
Yuzuru
(D Sc)



Instr
FUJII,
Tomomi
(D Sc)



Instr
AKUTAGAWA,
Tohru

Students:
KURIHARA, Eiji (MC)
SAKAI, Hisanobu (MC)

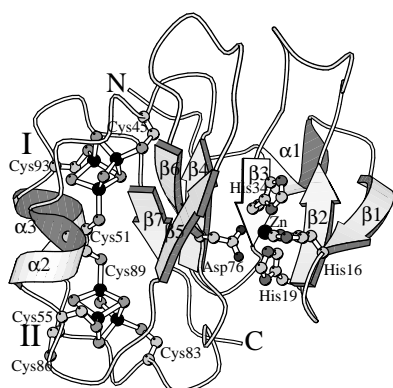


Figure 1. Schematic drawing of the *Sulfolobus* Fd molecule. β -strands are shown as gray arrows and α -helices are shown as gray spirals. The [3Fe-4S] clusters, the seven cysteines, the zinc ion and the four zinc-ligand residues are represented as ball-and-stick models. Fe-S cluster I and II are indicated as I and II, respectively.

cell dimensions of $a = b = 50.12 \text{ \AA}$ and $c = 69.52 \text{ \AA}$. The structure was determined by the isomorphous replacement method for the uranium and platinum derivatives, supplemented with anomalous dispersion effects from the iron atoms of the Fe-S clusters as well as the uranium atoms in the derivative. In the course of the structural analysis, an uninterpreted high density peak coordinated by three histidines and one aspartate in a tetrahedral manner suggested that the present Fd molecule might contain a divalent metal cation such as Zn^{2+} . The X-ray crystallographic identification of the metal ion was performed using anomalous dispersion effects characteristic for zinc which were measured with a tuneable synchrotron radiation source. Finally, the whole model of the Fd molecule was refined to an R factor of 0.173 at 2.0 \AA resolution.

The overall structure of the *Sulfolobus* Fd molecule is depicted in Fig. 1. The protein folding of the *Sulfolobus* Fd can be divided into two parts by a structural comparison of the present archaeal Fd with other bacterial dicluster Fds (Fig. 2). One part is the core-fold part (residues 37-103), which binds two [3Fe-4S] clusters and has a topologically conserved protein folding; a $(\beta\alpha\beta)_2$ fold, common to bacterial dicluster Fds, forms two antiparallel β -sheets, A ($\beta 4$ and $\beta 7$) and B ($\beta 5$ and $\beta 6$), and two α -helices, $\alpha 2$ and $\alpha 3$. The other part is the N-terminal extended part (residues 1-36), which is mainly formed by one-turn α -helix $\alpha 1$ and antiparallel β -sheet A' of strands 1-3. β -Sheet A' in the N-terminal part interacts with the terminal β -sheet A in the core-fold part through hydrogen bonds between strands $\beta 3$ and $\beta 4$ to form a larger five-stranded β -sheet, A'+A. As described above, the *Sulfolobus* Fd molecule contains a novel zinc-binding center, which had never been found in ferredoxins, at the interface between the core-fold part and the N-terminal extended part (Fig. 1). The zinc ion is tetrahedrally ligated by four amino acid residues, His 16, His 19 and His 34 from the N-terminal part, and Asp 76 from the core-fold part. Three ligand histidines, His 16, His 19 and His 34, to the zinc ion are located at the C-, N-

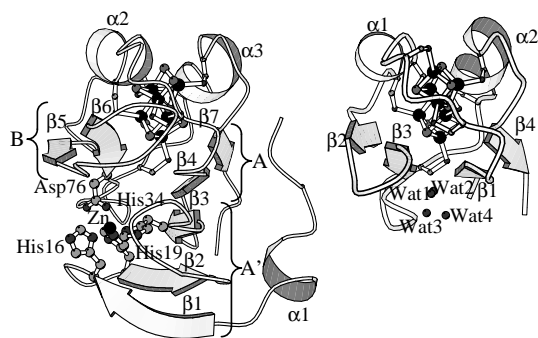


Figure 2. Schematic drawing of bacterial Fd molecules, viewed from the top of Figure 1. (left) The *Sulfolobus* Fd, (right) *Clostridium acidurici* Fd. The Fe-S clusters and the residues which participate in interaction between β -sheets A and B are represented with ball-and-stick models. The atoms of the Fe-S cluster ligating cysteine residues are only represented with small balls. β -Sheets A (strands $\beta 4$ and $\beta 7$), A' (strands $\beta 1$, $\beta 2$ and $\beta 3$) and B (strands $\beta 5$ and $\beta 6$) in the *Sulfolobus* Fd are indicated as A, A' and B, respectively.

and C-terminal ends of three β -strands, $\beta 1$ - $\beta 3$, respectively, which form β -sheet A' in the N-terminal extended part. The zinc ion binds tightly through the Zn-His coordinate bonds to β -sheet A' which interacts with β -sheet A through hydrogen bonds between $\beta 3$ and $\beta 4$ to form the larger sheet, A'+A. The last zinc ligand, Asp 76, is located at the C-terminal end of strand $\beta 6$ in β -sheet B. In this way, two β -sheets, A and B, in the core-fold part, are indirectly linked by both the zinc ligation between β -sheets B and A' and the hydrogen bonds between β -sheets A' and A (Fig. 2).

The core fold common to bacterial Fds adopts a quite simple $(\beta\alpha\beta)_2$ fold. In the core-fold part of bacterial dicluster Fds, β -sheets A and B are usually so apart from each other that they do not interact directly (Fig. 2). The unfolding of the core fold may begin with dissociation of the two β -sheets. If the interaction between the β -sheets is strong, the unfolding of the core fold would be unlikely to occur. Indeed, the *Sulfolobus* Fd seems to utilize the zinc ion, the N-terminal extension and the insertion in order to enhance the stability of the core fold through the indirect interaction between the two β -sheets. Therefore, thermoacidophilic archaeal Fds may acquire thermostability primarily by inserting the zinc ion in the interface between the extended N-terminal and the core-fold parts, as observed in the *Sulfolobus* Fd. It is expected that biochemical and biophysical studies on the roles of the zinc ion in thermoacidophilic archaeal Fds might lead to elucidation of the role of metal ions in protein thermostability.

References

1. Woese C R, Kandler O and Wheelis M L, *Proc. Natl. Acad. Sci. U.S.A.*, **87**, 4776-4579 (1990).
2. Wakagi T and Oshima T, *Biochim. Biophys. Acta*, **817**, 33-41 (1985).
3. Wakagi T, Fujii T and Oshima T, *Biochem. Biophys. Res. Commun.*, **225**, 489-493 (1996).

Two-component Response Regulators from *Arabidopsis thaliana* Contain a Putative DNA-binding Motif

Hiroe Sakai, Takashi Aoyama, Hidemasa Bono, and Atsuhiko Oka

An expression sequence tag database of higher plants was screened by *in silico* profile analysis for response regulators of the two-component regulatory system. Two closely related genes (*ARR1* and *ARR2*), corresponding to one of the extracted candidates, were isolated from *Arabidopsis thaliana*. The two genes were comparably expressed in all tissues, and at higher levels in the roots. The amino-terminal half of their translation products was highly conserved. This is where a phosphate receiver domain with the landmark aspartate residue and a putative DNA-binding domain were located. Their carboxyl-terminal halves, although less similar to each other, included glutamine-rich and proline-rich regions characteristic of the transcriptional activation domain of eukaryotes. This architecture resembles that of typical bacterial response regulators serving as transcription factors.

Keywords: *Arabidopsis* / Response regulator / Transcription factor / Two-component regulatory system

Extracellular stimuli received by living cells are processed through signal transduction pathways and result in orchestrated gene expression. A large number of intracellular signal transduction pathways have been studied with eukaryotic cells. Many plant proteins (or their genes) similar to the components involved in animal and fungus signal transduction pathways have been identified. Recently, the *Arabidopsis thaliana* genes *ETR1* and *CKII*, which are implicated in ethylene and cytokinin responses, respectively, have been shown to code for proteins similar to the sensor of a two-component regulatory system, which is the ubiquitous signal transduction system in bacteria (1). This suggests that the bacterial type of signal transduction pathway, or a similar one, may possibly exist in plant cells. To elucidate an entire plant

signal transduction pathway incorporating the two-component regulatory system, the functions executed by the plant response regulator components must be known. In this respect, an attempt has been made to clone plant response regulator genes, but no response regulator in which the signal receiver domain accompanies other known functional domains has been identified. We here show the presence of two *A. thaliana* response regulators with characteristics of transcription factors (2), like the majority of bacterial response regulators.

Using the profile method (3), the similarity score was calculated for each entry in the plant EST database. We extracted 21 EST sequences of *A. thaliana* and rice with high scores, and found that 11 of their central aspartate residues were accompanied by additional landmark resi-

MOLECULAR BIOLOGY AND INFORMATION — Molecular Biology —

Scope of research

Attempts have been made to elucidate structure-function relationships of genetic materials and various gene products. The major subjects are mechanisms involved in signal transduction and regulation of gene expression responsive to environmental stimuli, differentiation and development of plant organs, and plant-microbe interaction. As of December 1998, study is being concentrated on the roles of homeo domain proteins, MADS box proteins, and DDK response regulators of higher plants in developmental and signal transduction processes.



Prof
OKA, Atsuhiko
(D Sc)



Assoc Prof
AOYAMA, Takashi
(D Sc)



Instr
GOTO, Koji
(D Sc)

Students:

TSUKUDA, Mayumi (DC)
HOMMA, Takashi (DC)
OHGISHI, Maki (DC)
SAKAI, Hiroe (DC)
LIANG Yajie (DC)
YANO, Hiroyuki (DC)
UEDA, Yumi (MC)
OHASHI, Yohei (MC)

dues, the fore aspartate or rear lysine residues at distances suitable for the D-D-K signal receiver domain in the response regulator. These can be structurally classified into three groups I, II, and III. Since the group I candidates appeared to code for additional functional domains from their mRNA sizes (see below), we carried out cloning experiments for the corresponding genes with an *A. thaliana* genomic library. As a result, we isolated two closely related D-D-K receiver genes (*ARR1* and *ARR2*).

The starting and terminating sites of *ARR1* and *ARR2* transcription were estimated by 5'- and 3'-RACE analyses on a mixture of *A. thaliana* cDNA. The transcriptional unit was thus determined to be 3,093 bp long for *ARR1* and 3,508 bp long for *ARR2*. These sequence data were deposited in the DDBJ/EMBL/GenBank databases (AB016471 and AB016472). To determine the exon-intron organization of these two genes, PCR was done on an *A. thaliana* cDNA mixture with various sets of primers, and the resulting PCR fragments were sequenced. We found that *ARR1* and *ARR2* are split by four and five introns, respectively. The sizes of the mature mRNA for *ARR1* and *ARR2* were thus calculated to be 2,362 and 2,697 residues, respectively.

The *ARR1* and *ARR2* translation products consisted of 669 and 664 amino-acid residues, respectively. Both proteins had comparable domain architecture. The D-D-K signal receiver domain was located at the amino-terminal end of both (aa 37-150 for *ARR1* and aa 28-141 for *ARR2*), and 95% of the amino-acid residues were identical. A potential nuclear localization signal followed the receiver domain of both *ARR1* (aa 152-157) and *ARR2* (aa 143-148). Another highly similar region (96% identity) was aa 236-299 of *ARR1* and aa 215-278 of *ARR2*. This region showed strong resemblance to a segment found in various proteins with unknown functions. In addition, we noticed a weak but significant similarity of this region to the DNA-binding Myb oncoprotein, particularly to the potato Myb homolog MybSt1, and this region is called the Myb-like domain hereafter. In contrast to the strong resemblance of the amino-terminal half of the gene products, the carboxyl-terminal half (aa 300-669 of *ARR1* and aa 279-664 of *ARR2*) was not as highly conserved, and only 52% of the amino-acid residues were identical when the appropriate gaps were incorporated. Although the amino-acid sequence of this domain itself showed no obvious similarity to other proteins, this domain, particularly the one in *ARR1*, was rich in glutamine. It also had higher than average amounts of proline, serine, and phenylalanine residues.

Northern blot hybridization analysis of the *ARR1* and *ARR2* transcripts with specific probes was carried out by

using total RNA from roots, rosette leaves, cauline leaves, stems, flower buds/flowers, and siliques of *A. thaliana* that had been grown under the standard conditions. The results revealed that the expression patterns of the two genes are similar to each other, though the transcription level of *ARR1* is always slightly higher than that of *ARR2*, and that the two genes are transcribed in all tissues, and at higher levels in the roots. The mRNA sizes estimated from the Northern analysis were about 2.4 kb for *ARR1* and 2.8 kb for *ARR2*. These values are consistent with those calculated from the transcription unit and exon-intron organization of both genes.

To estimate the copy number of *ARR1* and *ARR2* on the *A. thaliana* chromosomes, Southern blot hybridization analysis was performed. Under high-stringency conditions, each probe of the entire coding-region produced a limited number of signal bands, which were expected from the genomic sequence. On the other hand, under low-stringency conditions several additional weak bands were detected. The bands with relatively higher signal intensities corresponded to the bands that were clearly visualized by the other probe under the high-stringency conditions. These results indicated that the *A. thaliana* genome contains one copy each of *ARR1* and *ARR2* and presumably a few additional cognate genes, constituting a small gene family.

To obtain information on localization of the *ARR1* and *ARR2* proteins in cells, their cDNAs were connected in-frame to GUS under the control of cauliflower mosaic virus 35S promoter, and then introduced into onion epidermal cells by the particle delivery system. Histological staining analysis revealed that either fusion protein is located in nuclei. Furthermore, when the D-D-K signal receiver domain was replaced by yeast GAL4 DNA binding domain, the resulting recombinant proteins conferred the ability to activate transcription of the reporter gene with the GAL4 target element in tobacco cells. These results strongly suggest that *ARR1* and *ARR2* actually work as a transcription factor in plant cells, as supposed from their architecture. This is the first report delineating plant response regulators in which the signal receiver domain accompanies other functional domains such as nuclear localization domain, transcriptional activation domain, and probable DNA-binding domain.

References

1. Oka A, *Tanpakushitsu-Kakusan-Kouso*, **40**, 1010-1021 (1995).
2. Sakai H, Aoyama T, Bono H, and Oka A, *Plant Cell Physiol.*, **39**, 1232-1239 (1998).
3. Dodd IB, Egan JB, *J. Mol. Biol.*, **194**, 557-564 (1987).

NLS (Nuclear Localization Signal) Prediction

Keun-Joon Park and Minoru Kanehisa

The nucleus of eukaryotic cells contains many nuclear proteins that function for delivery of molecular information between cytosol and nucleus, and for control of gene expression. After the synthesis on the ribosomes in the cytoplasm, these proteins enter the nucleus through pore complexes in the nuclear envelope. Nuclear proteins are transported into the nucleus, if they contain nuclear localization signals (NLSs). In this work we developed a method that predicts a location of NLS on a query protein sequence by computational analysis. We employed Hidden Markov Model (HMM) in our method to find NLSs in the amino acid sequences. The prediction performance was assessed by leave-one-out cross-validation.

keywords: Nuclear transport / Protein sorting / Database / Bioinformatics

In eukaryotic cells, there are functionally distinct, membrane-bounded compartments. The intracellular compartments in eukaryotic cells contain their own characteristic proteins with different functions. Most nuclear proteins move into nucleus through the nuclear pores that penetrate nuclear envelope (Fig. 1). Nuclear pore is formed by a large, complex structure known as the nuclear pore complex (NPC). The selective transport of proteins through the NPC is performed by their own nuclear localization signals (NLSs). The first NLS was found from SV40 T antigen as a short cluster of five contiguous positively charged residues in the sequence 126 PKKKRKV 132 (3). A family of simple NLSs of this type were generally characterized by one short basic

stretch of sequence (4-8 residues) containing several lysine and arginine residues. The precise location of an NLS within the amino acid sequence of a nuclear protein is not important unlike other signal peptides (4). Robbins et al. found other type of NLS in the nucleoplasmin, the major nuclear protein of the xenopus oocyte (5,6). This type of signal, known as bipartite NLS motif, contains two interdependent positively charged clusters separated by a mutation tolerant linker region of 10-12 amino acids.

In this study we developed a method that predicts the location of NLS and the possibility of a nuclear protein by computational analysis of NLSs. For this purpose, we constructed data sets from the SWISS-PROT protein sequence database (simple NLS 100 entries and bipartite

MOLECULAR BIOLOGY AND INFORMATION — Biological Information Science —

Scope of research

This laboratory aims at developing theoretical frameworks for understanding the information flow in biological systems in terms of genes, gene products, other biomolecules, and their interactions. Toward that end a new deductive database is being organized for known molecular and genetic pathways in living organisms, and computational technologies are being developed for retrieval, inference and analysis. Other studies include: functional and structural prediction of proteins from sequence information and development of sequence analysis tools.



Prof
KANEHISA, Minoru
(D Sc)



Instr
GOTO, Susumu
(D Eng)



Instr
OGATA, Hiroyuki
(D Sc)

Students:

SUZUKI, Kenji (DC)
KIHARA, Daisuke (DC)
KAWASHIMA, Shuichi (DC)
PARK, Keun-Joon (DC)
HATTORI, Masahiro (DC)
BONO, Hidemasa (DC)
IGARASHI, Yoshinobu (DC)
KATAYAMA, Toshiaki (DC)
SATO, Kiminobu (DC)
TAKAZAWA, Fumi (MC)
TANIGUCHI, Takeaki (MC)
NAKAO, Mitsuteru (MC)
OKUJI, Yoshinori (MC)
LIMVIPHUVADH, Vachiranee (RS)

Research Fellow:

SATO, Kazushige (RF)

NLS 75 entries). We used Hidden Markov Model (HMM) for predicting NLSs within the amino acid sequences and for calculating the strength of the signals. We trained two (simple and bipartite) HMMs for unaligned sequences of NLSs in our data sets.

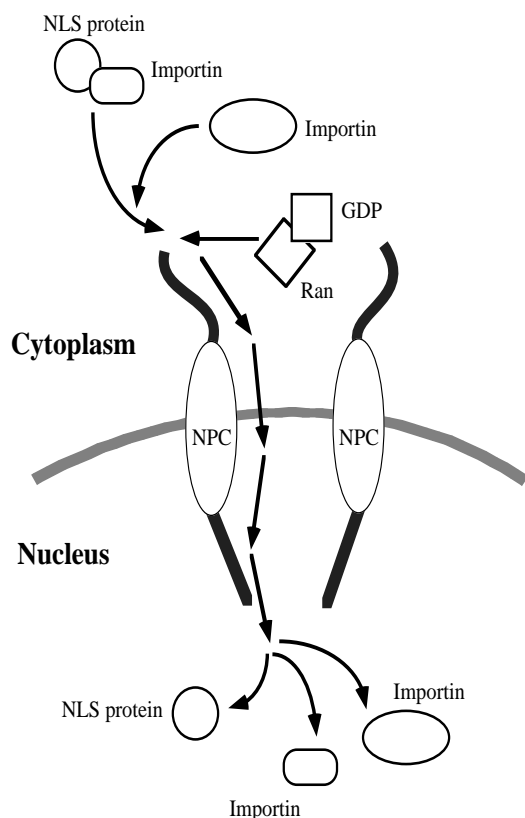


Figure 1. Nuclear protein import
(NLS: Nuclear Localization Signal; NPC: Nuclear Pore Complex)

The performance of the HMMs to recognize NLSs trained on the data sets may be improved by using calculation with fewer different kinds of amino acids (alphabet characters). In this work we changed all arginines (R) to lysines (K) in the sequences of the data sets and the query proteins, since these two positively charged residues would likely to have the same function in NLSs. It seems that the NLSs are usually situated at the extended loop structure that is accessible to the solvent (7). Therefore we examined the frequency of amino acid residues in the NLSs and their secondary structure propensity in order to reduce the number of amino acid types for training. Some amino acids were selected for HMM training and the other amino acid residues were changed into residue Xs in both of the two NLS cases.

To test the performance of the HMM, each protein sequence in the data set was selected once as a test sequence for the HMMs trained for the other sequence in the data set. Specifically, the performance was assessed by leave-one-out cross-validation; the leave-one-out idea is often called "jack-knife test". In the training step, one NLS is left out from the training set. Then the protein sequence containing the NLS is used for checking the performance of the trained HMM. The HMM for simple NLSs was trained for 99 from 100 samples and tested on the remaining one. This process was repeated 100 times for different test sequence. The second HMM for bipartite NLSs was trained for 74 from 75 data set entries and yielded 75 different HMMs. We examined whether two HMMs can recognize their own NLS sequences in their data set or not. As a result, the prediction accuracy of our method was 88.0% and 90.7% for simple and bipartite NLSs, respectively. In conclusion, we confirmed that the two HMMs could predict NLS in amino acid sequences with high performance.

Acknowledgments

This work was supported in part by a Grant-in-Aid for Scientific Research on Priority Areas 'Genome Science' from the Ministry of Education, Science, Sports and Culture in Japan. The computation time was provided by the Supercomputer Laboratory, Institute for Chemical Research, Kyoto University.

References

1. D. Kalderon, W.D. Richardson, A.F. Markham and A.E. Smith, *Nature*, **311**, 33 - 38 (1984).
2. J. Garcia-Bustos, J. Heitman and M.N. Hall, *Biochim. Biophys. Acta*, **1071**, 83 - 101 (1991).
3. J. Robbins, S.M. Dilworth, R.A. Laskey, and C. Dingwall, *Cell*, **64**, 615 - 623 (1991).
4. C. Dingwall and R.A. Laskey, *Trends Biochem. Sci.*, **16**, 478 - 481 (1991).
5. J. Löwe, D. Stock, B. Jap, P. Zwickl, W. Baumeister, R. Huber, *Science*, **268**, 533 - 539 (1995).

Simulation Study of Three-Dimensional Laser Cooling Method for Fast Stored Ion Beams

Takahiro Kihara, Hiromi Okamoto and Yoshihisa Iwashita

Three-dimensional (3D) laser cooling method of fast stored ion beams based on linear coupling mechanism is explored. We employ the tracking code "SAD", showing that resonant coupling remarkably enhances transverse cooling rates. Molecular dynamics (MD) code "SOLID" is also employed to study the effect of space charges and the possibility of beam crystallization.

Keywords : Beam-Cooling/ Coupling/ Simulation/ Space-Charge/ Storage Ring

To our current knowledge, Doppler laser cooling is the most promising technique in achieving the highest possible phase-space density of ion beams [1]. It has already been experimentally demonstrated that one can produce an ultra-cold beam close to the longitudinal space-charge limit [2, 3]. In contrast, laser cooling in the transverse directions has been much less effective. Therefore one may need to develop some novel approach in order to extend the powerful laser cooling force to the transverse degrees of freedom.

For this purpose, a novel method has been proposed in the previous publications [4, 5]. The idea is simple, that is, we develop a synchrotron coupling to indirectly increase the transverse cooling rates. The coupling source theoretically considered was the linear potential induced either by *momentum dispersion* in a regular RF cavity [4], or by a special *coupling cavity* operating in TM_{210} mode [5]. It has been proven that the transverse cooling rates can be most enhanced under the resonance conditions

$$v_s - v_x \approx \text{integer} \quad \text{and} \quad v_x - v_y \approx \text{integer}, \quad (1)$$

where v_x , v_y , and v_s are, respectively, the horizontal, vertical and longitudinal tunes.

In order to carry out reliable numerical experiments where realistic lattice structures of storage rings is taken into account, we employed the tracking code "SAD (Strategic Accelerator Design)" [6] to systematically explore the behavior of the beam at high temperature. As an example, we considered the lattice parameter of the ASTRID ring in Denmark [2], one of the two storage rings in which a laser cooling system has been installed (another is the TSR ring in Germany [3]). Under the typical operating condition of ASTRID, we obtain Fig. 1(a), where no transverse cooling is visible. On the other hand, Fig. 1(b) corresponds to the case where the lattice parameters have been modified so as to roughly satisfy the resonance conditions in Eq. (1). The effectiveness of the coupling scheme is evident.

The effect of particle Coulomb interactions dominates

NUCLEAR SCIENCE RESEARCH FACILITY — Beams and Fundamental Reaction —

Scope of research

Particle beams, accelerators and their applications are studied. Structure and reactions of fundamental substances are investigated through the interactions between beams and materials such as nuclear scattering. Tunable lasers are also applied to investigate the structure of unstable nuclei far from stability and to search for as yet unknown cosmological dark-matter particles in the Universe.



Prof
INOUE, Makoto
(D Sc)



Assoc Prof
MATSUKI, Seishi
(D Sc)



Instr
OKAMOTO, Hiromi
(D Sc)

Students

KAPIN, Valeri (RF)
TADA, Masaru (DC)
KISHIMOTO, Yasuhiro (DC)
AO, Hiroyuki (DC)
SHIBATA, Masahiro (MC)
OOISHI, Chikara (MC)

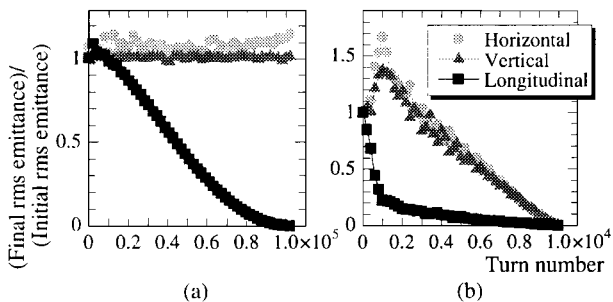


Figure 1. SAD simulation results. The time evolutions of root-mean-squared (rms) beam emittances are plotted. The case (a) corresponds to the ordinary operating mode of ASTRID while the lattice parameters have been modified in the case (b) such that the resonance conditions in Eq. (1) are satisfied.

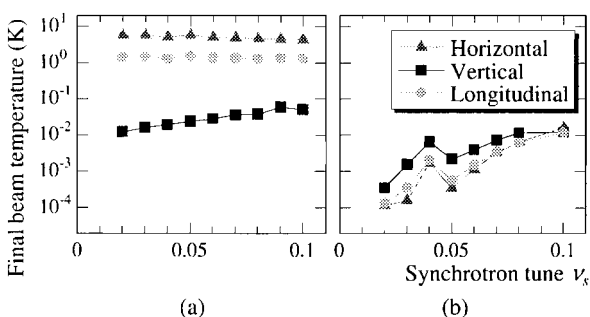


Figure 2. Equilibrium beam temperatures vs. operating synchrotron tune, obtained from SOLID. In the case (a), the same resonant ASTRID lattice as employed in Fig. 1(b) has been considered, while the case (b) corresponds to the modified TARN II lattice where the resonance conditions Eq. (1) are satisfied.

the beam at low temperature. Thus we need to examine the effect of space charges on the final temperature, employing the MD code "SOLID" [7]. Figure 2(a) illustrates the ν_s -dependence of the final beam temperature in the resonant ASTRID lattice. It is shown that the coupling method achieved transverse temperatures of the order of 1K. Beam crystallization is, however, still not achievable in this temperature region.

The lattice of a storage ring suitable for beam crystallization must fulfill the so-called maintenance condition given by [8]

$$\max(\nu_x, \nu_y) < N_l/2\sqrt{2} \quad (2)$$

where N_l is the lattice superperiodicity. Since ASTRID does not satisfy this necessary condition of beam crystallization, we now consider, among a wide range of choice, the lattice parameters of the storage ring TARN II [9]. The beam temperatures achieved in TARN II by means of the coupling method are plotted in Fig. 2(b). We see that the transverse temperatures have now become more than two orders of magnitude lower than those in the ASTRID case. Figure 3 displays the real-space profile of an equilibrium beam laser-cooled in TARN II. As anticipated, we see a 3D ordered structure formed.

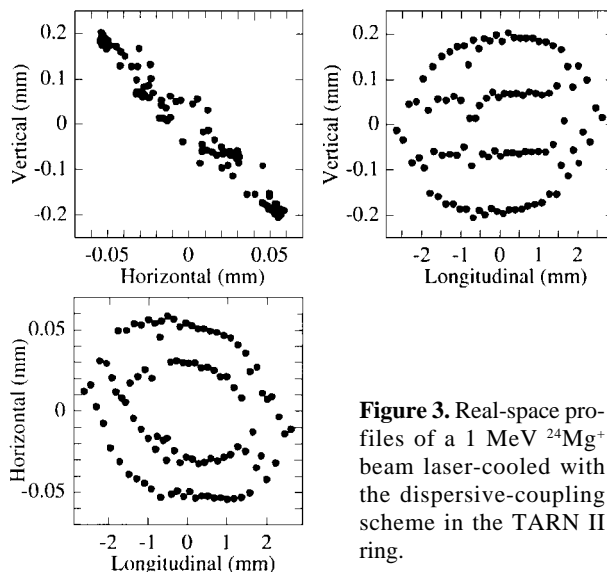


Figure 3. Real-space profiles of a 1 MeV $^{24}\text{Mg}^+$ beam laser-cooled with the dispersive-coupling scheme in the TARN II ring.

To summarise, we have studied the fundamental properties of the 3D laser cooling methods based on linear synchrotron coupling. It has been clearly demonstrated that the transverse cooling time can remarkably be shortened by using the coupling schemes. Provided that the lattice parameters of a ring satisfy the maintenance condition, equilibrium transverse temperature well below 1K could be reached very quickly, and beam crystallization is realized.

The MD simulation program was originally developed by Dr. X.-P. Li and J. Wei. Computation time was partially provided by the SAD cluster of KEK, and the Super-computer Laboratory, Institute for Chemical Research, Kyoto University.

References

1. D. J. Wineland and H. Dehmelt, *Bull. Am. Phys. Soc.* 20 (1975) 637 ; T. Hansch and A. Schawlow, *Opt. Commun.* 13 (1975) 68.
2. J. S. Hangst et al., *Phys. Rev. Lett.* 67 (1991) 1238.
3. S. Schroder et al., *Phys. Rev. Lett.* 64 (1990) 2901.
4. H. Okamoto, A. M. Sessler and D. Mohl, *Phys. Rev. Lett.* 72 (1994) 3977.
5. H. Okamoto, *Phys. Rev.* E50 (1994) 4982.
6. For the details of the SAD code, see : <http://www-acctheory.kek.jp/SAD/sad.html>
7. For the information of SOLID, see, e.g., J. Wei, X.-P. Li, and A. M. Sessler, *BNL Report BNL-52381* (1993).
8. See, e.g., J. Wei, A. Draeseke, A. M. Sessler, and X.-P. Li, *Crystalline Beams and Related Issues* (World Scientific Publishing Co. Pte. Ltd., Singapore, 1996) p. 229.
9. T. Katayama et al., in *Proceedings of the 2nd European Particle Accelerator Conference, 1990, (Nice, 1990)*, p. 577.

Design of the Superconducting RFQ for PIAVE Linac

Toshiyuki Shirai, Vladimir Andreev*, Giovanni Bisoffi*, Michele Comunian*,
Augusto Lombardi*, Andrea Pisent*, Anna M. Porcellato*

Two superconducting RFQs (SRFQ1 and SRFQ2) have been developed in INFN-LNL. The output beam energy is 578.3 keV/nucleon for $^{28+}\text{U}^{238}$. The SRFQ1 was designed based on the 90°-apart-stem structure and the RF characteristics were measured on the half scale model. The important decision in the design is to split the cavity into two sections because the electrode length of SRFQ1 is too long to perform the electron beam welding with the available machine. The field variation within $\pm 1\%$ is achieved even after the splitting.

Keywords : Superconducting RFQ/ PIAVE /Heavy ion accelerator

RFQ (radio frequency quadrupole) linacs are widely used for ion accelerators. Many laboratories and companies have been constructing RFQ linacs using the normal conducting cavity. The first superconducting RFQ has been developed in INFN-LNL. The power consumption is greatly reduced using the superconducting cavity, which enables to accelerate very heavy ions in the CW mode. The superconducting RFQ will be utilized in the new injector PIAVE (Positive Ion Accelerator for Very-low Energy) [1]. Main specification is shown in Table 1 [2]. There are two superconducting RFQ cavities (SRFQ1 and SRFQ2) in the project. Figure 1 shows the half scale model of SRFQ1.

There are some design constraints in the superconducting RFQ, as follows;

- (1) Low magnetic field on the surface (<300 Gauss),
- (2) Mechanically stable structure,

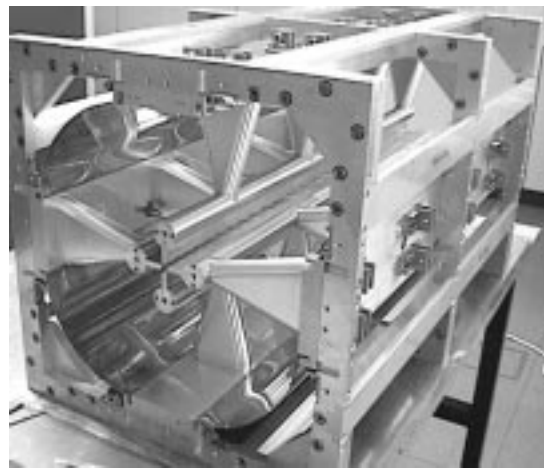


Figure 1. Half scale model of SRFQ1 made of aluminum except for the outer shell.

NUCLEAR SCIENCE RESEARCH FACILITY — Particle and Photon Beams —

Scope of research

Particle and photon beams generated with accelerators and their instrumentations both for fundamental research and practical applications are studied. The following subjects are being studied: Beam dynamics related to space charge force in accelerators: Beam handling during the injection and extraction processes of the accelerator ring: radiation mechanism of photon by electrons in the magnetic field: R&D to realize a compact proton synchrotron dedicated for cancer therapy: Control of the shape of beam distribution with use of nonlinear magnetic field: and Irradiation of materials with particle and photon beams.



Prof
NODA, Akira
(D Sc)



Assoc Prof
IWASHITA, Yoshihisa
(D Sc)



Instr
SHIRAI, Toshiyuki



Techn
TONGUU, Hiromu

Lecturer(part-time):

YAMADA, Satoru(Head; H.E. Acc. Div., National Institute of Radiological Sciences)

Students:

SUGIMURA, Takashi(DC)

KIHARA, Takahiro (DC)

FUJIEDA, Miho (DC)

URAKABE, Eriko (DC)

MORITA, Akio (MC)

HIRAMOTO, Kazuo(RF, D Eng)

* INFN-Laboratori Nazionali di Legnaro

This work is supported by Monbusho Grant-in-Aid for International Scientific Research : Joint Research, contact No. 08044076

- (3) Small stored energy (<4 J),
- (4) Short cavity length.
- (5) Uniform field distribution along the beam axis,
- (6) Good field balance among four quadrants (<1%).

The constraints (1), (2) and (3) are common problems to the superconducting cavity. The surface magnetic field should be well below the critical field of Nb at 4K (1). In order to feed RF power into the cavity, the resonant frequency should not shift (2) and the RF phase should be locked by the feedback control (3). The simulation results for the optimized geometry are shown in Table 1.

The condition (4) is a restriction from the fabrication. The components of the cavity are made of 3 mm thick niobium (Nb) sheet and they are assembled by the electron beam welding (EBW). The cavity geometry is limited by the available EBW machine. But the length of the SRFQ1 is 1378 mm, which is too long to perform the EBW. We decided to split the cavity into two sections. Each section is assembled separately and the outer shells of the two sections are finally welded by the EBW. The vane electrodes inside the cavity are still separated with 1 mm gaps.

The conditions (5) and (6) are general tasks for an RFQ design. We adopted the 90°-apart-stem RFQ structure [3]. It has a good field balance among the quadrants. Figure 2 shows the simulation results of the transverse electric field distribution along the beam axis. The broken line is a result in the original design. The big field steps exist at the vane cutting points. The solid line shows the field distribution when Nb strips are welded on the vane cutting point for the RF contacts. The field deviation becomes 0.3 %. Figure 3 shows the field distribution of the half scale model. It is measured by the standard bead-pull method. The split vanes are connected by Al strips and screws in the model. The field imbalance among the four quadrants is within ± 0.8 %, which is induced by the misalignment of the vane electrodes. The total field deviation is within ± 1.0 %. It is acceptable value from a point of view of the beam dynamics.

We have finished the cavity design of the SRFQ1 to satisfy the design constraints. The fabrication of the Nb components is in progress.

References

- [1] G. Bisoffi et al., "Prototype of a Superconducting RFQ for a Heavy Ion Injector Linac", Proc. of the 1997 Particle Accelerator Conference, Vancouver
- [2] A. Pisent et al., "Complete Simulation of the Heavy Ion Linac PIAVE", Proc. of the 1997 Particle Accelerator Conference, Vancouver

- [3] V.A. Andreev et al., "90°-apart-stem RFQ Structure for Wide Range of Frequencies", Proc. of the 1993 Particle Accelerator Conference, Washington

Table 1. Main specification of the SRFQs and the simulation results

	SRFQ1	SRFQ2
RF Frequency [MHz]	80.0	80.0
Output energy [keV/u]	341.7	578.3
Vane length [mm]	1378.0	746.1
Stored energy [J]	2.1	3.6
E_{\max} [MV/m]	25.5	25.5
B_{\max} [Gauss]	249	241
Field variation [%]	0.3	0.5

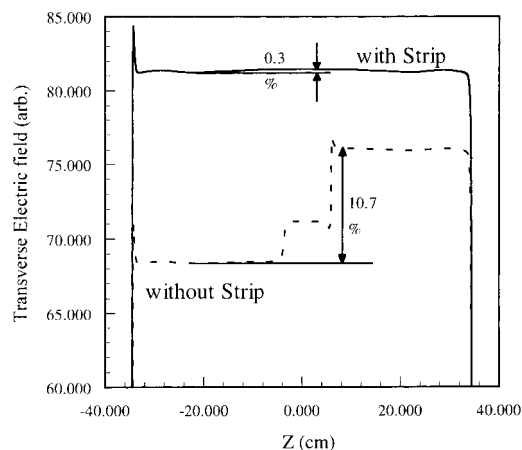


Figure 2. Simulation results of the transverse electric field distribution along the axis. The broken line corresponds to the original design. The solid line shows the field distribution with the Nb strips on the vane cutting points.

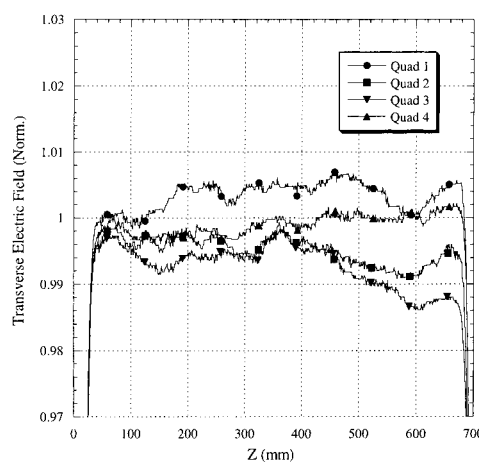


Figure 3. Field measurement results of the half scale model. The ordinate is the transverse electric field in four quadrants.

Mitochondrial Proteins Interacting with Guide RNAs

Hiroyuki Sugisaki

In mitochondria of kinetoplastid protozoa, many of mRNA transcripts of structure genes are modified within coding regions in a posttranscriptional processing characterized by the insertion and, less frequently, the deletion of uridine residues. This process, known as RNA editing, involves small RNA molecules, guide RNAs, which specify the sequence information required. The aim of this study was to identify mitochondrial proteins that are in direct physical contacts with gRNA molecules, thereby possibly responsible for the RNA editing reaction. Using an ultraviolet light-induced cross-linking technique and a gel retardation assay, seven proteins with apparent molecular weights ranging from 20 to 67 kDa in size were identified. Four species of the proteins were purified with DEAE-cellulose and phosphocellulose column chromatographies. One of them probably contacts with 3' poly(U)_n tails of the gRNA molecules because the binding of the protein was sensitive to the presence of oligo (U)_n.

Keywords: RNA editing/ kinetoplastid protozoa/ *C. fasciculata*

Many mitochondrial transcripts in kinetoplastid protozoa such as *Crithidia*, *Leishmania*, and *Trypanosoma* undergo remarkable posttranscriptional processing named RNA editing that is required for creation of functional mRNA. The location of editing domains, number of editing sites within a single editing domain and number of uridine residues to be added or deleted at each editing site are very specific to individual mRNAs, thus creating initiation and termination codons and extending open reading frames. The sequence information for editing is probably contained in small RNAs termed guide RNAs (gRNAs) which are complementary to edited mRNAs. Two models, the enzyme cascade model and the transesterification model, have been proposed for the mechanism of this process. Both models propose initial base pairing-mediated recognition of the preedited mRNA sequence immediately 3' of the region whose editing the gRNA directs with the 5 to 15 nucleotide 5' anchor se-

quence of gRNA. Thus, all gRNAs have an anchor region, but these differ in sequence between individual gRNAs. All gRNAs described to date are of similar size, averaging about 60 nucleotides, including a posttranscriptionally added 3' oligo(U)_n tail of approximately 10 to 15 nucleotides. Guide RNA and mRNA are thought to interact during editing in a ribonucleoprotein (RNP) complex. The minimal function of such a complex is presumably maintain the proximity of the mRNA 5' and 3' fragments. A more extensive function for the complex, perhaps involving catalysis, gRNA selection, or developmental regulation is also possible. The aim of this study was to identify mitochondrial proteins that are in direct physical contact with gRNA molecules, thereby possibly responsible for RNA editing.

To identify mitochondrial proteins that form stable, direct contacts with gRNA molecules, I used two different techniques, an ultraviolet (UV) light-induced cross-link

RESEARCH FACILITY OF NUCLEIC ACIDS

Scope of research

The following is the current major activities of this facility.

With emphasis on regulatory mechanisms of gene expression in higher organisms, the research activity has been focused on analysis of signal structures at the regulatory regions of transcriptional initiation and of molecular mechanisms involved in post-transcriptional modification by the use of eukaryotic systems appropriate for analysis. As of December 1994, studies are concentrated on the molecular mechanism of RNA editing in mitochondria of kinetoplastids.



Assoc Prof
SUGISAKI, Hiroyuki
(D Sc)



Instr
FUJIBUCHI, Wataru
(D Sc)



Techn
YASUDA, Keiko

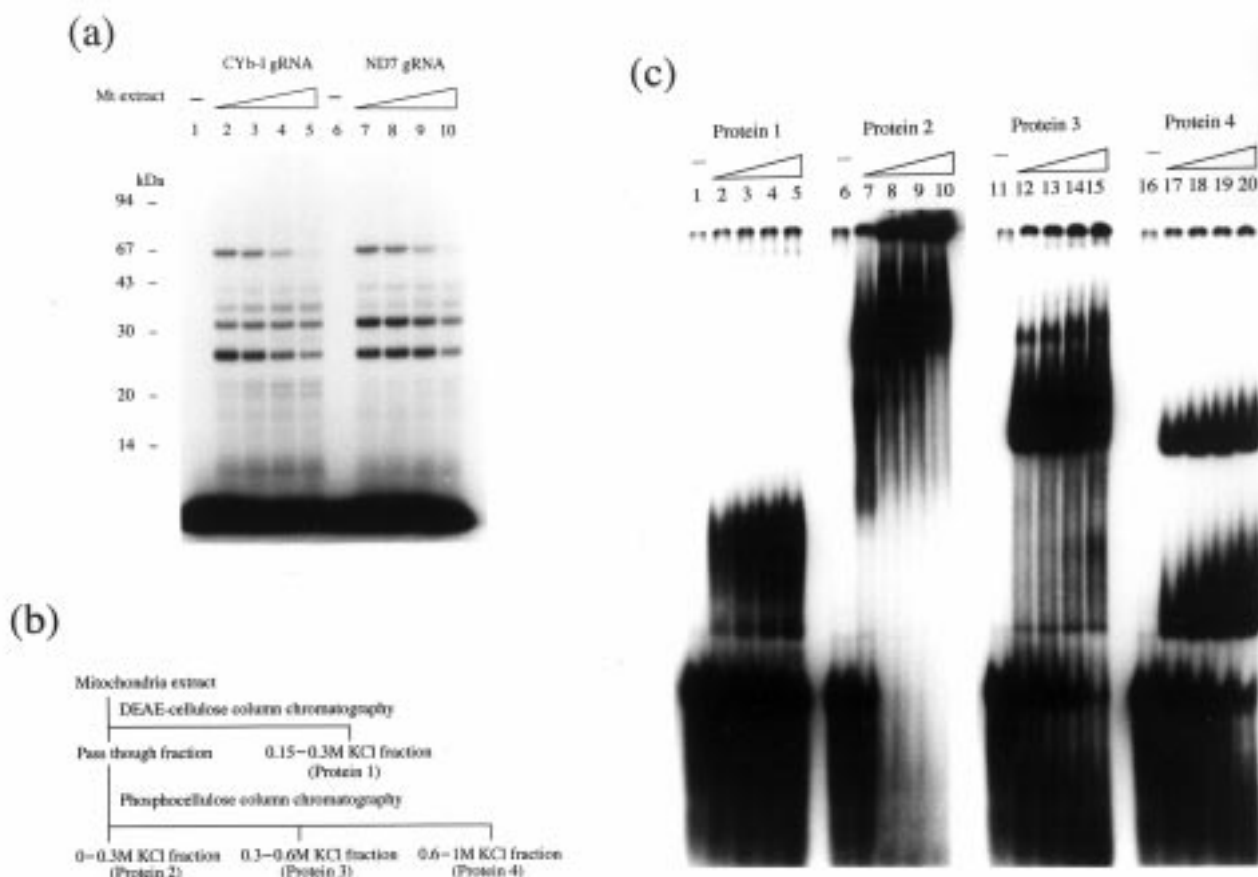


Fig. 1 (a) Protein cross-linking of ^{32}P -labeled CYb-I and ND7 gRNA with mitochondrial proteins of *C. fasciculata*. (b) Purification procedures of proteins interacted with CYb-I gRNA. (c) Patterns of a gel retardation assay with ^{32}P -labeled CYb-I gRNA and the purified protein fractions.

ing technique and a gel retardation assay. ^{32}P -Labeled gRNA molecules were incubated with the S100 mitochondrial extract of *C. fasciculata* in low monovalent cation concentration and subsequently irradiated at 254 nm. The reaction was performed in the presence of a defined concentration of tRNA molecules to account of non-specific RNA-protein interactions. Two gRNA substrates used in this study are specific for different editing domains of *C. fasciculata*, CYb-I and ND7 mRNAs and were labeled with ($\alpha^{32}\text{P}$)UTP by *in vitro* transcription. The transcripts contain a few vector-derived extrabases at their 5' end and have 3' oligo(U) tails of about 10 nucleotides. The cross-linked samples were extensively digested with ribonuclease, and the proteins were separated on a SDS-polyacrylamide gel. Proteins cross-linked to the gRNAs were detected by the radioactive oligonucleotides which remained to be covalently attached after the ribonuclease treatment while the none-cross-linked protein were stripped from the RNA by the denaturing conditions in electrophoresis. Seven mitochondrial proteins were identified with apparent molecular weights of 20, 22, 26, 32, 37, 40, and 65kDa [Fig. 1(a)]. The two different gRNA substrates gave essentially an identical cross-linking pattern, indicating the assembly of the same RNP complex upon mitochondrial extract

addition. Several major ribonucleoprotein complexes which can be resolved on 4% native polyacrylamide gels are formed during incubation of *in vitro*-transcribed gRNA with the mitochondrial extract. I made an attempt to purify the individual proteins interacted with gRNAs. The S100 extract was applied on a DEAE-cellulose column and separated to the pass through fraction and the absorbed fraction. The absorbed proteins were eluted with 0.4M KCl after washing the column with 0.15 M KCl. The pass through fraction was applied onto a phosphocellulose column and eluted with three steps, 0.3M, 0.6M and 1M KCl [Fig. 1(b)]. The separated protein fractions were further purified with hydroxyapatite column chromatography. Patterns of the gel retardation assay with the purified proteins and ^{32}P -labeled CYb-I gRNA are shown in Fig. 1(c). Protein IV probably contacts with 3' poly(U)n tails of the gRNA molecules because the binding of the protein was sensitive to the presence of oligo (U)n.

References

1. Sollner-Webb B, *Science*, 273, 1182-1183 (1996)
2. Simpson L, "mRNA editing". In *Eukaryotic Messenger RNA Processing* (Krainer, A., Ed.) *Frontiers in Molecular Biology*, IRL Press, London, 335-376.

LABORATORIES OF VISITING PROFESSORS

SOLID STATE CHEMISTRY — Structure Analysis —



Vis Prof
MAEKAWA, Sadamichi
(D Eng)

Professor

MAEKAWA, Sadamichi
Institute for Materials Research, Tohoku University
(2-1-1 Katahira, Aoba-ku, Sendai 980-8577)

Lecture at ICR

Physics of Transition Metal Oxides I
Physics of Transition Metal Oxides II
Physics of Transition Metal Oxides III



Vis Assoc Prof
SUZUKI, Yoshishige
(D Eng)

Associate Professor

SUZUKI, Yoshishige
Materials Science Division, Electrotechnical Laboratory
(1-1-4 Umezono, Tsukuba, Ibaraki 305-8568)

Lectures at ICR

Quantum Size Effects in Magnetic Materials - Basic Concepts
Quantum Size Effects in Magnetic Materials - Concrete Examples

FUNDAMENTAL MATERIAL PROPERTIES — Composite Material Properties —



Vis Prof
KATO, Katsuhiko
(D Eng)

Professor

KATO, Katsuhiko (D Eng)
Deputy Director, Functional & Biomedical Products Division,
Toyobo Co. Ltd.
President, Nippon Dyneema Co. Ltd.

Lectures at ICR

Recent Progress in High Performance Industrial Fiber
“Super” Fibers and Their Characteristics
New Rigid-Rod Polymer - PBO Fiber;
Fiber-Making, Properties, and Its Industrial Application
UHMW Polyethylene Fiber
R & D Story of “Super” Fibers



Vis Assoc Prof
FUKAHORI, Yoshihide
(D Eng)

Associate Professor

FUKAHORI, Yoshihide (D Eng)
Manager, Materials Development Department
Bridgestone Corporation (Totsuka-ku-1, Yokohama, 244-8510)

Lectures at ICR

- (1) A new polymer (a thermo-setting elastomer reinforced with continuous hard structures)
- (2) A new polymer (a polymer physical gel with co-continuous structures)
- (3) Rubber elasticity (theories and numerical treatments)
- (4) Tribology of polymers (friction and wear)

SYNTHETIC ORGANIC CHEMISTRY —Synthetic Theory —



Professor
KOGA, Kenji
(D Pharm Sci)

Professor

KOGA, Kenji (D Pharm Sci)
Nara Institute of Science and Technology (Ikoma-shi, Nara 630-0101)

Lectures at ICR

Synthesis of Lithium Amide and an Approach to the Asymmetric Catalytic Process



TOBE, Yoshito
(D Eng)

TOBE, Yoshito (D Eng)

Department of Fundamental Chemical Engineering, Osaka University (Toyonaka-shi, Osaka 560-8531)

Lecture at ICR

Enthalpy-Entropy Compensation in Asymmetric Recognition

PUBLICATIONS

STATES AND STRUCTURES

I. Atomic and Molecular Physics

Tokesi K, Kover L, Varga D, Toth J and Mukoyama T: Effects of surface loss in REELS spectra of silver, *Surface Rev. Lett.*, **4**, 955-958 (1997).

Iwazumi T, Kobayasi K, Kisimoto S, Nakamura T, Nanao S, Ohsawa D, Katano R and Isozumi Y: Magnetic resonance effect in x-ray resonant raman scattering, *Phys. Rev.* **B56**, R14267 (1997).

Iwazumi T, Kobayasi K, Kisimoto S, Nakamura T, Nanao S, Ohsawa D, Katano R, Isozumi Y and Maruyama H: Magnetic circular dichroism of lanthanoid $L_{\beta_{2,15}}$ fluorescence spectra of magnetic lanthanoid compounds, *J. Electron Spectrosc. Related Phenom.*, **92**, 257-260 (1998).

Nakamura T, Nanao S, Iwazumi T, Kobayasi K, Kisimoto S, Ohsawa D, Katano R and Isozumi Y: X-ray magnetic circular dichroism of multielectron excitation by fluorescence spectroscopy, *J. Electron Spectrosc. Related Phenom.*, **92**, 261-264 (1998).

Song B, Nakamatsu H, Sekine R, Mukoyama T and Taniguchi K: Valence Band Structures of Titanium Nitride and Titanium Carbide Calculated with Chemically Complete Clusters, *J. Phys. Cond. Matter*, **10**, 9443-9454 (1998).

Song B, Nakamatsu H, Mukoyama T and Taniguchi K: Study of Valence Band Structure for TiO_2 (rutile) with DV-X α Calculations and Soft X-ray Emission Spectra, *Advances in X-Ray Chemical Analysis, Japan*, **29**, 191-202 (1998).

Hirata M, Sekine R, Onoe J, Nakamatsu H, Mukoyama T, Takeuchi K and Tachimori S: Electronic Structures of Actinyl Nitrate-triethyl Phosphate Complexes using the DV-DS method, *J. Alloys Compounds*, **271-273**, 128-132 (1998).

Kowada Y, Tanaka I, Nakamatsu H, Mizuno M and Adachi H: *Calculations of Electronic Structures for Beginners*, Sankyo Shuppan, Tokyo, 1998 (in Japanese).

Kowada Y, Tanaka I, Nakamatsu H, Mizuno M and Adachi H: *Calculations of Electronic Structures for Beginners*, HanRimWon Press, Seoul, 1998 (in Korean).

Sekine R, Nakamatsu H, Mukoyama T, Onoe J, Hirata M, Kurihara M and Adachi H: Electronic Structures of Metal Carbides TiC and UC: Similarity and Dissimilarity, *Adv. Quantum Chem.*, **29**, 123-136 (1997).

Ichihara J, Takahashi M, Emura S, Tochio T, Ito Y and Mukoyama M: Acceleration of halogen-exchange reaction of lead (II) fluoride in organic solvent, in *the Abst. of Tenth International Conference on X-ray Absorption Fine Structure (XAFS X)*, Illinois Institute of Technology, Chicago, Illinois, USA, August 10-14, 1998, R5.3-13.

Emura S, Ito Y, Takahashi M and Mukoyama T: A new type of fine structures in x-ray absorption spectroscopy, in *the Abst. of Tenth International Conference on X-ray Absorption Fine Structure (XAFS X)*, Illinois Institute of Technology, Chicago, Illinois, USA, August 10-14, 1998, R4.2-4.

Yamaguchi K, Ito Y, Mukoyama T, Takahashi M and Emura S: Linear Inverse problem solution of the basic XAFS equation via Wavelet-Galerkin method, in *the Abst. of Tenth International Conference on X-ray Absorption Fine Structure (XAFS X)*, Illinois Institute of Technology, Chicago, Illinois, USA, August 10-14, 1998, T5.1-30.

Yamaguchi K, Ito Y, Mukoyama T, Takahashi M and Emura S: Reconstruction of one-dimensional potential from XAFS spectrum, in *the Abst. of Tenth International Conference on X-ray Absorption Fine Structure (XAFS X)*, Illinois Institute of Technology, Chicago, Illinois, USA, August 10-14, 1998, T5.1-31.

Ito Y, Tochio T, Vlaicu A, Osawa D, Mukoyama T, Muramatsu Y, Pererra R, Grush M, Callcott T and Shermann E: The contribution of the ligands around Cr to the resonant inelastic L x-ray emission spectra, in *the Abst. of the 12th International conference on Vacuum Ultraviolet radiation Physics*, August 3-7, 1998, San Francisco, California, USA.

Ito Y, Mukoyama T, Ashio K, Yamamoto K, Suga Y, Yoshikado Y, Julien C and Tanaka T: Ionic conduction and crystal structure of β - $Pb_{1-x}Sn_xF_2$ ($x < 0.3$), *Solid State Ionics* **106**, 291 (1998).

Yoshiaki Ito, Aurel M. Vlaicu, Tatsunori Tochio, Takeshi Mukoyama, Masao Takahashi, Shuichi Emura and Yoshiro Azuma: x-ray absorption features from multielectron excitations above Xe L edges, *Phys. Rev.* **A57**, 873 (1998).

Ito Y, Vlaicu A, Mukoyama T, Sato S, Yoshikado S, Julian C, Chong I, Ikeda Y, Takano M and Shermann E: Detailed structure of a Pb-doped $Bi_2Sr_2CuO_6$ superconductor, *Phys. Rev.* **B58**, 2851 (1998).

Vlaicu A, Tochio T, Ishizuka T, Osawa D, Ito Y, Mukoyama T, Nisawa A, Shoji T and Yoshikado S: Investigation of the $_{74}W$ L emission spectra and satellites, *Phys. Rev.* **A58**, 3544 (1998).

II. Crystal Information Analysis

Ogawa T, Isoda S, Suga T, Tsujimoto M, Hiragi Y and Kobayashi T: Analysis by SAXS and Cryo-TEM on Polymerization with a Surfactant, *Colloid & Polymer Science*, **106**, 141-143 (1997).

Kurata H, Wahlbring P, Isoda S and Kobayashi T: Importance of Relativistic Effects on Inelastic Scattering Cross-Sections for Quantitative Microanalysis, *Micron*, **28**, 381-388 (1997).

Kawase N, Isoda S, Kurata H, Murata Y, Takeda K and Kobayashi T: Polymerization Process of 1,6-di(N-carbazolyl)-2,4-hexadiyne (DCHD) Epitaxially Grown Films Studied by High-resolution Electron Microscopy, *Polymer*, **39**, 591-597 (1998).

Yoshida K, Tsujimoto M, Isoda S and Kobayashi T: Selective Crystal Growth in Organic Multilayer Formation, *Technical Report of IEICE*, **OME98-59**, 17-22 (1998) (in Japanese).

Ogawa T, Irie S, Isoda S, Kobayashi T and Whangbo M H: Simulation of Long-range Contrast Modulation in Scanning Tunneling Microscopy Image of Perylene-3,4,9,10-Tetracarboxylic-Dianhydride Monolayer on Graphite, *Jpn.J.Appl.Phys.*, **37**, 3864-3866 (1998).

Isoda S, Tsujimoto M, Yoshida K, Kobayashi T and Kamata T: Structure of the Green-phase of Bis(diphenylgloximato) platinum(II) with High χ^3 , *Mol. Cryst. & Liq. Cryst.*, **316**, 15-18 (1998).

Tosaka M, Tsuji M, Cartier L, Lotz B, Kohjiya S, Ogawa T, Isoda S and Kobayashi T: High Resolution TEM of the Melt-crystallized Modification of Syndiotactic Polystyrene, *Polymer*, **39**, 5273-5275 (1998).

Isoda S, Tsujimoto M, Yoshida K, Ogawa T, Kobayashi T and Kamata T: Structural Aspects of Reversible Control of Optical Activities of Bis(dimethylglyoximato) platinum(II) Thin Film, *Mol. Cryst. & Liq. Cryst.*, **316**, 71-74 (1998).

Terada S, Ogawa T, Nemoto T, Isoda S and Kobayashi T: Cryo-TEM on Structure Analysis of Metastable Polymorph of Hydrated Organic Crystal. I. Copper-oxinate Dihydrate, *Proc. The 14th International Conference on Electron Microscopy, Cancun*, **2**, pp.845-846 (1998).

Koshino M, Kurata H, Isoda S and Kobayashi T: Branching Ratio and L_2+L_3 Intensities of 3d-Transition Metals in Phthalocyanines and Their Amine Complexes, *Proc. The 14th International Conference on Electron Microscopy, Cancun*, **3**, pp.647-648 (1998).

Yoshida K, Tsujimoto M, Isoda S, Moriguchi S and Kobayashi T: Microscopic Analysis of On-top Crystal Nucleation in Organic Multilayers, *Proc. The 14th International Conference on Electron Microscopy, Cancun*, **2**, pp.891-892 (1998).

Hahakura S, Isoda S, Ogawa T, Moriguchi S and Kobayashi T: Direct Observation of Pt-particles Formed with a Surfactant with Cryogenic Transmission Electron Microscopy, *Proceed. Polymer Phasing Project Symposium on Multicomponent Polymer and Polyelectrolytes*, pp.107-110 (1998).

Isoda S, Kobayashi T and Hoshino A: STM Analysis on Interfacial Structures of Organic Epitaxy, *News letter, The division of Colloid and Surface Chemistry*, **23**, 6-9 (1998) (in Japanese).

Isoda S and Kobayashi T: Organic Hetero Epitaxy, *Molecular Electronics and Bioelectronics*, **9**, 80-87 (1998) (in Japanese).

Isoda S, Yoshida K, Tsujimoto M and Kobayashi T: Microscopic Analyses of Organic Double-layers, *Proc. Intern. Symp. Hybrid Analyses for Functional Nanostructure*, pp.89-92, (1998).

III. Polymer Condensed States Analysis

Kohjiya S and Ikeda Y: Polymer Solid Electrolytes from Poly(oxyethylene) Derivatives, *Mat. Sci. Res. Int.*, **4**, 73-78 (1998).

Manas Z, Abdullah I, Ahmad S and Kohjiya S: Effects of Dicumyl Peroxide and Liquid NR on the Physical Properties of NR/Polystyrene Blends, *Kaut. Gummi Kunst.*, **51**, 14-18 (1998).

Tanahashi H, Osanai S, Shigekuni M, Murakami K, Ikeda Y and Kohjiya S: Reinforcement of Acrylonitrile-Butadiene Rubber by Silica Generated in situ, *Rubber Chem. Technol.*, **71**, 38-52 (1998).

Hashim A S, Azahari B, Ikeda Y and Kohjiya S: The Effect of Bis(3-triethoxysilylpropyl) Tetrasulfide on Silica Reinforcement of Styrene-Butadiene Rubber, *Rubber Chem. Technol.*, **71**, 289-299 (1998).

Nishimoto A, Watanabe M, Ikeda Y and Kohjiya S: High Ionic Conductivity of New Polymer Electrolytes based on High Molecular Weight Polyether Comb Polymers, *Electrochimica Acta*, **43**, 1177-1184 (1998).

Yoon J R, Ikeda Y, Hashim A S and Kohjiya S: Die Wirkung der Bromierung auf die Eigenschaften von Ethylene-Propylen-Dien-Kautschuk in Anwesenheit von Divinylbenzol, *Gummi Fasern Kunst.*, **51**, 744-750 (1998).

Urayama K, Luo Z, Kawamura T and Kohjiya S: Phase Behavior of a Nematic Liquid Crystal in Polybutadiene Networks, *Chem. Phys. Lett.*, **287**, 342-346 (1998).

Kohjiya S, Tsubata H and Urayama K: Preparation of Copolymeric Gels Composed of Polydimethylsiloxane and Polyethylene Oxide Network Chains and Their Specific Characteristics, *Bull. Chem. Soc., Jpn.*, **71**, 961-971 (1998).

Urayama K and Kohjiya S: Extensive Stretch of Polysiloxane Network Chains with Random- and Super-coiled Conformations, *Eur. Phys. J. B.*, **2**, 75-78 (1998).

Urayama K, Kawamura T, Hirata Y and Kohjiya S: SAXS of Poly(dimethylsiloxane) Networks with Controlled Distributions of Chain Lengths between Crosslinks, *Polymer*, **39**, 3827-3833 (1998).

Kawamura T, Urayama K and Kohjiya S: Structure and Mechanical Properties of Bimodal PDMS Networks in the Swollen State, *Mater. Sci. Res. Int.*, **4**, 113-116 (1998).

Terakawa K, Muraoka K, Urayama K: Application of Epoxidized NR/Diamine Vulcanizates for Tyre Treads, *Kautschuk Gummi Kunst.*, **51**, 326-330 (1998).

Urayama K: Elastomer with Highest Extensibility, *Kohbunshi*, **47**, 572-573 (1998) (in Japanese).

Murakami S, Hirata Y, Murakami T, Kohjiya S, Nonoguchi M and Taniguchi K: New Design of the Small-Angle X-ray Scattering Spectrometer using Point Focus Optical System, *Beam Sci. & Technol.*, **3**, 5-9 (1998).

Murakami T, Murakami S and Ikeda Y: X-ray Scattering Studies on Elastomers, *J. Soc. Rubber Ind., Jpn.*, **71**, 129-139 (1998) (in Japanese).

Ikeda Y, Kasai Y, Murakami S and Kohjiya S: Preparation and Mechanical Properties of Graded Styrene-Butadiene Rubber Vulcanizates, *J. Jap. Inst. Metals*, **62**, 1013-1017 (1998) (in Japanese).

Murakami S: Structural Development under the Drawing of Poly(ethylene naphthalene-2,6-dicarboxylate), *Kohbunshi-Kako*, **47**, 223-229 (1998) (in Japanese).

Tosaka M, Tsuji M, Cartier L, Lotz B, Kohjiya S, Ogawa T, Isoda S and Kobayashi T: High-resolution TEM of the Melt-Crystallized Modification of Syndiotactic Polystyrene, *Polymer*, **39**, 5273 - 5275 (1998).

Tosaka M, Tsuji M and Kohjiya S: Stacking Faults in Syndiotactic Polystyrene β -form Crystals, *Proc. of Regional Conference on Polymeric Materials '98, Penang*, 154 - 159 (1998).

Tosaka M, Tsuji M and Kohjiya S: High-resolution Transmission Electron Microscopy of Polymer Crystals, *Mater. Sci. Res. Int.*, **4**, 79 - 85 (1998).

Fujita M, Tosaka M, Tsuji M and Kohjiya S: Crystalline Core in

the Folded-Chain Edge-on Lamella Crystallized Epitaxially from Solution onto Alkali Halides, *Proc. of Regional Conference on Polymeric Materials '98, Penang*, 123 - 127 (1998).

Shimizu T, Tsuji M and Kohjiya S: A TEM Study on Natural Rubber Thin Films Crystallized under Molecular Orientation, *Mater. Sci. Res. Int.*, **4**, 117 - 120 (1998).

Shimizu T, Tsuji M and Kohjiya S: TEM Studies on Oriented Crystallization of Natural Rubber and Polychloroprene, *Proc. of Regional Conference on Polymeric Materials '98, Penang*, 99 - 103 (1998).

Novillo-L F A, Fujita M, Tsuji M and Kohjiya S: Preferential Orientation of Poly(ethylene 2,6-naphthalate) Melt-Crystallized on the Friction-Transfer Layer of PTFE, *Sen'i Gakkaishi*, **54**, 544 - 549 (1998).

Hirai A, Tsuji M, Yamamoto H and Horii F: In situ Crystallization of Bacterial Cellulose. III. Influences of Different Polymeric Additives on the Formation of Microfibrils as Revealed by Transmission Electron Microscopy, *Cellulose*, **5**, 201 - 213 (1998).

Hirai A, Tsuji M and Horii F: Helical Sense of Ribbon Assemblies and Splayed Microfibrils of Bacterial Cellulose, *Sen'i Gakkaishi*, **54**, 506 - 510 (1998).

INTERFACE SCIENCE

I. Solutions and Interfaces

Matubayasi N, Wakai C, and Nakahara M: Structural study of supercritical water. I. Nuclear magnetic resonance spectroscopy, *J. Chem. Phys.*, **107**, 9133-9140 (1997).

Fujii K, Arata Y, Tanaka H, and Nakahara M: Stabilization Energies and Rotational Motions in Clathrate Hydrate of Benzene Studied by Molecular Dynamics Simulation, *J. Phys. Chem. A*, **102**, 2635-2640 (1998).

Murata Y, Tsunashima K, Umemura J and Koizumi N: Ferroelectric Properties of Polyamides Consisting of Hepta- and Nonamethylenediamines, *IEEE Trans. Dielectrics El*, **5**, 96-102 (1998).

Kobayashi K, Umemura J, Horiuchi T, Yamada H, and Matsushige K: Structural Study on Self-Assembled Monolayers of Alkanedithiol Molecules, *Jpn. J. Appl. Phys.*, **37**, L297-L299 (1998).

Miura Y, Kimura S, Imanishi Y, and Umemura J: Self-Assembly of α -Helix Peptide/Crown Ether Conjugate upon Complexation with Ammonium-Terminated Alkanethiolate, *Langmuir*, **14**, 2761-2767 (1998).

Sakai H and Umemura J: Molecular Orientation in Langmuir Films of 12-Hydroxystearic Acid Studied by Infrared External Reflection Spectroscopy, *Langmuir*, **14**, 6249-6255 (1998).

Hasegawa T, Nishijo J, Umemura J: Binding Mechanism of Sucrose to Dipalmitoylphosphatidylcholine Langmuir Films by Fourier Transform Infrared Reflection-Absorption Spectroscopy and Quartz-Crystal Microbalance Technique, *J. Phys. Chem. B*, **102**, 8498-8504 (1998).

Cohen R, Exerowa D, Kolarov T, Yamanaka T, and Tano T: Foam Films Stabilized with Lysophosphatidylcholine: A Comparison of Microinterferometric and Fourier Transform Infrared Spectroscopy Thickness Measurements, *Langmuir*, **13**, 3172-

3176 (1997).

Hartley P, Matsumoto M, and Mulvaney P: Determination of the Surface Potential of Two-Dimensional Crystals of Bacteriorhodopsin by AFM, *Langmuir*, **14**, 5203-5209 (1998).

Watanabe H, Osaki K, Matsumoto M, Bossev D P, McNamee C E, Nakahara M, and Yao M- L: Nonlinear rheology for threadlike micelles of tetraethylammonium perfluorooctyl sulfonate, *Rheol. Acta.*, **37**, 470-485 (1998).

Matubayasi N, Wakai C, and Nakahara M: NMR Study of Water Structure in Supercritical Conditions, *Rev. High Pressure Sci. Tech.*, **7**, 1112-1114 (1998).

Matubayasi N, Gallicchio E, and Levy R M: On the local and nonlocal components of solvation thermodynamics and their relation to solvation shell models, *J. Chem. Phys.*, **109**, 4864-4872 (1998).

Umemura J: FT-IR and Raman Spectroscopy of LB Film, L Monolayer, and Bilayer Lipid Membrane, *Maku (Membrane)*, **23**, 177-185 (1998) (in Japanese).

Takemoto T, Umemura J, Tsutiya H, Kubota T, Ohara S, Terasawa S, Huehuki Y, Horinouchi M, Shimatani K, Hirano M, Inoue J, Inoue T, Ueda K, Matsuda M, Nagasaki T, Kurokawa S, Kitagawa R: Development of New Connection Technique in Electronics Parts and Peripheral Techniques, in *1995-97 San-Gaku-Kan Joint Research Project "Development of New Connection Techniques in Electronics Parts and Peripheral Techniques"*, Kyoto Promotion Foundation for Industrial Techniques, 1-21 (1998) (in Japanese).

Umemura J: Study of Action Mechanism of Soldering Flux by FT-IR Spectroscopy, in *1995-97 San-Gaku-Kan Joint Research Project "Development of New Connection Techniques in Electronics Parts and Peripheral Techniques"*, Kyoto Promotion Foundation for Industrial Techniques, 32-46 (1998) (in Japanese).

Umemura J: Study of Reaction between Metals and Soldering Flux by Infrared Reflection Absorption Spectroscopy, in *1995-97 San-Gaku-Kan Joint Research Project "Development of New Connection Techniques in Electronics Parts and Peripheral Techniques"*, Kyoto Promotion Foundation for Industrial Techniques, 47-62 (1998) (in Japanese).

Nakahara M: Proceedings of International Conference-AIRAPT-16 and HPCJ-38- on High Pressure Science and Technology, The Review of High Pressure Science and Technology, **7** (1998).

II. Molecular Aggregates

Sato N, Yoshida H and Tsutsumi K: Photoemission and Inverse Photoemission Studies on a Thin Film of *N,N'*-Dimethylperylene-3,4,9,10-bis(dicarboximide), *J. Elect. Spectrosc. Relat. Phenom.*, **88-91**, 861-865 (1998).

Oda M and Sato N: Theoretical Study on the Topochemical Nature in the Initiation Process of the Solid-State Thermal Isomerization Reaction of Methyl 4-(Dimethylamino)benzenesulfonate, *J. Phys. Chem. B*, **102**, 3283-3286 (1998).

Okuno T, Izuoka A, Ito T, Kubo S, Sugawara T, Sato N and Sugawara Y: Reactivity of Mesogenic Diacetylenes Coupled with Phase Transitions between Crystal and Liquid Crystal Phases, *J. Chem. Soc. Perkin Trans. 2*, 889-895 (1998).

Sato N: Manners for Presenting Physical Quantities and Units,

Kagaku To Kyoiku, **46**, 569-573 (1998). (in Japanese)

Sato N: New Development of Studies on Electronic Structure in Organic Semiconductors, *Kagaku (Kyoto)*, **53**, 70-71 (1998). (in Japanese)

Asami K: Dielectric analysis of polystyrene microcapsules using scanning dielectric microscope, *Colloid Polym. Sci.*, **276**, 373-378 (1998).

Asami K, Gheorghiu E and Yonezawa T: Dielectric behavior of budding yeast in cell separation, *Biochim. Biophys. Acta*, **1381**, 234-240 (1998).

Gheorghiu E and Asami K: Monitoring cell cycle by impedance spectroscopy: experimental and theoretical aspects, *Bioelectrochem. Bioenerg.*, **45**, 139-143 (1998).

Asami K: Dielectric Relaxation Spectroscopy of Biological Cell Suspensions: *Handbook on Ultrasonic and Dielectric Characterization Techniques for Suspended Particulates*, Hackley V A and Texter J (eds.), (The American Ceramic Society, Westerville, 1998), pp. 333-349.

Kita Y: *Principles and Developments of Methods for Measuring Electrical Properties of Materials*, Yano S and Kita Y (eds.), (Toray Research Center, Tokyo, 1998), pp. 10-42 and 131-163 (in Japanese).

III. Separation Chemistry

Suzuki M, Matsui M, Kihara S: Reduction of flavin mononucleotide at the aqueous/organic solution interface in the absence and presence of oxygen, *J. Electroanal. Chem.*, **438**, 147-151 (1997).

Li Q, Huang C, Yao G, Umetani S, Matsui M: Synthesis, Characterization and Luminescence of Tb³⁺ Mixed Ligand Complexes with 1-Phenyl-3-methyl-4-isobutyl-5-pyrazolone and Neutral Ligands, *J. Chinese Rare Earth Soc.*, **15**, 295-299 (1997).

Umetani S, Kawase Y, Le Q.T.H, Matsui M: Role of the Intramolecular Hydrogen Bond and the Ligand Rigidity in the Complexation of Trifluoroacetylcycloalkanes with Lanthanides: Novel Strategy for the Design of Organic Ligands of High Selectivity, *Inorg.Chim.Acta*, **267**, 201-207 (1998).

Sasaki T, Umetani S, Matsui M, Tsurubou S, Kimura T, Yoshida Z: Complex Formation of Lanthanide Ions with Sulfonated Crown Ethers in Aqueous Solution, *Bull.Chem.Soc.Jpn*, **71**(2), 371-377 (1998).

Sohrin Y, Fujishima Y, Ueda K, Akiyama S, Mori K, Hasegawa H, Matsui M: Dissolved niobium and Tantalum in the North Pacific, *Geophys. Res. Lett.*, **25**(7), 999-1002 (1998).

Sohrin Y, Iwamoto S, Akiyama S, Fujita T, Kugii T, Obata H, Nakayama E, Goda S, Fujishima Y, Hasegawa H, Ueda K, Matsui M: Determination of trace elements in seawater by fluorinated metal alkoxide glass-immobilized 8-hydroxyquinoline concentration and high-resolution inductively coupled plasma mass spectrometry detection, *Anal. Chim. Acta*, **363**, 11-19 (1998).

Li Q, Zhou D, Huang C, Yao G, Zhou Y, Umetani S, Matsui M: Synthesis, Characterization and Luminescence of Tb(III)-1-Phenyl-4-methyl-4-acyl-5-pyrazolone Ternary Complexes(in Chinese), *Acta Chimica Sinica*, **56**, 52-57 (1998).

Gao X.C, Cao H, Huang C, Li B, Umetani S: Electroluminescence of a Novel Terbium Complex, *Appl. Phys. Lett.*, **72**, 2217-2219 (1998).

Komatsu Y, Umetani S, Tsurubou S, Michiue Y, Sasaki T: Quantitative Separation of Alkaline Earth Metal Ions by Triple-Phase Separation Method, *Chem. Lett.*, 1167-1168 (1998).

Gao X, Huang C, Li B, Ibrahim K, Liu F, Umetani S: Electroluminescence from both a Light-emitting Layer and Hole Transport Layer: Special Evidence for Charge Carrier Tunneling Injection, *Chem. Phys. Lett.*, **297**, 530-536 (1998).

Hojo M, Hasegawa H, Tsurui H, Kawashima K, Minami S, Mizobe A: Formation of Stable Carbocations or Zwitterions by a Specific Interaction with Alkali Metal Ions in Acetonitrile, *Bull. Chem. Soc. Jpn.*, **71**, 1619-1627 (1998).

SOLID STATE CHEMISTRY

I. Artificial Lattice Alloys

Shinjo T: Training for Originality, *J. Magn. Soc. Jpn.*, **21**, 1157-1158(1997). (in Japanese)

Amaral L, Scorzelli R B, Brückman M E, Paesano A, Schmidt J E, Shinjo T and Hosoito N: Very Thin Fe/Ni Modulation Multilayer Films under Ion Bombardment, *J. Appl. Phys.*, **81**, 4773-4775(1997).

Ueda K, Sugimoto T, Tada T, Nishimura K, Endo S, Toyota N, Kohama M, Yamamoto K, Yamaguchi T, Suenaga Y, Munakata M, Kanehisa N, Shibamoto Y, Kai Y and Hosoito N: Temperature Dependence of Crystal Structures, and Electrical Conducting and Magnetic Properties in Plate Crystals of 1:2 Tetrafluorotetracyanoquinodimethane Mixed Tetramethyl-Ammonium and -Phosphonium Salts, *Mol. Cryst. Liq. Cryst.*, **296**, 323-333(1997).

Sugimoto T, Ueda K, Endo S, Toyota N, Kohama M, Yamamoto K, Morimoto H, Yamaguchi T, Suenaga Y, Munakata M, Hosoito N, Kanehisa N, Shibamoto N and Kai Y: Ferromagnetic Behavior of 1:2 TCNQ/TCNQ⁻ Mixed Salts at Room Temperature, *Mol. Cryst. Liq. Cryst.*, **305**, 217-226(1997).

Kageyama H, Kawasaki S, Mibu K, Takano M, Yoshimura K and Kosuge K: Mössbauer Observation of the Quantum Levels of Fe³⁺ Ions Doped in 1D Ising Ferromagnet Ca₃Co₂O₆, *Phys. Rev. Lett.*, **79**, 3258-3261(1997).

Ono T, Miyajima H, Shigeto K and Shinjo T: Magnetization Reversal in Submicron Magnetic Wire Studied by Using Giant Magnetoresistance Effect, *Appl. Phys. Lett.*, **72**, 1116-1117(1998).

Mibu K and Shinjo T: Magnetic Anisotropy in Fe/Rare Earth Multilayers, *Hyper. Int.*, **113**, 287-293(1998).

Mibu K, Ito T and Shinjo T: Hyperfine Fields in Sn Layers of Cr/Sn Multilayers, *Hyper. Int. (C)*, **3**, 405-408(1998).

Shinjo T and Ono T: Nanostructured Magnetism: Studies of Multilayers Prepared on Microstructured Substrates, *J Magn. Mater.*, **117-181**, 31-36(1998).

Mibu K, Nagahama T, Ono T and Shinjo T: Magnetoresistance of Quasi-Bloch-Wall Induced in NiFe/CoSm Exchange-Spring Bilayers, *J. Magn. Mater.*, **177-181**, 1267-1268(1998).

Emoto T, Hosoito N and Shinjo T: Magnetic Polarization in Au

Layers of Au/M (M=Fe, Co, and Ni) Multilayers with ^{119}Sn Probes Studied by Mössbauer Spectroscopy, *J. Magn. Magn. Mater.*, **189**, 136-148(1998).

Shigeto K, Ono T and Shinjo T: Magnetization Measurement of a Single Submicron Wire by Using Giant Magnetoresistance Effect, *J. Magn. Soc. Jpn.*, **22**, 549-551(1998). (in Japanese)

Nagahama T, Mibu K and Shinjo T: The Magnetization Process and Magnetoresistance of Exchange-Spring Bilayer Systems, *J. Phys. D: Appl. Phys.*, **31**, 43-49(1998).

Mibu K, Tanaka S and Shinjo T: Preparation and Mössbauer Study of Epitaxial Cr/Sn Multilayers, *J. Phys. Soc. Jpn.*, **67**, 2633-2636(1998).

Mibu K, Nagahama T, Shinjo T and Ono T: Magnetoresistance of Bloch-Wall-Type Magnetic Structures Induced in NiFe/CoSm Exchange-Spring Bilayers, *Phys. Rev. B*, **58**, 6442-6446(1998).

Hashizume H, Ishimatsu N, Sakata O, Iizuka T, Hosoi N, Namikawa K, Iwazumi T, Srajer G, Venkataraman C T, Lang J C, Nelson C S and Berman L E: Resonant X-ray Magnetic Scattering from the Twisted States of an Fe/Gd Multilayer, *Physica B*, **248**, 133-139(1998).

Lee D R, Park Y J, Park S H, Jeong Y H, Lee K-B, Ishimatsu N, Hashizume H and Hosoi N: Resonant X-ray Reflectivity Measurements of a Magnetic Multilayer [Gd/Fe] $_{10}$, *Physica B*, **248**, 146-151(1998).

Hamada S, Hosoi N, Ono T and Shinjo T: Micromagnetic Structure in Co/Au Multilayers Revealed by ^{57}Fe Mössbauer Probes, *J. Magn. Soc. Jpn.*, **22**, 405-408(1998). (in Japanese)

Mibu K, Nagahama T, Ono T and Shinjo T: Magnetoresistance of Bloch-Wall-Type Magnetic Structures in Exchange-Spring Bilayers, *J. Magn. Soc. Jpn.*, **22**, 613-616(1998). (in Japanese)

II. Quantum Spin Fluids

C.H.Lee, N, Kaneko, S.Hosoya, K. Krahashi, S.Wakimoto, K.Yamada, and Y.Endoh : Growth of Large Single Crystals Using the Improved Lamp-image Floating-zone Furnace: Application to $\text{La}_{2-x}\text{Sr}_x\text{CuO}_4$, *Supercond. Sci. Technol.*, **11**, 891-897 (1998).

Yamada K, Lee C H, Kurahashi K, Wada J, Kimura Y, Ueki S, Endoh Y, Hosoya S, Shirane G, Birgeneau R J, Greven M, Kastner M A and Kim Y: Doping Dependence of Spatially Modulated Dynamical Spin Correlations and Superconducting Transition Temperature in $\text{La}_{2-x}\text{Sr}_x\text{CuO}_4$, *Phys. Rev. B*, **57**, 6165-6172 (1998) .

Isawa K, Yaegashi Y, Ogota S, Nagano M, Sudo S and Yamada K : Thermoelectric power of delafossite-derived compounds, RCuO_{2+d} (R=Y, La, Pr, Nd, Sm, and Eu), *Phys. Rev. B*, **57**, 7950-7954 (1998).

Isawa K, Yaegashi Y, Ogota S, Nagano M, Sudo S, Ohashi M and Yamada K : Crystal structure refinement of the oxygen-rich RCuO_{2+d} (R=Y and La) delafossite by neutron diffraction, *Advances in Superconductivity*, **X**, 395-398 (1998).

Ohta H, Ikeuchi Y, Kimura S, Okubo S, Nojiri H, Motokawa M, Hosoya S, Yamada K, Endoh Y : High field AFMR measurement of Bi_2CuO_4 , *Physica B*, **246-247**, 557-560 (1998).

Yamada K : How Does the High-T_c Superconductivity Disappear by Overdoping? -A Scenario from a Neutron

Scattering Study on $\text{La}_{2-x}\text{Sr}_x\text{CuO}_{4-d}$, *Advances in Superconductivity*, **X**, 37-42 (1998).

Ishiguro A, Sawada A, Suzuki M, Hiraka H, Yamada K, Endoh Y, Komatsubara T : De Haas-van Alphen effect in CoS_2 , *J. Mag. Mag. Mater.*, **177-181**, 1355-1356 (1998).

Wakimoto S, Kurahashi K, Yamada K, Kato K, Koike Y and Endoh Y: Magnetism of lightly oxygenated $\text{La}_{2-x}\text{Bi}_x\text{CuO}_{4+d}$, *Physica B*, **241-243**, 634-636 (1998).

Hirota K, Yamada K, Tanaka I and Kojima H : Quasi-elastic incommensurate peaks in $\text{La}_{2-x}\text{Sr}_x\text{Zn}_{1-y}\text{Cu}_y\text{O}_{4-d}$, *Physica B*, **241-243**, 817-819 (1998).

Suzuki T, Goto T, Shinoda T, Fukase T, Kimura H, Yamada K, Ohashi M, Yamaguchi Y : Observation of modulated-magnetic long-range order in $\text{La}_{1.88}\text{Sr}_{0.12}\text{CuO}_4$, *Phys. Rev. B*, **57**, R3229-3232 (1998) .

Hayashi F, Ueda E, Soto M, Kurahashi K, Yamada K : Anisotropy of the Superconducting Order Parameter of $\text{Nd}_{2-x}\text{Ce}_x\text{CuO}_4$ Studied by STM/STS, *J. Phys. Soc. Jpn.*, **67**, 3234-3239 (1998).

Sugai S, Kitamori N, Hosoya S and Yamada K : Separation of Spin and Charge Densities in $\text{La}_2\text{NiO}_{4+d}$, *J. Phys. Soc. Jpn.*, **67**, 2992-2995 (1998) .

Niinae T, Ikeda Y, Bando Y, Kusano Y and Takada J: The Modulation and Synthesis for $\text{Bi}_2\text{Sr}_2\text{CuO}_d$ under Ambient Oxygen Partial Pressure, *Funtai oyobi Funmatsu Yakin*, **45**, 661-665 (1998) (in Japanese).

Ito Y, Vlaicu A-M, Mukoyama T, Sato S, Yoshikado S, Julien C, Chong I, Ikeda Y, Takano M and Sherman E Y: Detailed Structure of a Pb-Doped $\text{Bi}_2\text{Sr}_2\text{CuO}_6$ Superconductor, *Phys. Rev. B*, **58**, 2851-2858 (1998).

Nakanishi M, Uwazumi Y, Fujiwara M, Takada J, Kusano Y, Takeda Y and Ikeda Y: Lithium Intercalation/Deintercalation of the Bi-2212 Phase by Electrochemical Method, *Funtai oyobi Funmatsu Yakin*, **45**, 666-669 (1998) (in Japanese).

Kusano Y, Takada J, Fukuhara M, Doi A, Ikeda Y and Takano M: Morphological Effects of Grinding on Bismuth-Based Cuprate Superconductors, *J. Am. Ceram. Soc.*, **81**, 217-221 (1998).

Yamada T, Niinae T, Ikeda Y, Hiroi Z, Takano M and Bando Y: Phase Diagram of the $\text{NdO}_{1-x}\text{-SrO-CuO}$ System, *Funtai oyobi Funmatsu Yakin*, **45**, 114-118 (1998) (in Japanese).

Nagaoka T, Matsuda Y, Obara H, Sawa A, Terashima T, Chong I, Takano M and Suzuki M: Hall Anomaly in the Superconducting State of High-T_c Cuprates: Universality in Doping Dependence, *Phys. Rev. Lett.*, **80**, 3594-3597 (1998).

Fujita M, Frost C D, Arai M, Motokawa M, Akimitsu J, Bennington S M: Spin dynamics of the spin-Peierls system CuGeO_3 at various temperatures, *Physica B*, **241-243** (1998) 241-243

III. Multicomponent Materials

Kawasaki S, Takano M, Kanno R, Takeda T and Fujimori A: Phase Transition in Fe^{4+} ($3d^4$)-Perovskite Oxides Dominated by Oxygen-Hole Character, *J. Phys. Soc. Jpn.*, **67**, 1529-1532 (1998).

Kawasaki S, Takano M and Takeda Y: Physical Properties of

Co-Substituted Iron Perovskite Systems, *Solid State Ionics*, **108**, 221-226 (1998).

Hiroi Z, Chong I, Izumi M and Takano M: Two-Phase Microstructures in the Heavily Pb-Substituted Bi-2212 Single Crystals Serving as Efficient Pinning Centers, *Advances in Superconductivity X: Proceedings of the 10th International Symposium on Superconductivity (ISS'97), Oct. 27-30, 1997, Gifu, Japan (ed. Osamura K and Hirabayashi I), Springer-Verlag Tokyo*, 285-288 (1998).

Kusano Y, Takada J, Fukuhara M, Doi A, Ikeda Y and Takano M: Morphological Effects of Grinding on Bismuth-Based Cuprate Superconductors, *J. Am. Ceram. Soc.*, **81**, 217-221 (1998).

Ito Y, Vlaicu A-M, Mukoyama T, Sato S, Yoshikado S, Julien C, Chong I, Ikeda Y, Takano M and Sherman E Y: Detailed Structure of a Pb-Doped $\text{Bi}_2\text{Sr}_2\text{CuO}_6$ Superconductor, *Phys. Rev. B*, **58**, 2851-2858 (1998).

Hiroi Z and Horiuchi S: High-Voltage High-Resolution Electron Microscopy Study of Alkaline-Earth Copper Oxides, *Microscopy Research and Technique*, **40**, 251-264 (1998).

Kitaoka Y, Kobayashi T, Kôda A, Wakabayashi H, Niino Y, Yamakage H, Taguchi S, Amaya K, Yamaura K, Takano M, Hirano A and Kanno R: Orbital Frustration and Resonating Valence Bond State in the Spin-1/2 Triangular Lattice LiNiO_2 , *J. Phys. Soc. Jpn.*, **67**, 3703-3706 (1998).

Vander Griend D A, Boudin S, Poepelmeier K R, Azuma M, Toganoh H and Takano M: High Pressure Transformation of $\text{La}_4\text{Cu}_3\text{MoO}_{12}$ to a Layered Perovskite, *J. Am. Chem. Soc.*, **120**, 11518-11519 (1998).

Takeda Y, Okazoe C, Imanishi N, Yamamoto O, Kawasaki S and Takano M: Oxygen Doping in $\text{Ca}_{1-x}\text{Sr}_x\text{FeO}_{3-z}$ Perovskite Oxides by an Electrochemical Method, *J. Ceram. Soc. Jpn.*, **106**, 759-762 (1998).

Azuma M, Kaimori S and Takano M: High-Pressure Synthesis and Magnetic Properties of Layered Double Perovskites Ln_2CuMO_6 (Ln=La, Pr, Nd, and Sm; M=Sn and Zr), *Chem. Mater.*, **10**, 3124-3130 (1998).

Azuma M, Fujishiro Y, Takano M, Nohara M, Takagi H, Ohsugi S, Kitaoka Y and Eccleston R S: Impurity Effects on a Two-Leg Spin Ladder Compound SrCu_2O_3 , *J. Mag. Mag. Mat.*, **177-181**, 655-656 (1998).

Fujiwara N, Yasuoka H, Fujishiro Y, Azuma M and Takano M: Nuclear Magnetic Resonance in the Ladder System $\text{Sr}(\text{Zn}_x\text{Cu}_{1-x})_2\text{O}_3$, *J. Mag. Mag. Mat.*, **177-181**, 628-629 (1998).

Nagaoka T, Matsuda Y, Obara H, Sawa A, Terashima T, Chong I, Takano M and Suzuki M: Hall Anomaly in the Superconducting State of High- T_c Cuprates: Universality in Doping Dependence, *Phys. Rev. Lett.*, **80**, 3594-3597 (1998).

Inami T, Maegawa S and Takano M: Neutron-Diffraction Study on Na- and K-Jarosit, *J. Mag. Mag. Mat.*, **177-181**, 752-753 (1998).

Yamada T, Niinae T, Ikeda Y, Hiroi Z, Takano M and Bando Y: Phase Diagram of the $\text{NdO}_{1.5-x}\text{-SrO-CuO}$ System, *Funtai oyobi Funmatsu Yakin*, **45**, 114-118 (1998) (in Japanese).

Kobayashi N, Hiroi Z and Takano M: Partial Substitution Effects of the La site in Two-Leg Ladder Compounds $\text{LaCuO}_{2.5}$, *Funtai oyobi Funmatsu Yakin*, **45**, 119-124 (1998) (in Japanese).

Sugai S, Shinoda T, Kobayashi N, Hiroi Z and Takano M: Spin Gap at the Phase Transition between Spin Liquid and Long-Range Ordered State in $\text{La}_{1-x}\text{Sr}_x\text{CuO}_{2.5}$, *Rev. High Pressure Sci. Technol.*, **7**, 571-573 (1998).

Fujiwara N, Yasuoka H, Fujishiro Y, Azuma M and Takano M: NMR Study of Zn Doping Effect in Spin Ladder System SrCu_2O_3 , *Phys. Rev. Lett.*, **80**, 604-607 (1998).

Mizokawa T, Konishi T, Fujimori A, Hiroi Z, Takano M and Takeda Y: Cu 2p X-Ray Absorption and Cu 2p-3d Resonant Photoemission Spectroscopy of LaCuO_3 , *J. Electron Spectrosc. Relat. Phenomen.*, **92**, 97-101 (1998).

Azuma M, Takano M and Eccleston R S: Disappearance of the Spin Gap in a Zn-Doped 2-Leg Ladder Compound $\text{Sr}(\text{Cu}_{1-x}\text{Zn}_x)_2\text{O}_3$, *J. Phys. Soc. Jpn.*, **67**, 740-743 (1998).

Mizokawa T, Fujimori A, Namatame H, Takeda Y and Takano M: Electronic Structure of Tetragonal LaCuO_3 Studied by Photoemission and X-Ray-Absorption Spectroscopy, *Phys. Rev. B*, **57**, 9550-9556 (1998).

Hiroi Z, Chong I and Takano M: Two-Phase Microstructures Generating Efficient Pinning Centers in the Heavily Pb-Substituted $\text{Bi}_x\text{Sr}_{1-x}\text{CaCu}_3\text{O}_{8+d}$ Single Crystals, *J. Solid State Chem.*, **138**, 98-110 (1998).

IV. Amorphous Materials

Uchino T and Yoko T, Vibration of Alkali Cations in Borate Glasses from Molecular Orbital Calculations, *Solid State Ionics*, **105**, 91-96 (1998).

Uchino T and Yoko T, Localized Low Frequency Dynamics in SiO_2 Glass, *J. Chem Phys*, **108**, 8130-38 (1998).

Kitaoka K, Kozuka H and Yoko T, Preparation of Lead Lanthanum Zirconate Titanate (PLZT, $(\text{Pb}, \text{La})(\text{Zr}, \text{Ti})\text{O}_3$) Fibers by Sol-Gel Method, *J. Am. Ceram. Soc.*, **81**, 1189-96 (1998).

Ohyama M, Kozuka H and Yoko T, Sol-Gel Preparation of Transparent and Conductive Aluminum-Doped Zinc Oxide Films with Highly Preferential Crystal Orientation, *J. Am. Ceram. Soc.*, **81**, 1622-32 (1998).

Lin H, Kozuka H and Yoko T, Preparation of TiO_2 Films on Self-Assembled Monolayers by Sol-Gel Method, *Thin Solid Films*, **315**, 111-117 (1998).

Lin H, Kumon S, Kozuka H and Yoko T, Electrical Properties of Titania Films Prepared by Sol-Gel Method, *Thin Solid Films*, **315**, 266-272 (1998).

Uchino T, Tokuda Y and Yoko T, Vibrational Dynamics of Defect Modes in Vitreous, *Phys. Rev. B*, **58**, 5322-28 (1998).

Zhao G-L, Utsumi S, Kozuka H and Yoko T, Photoelectrochemical Properties of Sol-Gel-Derived Anatase and Rutile TiO_2 Films, *J. Mater. Sci.*, **33**, 3655-59 (1998).

Uchino T and Yoko T, Structure and Vibrational Properties of Sodium Disilicate Glass from Ab Initio Molecular Orbital Calculations, *J. Phys. Chem.*, **102**, 8372-78 (1998).

Kitaoka K, Takahara K, Kozuka H and Yoko T, Sol-Gel Processing of Transparent PLZT $((\text{Pb}, \text{La})(\text{Zr}, \text{Ti})\text{O}_3)$ Fibers, *J. Sol-Gel. Sci. Tech.*, **81**, 1189-96 (1998)

Takahashi M, Izuki M, Kanno R and Kawamoto Y, Upconversion

characteristics of Er³⁺ in transparent oxyfluoride glass-ceramics, *J. Appl. Phys.*, **83**(7), 3920-3922 (1998).

Takahashi M, Fujiwara T and Ikushima A.J., Defect formation in GeO₂-SiO₂ glass by UV-excited poling, *Jpn. J. Appl. Phys.*, **37**, 71-74 (1998).

Takahashi M, Fujiwara T, Kawachi T and Ikushima A J, Thermal equilibrium of Ge-related defects in GeO₂-SiO₂ glass, *Appl. Phys. Lett.*, **72**(16), 1287-1289 (1998).

Takahashi M, Kano M and Kawamoto Y, Compositional dependence of local vibrational around rare earth ion in SiO₂-PbF₂ glass-ceramics, *J. Phys.: Condens. Matters*, **10**(14), 3269-3274 (1998).

Shojiya M, Takahashi M, Kanno R, Kawamoto Y and Kadono K, Optical transitions of Er³⁺ ions in ZnCl₂-based glass, *J. Appl. Phys.*, **82**(12), 6259-66 (1998).

Fujiwara T, Takahashi M and Ikushima A J, Second-harmonic generation in UV-poled glass, *Jpn J. Appl. Phys.*, **37**, 15-18 (1998).

Shojiya M, Takahashi M, Kanno R, Kawamoto Y and Kadono K, Optical transitions of Nd³⁺ ions in ZnCl₂-based glass, *Appl. Phys. Lett.*, **72**(23), 882-884 (1998).

Higuchi H, Takahashi M, Kawamoto Y, Kadono K, Ohtsuki T, Peyghanbarian N and Kitamura N, Optical transitions and frequency upconversion emission of Er³⁺ ions in Ga₂S₃-GeS₂-La₂S₃ glasses, *J. Appl. Phys.*, **83**(1), 19-27 (1998).

Shigemura H, Shojiya M, Kanno R, Kawamoto Y, Kadono K and Takahashi M, Optical property and local environment of Ni²⁺ in fluoride glasses, *J. Phys. Chem.*, **102**(11), 1920-1925 (1998).

FUNDAMENTAL MATERIAL

PROPERTIES

I. Molecular Rheology

Osaki K, Watanabe H and Inoue T: On the Estimation of Stresses in Steady Shear Flow from the Dynamic Viscoelasticity for Polymeric Liquids, *J. Soc. Rheol. Jpn.*, **26**, 49-52 (1998).

Watanabe H: Rheology of Multiphase Polymeric Systems, in Araki T, Tran-Cong Q and Shibayama M ed., "Structures and Properties of Multiphase Polymeric Materials", Chapter 9, Marcel Dekker, New York, 317-360 (1998).

Watanabe H, Yao M-L, Osaki K, Shikata T, Niwa H, Morishima Y, Balsara N P and Wang H: Nonlinear Rheology and Flow-induced Structure in a Concentrated Spherical Silica Suspension, *Rheol. Acta*, **37**, 1-6 (1998).

Watanabe H, Sato T, Osaki K, Hamersky M, Chapman B and Lodge T: Diffusion and Viscoelasticity of Copolymer Micelles in a Homopolymer Matrix, *Macromolecules*, **31**, 3740-3742 (1998).

Watanabe H, Sato T, Osaki K, Aoki Y, Li L, Uchida H, Kakiuchi M and Yao M-L: Rheological Images of Poly(vinyl chloride) Gels. 4. Nonlinear Behavior in a Critical Gel State, *Macromolecules*, **31**, 4198-4204 (1998).

Aoki Y, Li L, Uchida H, Kakiuchi M and Watanabe H:

Rheological Images of Poly(vinyl chloride) Gels. 5. Effect of Molecular Weight Distribution, *Macromolecules*, **31**, 7472-7478 (1998).

Matsumiya Y, Watanabe H, Osaki K and Yao M-L: Dynamics of Dipole-Inverted Cis-Polyisoprene Chains in a Matrix of Long, Entangling Chains. 1. Effects of Constraint Release on the Eigenmodes of the Local Correlation Function, *Macromolecules*, **31**, 7528-7537 (1998).

Watanabe H, Matsumiya Y, Osaki K and Yao M-L: Dynamics of Dipole-Inverted Cis-Polyisoprene Chains in a Matrix of Long, Entangling Chains. 2. Effects of Constraint Release on the Coherence of the Subchain Motion, *Macromolecules*, **31**, 7538-7545 (1998).

Matsumiya Y, Watanabe H, Inoue T, Osaki K and Yao M-L: Rheo-Dielectric Behavior of Oligostyrene and Polyisoprene, *Macromolecules*, **31**, 7973-7975 (1998).

Watanabe H, Osaki K, Matsumoto M, Bossev D P, McNamee C E, Nakahara M and Yao M-L: Nonlinear Rheology of Threadlike Micelles of Tetraethylammonium Perfluorooctyl Sulfonate, *Rheol. Acta*, **37**, 470-485 (1998).

Watanabe H: Structure and Rheology of Block Copolymer Systems, *Fiber (Sen-i Gakkaishi)*, **4**, 391-395 (1998). (in Japanese)

Ryu DS, Inoue T and Osaki K: A Rheo-optical study of polymer crystallization in the process of elongation of films, *Polymer*, **39**, 2515-2520 (1998).

Inoue T, Kuwada S, Ryu D-S and Osaki K: Effect of Wavelength on Strain-Induced Birefringence of Polymers, *Polymer J.*, **31**, 929-934 (1998).

Inoue T, Ryu D-S and Osaki K: A Rheo-Optical Study on Polystyrene under Large Tensile Deformation around the Glass Transition Temperature, *Macromolecules*, **31**, 6977-6983 (1998).

Onogi T, Inoue T and Osaki K: Shear Birefringence Measurement on Amorphous Polymers around the Glass Transition Zone, *Nihon Reoroji Gakkaishi*, **26**, 49-52 (1998). (in Japanese)

II. Polymer Materials Science

Hansen J, Kanaya T, Nishida K, Kaji K, Tanaka T and Yamaguchi A: Role of Vibrational Softening in Fast Dynamics of an Amorphous Polyimide Far below T_g, *J. Chem. Phys.*, **108**, 6492-6497 (1998).

Bartos J, Klimova M, Kanaya T and Kaji K: Microscopic Dynamic Aspects of the Free Radical Decay Acceleration in sub-T_g Region in Atactic Poly(propylene), *Polymer*, **39**, 1107-1112 (1998).

Kanaya T, Tsukushi I, Kaji K, Gabrys B and Bennington S M: Heterogeneity of Amorphous Polymers with Various Fragility Indices As Studied in Terms of non-Gaussian Parameter, *J. Non-Cryst. Solids*, **235/237**, 212-218 (1998).

Tsukushi I, Kanaya T and Kaji K: Spatial Scale Concerning the Low-energy Excitation in Amorphous Polymers, *J. Non-Cryst. Solids*, **235/237**, 250-253 (1998).

Kanaya T, Takeshita H, Nishikoji Y, Ohkura M, Nishida K and Kaji K: Micro- and Mesoscopic Structure of Poly(vinyl alcohol) Gels Determined by Neutron and Light Scattering, *Supramolecular Science*, **5**, 215-221 (1998).

Hara K, Nakamura A, Hiramatsu N and Kanaya T: Low-energy Excitation in Hydrated Gel, *Physica*, **B241/243**, 982-983 (1998).

Kaji K: Glass Transition of Polymers, *Nippon Gomu Kyokaishi*, **71**, 125-128 (1998) (in Japanese).

Takeshita H, Kanaya T, Kaji K, Nishida K, Nishikoji Y, Ohkura M, Hierarchic Structure of Poly(vinyl alcohol) Gels, *Kobunshi Ronbunshu*, **55**, 595-602 (1998) (in Japanese).

Kanaya T: Relaxation Process in Glass-forming Polymers and Heterogeneity, *Koubunshi*, **47**, 302-305 (1998) (in Japanese).

Kanaya T, Zorn R, Tsukushi, I, Murakami S, Kaji K and Richter R: Orientational Effects on Low-energy Modes in Amorphous Poly(ethylene terephthalate) Fiber, *J. Chem. Phys.*, **109**, 10456-10463 (1998)

III. Molecular Motion Analysis

Masuda K and Horii F: CP/MAS ^{13}C NMR Analyses of the Chain Conformation and Hydrogen Bonding for Frozen Poly(vinyl alcohol) Solutions, *Macromolecules*, **31**, No. 17, 5810-5817 (1998).

Kawanishi H, Tsunashima Y and Horii F: A Nest of Structures in Dynamics of Cellulose Diacetate in *N, N*-dimethylacetamide in Quiescent Solution State Studied by Dynamic Light Scattering, *J. Chem. Phys.*, **109**, No. 24, 11027-11031 (1998).

Kaji H and Horii F: Analyses of the Local Order in Poly(ethylene terephthalate) in the Glassy State by Two-Dimensional Solid State ^{13}C Spin Diffusion Nuclear Magnetic Resonance Spectroscopy, *J. Chem. Phys.*, **109**, No. 11, 4651-4658 (1998).

Kawanishi H, Tsunashima Y, Okada S and Horii F: Change in Chain Stiffness in Viscometric and Ultracentrifugal Fields: Cellulose Diacetate in *N, N*-dimethylacetamide Dilute Solution, *J. Chem. Phys.*, **108**, No. 14, 6014-6025 (1998).

Hirai A, Tsuji M and Horii F: Helical Sense of Ribbon Assemblies and Splayed Microfibrils of Bacterial Cellulose, *Sen-i gakkaiishi*, **54**, No. 10, 506-510 (1998).

Nakaoki T, Ohira Y, Hayashi H and Horii F: Spontaneous Crystallization of the Planar Zigzag Form of Syndiotactic Polypropylene at 0°C, *Macromolecules*, **31**, No. 8, 2705-2706 (1998).

Hirai A, Tsuji M, Yamamoto H and Horii F: *In Situ* Crystallization of Bacterial Cellulose. III. Influences of Different Polymeric Additives on the Formation of Microfibrils as Revealed by Transmission Electron Microscopy, *Cellulose*, **5**, No. 3, 201-213 (1998).

Shen Y, Kaji H and Horii F: An Analytical Expression of Magic Angle Spinning Nuclear Magnetic Resonance Free Induction Decays in Two-Site Exchange Problems, *Chinese Phys. Lett.*, **5**, No.6, 453-454 (1998).

Kawaguchi T, Mamada A, Hosokawa Y and Horii F: ^2H NMR Analysis of the Phenylene Motion in Different Poly(ethylene terephthalate) Samples, *Polymer*, **39**, No.13, 2725-2732 (1998).

Horii F, Kaji H, Ishida H, Kuwabara K, Masuda K and Tai T: Solid-State NMR Analyses of the Structure and Dynamics of Polymers in the Different States, *J. Mol. Struct.*, **441**, 303-311 (1998).

Kaji H, Tai H and Horii F, Solid-State NMR Analyses of the Noncrystalline Structure and Relaxation of Glassy Polymers, *Koubunshi*, **47**, 316-317 (1998) (in Japanese).

Horii F: NMR Relaxations and Dynamics, in "Solid State NMR of Polymers", Ando I and Asakura T, Eds., Elsevier, 1998, pp. 51-81.

Horii F and Masuda K: Hydrogen-Bonded Polymers, in "Solid State NMR of Polymers", Ando I and Asakura T, Eds., Elsevier, 1998, pp. 713-736.

Horii F, Ed., Solid-State NMR and Materials, Special issue of *J. Mol. Struct.*, **441**, No. 2-3, 101-319 (1998).

Horii F, Ed., Collected Papers of the Annual Meeting of the Cellulose Society of Japan, Special issue of *Cellulose*, **5**, No. 2 and 3, 113-229 (1998).

ORGANIC MATERIALS CHEMISTRY

I. Polymeric Materials

Takaragi A, Minoda M, Miyamoto T and Watanabe J: Synthesis and Thermal Properties of Liquid Crystalline Side Chain Polymers with Pendant Cellobiose Residues, *Macromol. Chem. Phys.*, **199**, 1119-1126 (1998).

Takaragi A, Miyamoto T, Minoda M and Watanabe J: Thermotropic Liquid Crystalline Poly(Vinyl Ether)s with Pendant Cellobiose Residues: Synthesis and Mesophase Structure, *Macromol. Chem. Phys.*, **199**, 2071-2077 (1998).

Ide N, Sato T, Miyamoto T and Fukuda T: Thermoreversible Hydrogel of Short-Chain *O*-(2,3-Dihydroxypropyl)cellulose/Borax Aqueous Solution. Microscopic versus Macroscopic Properties, *Macromolecules*, **31**, 8878-8885 (1998).

Kajiwara K and Miyamoto T: Progress in Structural Characterization of Functional Polysaccharides, in "Polysaccharides: Structural Diversity and Functional Versatility", ed. by Dumitriu S, Marcel Dekker, Inc., New York, 1-55 (1998).

Miyamoto T, Tsujii Y and Yamamoto S: Functionalization of Cellulose-based Polysaccharides, *Kasen-Kouenshu*, **55**, 1-7 (1998) (in Japanese).

Ohno K, Ejaz M, Fukuda T, Miyamoto T and Shimizu Y: Nitroxide-Controlled Free Radical Polymerization of *p*-tert-Butoxystyrene. Kinetics and Applications, *Macromol. Chem. Phys.*, **199**, 291-297 (1998).

Ohno K, Tsujii Y, Miyamoto T, Fukuda T, Goto M, Kobayashi K and Akaike T: Synthesis of a Well-Defined Glycopolymer by Nitroxide-Controlled Free Radical Polymerization, *Macromolecules*, **31**, 1064-1069 (1998).

Okamura H, Ide N, Minoda M, Komatsu K and Fukuda T: Solubility and Micellization Behavior of C_{60} Fullerenes with Two Well-Defined Polymer Arms, *Macromolecules*, **31**, 1859-1865 (1998).

Ohno K, Goto A, Fukuda T, Xia J and Matyjaszewski K: Kinetic Study on the Activation Process in an Atom Transfer Radical Polymerization, *Macromolecules*, **31**, 2699-2701 (1998).

Goto A, Ohno K and Fukuda T: Mechanism and Kinetics of Iodide-Mediated Polymerization of Styrene, *Macromolecules*, **31**, 2809-2814 (1998).

Ejaz M, Yamamoto S, Ohno K, Tsujii Y and Fukuda T: Controlled Graft Polymerization of Methyl Methacrylate on Silicon Substrate by the Combined Use of the Langmuir-Blodgett and Atom Transfer Radical Polymerization Techniques, *Macromolecules*, **31**, 5934-5936 (1998).

Ohno K, Tsujii Y and Fukuda T: Synthesis of a Well-Defined Glycopolymer by Atom Transfer Radical Polymerization, *J. Polym. Sci., Polym. Chem.*, **36**, 2473-2481 (1998).

Ohno K, Fukuda T and Kitano H: Free Radical Polymerization of a Sugar Residue-Carrying Styryl Monomer with a Lipophilic Alkoxyamine Initiator: Synthesis of a Well-Defined Novel Glycolipid, *Macromol. Chem. Phys.*, **199**, 2193-2197 (1998).

Fukuda T, Goto A, Ohno K and Tsujii Y: Mechanism and Kinetics of Nitroxide-Controlled Free Radical Polymerization, in "Controlled Radical Polymerization (ACS Symposium Series 685)", ed. by Matyjaszewski K, pp. 180-199 (1998).

Ohno K and Fukuda T: Synthesis of New Types of Polymers by Living Radical Polymerization Technique, *Kobunshi-Kako*, **47**, 419-425 (1998) (in Japanese).

Yamamoto S, Miyamoto T, Kokubo T and Nakamura T: Preparation of Polymer-Silicate Hybrid Materials Bearing Silanol Groups and the Apatite Formation on/in the Hybrid Materials, *Polymer Bulletin*, **40**, 243-250 (1998).

Oyane A, Minoda M, Miyamoto T, Nakanishi K, Kim H-M, Miyaji F, Kokubo T and Nakamura T: Surface Modification of Ethylene-Vinylalcohol Copolymer for Inducing its Apatite-Forming Ability, *Bioceramics*, **11**, 687-690 (1998).

Kondo T and Miyamoto T: The Influence of Intramolecular Hydrogen Bonds on Handedness in Ethylcellulose /CH₂Cl₂ Liquid Crystalline Mesophases, *Polymer*, **39**, 1123-1127 (1998).

Takatsuka T, Oneichi Y, Matsuura A, Joko K, Kimura K, Miyamoto T and Arai M: Isolation of Cuticle-Degrading *Bacillus cereus* NS-11 and Properties of the Enzyme Produced by the Bacterium, *Seibutsu-Kogaku*, **76**, 43-50 (1998) (in Japanese).

Kajiwara K and Miyamoto T: Application of High-Technology Fibers in Sports, *Descende Sports Science*, **19**, 14-34 (1998) (in Japanese).

Mabuchi M, Ito S, Yamamoto M, Miyamoto T, Schmidt A and Knoll W: Nanostructure and Thermal Stability of the Polyglutamate Langmuir-Blodgett Films Probed by Interlayer Energy Transfer Method, *Macromolecules*, **31**, 8802-8808 (1998).

II. High-Pressure Organic Chemistry

Nishinaga T, Izukawa Y, Komatsu K: The Ring Inversion of Silacycloheptatriene and Cycloheptatriene. Comparison of the "Aromaticity" of Planar and Boat Conformers Estimated by Nucleus-Independent Chemical Shift (NICS), *J. Phys. Org. Chem.*, **11**, 475-477 (1998).

Nishinaga T, Izukawa Y, Komatsu K: Effects of Substituents on Silicon upon the Ring Inversion of Silolepines Annulated with Bicyclo[2.2.2]octene Frameworks, *Chem. Lett.*, **1998**, 269-270.

Fujiwara K, Murata Y, Wan TSM, Komatsu K: Synthesis of a Propargyl Alcohol Having a C₆₀ Cage, Its Transformation into C₆₀ Derivatives with Polar Functional Groups, and the Solubility Measurements, *Tetrahedron*, **54**, 2049-2058 (1998).

Okamura H, Ide N, Minoda M, Komatsu K, Fukuda T: Solubility and Micellization Behavior of C₆₀ Fullerenes with Two Well-Defined Polymer Arms, *Macromolecules*, **31**, 1859-1865 (1998).

Nishinaga T, Nakayama H, Nodera N, Komatsu K: Synthesis and Properties of 1,4-Dimethoxynaphtho[2,3]-annulated Dehydroannulenes, *Tetrahedron Lett.*, **39**, 7139-7142 (1998).

Nishinaga T, Kawamura T, Komatsu K: Synthesis and Structural Characterization of Novel Silver(I) Complexes of Tetradehydro[16]annulene Annulated with Bicyclo[2.2.2]octene Units, *Chem. Commun.*, **1998**, 2263-2264.

Komatsu K, Wang G-W, Murata Y, Tanaka T, Fujiwara K, Yamamoto K, Saunders M: Mechanochemical Synthesis and Characterization of the Fullerene Dimer C₁₂₀, *J. Org. Chem.*, **63**, 9358-9366 (1998).

Komatsu K: Dumbbell-Shaped Fullerene, *Kagaku*, **53**, 14-16 (1998) (in Japanese).

Komatsu K, Shiro M: Synthesis and X-Ray Structure Determination of the Dumbbell-Shaped Fullerene Dimer C₁₂₀, *Rigaku-Denki Journal*, **29**, 3-8 (1998) (in Japanese).

Komatsu K, Wang G-W, Shiro M, Murata Y, Tanaka T: Synthesis and Structural Determination of Fullerene Dimer C₁₂₀: Creation of Bucky Dumbbell, *Kagaku to Kougyou*, **51**, 774-776 (1998) (in Japanese).

SYNTHETIC ORGANIC CHEMISTRY

I. Synthrtic Design

Yamaguchi S, Iimura K, and Tamao K: Silole-Acetylene π -Electronic Systems with Low Bandgaps: Synthesis, Structure, and UV-vis Absorption Spectra of 2,5-Diethynylsilole Derivatives and Their Polymers, *Chem. Lett.*, 89-90 (1998).

Plack V, Sakhaii P, Fischer A, Jones P. G, Schmutzler R, Tamao K, and Sun G.-R: X-ray Analysis and NMR-Studies of *E*- and *Z*-1,2-bis(fluorodimethylsilyl)-1,2-diphenylethenes, *J. Organomet. Chem.*, **553**, 111-114 (1998).

Yamaguchi S, Jin R.-Z, and Tamao K: Modification of the Electronic Structure of Silole by the Substituents on the Ring Silicon, *J. Organomet. Chem.*, **559**, 73-80 (1998).

Yamaguchi S, Akiyama S, and Tamao K: Synthesis, Structures, Photophysical Properties, and Dynamic Stereochemistry of Tri(9-anthryl)silane Derivatives, *Organometallics*, **17**, 4347-4352 (1998).

Tanaka Y, Hada M, Kawachi A, Tamao K, and Nakatsuji H: Self-Condensation of Lithium (Methoxy)silylenoid: A Model Study by Ab Initio Calculation, *Organometallics*, **17**, 4573-4577 (1998).

Yamaguchi S, Itami Y, and Tamao K: Group 14 Metalloles Having Thienyl Groups on 2,5-Positions: Effects of Group 14 Elements on Their π -Electronic Structures, *Organometallics*, **17**, 4910-4916 (1998).

Yamaguchi S, Jin R.-Z, Ohno S, and Tamao K: Halodesilylation Route to 2,5-Difunctionalized 3,4-Dialkylsiloles and Their Derivatization to 2,2'-Bisilole, *Organometallics*, **17**, 5133-5138 (1998).

Katkevics M, Yamaguchi S, Toshimitsu A, and Tamao K: From Tellurophenes to Siloles. Synthesis, Structures, and

Photophysical Properties of 3,4-Unsubstituted 2,5-Diarylsiloles, *Organometallics*, **17**, 6796-5800 (1998).

Yamaguchi S and Tamao K: Silole-Containing σ - and π -Conjugated Compounds, *J. Chem. Soc., Dalton Trans., Perspective*, 3693-3702 (1998).

Yamaguchi S and Tamao K: Silole-Containing σ - and π -Conjugated Compounds, *J. Synth. Org. Chem., Jpn.*, **56**, 500-510 (1998) (in Japanese).

Tamao K and Toshimitsu A: Synthetic Applications of Hypervalent Compounds, *Kikan Kagaku Sosetsu*, **34**, 127-147 (1998) (in Japanese).

Noyori R, Shibasaki M, Suzuki K, Tamao K, Nakasuji K, and Narasaka K, Eds.: *Organic Chemistry II*, Tokyo Kagaku Doujin, 1998.

II. Fine Organic Synthesis

Ahn M, Tanaka K, and Fuji K: Diastereoselective reaction of 1,1'-binaphthyl ester enolates with carbonyl electrophiles, *J. Chem. Soc. Perkin trans I*, 185-191 (1998).

Fuji K, Oka T, Kawabata T and Kinoshita T: The first Synthesis of an Optically Active Molecular Bevel Gear with Only Two Cogs on Each Wheel, *Tetrahedron Lett.*, **39**, 1373-1376 (1998).

Fuji K, Kawabata T, Ohmori T, Shang M and Node M: Enantioselective Creation of Quaternary Carbon Centers through Addition-Elimination Reaction: Asymmetric Nitroolefination of 3-Substituted 2-Oxindoles, *Heterocycles*, **47**, 951-964 (1998).

Tsubaki K, Tanaka K, Kinoshita T and Fuji K: Complexation of C₆₀ with Hexahomoxacalix[3]arenes and Structures of Complexes in the Solid State, *Chem. Commun.*, 895-896 (1998).

Tsubaki K, Otsubo T, Tanaka K, Fuji K and Kinoshita T: Stepwise Construction of Some Hexahomoxacalix[3]arenes and Their Conformation in Solid State, *J. Org. Chem.*, **63**, 3260-3265 (1998).

Fuji K, Sakurai M, Kinoshita T and Kawabata T: Palladium-Catalyzed Asymmetric Reduction of Allylic Esters with a New Chiral Monodentate Ligand, 8-Diphenylphosphino-8'-methoxy-1,1'-binaphthyl, *Tetrahedron Lett.* **39**, 6323-6326 (1998).

Fuji K and Kawabata T: Memory of Chirality-A New Principle in Enolate Chemistry, *Chemistry. A European J.*, **4**, 373-376 (1998)

Tanaka K and Fuji K: Asymmetric Olefination Using Optically Active Phosphorous Reagents, *J. Synth. Org. Chem. Jpn.*, **56**, 521-531 (1998) (in Japanese).

BIOORGANIC CHEMISTRY

I. Bioorganic Reaction Theory

Dao D H, Kawai Y, Hida K, Hornes S, Nakamura K, Ohno A, Okamura M, Akasaka T: Stereochemical Control in Microbial Reduction. 30. Reduction of Alkyl 2-Oxo-4-phenylbutyrate as Precursors of Angiotensin Converting Enzyme (ACE) Inhibitors. *Bull. Chem. Soc. Jpn.*, **71**, 425-432 (1998).

Dao D H, Okamura M, Akasaka T, Kawai Y, Hida K, Ohno A: Stereochemical Control in Microbial Reduction. Part 31: Reduction of Alkyl 2-Oxo-4-arylbutyrates by Baker's Yeast under

Selected Reaction Conditions. *Tetrahedron: Asymmetry*, **9**, 2725-2737 (1998).

Kawai Y, Kunitomo J, Ohno A: First Determination of the Absolute Configuration of an Atropisomeric Flavin Derivative. *Acta Crystallogr.*, **C54**, 77-79 (1998).

Kawai Y, Matsuo T, Ohno A: Conformational Effect (Induced-Fit) on Catalytic Activity of α -Chymotrypsin. *Bull. Chem. Soc. Jpn.*, **71**, 2187-2196 (1998).

Kawai Y, Hayashi M, Inaba Y, Saitou K, Ohno A: Asymmetric Reduction of α,β -Unsaturated Ketones with a Carbon-Carbon Double-Bond Reductase from Baker's Yeast: *Tetrahedron Lett.*, **39**, 5225-5228 (1998).

Kawai Y, Hida K, Dao D H, Ohno A: Asymmetric Synthesis of β -Hydroxy Esters Having Three Consecutive Chiral Centers with a Reductase from Bakers' Yeast. *Tetrahedron Lett.*, **39**, 9219-9222 (1998).

Nakamura K: Highly Stereoselective Reduction of Ketones by *Geotrichum candidum*. *J. Mol. Catal. B: Enzym.*, **5**, 129-132 (1998).

Nakamura K, Matsuda T, Shimizu M, Fujisawa T: Asymmetric Reduction of Trifluoromethyl Ketones Containing a Sulfur Functionality by the Alcohol Dehydrogenase from *Geotrichum*. *Tetrahedron*, **54**, 8393-8402 (1998).

Nakamura K, Matsuda T: Asymmetric Reduction of Ketones by the Acetone Powder of *Geotrichum candidum*. *J. Org. Chem.*, **63**, 8957-8964 (1998).

Ohno A, Ishikawa Y, Yamazaki N, Okamura M, Kawai Y: NAD(P)⁺-NAD(P)H Models. 88. Stereoselection without Steric Effect but Controlled by Electronic Effect of a Carbonyl Group: Syn/Anti Reactivity Ratio, Kinetic Isotope Effect, and an Electron-Transfer Complex as a Reaction Intermediate. *J. Am. Chem. Soc.*, **120**, 1186-1192 (1998).

Ohno A: Stereoselection without Steric Effect but Controlled by Electronic Effect: Important Contribution of Ground State. *Bull. Chem. Soc. Jpn.*, **71**, 2041-2050 (1998).

Sugiyama T: Organic Synthesis by Means of Lanthanoids. Cerium (IV) Compounds in Organic Synthesis: Past, Present, and Future. *Kikan Kagaku Sosetsu*, **37**, 161-171 (1998) (in Japanese).

Sugiyama T, Mori S, Komatsu K, Ohno A: Cerium ammonium nitrate-formic acid promoted 1,3-dipolar cycloaddition of [60]fullerene with nitrile oxide from nitroalkanes. *Kidorui*, **32**, 56 (1998) (in Japanese).

Uenishi J, Hiraoka T, Hata S, Nishiwaki K, Yonemitsu O, Nakamura K, Tsukube H: Chiral Pyridines: Optical Resolution of 1-(2-Pyridyl)- and 1-[6-(2,2'-Bipyridyl)]ethanols by Lipase-Catalyzed Enantioselective Acetylation. *J. Org. Chem.*, **63**, 2481-2487 (1998).

Yasui S, Tsujimoto M, Okamura M, Ohno A: Stereoelectronic Effects on the One-Electron Donor Reactivity of Trivalent Phosphorus Compounds. Experimental and Theoretical Investigations. *Bull. Chem. Soc. Jpn.*, **71**, 927-932 (1998).

II. Bioactive Chemistry

Kamiuchi T, Abe E, Imanishi M, Kaji T, Nagaoka M, Sugiura Y: Artificial Nine Zinc-Finger peptide with 30 Base Pair Binding

Sites. *Biochemistry*, **37**, 13827-13834 (1998).

Yokono M, Saegusa N, Matsushita K, Sugiura Y: Unique DNA Binding Mode of the N-Terminal Zinc Finger of Transcription Factor Sp1. *Biochemistry*, **37**, 6824-6832 (1998).

Okahata Y, Niikura K, Sugiura Y, Sawada M, Morii T: Kinetic Studies of Sequence-Specific Binding of GCN4-bZIP Peptides to DNA Strands Immobilized on a 27-MHz Quartz-Crystal Microbalance. *Biochemistry* **37**, 5666-5672 (1998).

Matsushita K, Hagihara M, Sugiura Y: Participation of Oligomerization through C-terminal Domain Region of Sp1 in DNA Binding. *Biol. Pharm. Bull.*, **21**, 1094-1097 (1998).

Araki M, Okuno Y, Hara Y, Sugiura Y: Allosteric regulation of a ribozyme activity through ligand-induced conformational change. *Nucleic Acids Res.*, **26**, 3379-3384 (1998).

Araki M, Okuno Y, Sugiura Y: Modulation of a ribozyme activity by introducing aptamer domain: A model for the allosteric interactions. *Nucleic Acids Res. (Sym. Ser.)*, **39**, 227-228 (1998).

Ando T, Ishii M, Kajiura T, Kameyama T, Miwa K, Sugiura Y: A New Non-Protein Enediyne Antibiotic N1999A2: Unique Enediyne Chromophore Similar to Neocarzinostatin and DNA Cleavage Feature. *Tetrahedron Lett.*, **39**, 6495-6498 (1998).

Kato Y, Sugiura Y, Sunamoto J: Complex formation of neocarzinostatin chromophore and hydrophobized polysaccharide as an apoprotein model. *Proc. Japan. Acad.*, **74**, 116-121 (1998).

Imanishi M, Sugiura Y: Design of new zinc-finger proteins. *Chemistry*, **53**, 72-73 (1998) (in Japanese).

Yamada K, Ojika M, Kigoshi H, Sugiura Y: Bracken carcinogen. *Tanpakushitsu-Kakusan-Kouso*, **43**, 28-37 (1998) (in Japanese).

Futaki S: Creation of Ion Channel Function Using Synthetic Peptides. *J. Syn. Org. Chem. Jpn.*, **56**(2), 125-133 (1998).

Futaki S: Peptide Ion Channels: Design and Creation of Function. *Biopolymers (Peptide Science)*, **47**(1), 75-81 (1998).

Futaki S: Peptide Synthesis Aiming at Elucidation and Creation of Protein Functions. *Yakugaku Zasshi*, **118**(11), 493-510 (1998).

Tsutsumishita Y, Onda T, Okada K, Takeda M, Endou H, Futaki S, Niwa M: Involvement of H₂O₂ Production in Cisplatin-Induced Nephrotoxicity. *Biochem. Biophys. Res. Commun.*, **242**(2), 310-312 (1998).

Mori H, Kamada M, Maegawa M, Yamamoto S, Ando T, Futaki S, Yono M, Kido H, Samuel S. Koide: Enzymatic Activation of Immunoglobulin Binding Factor in Female Reproductive Tract. *Biochem. Biophys. Res. Commun.*, **246**(2), 409-413 (1998).

Tachibana R, Harashima H, Shono M, Azumano M, Niwa M, Futaki S, Kiwada H: Intracellular Regulation of Macromolecules using pH-sensitive Liposomes and Nuclear Localization Signal: Qualitative and Quantitative Evaluation of Intracellular Trafficking. *Biochem. Biophys. Res. Commun.*, **25**(2), 538-544 (1998).

Kamada M, Mori H, Maeda N, Yamamoto S, Kunimi K, Takikawa M, Maegawa M, Aono T, Futaki S, Samuel S. Koide: $\tilde{\epsilon}$ -Microseminoprotein/Prostatic Secretory Protein Is a Member of Immunoglobulin Binding Factor Family. *Biochim. Biophys. Acta*, **1388**(1), 101-110 (1998).

III. Molecular Clinical Chemistry

Tanaka S, Kawamata J, Shimohama S, Akaki H, Akiguchi I, Kimura J and Ueda K: Inferior temporal lobe atrophy and APOE genotypes in Alzheimer's disease: X-ray computed tomography, magnetic resonance imaging and Xe-133 SPECT studies. *Dement Geriatr Cogn Disord*, **9**, 90-98 (1998).

Ikemoto M., Tsunekawa S, Tanaka K, Tanaka A, Yamaoka Y, Ozawa K, Fukuda Y, Moriyasu F, Totani M, Kasai Y, Mori T and Ueda K: Liver-type arginase in serum during and after liver transplantation: a novel index in monitoring conditions of the liver graft and its clinical significance. *Clin Chim Acta*, **271**, 11-23 (1998).

Tokime T, Ueda K, Nozaki K and Kikuchi H: Enhanced poly(ADP-ribosyl)ation after focal ischemia in rat brain. *J Cerebral Blood Flow Metab*, **18**, 991-997 (1998).

Tanaka S, Chen X, Xia Y, Kang DE, Matoh N, Sundsmo M, Thomas RG, Katzman R, Thal LJ, Trojanowski JQ, Saitoh T, Ueda K and Masliah E, Association of CYP2D microsatellite polymorphism with Lewy body variant of Alzheimer's disease. *Neurology*, **50**, 1556-1562 (1998)

Masliah E, Mallory M, Alford M, Tanaka S and Hansen LA, Caspase dependent DNA fragmentation might be associated with excitotoxicity in Alzheimer disease. *J Neuropathol Exp Neurol*, **57**, 456-464 (1998).

Ariumi Y, Ueda K, Masutani M, Noda M, Copeland TD, Hatanaka M and Shimotohno K, In vivo phosphorylation of poly(ADP-ribose) polymerase is independent of its activation. *FEBS Lett*, **436**, 288-292 (1998).

MOLECULAR BIOFUNCTION

I. Functional Molecular Conversion

Sawai Y and Sakata K: An NMR Analytical Approach to Clarify the Antioxidative Molecular Mechanism of Catechins Using DPPH. *J. Agric. Food Chem.*, **46**, 111-114 (1998).

Ijima Y, Ogawa K, Watanabe N, Usui T, Ohnishi-Kameyama M, Nagata T, Sakata K: Characterization of β -Primeverosidase, Being Concerned with Alcoholic Aroma Formation in Tea Leaves to be Processed into Black Tea, and Preliminary Observations on Its Substrate Specificity. *J. Agric. Food Chem.*, **46**, 1712-1718 (1998).

Oka N, Ikegami A, Ohki M, Sakata K, Yagi A, Watanabe N: Citronellyl Disaccharide Glycoside as an Aroma Precursor from Rose Flowers. *Phytochemistry*, **47**, 1527-1529 (1998).

Guo W, Sasaki N, Fukuda M, Yagi A, Watanabe N, Sakata K: Isolation of An Aroma Precursor of Benzaldehyde from Tea Leaves (*Camellia sinensis* var. *sinensis* cv. *Yabukita*). *Biosci. Biotechnol. Biochem.*, **62**, 2052-2054 (1998).

Sakata K, Watanabe N, Usui T: Molecular Basis of Alcoholic Aroma Formation During Tea Processing. *Proceedings of the 3rd International Conference on Food Science and Technology*, Davis, California, in press (1998).

Sakata K and Watanabe S: Importance of Sugar Conjugates as Aroma Precursor in Plants—Molecular Mechanism of Alcoholic Aroma Formation in Tea Leaves and Flowers—, *J. Appl. Glycosci.*, **45**, 123-129 (1998) (in Japanese).

Sakata K: Function and Development of Biomaterials from Plants. 2. Chlorophyll Derivatives. in "Recent Development of Food Factors for the Diseases Prevention" (Niki E, Yoshikawa T, Osawa T eds), CMC, 254-262 (1998) (in Japanese).

Sakata K: 6. Antioxidants in Food. 6) Sea Weeds, in "Compilation of Antioxidants" (Yoshikawa T ed), Sentan-Igaku-sha, 157-164 (1998) (in Japanese).

Yamada T, Hiratake J, Aikawa M, Suizu Y, Saito Y, Kawato A, Suginami K, Oda J: Cysteine Protease Inhibitors Produced by the Industrial Koji Mold, *Aspergillus oryzae O-1018*, *Biosci. Biotech. Biochem.*, **62**, 907-914 (1998).

Sawa M, Imaeda Y, Hiratake J, Fujii R, Umeshita R, Watanabe M, Kondo H, Oda J: Toward the Antibody-Catalyzed Chemiluminescence. Design and Synthesis of Hapten, *Bioorg. & Med. Chem. Lett.*, **8**, 647-652 (1998).

Katoh M, Hiratake J, Oda J: ATP-Dependent Inactivation of *E. coli* γ -Glutamylcysteine Synthetase by L-Glutamic Acid γ -Monohydroxamate, *Biosci. Biotech. Biochem.*, **62**, 1455-1457 (1998).

Tokutake N, Hiratake J, Katoh M, Irie T, Kato H, Oda J: Design, Synthesis and Evaluation of Transition-State Analogue Inhibitors of *Escherichia coli* γ -Glutamylcysteine Synthetase, *Bioorg. & Med. Chem.*, **6**, 1935-1953 (1998).

Shibata H, Kato H, Oda J: Calcium Ion-Dependent Reactivation of a *Pseudomonas* Lipase by Its Specific Modulating Protein, Lip B, *J. Biochem. (Tokyo)*, **123**, 136-141 (1998).

Nakatsu T, Kato H, Oda J: Crystal Structure of Asparagine Synthetase Reveals a Close Evolutionary Relationship to Class II Aminoacyl-tRNA Synthetase, *Nature Struct. Biol.*, **5**, 15-19 (1998).

Shibata H, Kato H, Oda J: Molecular Property and Activity of Amino-Terminal Truncated Forms of Lipase Activator Protein, *Biosci. Biotech. Biochem.*, **62**, 354-357 (1998).

Shibata H, Kato H, Oda J: Random Mutagenesis of *Pseudomonas* Lipase Activator Protein, LipB, *Protein Eng.*, **11**, 467-472 (1998).

Nakajima K, Yamashita A, Akama H, Nakatsu T, Kato H, Hashimoto T, Oda J, Yamada Y: Crystal Structures of Two Tropinone Reductases: Different Reaction Stereospecificities in the Same Protein Fold, *Proc. Nat. Acad. Soc. USA*, **95**, 4876-4881 (1998).

II. Molecular Microbial Science

Li Y-F, Hata Y, Fujii T, Kurihara T and Esaki N. Crystal Structures of Reaction Intermediates of L-2-Haloacid Dehalogenase and Implications for the Reaction Mechanism, *J. Biol. Chem.*, **273**(24), 15035-15044 (1998)

Lim Y-H, Yoshimura T, Kurokawa Y, Esaki N and Soda K. Nonstereospecific Transamination Catalyzed by Pyridoxal Phosphate-dependent Amino Acid Racemases of Broad Substrate Specificity, *J. Biol. Chem.*, **273**(7), 4001-4005 (1998)

Liu J-Q, Kurihara T, Ichihara S, Miyagi M, Tsunasawa S, Kawasaki H, Soda K and Esaki N. Reaction Mechanism of Fluoroacetate Dehalogenase from *Moraxella* sp. B., *J. Biol. Chem.*, **273**(47), 30897-30902 (1998)

Gutierrez A, Yoshimura T, Fuchikami Y, Soda K and Esaki N. A Mutant D-Amino Acid Aminotransferase with Broad Substrate Specificity: Construction by Replacement of the Interdomain

Loop Pro119-Arg120-Pro121 by Gly-Gly-Gly, *Protein Engineering*, **11**(1), 53-58 (1998)

Sugio S, Kashima A, Kishimoto K, Peisach D, Petsko G A, Ringe D, Yoshimura T and Esaki N. Crystal Structures of L201A Mutant of D-Amino Acid Aminotransferase at 2.0Å Resolution: Implication of Structural Role of Leu201 in Transamination, *Protein Engineering*, **11**(8), 613-619 (1998)

Uo T, Yoshimura T, Shimizu S and Esaki N. Occurrence of Pyridoxal 5'-Phosphate-Dependent Serine Racemase in Silkworm, *Bombyx mori*, *Biochem. Biophys. Res. Com.*, **246**(1), 31-34 (1998)

Yoshimune K, Yoshimura T and Esaki N. Hsc62, A New DnaK Homologue of *Escherichia coli*, *Biochem. Biophys. Res. Com.*, **250**(1), 115-118 (1998)

Fuchikami Y, Yoshimura T, Gutierrez A, Soda K and Esaki N. Construction and Properties of a Fragmentary D-Amino Acid Aminotransferase, *J. Biochem.*, **124**(5), 905-910 (1998)

Kurokawa Y, Watanabe A, Yoshimura T, Esaki N and Soda K. Transamination as a Side-Reaction Catalyzed by Alanine Racemase of *Bacillus stearothermophilus*, *J. Biochem.*, **124**(6), 1163-1169 (1998)

Li Y-F, Hata Y, Fujii T, Kurihara T and Esaki N. X-Ray Structure of a Reaction Intermediate of L-2-Haloacid Dehalogenase with L-2-Chloropropionamide, *J. Biochem.*, **124**(1), 20-22 (1998)

Choo D-W, Kurihara T, Suzuki T, Soda K and Esaki N. A Cold-Adapted Lipase of an Alaskan Psychrotroph, *Pseudomonas* sp. B11-1: Gene Cloning, Purification and Characterization, *Appl. Environ. Microbiol.*, **64**(2), 486-491 (1998)

Gorlatova N, Tchorzewski M, Kurihara T, Soda K and Esaki N. Purification, Characterization, and Mechanism of a Flavin Mononucleotide-Dependent 2-Nitropropane Dioxygenase from *Neurospora crassa*, *Appl. Environ. Microbiol.*, **64**(3), 1029-1033 (1998)

Lim Y-H, Yoshimura T, Soda K and Esaki N. Stereospecific Labeling at α -Position of Phenylalanine and Phenylglycine with Amino Acid Racemase, *J. Ferment. Bioeng.*, **86**(4), 400-402 (1998)

Liu L, Yoshimura T, Endo K, Kishimoto K, Fuchikami Y, Manning M J, Esaki N and Soda K. Compensation for D-Glutamate Auxotrophy of *Escherichia coli* WM335 by D-Amino Acid Aminotransferase Gene and Regulation of *murI* Expression. *Biosci. Biotech. Biochem.*, **62**(1), 193-195. (1998)

MOLECULAR BIOLOGY AND INFORMATION

I. Biopolymer Structure

Hata Y, Li Y.-F., Fujii T, Akutagawa T and Esaki N: Crystallographic Analysis of the Catalytic Mechanism of L-2-Haloacid Dehalogenase, *3rd Conference of the Asian Crystallographic Association*, 15P5 (1998).

Hata Y, Li Y.-F., Fujii T, Hisano T, Nishihara M., Kurihara T and Esaki N: X-ray Crystal Structure of Reaction Intermediate of L-2-Haloacid Dehalogenase, *Photon Factory Activity Report*, **15**, 27 (1997).

Ishiguro R, Matsumoto T and Takahashi S: The relationship between the behavior of the α -helical peptide in phospholipid

bilayer and its fusion activity, *Colloids & Surfaces, Ser. B* **11**, 153-165 (1998).

Li Y.-F., Hata Y, Fujii T, Hisano T, Nishihara M, Kurihara T and Esaki N: Crystal Structures of Reaction Intermediates of L-2-Haloacid Dehalogenase and Implications for the Reaction Mechanism, *J. Biol. Chem.*, **273**, 15035-15044 (1998).

Li Y.-F., Hata Y, Fujii T, Kurihara T and Esaki N: X-Ray Structure of a Reaction Intermediate of L-2-Haloacid Dehalogenase with L-2-Chloropropionamide, *J. Biochem.*, **124**, 20-22 (1998).

Miyajima Y, Fukushima J, Kawamoto S, Okuda K, Shibano Y, Hata Y and Morihara K: Site-Directed Mutagenesis of His-176 and Glu-177 in *Pseudomonas aeruginosa* Alkaline Protease: Effect on Catalytic Activity, *J. Ferment. Bioeng.*, **84**, 588-590 (1997).

Miyajima Y, Hata Y, Fukushima J, Kawamoto S, Okuda K, Shibano Y and Morihara K: Long-Range Effect of Mutation of Calcium Binding Asparates on the Catalytic Activity of Alkaline Protease from *Pseudomonas aeruginosa*, *J. Biochem.*, **123**, 24-27 (1998).

Yamamoto Y, Okajima T, Fukazawa Y, Fujii T, Hata Y and Sawada S: Conformational Analysis of a Fluorescent Rotor, 6-(2,2-Dicyanovinyl)-1-(2-hydroxyethyl)-1,2,3,4-tetrahydroquinoline, *J. Chem. Soc. Perkin Trans.*, **2**, 561-564 (1998).

Yoshimura Y, Kameyama K, Aimoto S, Takagi T, Goto Y and Takahashi S: Formation of protein- and peptide-membrane assemblies and membrane fusion, *Progr. Colloid Polymer Sci.* **106**, 219-222 (1997).

II. Molecular Biology

Liang Y, Aoyama T, and Oka A: Structural Characterization of the *virB* Operon on the Hairy-root-inducing Plasmid A4. *DNA Research*, **5**, 87-93 (1998).

Ito M, Kato H, Oka A, and Honda G: Phylogenetic Analysis of Japanese *Perilla* Species by Using DNA Polymorphisms. *Natural Medicines*, **52**, 248-252 (1998).

Yamada T, Imaishi H, Oka A, and Ohkawa H: Molecular Cloning and Expression in *Saccharomyces cerevisiae* of Tobacco NADPH-Cytochrome P450 Oxidoreductase cDNA. *Biosci Biotechnol Biochem*, **62**, 1403-1411 (1998).

Sakai H, Aoyama T, Bono H, and Oka A: Two-Component Response Regulators from *Arabidopsis thaliana* Contain a Putative DNA-binding Motif. *Plant Cell Physiol*, **39**, 1232-1239 (1998).

Aoyama, T: Glucocorticoid-inducible Gene Expression in Plants. In *Inducible Gene Expression in Plants* (P. Reynolds ed.), CAB International (Wallingford), pp 44-59 (1998).

McNellis TW, Mudgett MB, Li K, Aoyama T, Horvath D, Chua N-H, and Staskawicz BJ: Glucocorticoid-inducible Expression of a Bacterial Avirulence Gene in Transgenic *Arabidopsis* Induces Hypersensitive Cell Death. *Plant J*, **14**, 247-257 (1998).

Kato H, Honma T, and Goto K: *CENTRORADIALIS/TERMINAL FLOWER 1* Gene Homolog is Conserved in *N. tabacum*, a Determinate Inflorescence Plant. *J Plant Res*, **111**, 289-294 (1998).

III. Biological Information Science

Bono H and Kanehisa M: From Genome Information to Blueprint for Life. *CICSJ Bulletin*, **16**, 15-19 (1998) (in Japanese).

Bono H, Goto S, Fujibuchi W, Ogata H and Kanehisa M: Systematic Prediction of Orthologous Units of Genes in the Complete Genomes. *Genome Informatics*, **9**, 32-40 (1998).

Bono H, Ogata H, Goto S and Kanehisa M: Reconstruction of Amino Acid Biosynthesis Pathways from the Complete Genome Sequence. *Genome Res.*, **8**, 203-210 (1998).

Fujibuchi W, Ogata H, Matsuda H and Kanehisa M: Automatic Detection of Gene Clusters by P-quasi Complete Linkage Grouping. *Genome Informatics*, **9**, 300-301 (1998).

Fujibuchi W, Sato K, Ogata H, Goto S and Kanehisa M: KEGG and DBGET/LinkDB: Integration of Biological Relationships in Divergent Molecular Biology Data. In *Knowledge Sharing Across Biological and Medical Knowledge Based Systems*, Technical Report WS-98-04, pp. 35-40, AAAI Press (1998).

Goto S: Current Status of Integrated Database. *Kagaku to Seibutsu*, **36**, 319-324 (1998) (in Japanese)

Goto S, Nishioka T and Kanehisa M: LIGAND: Chemical Database for Enzyme Reactions. *Bioinformatics*, **14**, 591-599 (1998).

Goto S, Shiraishi K, Okamoto K, Ishida H, Asanuma S, Bono H, Ogata H, Fujibuchi W and Kanehisa M: Constructing and Annotating GENES Database in KEGG. *Genome Informatics*, **9**, 226-227 (1998).

Igarashi Y and Kanehisa M: The Construction of the Knowledge Base of Immune System. *Genome Informatics*, **9**, 302-303 (1998).

Kanehisa M: Databases of Biological Information. *Trends Guide to Bioinformatics*, pp. 24-26 (1988).

Kanehisa M: Editorial: Grand challenges in Bioinformatics. *Bioinformatics*, **14**, 309 (1998).

Kanehisa M: KEGG - From Genes to Biochemical Pathways. In *Molecular Biology Databases* (Letovsky, S., ed.), in press, Kluwer Academic Press (1998).

Kawashima S, Ogata H and Kanehisa M: Extracting Regulatory Signals from the Upstream Region of Co-expressed Genes Derived from DNA Microarray Experiments. *Genome Informatics*, **9**, 306-307 (1998).

Kihara D and Kanehisa M: The Human Genome Project and Bioinformatics. In *Gendai Igaku no Kiso* (Kajiro T and Muramatsu M eds.), vol. 1, chap. 11, pp.215-235, Iwanami Shoten Publishers (1998) (in Japanese).

Kihara D, Shimizu T, and Kanehisa M: Prediction of Membrane Proteins Based on Classification of Transmembrane Segments. *Protein Eng.*, **11**, 961-970 (1998).

Nakao M, Sato K, Kamiya T, Kimura Y and Kanehisa M: Genome-scale Gene Expression Profiles Mapped onto the Pathway and Genome Maps in KEGG. *Genome Informatics*, **9**, 230-231 (1998).

Ogata H, Fujibuchi W and Kanehisa M: Detection of Co-regulated Genes by Comparative Analysis of Microbial

Genomes. *Genome Informatics*, **9**, 304-305 (1998).

Ogata H, Goto S, Fujibuchi W and Kanehisa M: Computation with the KEGG Pathway Database. *BioSystems*, **47**, 119-128 (1998).

Sakai H, Aoyama T, Bono H and Oka A: Two-component Response Regulators from *Arabidopsis thaliana* Contain a DNA-binding Myb-like Motif. *Plant and Cell Physiology*, **39**, 1232-1239 (1998)

Sato K and Kanehisa M: A Library of Protein-ligand Interaction Sites for de novo Ligand Design. *Genome Informatics*, **9**, 298-299 (1998).

Takagi T, Kanehisa M eds: Introduction to GenomeNet Databases, 2nd ed., Kyoritsu Shuppan, Tokyo (1998) (in Japanese).

Takazawa F, Sasai M Kanehisa M: Protein Folding Simulation and Self-Consistent Potential Functions. *Genome Informatics*, **9**, 308-309 (1998).

Taniguchi T and Kanehisa M: Construction of Ortholog/Paralog Group Table for PTS. *Genome Informatics*, **9**, 296-297 (1998).

Tomii K and Kanehisa M: A Comparative Analysis of ABC Transporters in the Complete Microbial Genomes. *Genome Res.*, **8**, 1048-1059 (1998).

Tomii K and Kanehisa M: Systematic Detection of Protein Structural Motifs. In *Pattern Discovery in Molecular Biology* (Wang, J.T., Shapiro, B.A., and Shasha, D., eds.), in press, Oxford Univ. Press (1998).

NUCLEAR SCIENCE RESEARCH FACILITY

I. Particle and Photon Beams

II. Beams and Fundamental Reaction

Ao H, Iwashita Y, Shirai T, Noda A and Inoue M: Fabrication of Disk-And-Washer, *Proc. of the APAC98, March 1998, Tsukuba, Japan*, 187-189 (1998)

Noda A, Inoue M, Iwashita Y, Morita A, Shirai T, Urakabe E, Hiramoto K, Nishi M, Tadokoro M, Hirota J, Saito K, Umezawa M, Noda K, Kanai T and Fujita Y: Development of Compact Proton Accelerator Facility Dedicated For Cancer Therapy. *Proc. of the APAC98, March 1998, Tsukuba, Japan*, 787-789 (1998)

Hayakawa Y, Seto M, Maeda Y, Shirai T and Noda A: Analysis of the Angular Distribution and the Intensity of Parametric X-ray Radiation in a Bragg Case". *Journal of the Physical Society of Japan*, **67**, 3, 1044-1049. (1998)

Noda A: Colliding or Merging Beam Section, *Proc. of the 6th European Particle Accelerator Conference, EPAC-98, Stockholm, Sweden*, 538-540. (1998)

Kapin V, Inoue M and Noda A: Design Study of A Multiple-Beam RFQ Version of a High-Current Linac Injector for a Neutron Source, *Proc. of the 6th European Particle Accelerator Conference, EPAC-98, Stockholm, Sweden*, 725-727 (1998)

Pisent A, Andreev V, Bassato G, Bezzon G, Bisoffi G, Canella S, Cervellera F, Chiurlotto F, Comunian M, Lombardi A, Moisisio M, Poggi M, Porcellato A, Ziomi L, Shirai T, Scarpa F, Facco A, Favaron P, Fortuna G, Tovo E, Tovo R: The New LNL Injector PIAVE, based on a Superconducting RFQ, *Proc. of the 6th*

European Particle Accelerator Conference, EPAC-98, Stockholm, Sweden, 758-760 (1998)

Bisoffi G, Andreev V, Chiurlotto F, Comunian M, Corradin E, Lombardi A, Meccariello G, Pisent A, Porcellato A, Shirai T, Tovo E, Tovo R: Experimental Results on the Stainless Steel Prototype of a Superconducting RFQ, *Proc. of the 6th European Particle Accelerator Conference, EPAC-98, Stockholm, Sweden*, 1840-1842 (1998)

Kihara T, Okamoto H, Iwashita Y, Oide K, Lamanna G, Wei J: Simulation Study of Three-Dimensional Laser Cooling Schemes for Fast Stored Beams, *Proc. of the 6th European Particle Accelerator Conference, EPAC-98, Stockholm, Sweden*, 1040-1042 (1998)

Morita A, Iwashita Y and Noda A: Tune Value Evaluation for Combined Function Lattice, *Proc. of the 6th European Particle Accelerator Conference, EPAC-98, Stockholm, Sweden*, 1309-1311(1998)

Iwashita Y and Noda A: Massless Septum with Hybrid Magnet. *Proc. of the 6th European Particle Accelerator Conference, EPAC-98, Stockholm, Sweden*, 2109-2110. (1998)

Noda A, Fujita H, Inoue M, Iwashita Y, Morita A, Shirai T, Sugimura T and Tonguu H: Slow Extraction System of Stretcher Ring, KSR, *Proc. of the 6th European Particle Accelerator Conference, EPAC-98, Stockholm, Sweden*, 2120-2122. (1998)

Noda A, Inoue M, Iwashita M, Morita A, Shirai T, Nishi M, Hiramoto K, Tadokoro M and Umezawa M: Combined Function Proton Synchrotron Dedicated for Cancer Therapy, *Proc. of the First Symposium on Accelerator and Related Technology for Application, Tokyo, Japan*, 13-16. (1998)

Urakabe E, Inoue M, Iwashita Y, Kanai T, Kanazawa M, Kitagawa A, Shimbo M, Suda M, Tomitani T, Torikoshi M, Nishio T, Noda A, Noda K, Futami Y, Matsufuji N, Minohara S, Mizota M: Irradiation Field Formation Using the Spot Scanning, *Proc. of the First Symposium on Accelerator and Related Technology for Application, Tokyo, Japan*, 21-24 (1998)

Fujieda M, Mori Y, Nakayama H, Ohmori C, Saito K, Sato Y, Tanabe Y, Uesugi T and Yamamoto M: Magnetic Alloys for High Intensity Proton Synchrotron, *Beam Science and Technology*, **3**, 1-4 (1998)

Awata T, Yajima K, Imai M, Itoh A, Imanishi N, Sugimura T, Shirai T, Noda A: Study of Resonant Transition Radiation X rays, *Beam Science and Technology*, **3**, 10-13 (1998)

Iwashita Y: A Possible Massless Septum Magnet for High Intensity Synchrotron, *Beam Science and Technology*, **3**, 14 (1998)

Tonguu H, Fujita H, Inoue M, Iwashita Y, Noda A, Shirai T, and Sugimura T: Present Status of the Vacuum System for KSR, *Beam Science and Technology*, **3**, 15-17 (1998).

Hill J. E., Inagaki T, Jung C. K., Kobayashi T, Kohama M, Maruyama T, Nishikawa K, Shirai T, Suh E.S. and Taino M: Tests of Beam Monitoring Equipment for a Neutrino Experiment, *Beam Science and Technology*, **3**, 18-22 (1998)

Morita A, Iwashita Y and Noda A: Tune Value Evaluation for Combined Function Lattice, *Beam Science and Technology*, **3**, 23-26 (1998)

Shirai T, Sugimura T, Iwashita Y, Kakigi S, Fujita H, Tonguu H, Noda A and Inoue M: Design of the Injector Linac for KSR, *Beam Science and Technology*, **3**, 27-30, (1998)

Noda A, Fujita H, Inoue M, Iwashita Y, Shirai T, Sugimura T and Tonguu H: Electrostatic Septum for Slow Extraction at KSR, *Beam Science and Technology*, **3**, 31-33 (1998)

Noda A, Fujita H, Inoue M, Iwashita Y, Okamoto H, Shirai T, Sugimura T and Tonguu H: KSR as a Pulse Stretcher, *Proc. of the 1997 Particle Accelerator Conference, Vancouver, B.C., Canada*, 339-341 (1997)

Bisoffi G, Andreev V, Bissiato E, Chiurlotto F, Comunian M, Corradini E, Dewa H, Lombardi A, Pisent A, Porcellato A.M., Shirai T, Tovo E, Tovo R: Prototype of a Superconducting RFQ for a Heavy Ion Injector Linac, *Proc. of the 1997 Particle Accelerator Conference, Vancouver, B.C., Canada*, 1087-1089 (1997)

Iwashita Y, H. Ao, Noda A, Okamoto H, Shirai T, Inoue M: Fabrication of Biparabolic DAW Cavity, *Proc. of the 1997 Particle Accelerator Conference, Vancouver, B.C., Canada*, 1203-1205 (1997)

Sugimura T, Shirai T, Tonguu H, Iwashita Y, Noda A and Inoue M: Present Status of The Electron Linac as The Injector for KSR, *Proc. of the 1997 Particle Accelerator Conference, Vancouver, B.C., Canada*, 1206-1208 (1997)

Kihara T, Okamoto H, Iwashita Y, The Coupling-Cavity Scheme for Three-Dimensional Laser Cooling, *Proc. of the 1997 Particle Accelerator Conference, Vancouver, B.C., Canada*, 1798-1800 (1997)

Ikegami M and Okamoto H: Halo Formation from Axisymmetric Breathing Beams, *Proc. of the 1997 Particle Accelerator Conference, Vancouver, B.C., Canada*, 1911-1913 (1997)

Fujieda M, Mori Y, Nakayama H, Ohmori C, Sawada S, Tanabe Y, Ezura E, Takagi A, Toda M, Yoshii M, Tanabe T and Uesugi T: Studies of Magnetic Cores for JHF Synchrotrons, *Proc. of the 1997 Particle Accelerator Conference, Vancouver, B.C., Canada*, 2992-2994 (1997)

Ohmori C, Fujieda M, S. Machida, Mori Y, Nakayama H, K. Saito, Sawada S, Tanabe Y, M. Yamamoto, Ezura E, Takagi A, Toda M, Yoshii M, T. Tanabe and T. Uesugi: A Wideband Cavity for JHF Synchrotrons, *Proc. of the 1997 Particle Accelerator Conference, Vancouver, B.C., Canada*, 2995-2997 (1997)

Tadokoro M, Hirota J, K. Hiramoto, Umezawa M, Kakiuchi S, Iwashita Y, Noda A, Shirai T and Inoue M: A Combined Function Magnet for a Compact Synchrotron, *Proc. of the 1997 Particle Accelerator Conference, Vancouver, B.C., Canada*, 3294-3296 (1997)

Urakabe E, Inoue M, Iwashita Y, Shirai T, Sugimura T, Noda A, Kanazawa M, Torikoshi M, Noda K, Yamada S, Tadokoro M, Nishi M, Fujita Y: Performance of Parallel Plate Ionization Chamber for Medical Irradiation, *Proc. of the 1997 Particle Accelerator Conference, Vancouver, B.C., Canada*, 3819-3821 (1997)

Iwashita Y: Accuracy of Eigenvalue Obtained with Hybrid Elements on Axisymmetric Domains, *IEEE Trans. MAG-34*, 5 2543-2546 (1998)

Iwashita Y: General Eigenvalue Solver with Zero and Upper Filters for Large Sparse Symmetric Matrix, *Proc. of the IEEE CEFC'98, Tucson, Arizona*, 253 (1998)

Urakabe E, Hiramoto K, Inoue M, Iwashita Y, Kanazawa M, Morita A, Nishi M, Norimine T, Noda A, Noda K, Ogawa H, Shirai T, Torikoshi M, Umezawa M, Yamada S, and Fujita Y: Ribbon Beam Irradiation Formed by Multipole Magnets, *Proc*

of the XXVII PTCOG Meeting, Chiba, The Official Journal of The Japanese Society for Therapeutic Radiology and Oncology, **9 Suppl. 2** 108-111 (1998)

Yamamoto M, Uesugi T, Ohmori C, Saito K, Souda M, Sawada S, Tanabe T, Tanabe Y, Nakayama H, Hashimoto Y, Fujieda M, Machida S, Mori Y, Yan T, Ezura E, Takagi A, Toda M and Yoshii M: Beam Loading in JHF 50-GeV Proton Synchrotron, *Proc. of the 11th Symposium on Accelerator Technology and Science, Nishiharima, Hyogo, Japan*, 227-229 (1997)

Mori Y, Ezura E, Fujieda M, Koba K, Machida S, Ohmori C, Saito K, Sawada S, Takagi A, Tanabe Y, Toda M, Yamamoto M, Yoshii M and Uesugi T: A New Type of RF Cavity for High Intensity Proton Synchrotron, *Proc. of the 11th Symposium on Accelerator Technology and Science, Nishiharima, Hyogo, Japan* 224-226 (1997)

Koba K, Arakawa D, Fujieda M, Ikegami K, Kubota C, Machida S, Mori Y, Ohmori C, Saito K, Shibuya S, Takagi A, Toyama T, Uesugi T, Watanebe M, Yamamoto M and Yoshii M: Longitudinal Impedance Tuner Using High Permeability Material, *Proc. of the 11th Symposium on Accelerator Technology and Science, Nishiharima, Hyogo, Japan* 409-411 (1997)

Afanasev S, Anisimov Y, Fujieda M, Fukui S, Hasegawa T, Horikawa N, Isupov A, Iwata T, Izotov A, Kageya T, Koba K, Kolesnikov V, Litvinenko A, Malakhov A, Matsuda T, Miyachi Y, Nikiforov A, Perelygin V, Reznikov S, Rukoyatkin P, Semenova A, Semenova I, Wakai A and Zolin L: Tensor Analyzing Power T(20) for Cumulative Pion Production from Deuterons in a GeV Energy Region, *Nucl. Phys.* **A625** 817-831 (1997)

Yoshimura T, Okihana A, Warner R.E., Chant N.S., Roos P.G., Samanta C, Kakigi S, Koori N, Fujiwara M, Matsuoka N, Tamura K, Kubo E, Ushiro K: Alpha spectroscopic factors for ${}^6\text{Li}$, ${}^7\text{Li}$, ${}^9\text{Be}$ and ${}^{12}\text{C}$ from the (p, pa) reaction at 296 MeV, *Nuclear Physics* **A641** 3-20 (1998)

Fujieda M, Koba K, Mori Y, Nakayama H, Ohmori C, Saito K, Satoh Y, Tanabe Y, Takagi A, Toda Y, Uesugi T, Yamamoto M, Yan T and Yoshii M: A New Type of RF Cavity for High Intensity Proton Synchrotron Using High Permeability Magnetic Alloy, *Proc. of 6th European Particle Accelerator Conference, Stockholm, Sweden, 22-26 Jun 1998*, 299-301 (1998)

Fujieda M, Machida S, Mori Y, Nakayama H, Ohmori C, Sato Y, Tanabe Y, Uesugi T, Yamamoto M, Takagi A, Toda M, Yoshii M and Iwashita Y: MA Loaded Cavity for Barrier Bucket Experiment, *Proc. of 6th European Particle Accelerator Conference, Stockholm, Sweden, 22-26 Jun 1998*, 1796-1798 (1998)

Tanabe Y, Fujieda M, Mori Y, Nakayama H, Ohmori C, Saito K, Sato Y, Uesugi T, Yamamoto M, Yan T, Ezura E, Takagi A and Yoshii M: Evaluation of Magnetic Alloys for JHF RF Cavity, *Proc. of 1st Asian Particle Accelerator Conference, Tsukuba, Japan, 23-27 Mar 1998*, 390-392 (1998)

Nakayama H, Ezura E, Fujieda M, Ohmori C, Saito K, Sato Y, Sawada S, Takagi A, Tanabe Y, Toda M, Uesugi T, Yamamoto M and Yoshii M: A Measurement System Using GP-IB for a Magnetic Core Test Cavity, *Proc. of 1st Asian Particle Accelerator Conference, Tsukuba, Japan, 23-27 Mar 1998*, 393-395 (1998)

Sato Y, Fujieda M, Mori Y, Nakayama H, Ohmori C, Saito K, Tanabe Y, Uesugi T, Yamamoto M, Yan T, Toda M, Takagi A and Yoshii M: Push Pull Amplifier for MA-Loaded Cavity, *Proc. of 1st Asian Particle Accelerator Conference, Tsukuba, Japan, 23-27 Mar 1998*, 396-398 (1998)

Yamamoto M, Ezura E, Fujieda M, Hashimoto Y, Kobayashi H, Nakayama H, Machida S, Mori Y, Ohmori C, Ohsaka S, Saito K, Sato Y, Souda M, Takagi A, Tanabe Y, Toda M, Uesugi T, Yan T and Yoshii M: Beam Loading Effects in JHF Synchrotron, *Proc. of 1st Asian Particle Accelerator Conference, Tsukuba, Japan, 23-27 Mar 1998*, 399-401 (1998)

Nakayama H, Ezura E, Fujieda M, Ohmori C, Saito K, Sato Y, Sawada S, Souda M, Takagi A, Tanabe Y, Toda M, Uesugi T, Yamamoto M, Yoshii M and Yan T: Higher Harmonics Beam Loading Compensation for a Broad Band MA-Loaded RF Cavity, *Proc. of 1st Asian Particle Accelerator Conference, Tsukuba, Japan, 23-27 Mar 1998*, 402-404 (1998)

Fujieda M, Iwashita Y, Mori Y, Nakayama H, Ohmori C, Saito K, Sato Y, Sawada S, Takagi A, Tanabe Y, Toda M, Uesugi T, Yamamoto Y, Yan T and Yoshii M: An RF Cavity for Barrier Bucket Experiment in the AGS, *Proc. of 1st Asian Particle Accelerator Conference, Tsukuba, Japan, 23-27 Mar 1998*, 408-410 (1998)

Yan T, Fujieda M, Mori Y, Souda M, Ohmori C, Saito K, Sato Y, Tanabe Y, Uesugi T, Yamamoto M: The Characteristics of Different Magnetic Material for RF Cavity under Perpendicular Magnetization, *Proc. of 1st Asian Particle Accelerator Conference, Tsukuba, Japan, 23-27 Mar 1998*, 417-419 (1998)

Koba K, Arakawa D, Fujieda M, Okegami K, Kuboto C, Machida

S, Mori Y, Ohmori C, Shinto K, Shibuya S, Takagi A, Toyama T, Uesugi T, Watanebe M, Yamamoto M and Yoshii M: Longitudinal Impedance Tuner Using High Permeability Material, *Proc. of 1st Asian Particle Accelerator Conference, Tsukuba, Japan, 23-27 Mar 1998*, 450-452 (1998)

Ohmori C, Fujieda M, Hashimoto Y, Mori Y, Nakayama H, Saito K, Sato Y, Souda M, Tanabe Y, Uesugi T, Yamamoto M, Ezura E, Takagi A, Toda M, Yan T and Yoshii M: RF Systems for JHF Synchrotrons, *Proc. of 1st Asian Particle Accelerator Conference, Tsukuba, Japan, 23-27 Mar 1998*, 602-604 (1998)

RESEARCH FACILITY OF NUCLEIC

ACIDS

Fujibuchi, W, Sato, K, Ogata, H, Goto, S and Kanehisa, M: KEGG and DBGET/LinkDB: Integration of biological relationships in divergent molecular biology data. In "Knowledge Sharing Across Biological and Medical Knowledge Based Systems", Technical Report WS-98-04, pp. 35-40, AAAI Press (1998).

Fujibuchi, W, Ogata, H, Matsuda, H and Kanehisa, M: Automatic Detection of Gene Clusters by P-Quasi Complete Linkage Grouping. *9th Workshop on Genome Informatics*, 300-301 (1998).

SEMINARS

Professor Mitsuo Sawamoto
Graduate School of Engineering, Kyoto University, Kyoto,
Japan
“Living Radical Polymerization: Recent Advances”
Monday 12 January 1998

Professor Roger McMacken
Department of Biochemistry, School of Hygiene and
Public Health, Johns Hopkins University, USA
“The Role of Molecular Chaperones in the Initiation of
Bacteriophage Lambda DNA Replication”
Monday 19 January 1998

Professor Jean-Pierre Majoral
CNRS, Toulouse, France
“Phosphorus Containing Dendrimers; a New Class of
Macromolecules”
Tuesday 20 January 1998

Professor Mitsuru Akashi
Faculty of Engineering, Kagoshima University,
Kagoshima, Japan
“Synthesis of Polystyrene-Nanosphere with Functional
Surface by Macromonomer Polymerization Technique”
Wednesday 21 January 1998

Dr. Marie-Emmanuelle Couprie
LURE, Centre Universitaire de Paris-Sud, FRANCE
“The Super-ACO Free Electron Laser Source in the UV”
Friday 23 January 1998

Professor Ivan K. Schuller
University of California, San Diego, USA
“Exchange Interaction between Magnetic Layers”
Wednesday 28 January, 1998

Professor Mitsuo Takai
Hokkaido University, Japan
“Biosynthesis and Molecular Structure of Cellulose”
Wednesday 28 January 1998

Professor Masayoshi Watanabe
Faculty of Engineering, Yokohama National University,
Japan
“Ion Dynamics in Polymer Matrix and Polymer Solid
Electrolytes”
Friday 30 January 1998

Professor Michiya Fujiki
NTT Basic Research Laboratories, Japan
1. “One Dimensional Self-Assemblies of Optically
Inactive and Optically Active Phthalocyanine Derivatives:
Molecular Design, Structure and Properties”
2. “Inversion of Helicity of Optically Active Synthetic
and Biological Polymers”
Friday 30 January 1998

Dr Yuichi Shimakawa
NEC
“Pyrochlore and Spinel Mangan Oxides
-Synthesis, Structure, GMR and Secondary Battery-”
Thursday 5 February 1998

Professor Toshio Yamaguchi
Department of Chemistry, Faculty of Science, Fukuoka
University, Japan
“Structure of Hydrogen-Bonding Liquids and Solutions
at Sub- and Super-Critical Conditions”
Thursday 10 February 1998

Professor Gustaff Van Tendeloo
EMAT University of Antwerp
“Better superconducting materials by TEM”
Tuesday 10 February 1998

Professor Wolfgang Krätschmer
Max-Planck Institute for Solid Physics, Heidelberg,
Germany
“Fullerene Research in Heidelberg”
Monday 16 February 1998

Professor Takashi Odagaki
Department of Physics, Faculty of Science
Kyushu University, Japan
“Theory and Scenario of Glass Transition”
Friday 27 February 1998

Dr. King Y Ng
Fermi National Accelerator Laboratory, USA
“Dynamics of the barrier bucket and its application”
Friday 27 February 1998

Professor M. Hara
Department of Chemical and Biochemical Engineering,
Rutger University, USA
“Effects of Ionic Interactions on Mechanical Properties
of Polymers and Polymer Blends/Composites”
Monday 16 March 1998

Professor Yoshinobu Isono
Faculty of Engineering, Nagaoka University of
Technology, Japan
“Non-linear Viscoelasticity and Structural Change in
Entanglements for Concentrated Polymer Solution
Systems”
Tuesday 17 March 1998

Professor Peter A. Grünberg
Forschungszentrum Jülich, Germany
“Layered Magnetic Structures in Research and
Application”
Friday 20 March, 1998

Professor Joanna Strosznajder
Laboratory of Cellular Signaling, Polish Academy of
Sciences, Medical Research Center, Poland
“Effect of Alzheimer's Disease-Related Amyloid β
Peptides on Calcium and Phosphoinositides Signaling in
Brain Cortex”
Monday 23 March 1998

Professor Ben L. Feringa
Department of Chemistry, University of Groningen, The
Netherlands

“Chiroptical Molecular Switches”
Wednesday 25 March 1998

Professor Philip Boudjouk
North Dakota State University, U.S.A.
“Silole Chemistry: Anions and Nucleophilic Substitution at Silicon”
Thursday 26 March 1998

Professor Antoine Kahn
Princeton University, USA
“Electronic Properties of Interfaces of Organic Molecular Semiconductors with Application to Electroluminescent Devices”
Wednesday 1 April 1998

Professor Franoise Brochard-Wyart
University of Paris VI, Paris, France
“Wetting by Polymer Solutions”
Tuesday 7 April 1998

Professor Pierre Gilles de Gennes
College de France, Paris, France
“Artificial Muscle”
Tuesday 7 April 1998

Professor Wei-Min Dai
Hong Kong University of Science and Technology
“Recent Progress in Asymmetric Wittig Reaction of Chiral Arsonium Ylids and Regioselective Allylic Rearrangement for Ene-yne Synthesis”
Thursday 9 April 1998

Professor Dieter Richter
Institut für Festkörperforschung, Forschungszentrum Jülich GmbH, Jülich, Germany
“Polymer Dynamics at Short and Long Length Scales”
Thursday 23 April 1998

Professor Robert West
University of Wisconsin, Madison, U.S.A.
“Cyclic Organosilicon Compounds with “Aromatic” Properties”
Friday 24 April 1998

Professor Hiroshi Kihara
Kansai Medical University
“Protein Folding Under Sub-zero Temperature”
Monday 2 May 1998

Dr. Manabu Ishitani
Department of Plant Sciences, University of Arizona, Tucson AZ 85721 USA
“COS-, HOS- and LOS-Genes Regulating Plants Responses to Salt, Water and Temperature Stresses”
Monday 5 May 1998

Professor Vesselin Vassilev Dimitrov
Nagaoka University of Technology
“Polarizability, Optical Basicity and Nonlinear Optical properties of Simple Oxides”
Thursday 14 May 1998

Professor Seizou Miyata

Graduate School of Bio-Applications & Systems Engineering, Tokyo University of Agriculture and Technology, Tokyo, Japan
“Conducting Polymers and Organic Electroluminescence Devices”
Friday 8 May 1998

Professor Wolfgang Kreis
Dept. of Pharmaceutical Biology, Erlangen-Nuremberg University, Germany
“Cardenolide Biosynthesis and Biotransformation in Digitalis and Isoplexis”
Monday 11 May 1998

Professor M. David Curtis
University of Michigan, U.S.A.
“Properties of New Conjugated Polymers Based on Bithiazoles, Bisoxazoles and Furans”
Monday 25 May 1998

Professor Minoru Terano
School of Material Science, Japan Advanced Institute of Science and Technology, Japan
“Catalyst for Polymerization of Olefins: Industrial Developments and Fundamental Research”
Tuesday 26 May 1998

Dr. Toru Tanimori
Department of Physics, Tokyo Institute of Technology
“Development of 2D MicroStrip Gas Chamber as a Time-resolved Area Detector”
Friday 29 May 1998

Professor Kenneth S. Schweizer
Department of Materials Science and Engineering
University of Illinois, USA
“Structure, Phase Behavior, and Diffusion in Diblock Melts and Solutions”
Monday 1 June 1998

Professor Rufina G. Alamo
Florida Agricultural & Mechanical University, The Florida State University, USA
“Crystallization, Morphology and Melting Behavior of Polypropylenes”
Tuesday 2 June 1998

Professor Redouane Borsali
Cermav-CNRS, Grenoble, France
“Structure and Dynamics of Polyelectrolyte Solutions: Light and Neutron Scattering Experiments”
Thursday 4 June 1998

Professor Gerhard Wegner
Max-Planck-Institute for Polymer Research, Mainz, Germany
“Novel Architectures of Polyelectrolytes and Ionic Conductors”
Friday 5 June 1998

Professor Jean-Michel Guenet
Laboratoire d'Ultrasons et de Dynamique des Fluides Complexes Université Louis Pasteur, France
“Thermoreversible gelation of PVC: the mechanisms involved and their impact on rheological properties”

Monday 8 June 1998

Professor Herbert Dautzenberg
Max-Planck-Institut für Kolloid und
Grenzflächenforschung Teltow-Seehof, Germany
“Polyelectrolyte Complex Formation in Highly
Aggregating Systems”
Tuesday 9 June 1998

Professor Long Y. Chiang
Center for Condensed Matter Sciences, National Taiwan
University, Taipei, Taiwan
“Synthesis of Star-burst Conductive Conjugated Polymers
Based on Reactive Polyfunctional C₆₀ Precursors”
Thursday 11 June 1998

Professor Yasuhiko Shirota
Department of Material Chemistry
Faculty of Engineering, Osaka University, Japan
“Photo-electric Functional Materials and Applications to
Devices”
Monday 6 July 1998

Dr. Ian. L. Hosier
J. J. Thomson Physical Laboratory, University of Reading,
Reading, UK
“Chemical Etching Procedure”
Tuesday 14 July 1998

Dr. Takeichiro Yokoi
High Energy Accelerator Research Organization (KEK)
Tanashi
“Next generation secondary beamline for JHF”
Thursday 20 August 1998

Dr. Tsuru Kamata
Laboratory of Biochemical Physiology
National Cancer Institute, USA
“Regulation of the Ras Signaling Pathway and Its Role in
the Generation of Reactive Oxygen Species”
Wednesday 2 September 1998

Dr. Augusto Lombardi
Laboratori Nazionali di Legnaro, Istituto Nazionale di
Fisica Nucleare, (INFN-LNL), Italy
“PIAVE: the new positive ion injector at Legnaro”
Wednesday 2 September 1998

Professor Andreas Hirsch
Department of Organic Chemistry, University of Erlangen,
Erlangen, Germany
“Buckminsterfullerene as Building Block for New
Macromolecular and Supramolecular Nanostructures”
Friday 4 September 1998

Professor H. Henning Winter
Department of Chemical Engineering, University of
Massachusetts at Amherst, USA
“Conoscopic Observation of Shear Introduced Rotation
of Liquid Crystalline Molecules”
Monday 7 September 1998

Professor Ronald G. Larson
Department of Chemical Engineering, University of
Michigan, USA

“Single Molecule Hydrodynamics of Long DNA
Molecules”
Thursday 10 September 1998

Professor Yves Rubin
Department of Chemistry and Biochemistry, University
of California, Los Angeles, Los Angeles, U.S.A.
“Highly Unsaturated Compounds on the Way to Fullerenes
and Their Endohedral Metal Complexes”
Saturday 12 September 1998

Dr. Masahiro Okamura
The Institute of Physical and Chemical Research
“Helical Dipole Magnets for RHIC”
Wednesday 30 September 1998

Professor Ajay Gupta
Inter University Consortium for DAE Facilities, India
“Effects of the Interface Structure on the Magnetic
Properties of Metallic Multilayers”
Thursday 1 October, 1998

Dr. Robert V. Law
Department of Chemistry, Imperial College, UK
“Solid-State NMR Studies of Highly Crosslinked
Polymers”
Friday 2 October 1998

Professor Gregory Soh-Yu Yeh
Department of Chemical Engineering and Polymer
Physics, The University of Michigan, Michigan, USA
“Polymer Structure: Melt, Glass vs. Crystallized State”
Friday 2 October 1998

Professor Klaus Jurkschat
University of Dortmund, Germany
“On the Chemistry of Stannasiloxanes”
Monday 5 October 1998

Professor Kwang-Sup Lee
Chemistry Division, Materials Chemistry Branch, Naval
Research Lab., USA
“Highly Efficient and Thermally Stable Nonlinear Optical
Materials”
Friday 9 October 1998

Dr. Rajai H. Atalla
USDA Forest Service, Forest Products Laboratory, USA
“Biogenesis of wood cell walls”
Friday 18 October 1998

Dr. Kenji Oeda
Biotechnology Laboratory, Sumitomo Chemical Co., Ltd.,
Takarazuka, Japan
(1) “Variation of G box (CACGTG) Sequences and
Control of Gene Expression”; (2) “Adaptive Responses
to Strong Light Stress”; (3) “Progress in Commercial
Transgenic Plants”
Monday 19 October 1998

Dr. Jean Claude Wittmann
Institut Charles Sadron, CNRS-ULP, France
“Orientation of Monomers, Oligomers and Polymers on
Friction-Transferred Poly(tetrafluoroethylene) Layers”
Monday 19 October 1998

Professor M. A. Bennett
University of Australia, Australia
“Cyclometallated Triphenylphosphine: a Versatile Ligand”
Tuesday 20 October 1998

Professor Naoto Nagaosa
Department of Applied Physics, The University of Tokyo
“Spin, Charge and Orbital”
Saturday 24 October 1998

Professor Hiroo Hashizume
Tokyo Institute of Technology, Japan
“Magnetic Structures of Fe/Gd Multilayers Studied by Resonant X-Ray Scattering”
Friday 30 October, 1998

Prof. Eberhard Jaeschke
Berliner Elektronenspeicherring Gesellschaft fuer Synchrotronstrahlung mbH (BESSY), Germany
“BESSY-II, the High Brightness Source in operation -- Commissioning experience and Future plans”
Friday 30 October 1998

Professor Yasuhiro Takahashi
Faculty of Science, Osaka University, Japan
“Structural Irregularity of Crystalline Polymers”
Friday 30 October 1998

Dr. Yoshiaki Mizuno
Institute for Materials Research, Tohoku University
“Superexchange Coupling of 90° Bond System-Li₂CuO₂-”
Monday 2 November 1998

Professor Mark D. Ediger
Department of Chemistry
University of Wisconsin, USA
“Special Inhomogeneity of Super-Cooled Liquids”
Thursday 5 November 1998

Professor Lech Thomas Baczewski
Institute of Physics, Polish Academy of Sciences, Poland
“Structural and Magnetic Properties of RE(Gd/Tb) Thin Films”
Friday 6 November, 1998

Professor Samuel D. Bader
Argonne National Laboratory, USA
“Study of Surface Magnetism using Surface Magneto-Optical Kerr Effect (SMOKE)”
Tuesday 10 November, 1998

Professor Yuri Feldman
Hebrew University of Jerusalem, Israel
“Cooperative Relaxation of Water Confined at Porous Glasses”
Monday 16 November 1998

Professor Ernst Bauer
Arizona State University, USA
“Spin-Polarized LEEM Studies of Thin Co Film Systems”
Tuesday 17 November, 1998

Dr. Derck Schlettwein

Institute of Applied and Physical Chemistry,
University of Bremen, Germany
“Influence of Molecular Structure on Thin Film Growth, and Electrical Properties of Substituted Phthalocyanines”
Tuesday 17 November 1998

Professor Yoshiharu Tsujita
Nagoya Institute of Technology, Nagoya, Japan
“Sorption, Diffusion, and Permeation of Gases in Polymeric Membrane”
Thursday 19 November 1998

Professor Nagao Kobayashi
Tohoku University, Japan
“Effects of Size, Symmetry and Substitution on Spectroscopic and Electrochemical Properties of Phthalocyanines”
Thursday 19 November 1998

Dr Bruce Normand
Institute of Physics, University of Basel
“Two-band Superconductivity in the Doped Spin Ladder La_{1-x}Sr_xCuO_{2.5}”
Friday 20 November 1998

Dr. Hisaaki Taniguchi
Division of Biomedical Polymer Science, Institute for Comprehensive Medical Science, Fujita Health University
“What does 'Dalton' talk? Applications of Mass Spectrometry to Structural Analysis of Biopolymers”
Tuesday 24 November 1998

Dr. Yoshihide Fukahori
Materials Development Department, Bridgestone Corporation, Japan
“Non-linear Creep Phenomena in Polymers”
Friday 27 November 1998

Professor Peter J. Rossky
University of Texas, Austin, USA
“Ionic Solvation in Supercritical Water: Structural, Thermodynamic, and Transport Properties”
Monday 7 December 1998

Professor Peter Kralchevsky
Faculty of Chemistry, Sofia University, Bulgaria
“Thermodynamics and Hydrodynamics of Thin Liquid Films”
Wednesday 9 December 1998

Dr. Grahame Rees
Rutherford Appleton Laboratory, England
“Revised Designs for the Linac and Rings of the European Spallation Neutron Source”
Friday 11 December 1998

Dr. Masafumi Harada
KU-VBL, Kyoto University, Japan
“Structural Analysis of Transition Metal Clusters Using EXAFS, SAXS, and DFT”
Wednesday 11 November 1998

Dr. Yoshihide Fukahori
Materials Development Department, Bridgestone Corporation, Japan

“Tribology of Polymers (Friction and Wear)”
Friday 11 December 1998

Dr. Eugene V. Koonin
National Center for Biotechnology Information
“Protein Fold Recognition using Sequence Profiles and
Phylogenetic Distribution of Protein Folds”
Monday 14 December 1998

Professor Masayasu Inoue
First Department of Biochemistry
Osaka City University School of Medicine
“Reactive Oxygen and Biocurrent”
Monday 14 December 1998

Dr. Toshio Kokubo
Research Center Kyoto, Bayer Yakuhin, Ltd.
“Improvement of Enzymes by Evolutionary Molecular
Engineering”
Tuesday 15 December 1998

Professor Robin K. Harris
Department of Chemistry, University of Durham, UK
“Recent NMR developments for solid fluorinated organic

compounds and solid fluoropolymers”
Thursday 16 December 1998

Professor Masakatsu Misawa
Department of Chemistry, Faculty of Science, Niigata
University
“Basis of Neutron Scattering Spectroscopy of Fluids”
Monday 21 December 1998

Professor Masakatsu Misawa
Department of Chemistry, Faculty of Science, Niigata
University
“Neutron Scattering Study of the Phase Separation of
Solutions and the Structure of Supercritical Fluids”
Thursday 22 December 1998

Professor Akihiro Tsutsumi
Hokkaido University, Japan
“Orientation and Chain Dynamics of Polypeptides as
Studied by Solid-State ^2H NMR”
Tuesday 22 December 1998

THESIS

- SHIBATA, Hiroyuki
D Agr, Kyoto University
"Molecular Mechanism of Lipase Activator Protein from *Pseudomonas aeruginosa*"
Supervisor: Professor Oda J
23 January 1998
- YAMAZAKI, Norimasa
D Sc, Kyoto University
"On the Stereochemistry of Reduction of Nicotinamide Coenzyme Model Compounds"
Supervisor: Professor Ohno A
23 January 1998
- CHOO, Dong-Won
D Agr, Kyoto University
"Enzymological Studies of Lipases from Psychrotrophic Bacteria"
Supervisor: Professor Esaki N
23 January 1998
- KISHIMOTO, Kazuhisa
D Agr, Kyoto University
"Protein Engineering Studies of D-Amino Acid Aminotransferase"
Supervisor: Professor Esaki N
23 January 1998
- LIU, Li-Dong
D Agr, Kyoto University
"Structure, Function and Regulation of Glutamate Racemase"
Supervisor: Professor Esaki N
23 January 1998
- ODA, Masao
"Experimental and Theoretical Studies on Thermal Isomerization Reaction of Methyl 4-(Dimethylamino)benzenesulfonate in the Crystalline State"
Supervisor: Professor Sato N
23 March 1998
- SAKAI, Hiroshi
D Sc, Kyoto University
"Characterization of Molecular Orientation in Langmuir Monolayers on the Water Surface by Infrared External Reflection Spectroscopy"
Supervisor: Associate Professor Umemura J
23 March 1998
- OKA, Takahiro
D Pharm Sci, Kyoto University
"Studies on the New Atropisomer of Diaryl Ether-Type"
Supervisor: Professor Fuji K
23 March 1998
- SUZUKI, Hideo
"a-alkylation of Amino Acid Derivatives Based on Memory of Chirality"
Supervisor: Professor Fuji K
23 March 1998
- TAKASU, Kiyoshei
"Studies on the Structure and Function of the Compounds with *cis*-2,5-Diphenylpiperazine Skeleton"
Supervisor: Fuji K
23 March 1998
- ASAHARA, Masahiro
D Eng, Kyoto University
"The Chemistry of Neutral Hypercoordinate Oligosilanes"
Supervisor: Professor Tamao K
23 March 1998
- KANDO, Masaki
D Sc, Kyoto University
"Experimental Study of Electron Acceleration by Laser Wake Field"
Supervisor: Professor Noda A
23 March 1998.
- MURATA, Yasujiro
D Eng, Kyoto University
"Studies on Synthesis and Properties of Fullerene Derivatives Possessing Novel Structures"
Supervisor: Professor Komatsu K
23 March 1998
- KOBAYASHI, Naoya
D Sc, Kyoto University
"High Pressure Synthesis and Properties of Cupric Oxides with Alkaline Earth Elements"
Supervisor: TAKANO, M
24 March 1998
- POULSEN, Niels Jakob
D Sc, Kyoto University
"High Pressure Synthesis and Physical Properties of (Ba, K)V(S, Se)₃"
Supervisor: TAKANO, M
24 March 1998
- SAWA, Masaaki
D Agr, Kyoto University
"Studies on the Generation of Catalytic Antibodies for Chemiluminescence and Glycoside Hydrolysis"
Supervisor: Professor Oda J
25 May 1998
- AOYAGI, Amane
D Agr, Kyoto University
"Time-resolved Crystallographic Studies on Glutathione Synthetase"
Supervisor: Professor Oda J
25 May 1998
- GUTIERREZ, Aldo
D Agr, Kyoto University
"Role of Interdomain Loop of D-Amino Acid Aminotransferase"
Supervisor: Professor Esaki N
25 May 1998

PARK, Chung
D Agr, Kyoto University
“Enzymological Studies of Bacterial DL-2-Halo Acid Dehalogenases”
Supervisor: Professor Esaki N
25 May 1998

YAMASHITA, Atsuko
D Agr, Kyoto University
“Structural Basis for the Reaction of Tropinone Reductase-II Analyzed by X-ray Crystallography”
Supervisor: Professor Oda J
25 May 1998

KAWAGUCHI, Tatsuya
D Eng, Kyoto University
“Neutron Scattering Studies on Dynamics of Amorphous Polymers”
Supervisor: Professor Kaji K
25 May 1998

FUJIBUCHI, Wataru
D Sc, Kyoto University
“Analysis of Gene Clusters Based on Complete Genome Comparisons”
25 May 1998

OGATA, Hiroyuki
D Sc, Kyoto University
“Analysis of Genome Organization and Metabolic Pathways Based on a Network Comparison Technique”
25 May 1998

TOMII, Kentaro
D Sc, Kyoto University
“A Comparative Analysis of ABC Transporters in the Complete Genomes of Seven Microorganisms”
25 May 1998

FUJIBUCHI, Wataru
D Sc, Kyoto University
“Analysis of Gene Clusters Based on Complete Genome Comparisons”
25 May 1998

OGATA, Hiroyuki
D Sc, Kyoto University
“Analysis of Genome Organization and Metabolic Pathways Based on a Network Comparison Technique”
25 May 1998

TOMII, Kentaro
D Sc, Kyoto University
“A Comparative Analysis of ABC Transporters in the Complete Genomes of Seven Microorganisms”
25 May 1998

FURUTA, Takumi
“Synthesis and Function of New Spiriral Molecules with Atropisomerism”
Supervisor: Fuji K
25 May 1998

SHANG, Mu-Hong
“Studies on the Creation of Quaternary Carbon Centers

via Addition-Elimination Process”
Supervisor: Fuji K
23 July 1998

SAKURAI, Minoru
“Development of New Optically Active Monodentate Phosphine Ligand”
Supervisor: Fuji K
23 July 1998

KITAYAMA, Takashi
D Sc, Kyoto University
“Asymmetric Syntheses with Microbes and Total Syntheses of Bioactive Substances”
Supervisor: Professor Ohno A
23 July 1998

LI, Yong-Fu
D Agr, Kyoto University
“Catalytic Mechanism of L-2-Haloacid Dehalogenase from *Pseudomonas* sp. YL”
Supervisor: Professor Esaki N
24 September 1998

IDE, Nobuhiro
D Eng, Kyoto University
“Studies on Cross-Linking and Gelation Processes in Polymer Systems”
Supervisor: Professor Miyamoto T
24 September 1998

TAKARAGI, Akira
D Eng, Kyoto University
“Studies on Synthesis and Properties of Some Novel Cello-Oligosaccharide and Cellulose Derivatives”
Supervisor: Professor Miyamoto T
24 September 1998

OKAMURA, Haruyuki
D Eng, Kyoto University
“Synthesis and Properties of Fullerene-Containing Polymers with Well-Defined Structures”
Supervisor: Professor Miyamoto T
24 November 1998

JIN, Ren-Zhi
D Eng, Kyoto University
“Functionalized Siloles and Their Application to Polysiloles”
Supervisor: Professor Tamao K
24 November 1998

YAJIMA, Ryuichi
D Sc, Kyoto University
“The Development of Highly-Sensitive Assay Method for the Activity of Neuropeptide-Processing Enzymes and Its Application: The Axonal Transport of These Enzymes in Rat Sciatic Nerves”
Supervisor: Professor Ohno A
24 November 1998

TANAKA, Yoko
D Eng, Kyoto University
“Theoretical and Experimental Studies on the Reactivities of Group 14 Inter-elements Compounds”

Supervisor: Professor Tamao K
24 November 1998

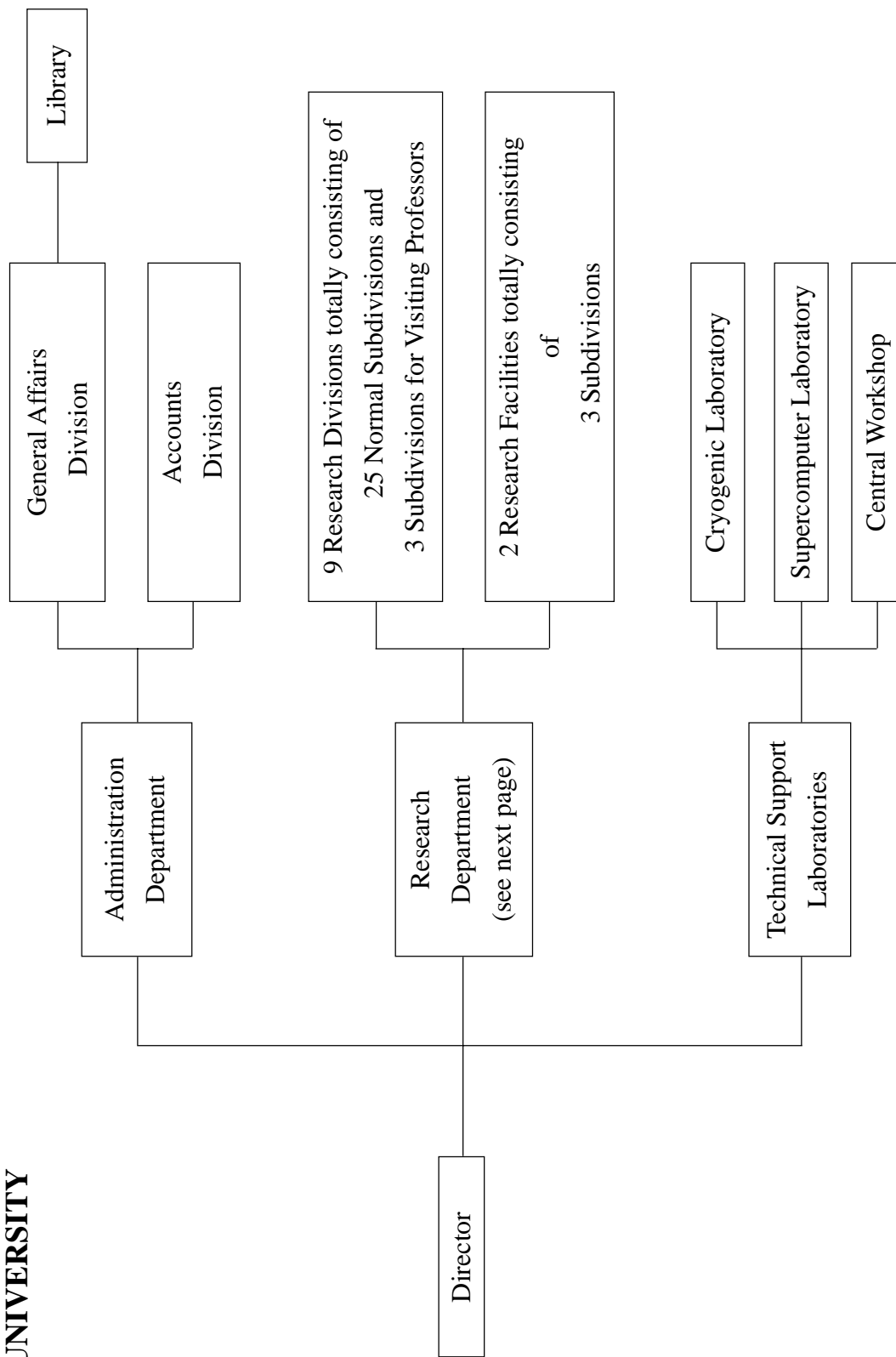
YOSHIDA, Yumi
D Sc, Kyoto University
“Electrochemical Understanding of Distribution of Ions
at Aqueous/Organic or Aqueous/Membrane Interfaces and
Membrane Potential”
Supervisor: Professor Matsui M

24 November 1998

TANO, Takanori
D Sc, Kyoto University
“Structural Characterization of Black Lipid Films in Air
by Fourier Transform Infrared Spectroscopy”
Supervisor: Associate Professor Umemura J
24 November 1998

ORGANIZATION AND STAFF

**INSTITUTE FOR CHEMICAL RESEARCH
KYOTO UNIVERSITY**



INSTITUTE FOR CHEMICAL RESEARCH, KYOTO UNIVERSITY As of 31 December 1998
RESEARCH DIVISION (G: Laboratory for Visiting Professors)

Research Division	Subdivision (Laboratory)	Related Graduate School <i>Graduate School of / Division of Science / Physics I</i>	Professor	Associate Professor	Instructor
States and Structure	I. Atomic and Molecular Physics		MUKOYAMA, Takeshi	ITO, Yoshiaki	KATANO, Rintarou NAKAMATSU, Hirohide
	II. Crystal Information Analysis	<i>Science / Chemistry</i>	KOBAYASHI, Takashi	ISODA, Seiji	OGAWA, Tetsuya NEMOTO, Takashi
	III. Polymer Condensed States	<i>Engineering / Polymer Chemistry</i>	KOHIYA, Shinzo	TSUJI, Masaki	URAYAMA, Kenji TOSAKA, Masatoshi MURAKAMI, Syozo
Interface Science	I. Solutions and Interfaces	<i>Science / Chemistry</i>	NAKAHARA, Masaru	UMEMURA, Junzo	MATSUMOTO, Mutsuo MATUBAYASHI, Nobuyuki
	II. Molecular Aggregates	<i>Science / Chemistry</i>	SATO, Naoki	ASAMI, Koji	KITA, Yasuo YOSHIDA, Hiroyuki
Solid State Chemistry	III. Separation Chemistry	<i>Science / Chemistry</i>	MATSUI, Masakazu	UMETANI, Shigeo	SASAKI, Yoshihiro HASEGAWA, Hiroshi
	I. Artificial Lattice Alloys	<i>Science / Chemistry</i>	SHINJO, Teruya	HOSOITO, Nobuyoshi	MIBU, Ko
	II. Quantum Spin Fluids	<i>Science / Chemistry</i>	YAMADA, Kazuyoshi	TERASHIMA, Takahito	IKEDA, Yasunori
Fundamental Material Properties	III. Multicomponent Materials	<i>Science / Chemistry</i>	TAKANO, Mikio	HIROL, Zenji	AZUMA, Masaki
	IV. Amorphous Materials	<i>Engineering / Molecular Engineering</i>	YOKO, Toshinobu	UCHINO, Takashi	TAKAHASHI, Masahide
	G. Structure Analysis	<i>Engineering / Molecular Engineering</i>	KOMATSU, Takayuki	TAKAGI, Hidenori	
	I. Molecular Rheology	<i>Engineering / Polymer Chemistry</i>	OSAKI, Kunihiko	WATANABE, Hiroshi	INOUE, Tadashi
	II. Polymer Materials Science	<i>Engineering / Molecular Engineering</i>	KAJI, Keisuke	KANAYA, Toshiji	NISHIDA, Koji
Organic Chemistry	III. Molecular Dynamic Characteristics	<i>Engineering / Molecular Engineering</i>	HORII, Fumiaka	TSUNASHIMA, Yoshisuke	KAJI, Hironori
	G. Composite Material Properties	<i>Engineering / Polymer Chemistry</i>	TANAKA, Michihiro	FUJIKI, Michiya	
Synthetic Organic Chemistry	I. Polymeric Materials	<i>Engineering / Energy & HC Chemistry</i>	MIYAMOTO, Takeaki	FUKUDA, Takeshi	TSUJII, Yoshinobu MINODA, Masahiko
	II. High-Pressure Organic Chemistry	<i>Engineering / Energy & HC Chemistry</i>	KOMATSU, Koichi		MORI, Sadayuki KUDO, Kiyoshi
Bioorganic Chemistry	I. Synthetic Design	<i>Engineering / Energy & HC Chemistry</i>	TAMAO, Kohei	TOSHIMITSU, Akio	NISHINAGA, Tohru KAWACHI, Aisushi
	II. Fine Organic Synthesis	<i>Pharmaceutical Sci. / Pharmac. Chem.</i>	FUJI, Kaoru	KAWABATA, Takeo	YAMAGUCHI, Shigehiro
Molecular Biofunction	G. Synthetic Theory	<i>Science / Chemistry</i>	NAKATA, Tadashi	YAMADA, Haruo	TUBAKI, Kzunori
	I. Bioorganic Reaction Theory	<i>Pharmaceutical Sci. / Drug System</i>	OHNO, Aisuyoshi	NAKAMURA, Kaoru	KAWAI, Yasushi SUGIYAMA, Takashi
	II. Bioactive Chemistry	<i>Medicine / Internal Medicine</i>	SUGIURA, Yukio	FUTAKI, Shiro	MORII, Takashi
Molecular Biology and Information	III. Molecular Clinical Chemistry	<i>Agriculture / Agricul. Chem.</i>	UEDA, Kunhiro	TANAKA, Seigo	ADACHI, Yoshitumi
	I. Functional Molecular Conversion	<i>Agriculture / Agricul. Chem.</i>	SAKATA, Kanzo	HIRATAKE, Jun	KATO, Hiroaki MIZUTANI, Masaharu
Nuclear Science Research Facility of Nucleic Acids	II. Molecular Microbial Science	<i>Science / Biophysics</i>	ESAKI, Nobuyoshi	YOSHIMURA, Tohru	KURIHARA, Tatsuo
	I. Biopolymer Structure	<i>Science / Biophysics</i>	TAKAHASHI, Sho	HATA, Yasuo	HIRAGI, Yuzuru FUJII, Tomomi
Nuclear Science Research Facility of Nucleic Acids	II. Molecular Biology	<i>Science / Biophysics</i>	OKA, Atsuhiko	AOYAMA, Takashi	AKUTAGAWA, Tohru
	III. Biological Information Science	<i>Science / Biophysics</i>	KANEHISA, Minoru		GOTO, Susumu OGATA, Hiroyuki
Nuclear Science Research Facility of Nucleic Acids	I. Particle and Photon Beams	<i>Science / Physics I</i>	NODA, Akira	IWASHITA, Yoshihisa	SHIRAI, Toshiyuki
	Beams and Fundamental Reaction	<i>Science / Physics II</i>	INOUE, Makoto	MATSUKI, Seishi	OKAMOTO, Hiromi
Nuclear Science Research Facility of Nucleic Acids	II. Biological Information Science	<i>Science / Biophysics</i>	KANEHISA, Minoru	SUGISAKI, Hiroyuki	FUJIBUCHI, Wataru
	I. Particle and Photon Beams	<i>Science / Physics I</i>	NODA, Akira	IWASHITA, Yoshihisa	SHIRAI, Toshiyuki
Nuclear Science Research Facility of Nucleic Acids	Beams and Fundamental Reaction	<i>Science / Physics II</i>	INOUE, Makoto	MATSUKI, Seishi	OKAMOTO, Hiromi
	II. Biological Information Science	<i>Science / Biophysics</i>	KANEHISA, Minoru	SUGISAKI, Hiroyuki	FUJIBUCHI, Wataru

PERSONAL

Retirement

Professor Masakazu Matsui

(Interface Science, Division of
Separation Chemistry)



On the 31st of March, 1999, Dr. Masakazu Matsui retired from Kyoto University after 38 years of service to the University and was honored with the title of Professor Emeritus of Kyoto University.

Dr. Matsui was born in Hyogo on the 13th of July, 1935. After graduation from Faculty of Science, Kyoto University in 1959, he continued his studies on the synthesis and application of α -dioximes for metal analysis as a graduate student. In 1961, he was appointed an instructor of the Laboratory of Radiochemistry, Institute for Chemical Research, Kyoto University, under the supervision of the Emeritus Professor Tsunenobu Shigematsu. He was granted a doctoral degree from Kyoto University in 1966 for his studies on coprecipitation mechanism with calcium oxalate. On a leave of absence in the year 1969 to 1970, he worked on the ion-selective electrode in cooperation with Professor H. Freiser at Arizona University. In 1972, Dr. Matsui was promoted to Associate Professor at the Laboratory of Radiochemistry, Institute for Chemical Research, Kyoto University. In 1982, he was appointed full Professor of Kyoto University and directed the Laboratory of Radiochemistry (present name, Interface Science III), Institute for Chemical Research. At the Graduate School of Science, Kyoto University, he gave lectures on Radiochemistry, Analytical Chemistry and Geochemistry, and supervised the dissertation works of many graduate student. His sincere and warmhearted character has been admired by his friends, colleagues and students.

Dr. Matsui devoted himself to the Japan Society for Analytical Chemistry, and officiated as Vice-President of the Society between 1994-1995. He was a member of the interdisciplinary committee of world cultural council, and the trustee of Japan Society of Solvent Extraction Chemistry and others. He has also chaired the International Symposium on New Sensors and Methods

for Environmental Characterization.

During the past 37 years, his research interest encompassed a wide array of radiochemistry, separation chemistry, inorganic chemistry, molecular recognition, environmental chemistry and geochemistry. His contribution to the Institute through both academic and administrative activities is hereby gratefully acknowledged, and his academic achievements are briefly described below.

Dr. Matsui's work has been concerned with selective complex formation systems based on the concept of molecular recognition, and the separation chemistry in the selective metal chelate system employing the new ligands. He designed and synthesized a new series of ligands (host molecules), in particular, β -diketone, acylpyrazolone and polypyrazolylborate derivatives that have novel functions with improved stability and separability of metal ions and guest molecules. His research interest in molecular recognition was highlighted by the X-ray crystallography of metal chelate complexes. He extensively investigated various mechanisms of ion size discrimination derived from structures of the ligand and complexes, such as bite size, rigidity and interligand contact. As a geochemical aspect of his research, he established novel analytical methods for trace elements in the hydrosphere and studied their applications. He also elucidated circulation and biochemistry of minor and trace elements in the open ocean and Lake Biwa. Owing to his brilliant achievements, he was awarded a prize from Japan Society for Analytical Chemistry in 1995.

Thus, Dr. Matsui has shown us an ideal direction of the academic research that the successful application can be attained only by a thorough understanding of the fundamental phenomena. This principle will remain as a firm basis underlying the research work in the Institute.

Retirement

Professor Atsuyoshi OHNO

(Bioorganic Chemistry,
Division of Bioorganic Reaction Theory)



On the 31st of March, 1999, Dr. Atsuyoshi Ohno retired from Kyoto University after 26 years of service to the University and was honored with the title of Professor Emeritus of Kyoto University.

Dr. Ohno was born in Hiroshima on the 13th of February, 1936. After graduation from Department of Chemistry, Faculty of Science, Kyoto University in 1958, he continued his studies as a graduate student. In 1960, he was appointed a technical officer of the Radiation Center of Osaka Prefecture, under the supervision of the Professor Shigeru Oae. He was granted a doctoral degree from Osaka City University in 1963 for his studies on the neighboring participation of sulfur to carbanion stabilization. In 1963, he stayed at the Department of Chemistry, Massachusetts Institute of Technology and studied reaction mechanism of S_N2 type hydrolysis with Professor C. G. Swain. In 1965, he moved to the Department of Chemistry, Purdue University and studied kinetic and theoretical studies of carbanion chemistry with Professor R. E. Davis. In 1966, Dr. Ohno was promoted to Research Fellow at Sagami Chemical Research Center. In 1969, he was promoted to the chief researcher of the same center. In 1974, Dr. Ohno was promoted to Associate Professor of Institute for Chemical Research, Kyoto University. In 1989, he was appointed full Professor of Kyoto University and directed the Laboratory of Bioorganic Chemistry.

During the past 40 years, his research interest encompassed a wide array of physical organic chemistry, bioorganic chemistry, and synthetic organic chemistry. Following his early studies on the mechanism of sulfur-stabilized carbanion, he developed a series of basic organic

reaction mechanism. His idea of assistance of 3d-orbital of sulfur on stabilization of carbanion prompted numerous organic chemists to use the sulfur stabilized carbanion in synthetic organic chemistry. He synthesized a series of model compounds of NADH, and carried out the stereoselective reduction of ketones with high enantioselectivity. He proposed a novel mechanism of the reaction with nicotinamide cofactor, namely, in the reaction of transfer of (net) hydride, electron transfer proceeds prior to hydrogen transfer and multi-step electron-proton-electron transfer was observed in the model reaction. His proposal raised a big controversy among organic chemists and biochemists during two decades and finally, multi-step mechanism was supported as the standard mechanism.

He synthesized a chiral 5-deazaflavin model and several NADH models which had axial chiralities and he found conversion of a central chirality into an axial chirality (chirality sink) or vice versa in the oxidation or reduction of these model compounds.

He used bakers' yeast as a biocatalyst to reduce various ketones into the corresponding chiral alcohols in high enantioselectivities. He found a new system for artificial control of the stereoselectivity of microbial reductions.

He served as editors of Bulletin of the Chemical Society of Japan, Chemistry Letters, Reviews on Heteroatom Chemistry, and Heteroatom Chemistry.

He gave lectures on advanced bioorganic chemistry at the graduate school of science at Kyoto University and supervised dissertation works of graduate students. His sincere and warmhearted character has been admired by his friends, colleagues, and students.

TANO, Takanori	10	UEDA, Momoko	46	YAMADA, Satoru	54
TATSUMI, Masao	22	UEDA, Yumi	50	YAMADA, Takahiro	20
TERADA, Shohei	6	UEMATSU, Takehiko	24	YAMAGUCHI, Koichiro	4
TERADA, Tomoko	36	UENO Yukiyo	8	YAMAGUCHI, Shigehiro	34
TERAKAWA, Katsumi	8	UMEMOTO, Shin-ichi	38	YAMAMOTO, Hiroyoshi	26
TERASHIMA, Takahito	18	UMEMURA, Junzo	10	YAMAMOTO, Kensaku	36
TERASHIMA, Takashi	20	UMETANI, Shigeo	14	YAMAMOTO, Shuichi	30
TOBE, Yoshito	61	UNO, Yumiko	40	YAMANAKA, Rio	38
TOCHIO, Tatsunori	4	UO, Takuma	46	YAMASHITA, Ryoji	26
TOGANO, Hiroki	20	URAKABE, Eriko	54	YAMAUCHI, Takahiro	46
TOHDO Fumiko	46	URAYAMA, Kenji	8	YAMAUCHI, Kayoko	40
TOKUDA, Youmei	22	UTSUNOMIYA, Machiko	46	YAMAZAKI, Norimasa	38
TONGUU, Hiromu	54			YANG, Xiaosheng	36
TOSAKA, Masatoshi	8			YANO, Hiroyuki	50
TOSHIMITSU, Akio	34	[V]		YASUDA, Keiko	58
TOYA, Hiroshi	10	VLAICU, A. Mihai	4	YASUI, Jun	4
TROSZNAJDER, Robert	42			YASUMOTO, Mitsuo	32
TSUJI, Hayato	34	[W]		YOKO, Toshinobu	22
TSUJI, Masaki	8	WAKAI, Chihiro	10	YOKOI, Tomoko	12
TSUJII, Yoshinobu	30	WAKAMIYA, Atsushi	32	YOKOYAMA, Keisuke	8
TSUJIMOTO, Masahiko	6	WATANABE, Akira	46	YOSHIDA, Hiroshi	36
TSUJINO, Yasuo	10	WATANABE, Hiroshi	24	YOSHIDA, Hiroyuki	12
TSUKIGI, Kaori	22	WATANABE, Tasuku	46	YOSHIDA, Kaname	6
TSUKUDA, Mayumi	50	WATANABE, Toshiyuki	36	YOSHIDA, Masato	36
TSUKUSHI, Itaru	26	WEI, Yun-Lin	46	YOSHIDA, Yumi	14
TSUNASHIMA, Yoshisuke	28	WILLIAMS, Tyler	42	YOSHIMUNE, Kazuaki	46
TSUTSUMI, Kiyohiko	12			YOSHIMURA, Tohru	46
TUBAKI, Kzunori	36	[X]			
		[Y]		[Z]	
[U]		YAJI, Toyonari	6	ZHAO, Gaoling	22
UCHINO, Takashi	22	YAMADA, Kazuyohi	18	ZHOU, Qi	30
UEDA, Kunihiko	42	YAMADA, Kenji	30		

KEYWORD INDEX

[A]		[G]		Polymacromonomer	30
α -Chymotrypsin	38	Germanosilicate glasses	22	polymerization process	6
Ab initio MO calculation	12	Germyllithium	34	Protein sorting	52
Alamethicin	12	Giant magnetoresistance	16	Pyridoxal phosphate	46
Alkaloids	44	Global mode	24	[Q]	
Alzheimer's disease	42	[H]		[R]	
Amino acid racemase	46	Heavy ion accelerator	54	Response regulator	50
Arabidopsis	50	High density polyethylene	8	Rheo-dielectric behavior	24
Arsenic	14	High pressure synthesis	20	RNA editing	58
Arsenic methylation	14	Hydrothermal reaction	10	[S]	
Artificial protein	40	[I]		Segmental mode	24
Atropisomer	36	Induced-Fit Theory	38	SEM	8
[B]		Internal motions	28	Shear flow	28
Beam-Cooling	56	Ion transport	12	Shear-thinning	24
$\text{Bi}_{2+x}\text{Sr}_{2-x}\text{CuO}_{6+d}$	18	Ion-channel	12	Silver complex	32
Bilayer lipid membrane	12	Iron-sulfur cluster	48	Simulation	56
Binaphthyl ether	36	[J]		Sol-gel method	22
Bioinformatics	52	[K]		Solid-state structure	34
[C]		kinetoplastid protozoa	58	Space-Charge	56
<i>C. fasciculata</i>	58	[L]		Speciation	14
C1 chemistry	10	Lewy body	42	Spin gap	20
C_{60}	32	Living cationic polymerization	30	Stereochemistry	46
Cannizzaro reaction	10	Low temperature high resolution imaging	6	Stereospecificity	44
Catalytic Activity	38	[M]		Storage Ring	56
Characteristic Wavelength	26	Magnetic domain wall	16	Submicron magnetic wire	16
Chelation	34	Magnetization reversal	16	Substitution	18
Controlled radical polymerization	30	Mechanochemistry	32	Superconducting RFQ	54
Cooperative domain structure	24	Medium Viscosity	38	Superconductivity	18
Coupling	56	Melt Crystallization	26	[T]	
Cycloaddition	32	Methyl cation transfer	12	Thermal isomerization	12
CYP2D6	42	Microphase Separation	26	Thermostability	48
[D]		Microsatellite	42	TiC	4
Database	52	Microwave digestion	14	TiN	4
Defect	22	Modulation	18	Transcription factor	40,50
Deformation	8	Molecular gear	36	Tropinone reductase	44
Dehydroannulene	32	Molecular orbital	4	Two-component regulatory system	50
Diffusion	28	Multi finger	40	[U]	
1 dimensional magnet	20	[N]		Ultraviolet irradiation	14
2-(Dimethylamino)phenyl ligand	34	NADPH	44	[V]	
1,6-di(N-carbazoyl)-2,4-hexadiyne	6	Natural water	14	[W]	
Diselenadigermetane	34	NMR	10	[X]	
DNA recognition	40	Nuclear transport	52	X-ray analysis	48
Dynamic coupling	28	[O]		X-ray crystallography	44
Dynamic light scattering	28	Organic solid-state reaction	12	X-ray diffraction	8
[E]		Organoarsenicals	14	X-ray emission spectra	4
Electronic structure	4	[P]		[Y]	
Enzymatic reaction	44	Parkinson's disease	42	[Z]	
Extended cluster model	4	PET	26	Zinc	48
Extruded blown film	8	Phase diagram	18	Zinc-finger protein	40
[F]		Photosensitivity	22		
Fiber Grating	22	PIAVE	54		
Formaldehyde	10				